



## ANOVEL ENANTIOSELECTIVE AMINOCATALYTIC PROCESSES BY MEANS OF VINYLOGOUS REACTIVITY AND PHOTOREDOX CATALYSIS

David Bastida Borrell

**ADVERTIMENT.** L'accés als continguts d'aquesta tesi doctoral i la seva utilització ha de respectar els drets de la persona autora. Pot ser utilitzada per a consulta o estudi personal, així com en activitats o materials d'investigació i docència en els termes establerts a l'art. 32 del Text Refós de la Llei de Propietat Intel·lectual (RDL 1/1996). Per altres utilitzacions es requereix l'autorització prèvia i expressa de la persona autora. En qualsevol cas, en la utilització dels seus continguts caldrà indicar de forma clara el nom i cognoms de la persona autora i el títol de la tesi doctoral. No s'autoritza la seva reproducció o altres formes d'explotació efectuades amb finalitats de lucre ni la seva comunicació pública des d'un lloc aliè al servei TDX. Tampoc s'autoritza la presentació del seu contingut en una finestra o marc aliè a TDX (framing). Aquesta reserva de drets afecta tant als continguts de la tesi com als seus resums i índexs.

**ADVERTENCIA.** El acceso a los contenidos de esta tesis doctoral y su utilización debe respetar los derechos de la persona autora. Puede ser utilizada para consulta o estudio personal, así como en actividades o materiales de investigación y docencia en los términos establecidos en el art. 32 del Texto Refundido de la Ley de Propiedad Intelectual (RDL 1/1996). Para otros usos se requiere la autorización previa y expresa de la persona autora. En cualquier caso, en la utilización de sus contenidos se deberá indicar de forma clara el nombre y apellidos de la persona autora y el título de la tesis doctoral. No se autoriza su reproducción u otras formas de explotación efectuadas con fines lucrativos ni su comunicación pública desde un sitio ajeno al servicio TDR. Tampoco se autoriza la presentación de su contenido en una ventana o marco ajeno a TDR (framing). Esta reserva de derechos afecta tanto al contenido de la tesis como a sus resúmenes e índices.

**WARNING.** Access to the contents of this doctoral thesis and its use must respect the rights of the author. It can be used for reference or private study, as well as research and learning activities or materials in the terms established by the 32nd article of the Spanish Consolidated Copyright Act (RDL 1/1996). Express and previous authorization of the author is required for any other uses. In any case, when using its content, full name of the author and title of the thesis must be clearly indicated. Reproduction or other forms of for profit use or public communication from outside TDX service is not allowed. Presentation of its content in a window or frame external to TDX (framing) is not authorized either. These rights affect both the content of the thesis and its abstracts and indexes.

UNIVERSITAT ROVIRA I VIRGILI  
ANovel ENANTIOSELECTIVE AMINOCATALYTIC PROCESSES BY MEANS OF VINYLLOGOUS  
REACTIVITY AND PHOTOREDOX CATALYSIS  
David Bastida Borrell

UNIVERSITAT ROVIRA I VIRGILI  
NOVEL ENANTIOSELECTIVE AMINOCATALYTIC PROCESSES BY MEANS OF VINYLLOGOUS  
REACTIVITY AND PHOTOREDOX CATALYSIS  
David Bastida Borrell

David Bastida Borrell

**Novel Enantioselective Aminocatalytic  
Processes by means of Vinylogous Reactivity  
and Photoredox Catalysis**

Doctoral Thesis

Supervised by Prof. Paolo Melchiorre

ICIQ – Institut Català d'Investigació Químic



UNIVERSITAT ROVIRA I VIRGILI

Tarragona

2015

UNIVERSITAT ROVIRA I VIRGILI  
NOVEL ENANTIOSELECTIVE AMINOCATALYTIC PROCESSES BY MEANS OF VINYLLOGOUS  
REACTIVITY AND PHOTOREDOX CATALYSIS  
David Bastida Borrell



Prof. Paolo Melchiorre, ICREA Research Professor & ICIQ Group Leader

I STATE that the present study, entitled “Novel Enantioselective Aminocatalytic Processes by means of Vinylogous Reactivity and Photoredox Catalysis”, presented by David Bastida Borrell to receive the degree of Doctor, has been carried out under my supervision at the Institut Català d'Investigació Química (ICIQ).

Tarragona, November the 4<sup>th</sup> 2015

Doctoral Thesis Supervisor

Prof. Paolo Melchiorre

UNIVERSITAT ROVIRA I VIRGILI  
NOVEL ENANTIOSELECTIVE AMINOCATALYTIC PROCESSES BY MEANS OF VINYLLOGOUS  
REACTIVITY AND PHOTOREDOX CATALYSIS  
David Bastida Borrell

## Acknowledgements

Després d'aquests darrers anys tant intensos a l'ICIQ, no haguessin sigut lo mateix o no haguessin sigut possibles sense la contribució de molta gent. Aquí un breu reconeixement a tots ells.

En primer lloc, voldria agrair al Prof. Paolo Melchiorre, la possibilitat d'haver realitzat la tesis en el seu grup de recerca. Apart de la formació química i el temps dedicat a la meva persona, també li voldria agrair tots els valors transmesos així com la passió per aquesta "feina".

També voldria agrair a les persones que varen fer possible l'estada durant 4 mesos a BASF, Dr. Klaas Lohmann i Dra. Ana Escribano, els quals em van acollir en el centre de recerca a Alemanya. Voldria agrair a tots els actuals i antics membres del grup, el seu suport i ajuda durant aquests anys. En especial voldria fer menció a aquells amb els quals vaig tenir la sort de col·laborar mes estretament. Dr. Yankai Liu, aquell qui em va iniciar dins el laboratori i de qui vaig aprendre moltíssim dins la vitrina. Dr. Indranil Chatterjee amb el qual vaig tenir la sort de compartir el naixement de la seva filla. Dr. John J. Murphy amb el qual hem portat a terme el darrer projecte, el seu optimisme i dedicació han estat contagiosos. També al Mattia i Ana aquells amb qui he compartit mes anys en el grup.

Voldria agrair a tots els membres de l'àrea de suport de l'ICIQ, per la seva professionalitat.

A tots els amics que he fet aquets quatre anys en el centre Jordi, Carla, Anna, Imma, José Luis, Marc, Xue, Miriam, Toni, Paco i un llarg etcètera... als jugadors de futbol del dijous.

Al Josep Cornellà amb qui vaig compartir laboratori durant 2 anys, també gracies a ell, el treball al laboratori va deixar un dia de ser treball.

A tota la gent de Tremp (la CCCCCoLLA i les YOKOS) i Guàrdia (komando Guardia) tot i que cansats de que no pugui tant per que molts cops havia de treballar un cap de setmana allà dalt amb "vates" em feia renovar i incrementar les forces.

A la Paula per suposat, pel seu suport incondicional. A ella he d'agrar-li tota la paciència durant aquest temps, el acceptar que no sempre ella ha estat abans de la química, el aguantar els mals dies del laboratori, les jornades maratonianes, sense ella hagués estat molt més difícil arribar fins aquí.

A la meva família, perquè sempre han estat al meu costat, m'han donat suport i empenta, encara que sempre costa explicar que realment fas, la seva curiositat i estima sempre m'han ajudat a seguir endavant. Especialment al meu pare, de qui podria dir que aquesta tesi es en gran part seva, per la educació i valors que m'ha donat al llarg de la meva vida, sense els quals mai hauria pogut arribar fins al dia d'avui.



Support from the Institute of Chemical Research of Catalonia (ICIQ) Foundation, from MICINN (grant CTQ2010-15513), MINECO (CTQ2013-45938-P) and from the European Research Council (ERC Starting grant agreement no. 278541—ORGA-NAUT) are gratefully acknowledged.

I am personally grateful to European Research Council (ERC Starting grant agreement no. 278541—ORGA-NAUT) for a doctoral fellowship.



## List of Publications

Some of the results presented in this thesis have been published:

- *Asymmetric Vinylogous Aldol Reaction via H-Bond-Directing Dienamine Catalysis;*  
**Bastida, D.**; Liu, Y.; Tian, X.; Escudero-Adán, E.; Melchiorre, P. *Org. Lett.* **2013**, *15*, 220.
- *Vinylogous Organocatalytic Triple Cascade Reaction: Forging Six Stereocenters in Complex Spiro-Oxindolic Cyclohexanes*  
Chatterjee, I.; **Bastida, D.**; Melchiorre, P. *Adv. Synth. Catal.* **2013**, *355*, 3124- 3130
- *Enantioselective catalytic construction of quaternary carbon stereocentres by iminium ion trapping of photochemically generated radicals;*  
**Bastida, D.**; Murphy, J. J., Paria, S., Melchiorre, P. Manuscript in preparation

UNIVERSITAT ROVIRA I VIRGILI  
NOVEL ENANTIOSELECTIVE AMINOCATALYTIC PROCESSES BY MEANS OF VINYLLOGOUS  
REACTIVITY AND PHOTOREDOX CATALYSIS  
David Bastida Borrell

“Perquè viure és combatre la peresa  
de cada instant, i restablir la fonda  
dimensió de cada cosa dita, podem  
amb cada gest guanyar nous àmbits,  
i amb cada mot acrièixer l'esperança.  
Serem allò que vulguem ser.”

Miquel Martí i Pol

UNIVERSITAT ROVIRA I VIRGILI  
NOVEL ENANTIOSELECTIVE AMINOCATALYTIC PROCESSES BY MEANS OF VINYLLOGOUS  
REACTIVITY AND PHOTOREDOX CATALYSIS  
David Bastida Borrell

UNIVERSITAT ROVIRA I VIRGILI  
NOVEL ENANTIOSELECTIVE AMINOCATALYTIC PROCESSES BY MEANS OF VINYLLOGOUS  
REACTIVITY AND PHOTOREDOX CATALYSIS  
David Bastida Borrell

*A la meua família*

UNIVERSITAT ROVIRA I VIRGILI  
NOVEL ENANTIOSELECTIVE AMINOCATALYTIC PROCESSES BY MEANS OF VINYLLOGOUS  
REACTIVITY AND PHOTOREDOX CATALYSIS  
David Bastida Borrell

## Table of Contents

<b>Chapter I. Introduction</b> .....	1
1.1. Activation Modes in Organocatalysis.....	1
1.1.1. Aminocatalysis.....	2
Iminium Ion Activation.....	3
Enamine Activation.....	4
1.1.2. Aminocatalytic Vinylogous Reactivity.....	4
1.1.3. The Tools of Aminocatalysis.....	5
Secondary Amine Catalysts.....	5
Primary Amine Catalysts.....	5
Mechanisms of Stereochemical Induction in Aminocatalysis.....	6
1.1.4. Hydrogen Bond Donor Catalysis.....	7
1.2. Aminocatalytic Cascade Reactions.....	8
1.3. Visible light Photoredox Catalysis and Aminocatalysis.....	9
1.4. Summary of the Thesis Research.....	11
<b>Chapter II. Asymmetric Vinylogous Aldol Reaction via H-Bond-Directing Dienamine Catalysis</b> .....	13
2.1. Background.....	13
2.2. Asymmetric Direct Vinylogous Aldol Reaction.....	19
2.2.1. Precedents of Asymmetric Vinylogous Aldol Reaction.....	19
2.2.2. Our Strategy: Results and Discussion.....	21
2.2.3. Mechanistic Studies.....	31
2.2.4. Conclusions.....	36
2.3. Experimental Section.....	36
2.3.1. General Information.....	36
2.3.2. General Procedure for the Vinylogous Aldol Reaction.....	38
2.3.4. Intermediate Characterization: NMR Spectroscopic Studies.....	47



<b>Chapter III. Vinylogous Organocatalytic Triple Cascade Reaction: Forging Six Stereocenters in Complex Spiro-Oxindolic Cyclohexanes .....</b>	<b>53</b>
3.1. Background .....	53
3.1.1. Amine-Catalyzed Cascade Reactions .....	55
3.1.2. Cascade Reactions and the Vinylogy Principle .....	57
3.1.3. Organocatalytic Asymmetric 1,6-Conjugate Additions .....	59
3.2. Results and Discussion .....	63
3.2.1. Conclusions .....	74
3.3. Experimental Section .....	74
3.3.1. Preparation of the Linear 2,4-dienals 30 .....	76
3.3.2. Preparation of 3-olefinic Oxindoles 24. ....	78
3.3.3. General Procedure of the Triple Vinylogous Cascade Reactions .....	80
3.3.4. Characterization of the Cascade Products .....	81
3.3.5. General Procedure for the Epoxidation of Compounds 34 .....	90
3.3.6. NMR Conformational Studies .....	91
3.3.7. Single Crystal X-Ray Diffraction Data .....	92
<b>Chapter IV. Photochemical Enantioselective <math>\beta</math>-Alkylation of Enones by Means of Iminium Ion Activation .....</b>	<b>95</b>
4.1. The Project Idea, the Precedents and the Challenges Behind .....	95
4.2. Generating Carbon-Centered Radicals using Photoredox Catalysis .....	99
4.3. Principles of Photochemistry and Photoredox Catalysis .....	99
4.3.1. Intramolecular Photophysical Processes of the Excited State .....	100
4.3.2. Intermolecular Photophysical Processes of the Excited State .....	100
4.3.3. Photoinduced Proton-Coupled Electron Transfer and Hydrogen Atom .....	102
4.4. Polyoxometalates and TBADT as Photoredox Catalysts .....	103
4.5. Research Project and Initial Trials .....	105
4.6. Enantioselective $\beta$ -Quaternarization of Cyclic Enones .....	109
4.7. Results and Discussion .....	110

4.7.1.	Final Optimization Studies.....	114
4.7.2.	Synthetic Route for the Preparation of Catalyst XXIX and Analogous Thereof .....	114
4.7.3.	Light Source.....	116
4.8.	ANNEX 1. Synthetic Efforts Toward the Preparation of the Carbazole-Derived Organocatalysts .....	121
4.8.1.	Route 1: S <sub>N</sub> 2 Substitution.....	122
4.8.2.	Route 2: Photoinduced, Copper-Catalyzed Couplings of Carbazoles. ....	124
4.8.3.	Preparation of Catalyst XXIX using the Michael Addition as a Key Step.....	125
4.9.	Experimental Section.....	128
4.9.1.	Preparation of Different Carbazole Compounds. ....	129
4.9.2.	Preparation of Different Carbazole Derivatives type Catalysts XXIX.....	134
4.9.3.	Resolution of the Enantiopure Primary Amine Catalysts.....	136
4.9.4.	Preparation of Starting Enones and Benzodioxole. ....	141
4.9.5.	General Procedure of the Photochemical Enantioselective $\beta$ -Alkylation of Enones. ....	145
4.9.6.	Single Crystal X-Ray Diffraction Data .....	147
4.9.7.	NMR traces of compound 23a and catalyst XXXIX .....	151
4.9.8.	HPLC traces of compound 23a.....	153
4.10.	ANNEX 2. Features, Descriptions and Technical Issues of the Irradiation Systems....	154

UNIVERSITAT ROVIRA I VIRGILI  
NOVEL ENANTIOSELECTIVE AMINOCATALYTIC PROCESSES BY MEANS OF VINYLLOGOUS  
REACTIVITY AND PHOTOREDOX CATALYSIS  
David Bastida Borrell

## Chapter I

### Introduction

---

Aim of the chapter is to contextualize this thesis providing the historical research background while briefly describing the reactivity concepts that have been crucial to the development of the present research. The thesis deals with catalysis and its application in chemical processes. By definition, a *catalyst* is a species that accelerates a chemical transformation by lowering the energy necessary to reach the transition state but without modifying the overall standard Gibbs energy change in the reaction. Moreover, such species remain unreacted, and it is not consumed throughout the reaction.

Within the realm of catalysis, enantioselective approaches<sup>1</sup> have attracted tremendous attention because of the possibility to convert achiral substrates into enantiomerically pure products with the help of only a small amount of chiral catalysts. Bio-catalysts and chiral organometallic catalysts have historically played a crucial role for developing asymmetric transformations. However, in the last fifteen years a new mode of catalysis emerged as a powerful alternative: *enantioselective organocatalysis*, which relies on the use of simple, enantiopure, small organic molecules to perform enantioselective transformations.<sup>2</sup>

#### 1.1. Activation Modes in Organocatalysis

Developing new catalytic reactions is a must to address the synthetic challenges faced by organic chemists. In the realm of enantioselective organocatalysis, this task is associated with the development of new generic catalytic modes of action, induction and reactivity. When an activation mode has been established, it is relatively straightforward to use it as a platform for the design of a wide range of new enantioselective reactions.<sup>2</sup> A generic activation mode provides a reactive species that can participate in many types of transformations with high enantioselectivity. Such reactive species arise from the interaction of a chiral catalyst with a key functional group of the substrate in a highly organized and predictable manner. Based on the nature of the interaction between the catalyst and the substrate, the generic organocatalytic activation modes can be categorized in *covalent*-based and *noncovalent*-based activations.<sup>3</sup>

---

<sup>1</sup> R. Noyori, Asymmetric Catalysis: Science and Opportunities (Nobel Lecture). *Angew. Chem. Int. Ed. Engl.* **2002**, *41*, 2008.

<sup>2</sup> D. W. C. MacMillan, The Advent and Development of Organocatalysis. *Nature*, **2008**, *455*, 304.

<sup>3</sup> E. N. Jacobsen, D. W. C. MacMillan, Organocatalysis. *Proc. Natl. Acad. Sci. USA*, **2010**, *107*, 20618.

Catalysts activating the substrate by forming a covalent bond are among the most widely used. Chiral primary and secondary amines belong to this class, participating in many reactions by activating the carbonyl compounds upon condensation and reversible formation of an enamine, an iminium ion,<sup>4</sup> or a SOMO intermediate<sup>5</sup> as the reactive species. Those three activation modes, which rely on strong, directional interactions, have provided the synthetic community with reliable synthetic platforms for generating stereogenic centers at the  $\alpha$  and  $\beta$  positions of unmodified carbonyl compounds.

Concerning the catalysis by noncovalent interactions, hydrogen-bonding interactions<sup>6</sup> have shown a clear utility in enantioselective synthesis. Although the interactions involved are generally weaker, less directional and less distance-dependent than their covalent counterparts, they have been shown to operate in concert through a cooperative effect, ensuring high level of transition state structural organization, and thus enantioselectivity. Another important catalytic approach, also classified as a noncovalent activation mode, involves the interaction of ionic species with chiral neutral, anionic or cationic organocatalysts. This field is referred to as ion-pairing catalysis.<sup>7</sup>

In the following sections, the generic organocatalytic modes of activation that have been crucial to address specific synthetic challenges identified within this PhD studies are highlighted.

### 1.1.1. Aminocatalysis

The use of chiral amine catalysts for the asymmetric functionalization of unmodified carbonyl compounds was firstly reported in the early 1970s by Hajos, Parrish, Eder, Sauer and Wiechert.<sup>8</sup> In 2000, two independent reports conceptualized the modern field of asymmetric aminocatalysis: the proline-catalyzed intermolecular Aldol reaction, published by List, Lerner and Barbas (Figure 1a),<sup>9</sup> and the asymmetric amine-catalyzed Diels-Alder reaction,<sup>10</sup> developed by MacMillan (Figure 1b). After these seminal publications, aminocatalysis was brought to the

---

<sup>4</sup> P. Melchiorre, M. Marigo, A. Carlone, G. Bartoli. Asymmetric Aminocatalysis - Gold Rush in Organic Chemistry. *Angew. Chem. Int. Ed.* **2008**, *47*, 6138.

<sup>5</sup> T. D. Beeson, A. Mastracchio, J.-B. Hong, K. Ashton, D. W. C. MacMillan. Enantioselective Organocatalysis Using SOMO Activation. *Science* **2007**, *316*, 582.

<sup>6</sup> M. S. Taylor, E. N. Jacobsen. Asymmetric Catalysis by Chiral Hydrogen-Bond Donors. *Angew. Chem. Int. Ed.* **2006**, *45*, 1520.

<sup>7</sup> K. Brak, E. N. Jacobsen. Asymmetric Ion-Pairing Catalysis. *Angew. Chem. Int. Ed.* **2013**, *52*, 534. b) M. Mahlau, B. List. Asymmetric Counteranion-Direct Catalysis: Concept, Definition, and Application. *Angew. Chem. Int. Ed.* **2013**, *52*, 518

<sup>8</sup> U. Eder, G. Sauer, R. Wiechert, New Type of Asymmetric Cyclization to Optically Active Steroid CD Partial Structures. *Angew. Chem. Int. Ed. Engl.* **1971**, *10*, 496; b) Z. G. Hajos, D. R. Parrish, Asymmetric Synthesis of Bicyclic Intermediates of Natural Product Chemistry. *J. Org. Chem.* **1974**, *39*, 1615

<sup>9</sup> B. List, R. A. Lerner, C. F. Barbas III. Proline-Catalyzed Direct Asymmetric Aldol Reactions. *J. Am. Chem. Soc.* **2000**, *122*, 2395.

<sup>10</sup> K. A. Ahrendt, C. J. Borths, D. W. C. MacMillan. New Strategies for Organic Catalysis: The First Highly Enantioselective Organocatalytic Diels-Alder Reaction. *J. Am. Chem. Soc.* **2000**, *122*, 4243.

forefront of the scientific community and became an appealing and competitive field of chemical research in asymmetric synthesis.<sup>4</sup>

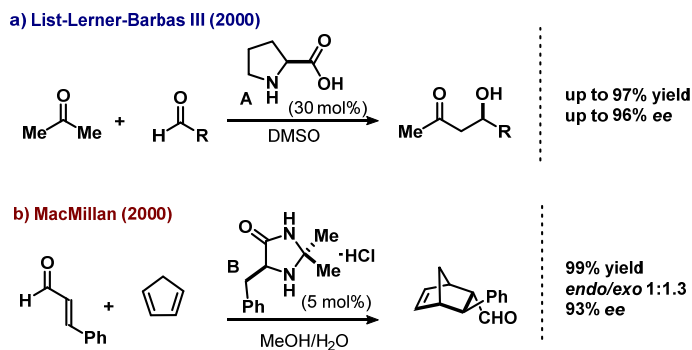


Figure 1. Seminal publications in asymmetric aminocatalysis.<sup>9,10</sup>

### Iminium Ion Activation

Iminium ion activation is based on the use of chiral amines for the direct asymmetric  $\beta$ -functionalization of  $\alpha,\beta$ -unsaturated carbonyl compounds (Figure 2).<sup>11</sup>

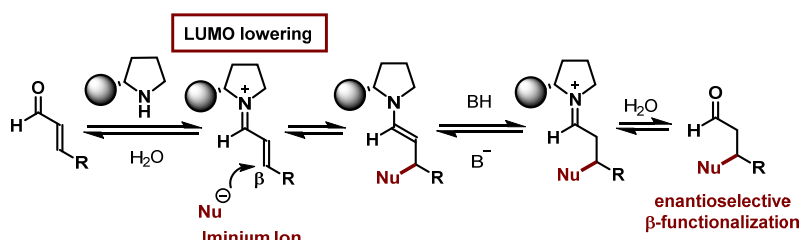


Figure 2. Iminium ion activation. Nu = nucleophile. The grey circle represents the chiral catalyst scaffold.

Initial condensation between the amine catalyst and the  $\alpha,\beta$ -unsaturated carbonyl compound renders the positively charged iminium ion intermediate. This species has a lower energy of the lowest unoccupied molecular orbital (LUMO) with respect to the original unsaturated carbonyl (LUMO lowering activation). For conjugated  $\pi$  systems, the electronic redistribution induced by the iminium ion intermediates facilitates nucleophilic additions and allows the asymmetric  $\beta$ -functionalization of carbonyl compounds.<sup>12</sup> In the case of isolated  $\pi$ -systems, the LUMO-lowering effect increases the  $\alpha$ -proton acidity. This induces a fast deprotonation, which leads to the generation of the enamine.

<sup>11</sup> A. Erkkilä, I. Majander, P. M. Pihko. Iminium Catalysis. *Chem. Rev.* **2007**, *107*, 5416.

<sup>12</sup> G. Lelais, D. W. C. MacMillan. Modern Strategies in Organic Catalysis: The Advent and Development of Iminium Activation. *Aldrichimica Acta* **2006**, *39*, 79.

### Enamine Activation

Enamine activation describes the reactions promoted by an in situ generated enamine, which is a nucleophilic enolate equivalent (Figure 3).<sup>13</sup>

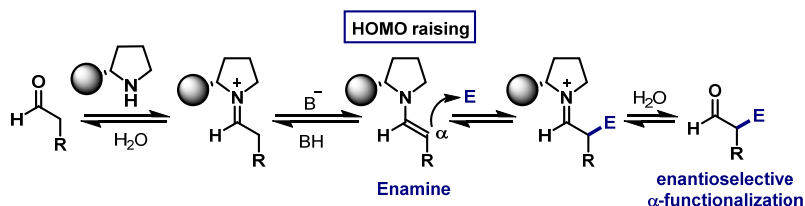


**Figure 3.** Enamine activation. E = electrophile. The grey circle represents the chiral catalyst scaffold

The reversible condensation of a catalytic amount of a secondary amine with an enolizable carbonyl compound leads to a positively charged intermediate (an iminium ion) that induces an increase of the acidity of the  $\alpha$  proton. This drives a fast deprotonation, which leads to the generation of the enamine. The enamine intermediate is characterized by a higher energy level of the highest occupied molecular orbital (HOMO) with respect to the parent enol form (HOMO raising activation). This determines the activation of the  $\alpha$ -carbon toward nucleophilic addition thus allowing for the asymmetric  $\alpha$ -functionalization of unmodified carbonyl compounds.<sup>14</sup>

#### 1.1.2. Aminocatalytic Vinylogous Reactivity

The principle of vinylogy, introduced by Fuson in 1935, recognizes the propagation of the inductive effects through a  $\pi$ -system.<sup>15</sup> In 2006, Jørgensen merged this principle with aminocatalysis to develop an enantioselective direct  $\gamma$ -amination of enals.<sup>16</sup> This study demonstrated that organocatalytic modes of activation, such as enamine activation, could potentially be extended to more remote positions. This approach opened the door to access stereoselective  $\gamma$ - or  $\epsilon$ -functionalizations of unsaturated carbonyl compounds via dienamine or trienamine activations (HOMO raising strategy). Following the same principle, iminium ion could be extended to the  $\delta$  position of polyunsaturated carbonyl compounds via vinylogous iminium ion catalysis (LUMO lowering strategy, Figure 4).<sup>17</sup>

<sup>13</sup> S. Makherjee, J. W. Yang, S. Hoffmann, B. List. Asymmetric Enamine Catalysis. *Chem. Rev.* **2007**, *107*, 5471.

<sup>14</sup> a) K. L. Jensen, G. Dickmeiss, H. Jiang, Ł. Albrecht, K. A. Jørgensen, The Diarylprolinol Silyl Ether System: A General Organocatalyst. *Acc. Chem. Res.*, **2012**, *45*, 248. b) S. Bertelsen, K. A. Jørgensen. Organocatalysis – After the Gold Rush. *Chem. Soc. Rev.* **2009**, *38*, 2178.

<sup>15</sup> R. C. Fuson, The Principle of Vinylogy. *Chem. Rev.* **1935**, *16*, 1.

<sup>16</sup> S. Bertelsen, M. Marigo, S. Brandes, P. Dinér, K. A. Jørgensen, Dienamine Catalysis: Organocatalytic Asymmetric  $\gamma$ -Amination of  $\alpha,\beta$ -Unsaturated Aldehydes. *J. Am. Chem. Soc.* **2006**, *128*, 12973.

<sup>17</sup> I. D. Jurberg I. Chatterjee, R. Tannert, P. Melchiorre, When Asymmetric Aminocatalysis Meets the Vinylogy Principle. *Chem. Comm.* **2013**, *49*, 4869.

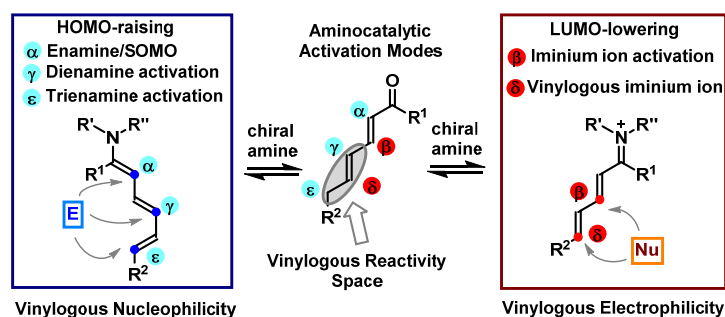


Figure 4. Vinylogous reactivity and aminocatalysis.

### 1.1.3. The Tools of Aminocatalysis

#### Secondary Amine Catalysts

The most general catalysts used in aminocatalysis are depicted in Figure 5 (primary amines on the left panel, secondary amines on the right). As aforementioned, L-proline (**A**) and MacMillan's imidazolidinones (**B**) found early applications in the pioneering works published in 2000 (Figure 1). In 2005, two independent groups simultaneously reported on organocatalytic highly stereoselective transformations catalyzed by  $\alpha,\alpha$ -diphenylprolinol trimethylsilyl protected derivatives (**C**).<sup>17</sup> Such family of versatile catalysts had become widely used in aminocatalysis, and they are simply named after the inventors: the Jørgensen-Hayashi catalysts.<sup>18</sup> The crucial aspects of these catalysts is that they could promote mechanistically unrelated reactions with high efficiency (enamine and iminium ion activations, and their vinylogous counterparts), a merit that made diarylprolinol silyl ethers the "workhorses" of aminocatalysis.<sup>19</sup>

#### Primary Amine Catalysts

Primary amines have been recognized as a new tool for expanding the synthetic applicability of aminocatalysis. Primary amines are characterized by a superior ability to effectively functionalize sterically biased carbonyls (*e.g.* simple ketones as well as  $\alpha$ -branched substituted aldehydes and ketones, and their  $\alpha,\beta$ -unsaturated counterparts), because they are less influenced by the structural features of the substrates.<sup>20</sup> In comparison to cyclic secondary amines, however, primary amines present a tautomeric imine-enamine equilibrium almost

<sup>18</sup> J. Franzén, M. Marigo, D. Fielenbach, T. C. Wabnitz, A. Kjærsgaard, and K. A. Jørgensen, A General Organocatalyst for Direct  $\alpha$ -Functionalization of Aldehydes: Stereoselective C–C, C–N, C–F, C–Br, and C–S Bond-Forming Reactions. Scope and Mechanistic Insights, *J. Am. Chem. Soc.*, **2005**, *127*, 18296; b) Y. Hayashi H. Gotoh, T. Hayashi, M. Shoji, Organocatalysis Diphenylprolinol Silyl Ethers as Efficient Organocatalysts for the Asymmetric Michael Reaction of Aldehydes and Nitroalkenes, *Angew. Chem. Int. Ed.* **2005**, *44*, 4212.

<sup>19</sup> D. Seebach, U. Grošelj, D. M. Badine, W. B. Schweizer, A. K. Beck. Isolation and X-Ray Structures of Reactive Intermediates of Organocatalysis with Diphenylprolinol Ethers and with Imidazolidinones A Survey and Comparison with Computed Structures and with 1-Acylimidazolidinones: The 1,5-Repulsion and the Geminal-Diaryl Effect at Work. *Helv. Chim. Acta*, **2008**, *91*, 1999.

<sup>20</sup> P. Melchiorre, Cinchona-based Primary Amine Catalysis in the Asymmetric Functionalization of Carbonyl Compounds, *Angew. Chem. Int. Ed.* **2012**, *51*, 9748.



completely shifted towards the imine<sup>21</sup> along with a reduced nucleophilicity. In addition, the less congested intermediates result in an inferior control of the E/Z selectivity, which is essential to obtain high level of stereoselectivity in aminocatalytic reactions.<sup>22</sup>

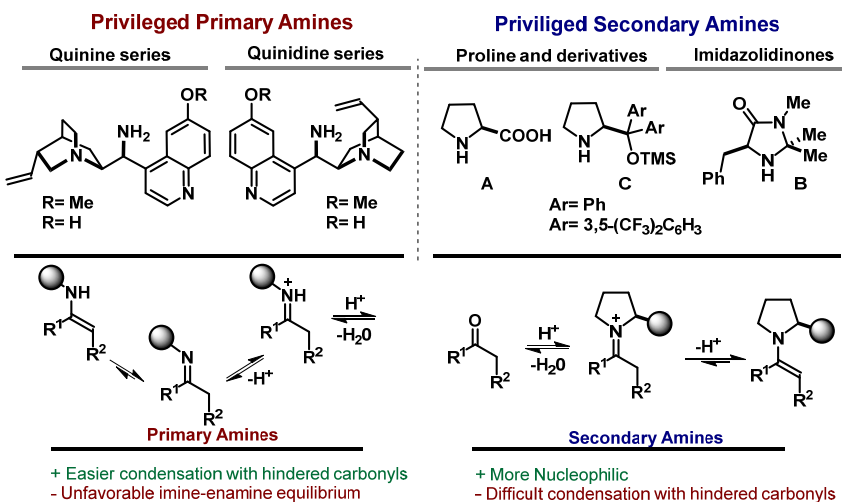


**Figure 5.** Privileged primary and secondary amine catalysts and some of their peculiarities. The grey circle represents the chiral catalyst scaffold.

### Mechanisms of Stereochemical Induction in Aminocatalysis.<sup>23</sup>

The excellent ability of chiral secondary amine catalysts to control the stereoselectivity of the processes was rationalized on the basis of two different mechanistic paths. Aminocatalysts containing an internal acidic group, such as L-proline, use it as a hydrogen bond donor to drive the approximation of the electrophile to one of the prochiral faces of the enamine or dienamine (Figure 6). This approximation requires the incoming electrophile to contain an H-bond acceptor moiety (that is, a lone pair on a heteroatom).

<sup>21</sup> R. A. Clark, D. C. Parker. Imine-Enamine Tautomerism. I. 2-(N-Cyclohexylimino)-1,3-diphenylpropane. *J. Am. Chem. Soc.*, **1971**, *122*, 7257.

<sup>22</sup> B. Capon, Z. P. Wu. Comparison of the Tautomerization and Hydrolysis of Some Secondary and Tertiary Enamines. *J. Org. Chem.* **1990**, *55*, 2317.

<sup>23</sup> A. Erkkilä, I. Majander, P. M. Pihko, Asymmetric Organocatalysis, Enamine Catalysis, *Top. Curr. Chem.* **2010**, *291*, 29.

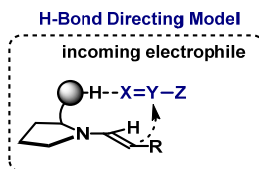


**Figure 6.** Hydrogen bond-assisted stereochemical model.

On the other hand, some aminocatalysts use a bulky group to control the stereoselectivity of the process. This group, acting as a steric control element, is crucial to induce a single geometry of the covalent intermediate while selectively shielding one of the prochiral faces of the enamine or iminium ion intermediate. The latter effects forces the approximation of the reacting partner from the opposite side of the shielding group (*Steric Control Approach*, Figure 7).

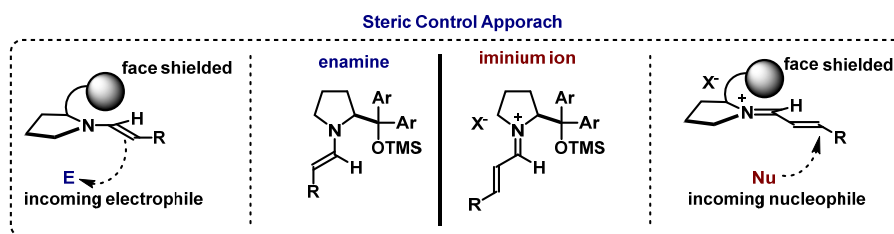


**Figure 7.** Steric control stereochemical model with cyclic secondary amine catalysts. The grey circle represents the chiral catalyst scaffold.

#### 1.1.4. Hydrogen Bond Donor Catalysis

H-Bond donor catalysis is a type of non-covalent catalysis, which utilizes a proton as the smallest Lewis acid. Two types of H-bond catalysis are suitable for the activation of electrophiles. On one side, specific acid catalysis, which activates the substrate (for example a carbonyl group) *via* protonation. On the other side, general acid catalysis, which uses the simultaneous sharing of a hydrogen atom between the catalyst (H-bond donor) and the substrate (H-bond acceptor). This allows for a lowering of the LUMO energy (Figure 8a) and the stabilization of the transition state.<sup>24</sup>

<sup>24</sup> K. Etsenbach-Effers, A. Berkessel, Noncovalent Organocatalysis Based on Hydrogen Bonding: Elucidation of Reaction Paths by Computational Methods. *Top. Curr. Chem.* **2010**, *291*, 1-27.

A large variety of either single or dual H-bond donors has emerged as suitable catalysts for the activation of different electrophiles.<sup>25</sup> Carbonyl compounds and imines, N-acyl iminium ions or nitro compounds, among others, were successfully activated, being ureas and thioureas the most general applicable class of H-bond donors in enantioselective organocatalysis.<sup>26</sup>

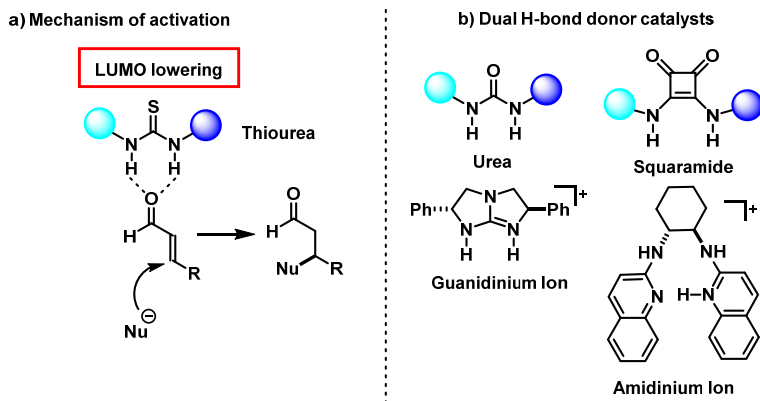


**Figure 8.** a) Activation mechanism of the thiourea-based dual H-bond donor catalysts. b) Representative dual H-bond donors catalysts. Blue circles represent the chiral catalyst scaffold.

## 1.2. Aminocatalytic Cascade Reactions

Aminocatalytic processes are flexible and versatile, and provide the possibility of integrating mechanistically distinct modes of catalysis in a single sequence (cascade reactions). To fully harness the synthetic power of aminocatalysis, it was crucial to identify the iminium ion/enamine activation sequence as an approach toward highly efficient asymmetric cascade transformations. The strategy is based on the conjugate addition of a nucleophile to an  $\alpha,\beta$ -unsaturated aldehyde or ketone followed by the  $\alpha$ -functionalization of the resulting saturated carbonyl (Figure 9). In this well-defined sequence, the chiral amine plays an important role in both steps. This strategy allows chemists to access, in a single pot operation, highly functionalized substrates with high levels of enantiocontrol.<sup>27</sup> It is worth mentioning that, currently, this approach is widely employed in developing new asymmetric organocatalytic domino reactions and it is an important tool for the generation of stereochemically dense scaffolds in a single pot operation from simple substrates.

<sup>25</sup> M. S. Taylor, E. N. Jacobsen. Asymmetric Catalysis by Chiral Hydrogen-Bond Donors. *Angew. Chem. Int. Ed.*, **2006**, *45*, 1520.

<sup>26</sup> A. G. Doyle, E. N. Jacobsen, Small-Molecule H-Bond Donors in Asymmetric Catalysis. *Chem. Rev.* **2007**, *107*, 5713.

<sup>27</sup> D. Enders, C. Grondal, M. R. M. Hüttl, Asymmetric Organocatalytic Domino Reactions, *Angew. Chem. Int. Ed.* **2007**, *46*, 1570.

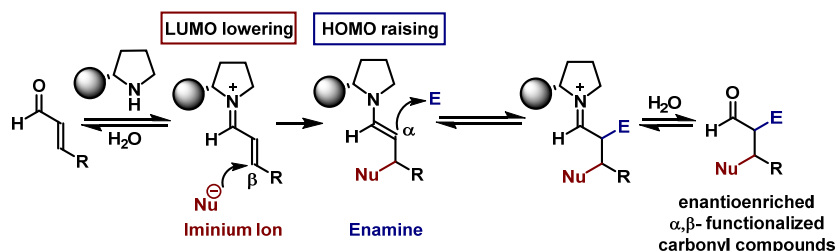


**Figure 9.** Aminocatalytic cascade reactions, Nu= Nucleophile, E= Electrophile. The grey circle represents the chiral catalyst scaffold.

### 1.3. Visible light Photoredox Catalysis and Aminocatalysis.

Visible light photoredox catalysis exploits the ability of metal complexes<sup>28</sup>, dyes<sup>29</sup>, and metal oxides semiconductors<sup>30</sup> to absorb light and, from the generated excited states, to engage in single electron transfer (SET) processes with organic molecules. The combination of this activation mode with aminocatalysis has been introduced by MacMillan in 2008 (Figure 10).<sup>31</sup> Merging photoredox catalysis and enamine catalysis enabled the asymmetric alkylation of aldehydes, which has been a widely sought but elusive transformation at that time. The key to this achievement was the generation of an open shell species reacting in a series of consecutive low barrier steps instead of the high barrier two-electron pathway. This is in contrast to nearly all organocatalytic reactions, where new bonds are formed in a polar pathway. The rapidly growing interest in the combination of organocatalysis and photoredox catalysis is justified by the possibility of accessing open-shell species, which participate in bond constructions that are unavailable using asymmetric organocatalysis alone. Indeed, the unique reactivity of radical intermediates enables unconventional transformations that cannot be achieved using classical “polar” approaches.

<sup>28</sup> C. K. Prier, D. A. Rankic, D. W. C. MacMillan, Visible Light Photoredox Catalysis with Transition Metal Complexes: Applications in Organic Synthesis, *Chem. Rev.* **2013**, *113*, 5322.

<sup>29</sup> S. Fukuzumi, K. Ohkubo, Organic Synthetic Transformations Using Organic Dyes as Photoredox Catalysts, *Org. Biomol. Chem.* **2014**, *12*, 6059.

<sup>30</sup> M. R. Hoffmann, S. T. Martin, W. Choi, D. W. Bahnemann, Environmental Applications of Semiconductor Photocatalysis, *Chem. Rev.* **1995**, *95*, 69.

<sup>31</sup> D. A. Nicewicz, D. W. C. MacMillan, Merging Photoredox Catalysis with Organocatalysis: The Direct Asymmetric Alkylation of Aldehydes, *Science*, **2008**, *322*, 77.

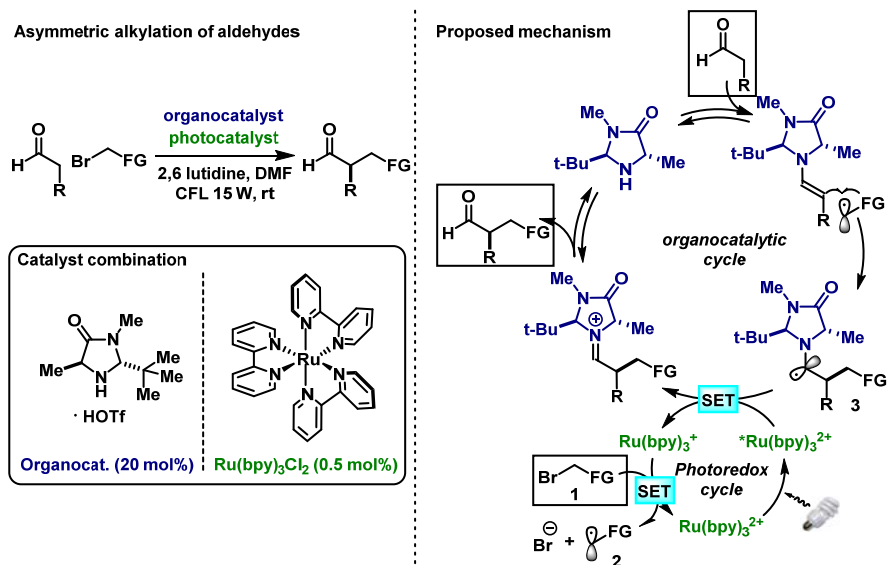


**Figure 10.** Reaction and mechanism of the enantioselective alkylation of aldehydes

The mechanism of this transformation consists on the merging of two catalytic cycles, visible light photoredox catalysis and aminocatalysis (Figure 10). Initially, photoredox active catalyst  $\text{Ru}(\text{bpy})_3^{2+}$  absorbs visible light to reach the excited state  $^*\text{Ru}(\text{bpy})_3^{2+}$ . This excited state has the particular feature to be, at the same time, a good oxidant and a good reductant. In this specific case, it was demonstrated that an initial sacrificial amount of the enamine had to be oxidized to generate the highly reducing  $\text{Ru}(\text{bpy})_3^+$ . This specie could reduce electron-deficient alkyl bromides **1** to generate, after fragmentation of the radical anion (mesolysis), the highly reactive electrophilic alkyl radical **2**. This radical is then selectively trapped by the electron-rich chiral enamine. This addition leads to an  $\alpha$ -amino-radical **3**, which is easily prone to oxidation by  $^*\text{Ru}(\text{bpy})_3^{2+}$ . The SET enables the regeneration of  $\text{Ru}(\text{bpy})_3^+$  and the iminium ion which, after hydrolysis, generates the chiral alkylation product while releasing the aminocatalyst.

## 1.4. Summary of the Thesis Research

The following chapters illustrate how the effective tools of organocatalysis and the different activation modes have been exploited to develop new catalytic enantioselective transformations. Chapter II discusses the development of an enantioselective  $\gamma$ -aldol reaction between 3-methyl 2-cyclohexen-1-one and  $\alpha$ -keto-esters. Key to success was the design of a bifunctional primary amine-thiourea catalyst that can combine H-bond-directing activation and vinylogous reactivity, specifically dienamine catalysis, to secure high levels of enantiocontrol (Figure 11).

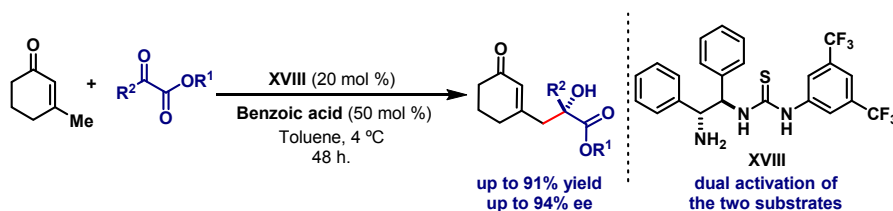


**Figure 11.** Asymmetric vinylogous aldol reaction via H-bond-directed dienamine catalysis

Chapter III describes the successful implementation of a triple cascade reaction catalyzed by a chiral secondary amine to afford the remote  $\delta$ -functionalization of dienals. This strategy overrides the intrinsic problems of site-selectivity and remote stereocontrol, furnishing highly functionalized spiro-oxindolic cyclohexane compounds with six contiguous stereocenters (Figure 12).

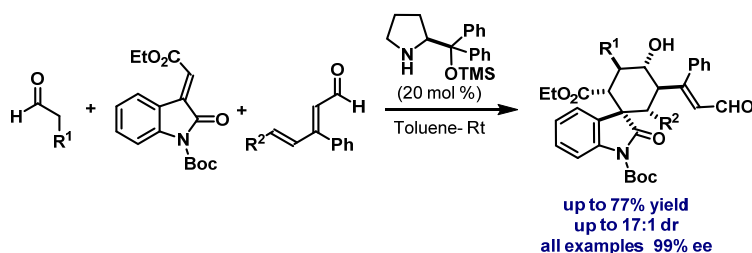


**Figure 12.** Vinylogous organocatalytic triple cascade reaction.

Chapter IV deals with an unprecedented transformation in aminocatalysis, namely the stereoselective interception of carbon-centered radicals by means of transiently generated chiral iminium ions. The chemistry provides stereoselective  $\beta$ -functionalizations of enones which are not achievable using polar pathways. Highly reactive nucleophilic carbon-centered radicals are generated by means of photoredox catalysis to then react with the in-situ generated iminium ion. A newly designed chiral primary amine was needed to ensure a high level of efficiency (Figure 13). The highly enantioselective formation of carbon quaternary stereocenters is achieved starting from  $\beta$ -alkyl substituted cyclohexenones.

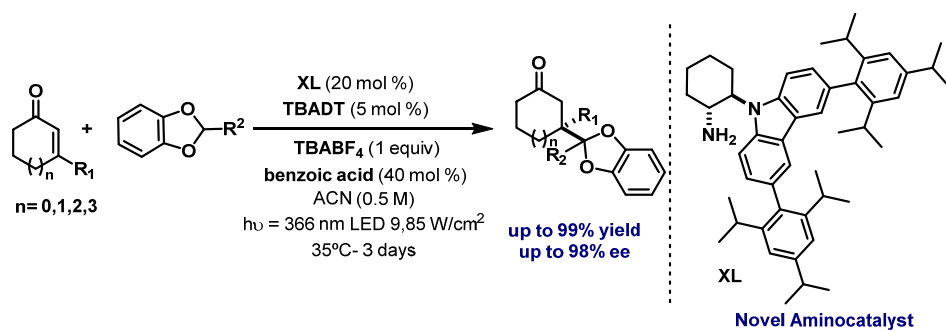


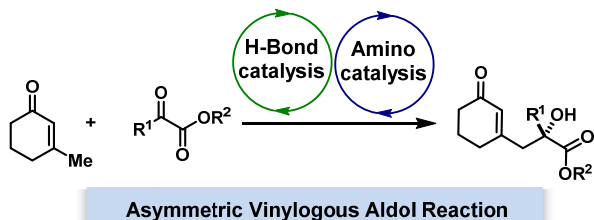
**Figure 13.** Light-driven enantioselective  $\beta$ -alkylation of enones by means of radical iminium ion trapping. TBADT= tetrabutylammonium decatungstate, TBABF<sub>4</sub>= tetrabutylammonium tetrafluoroborate.

## Chapter II

# Asymmetric Vinylogous Aldol Reaction via H-Bond-Directing Dienamine Catalysis

### Target

Developing an asymmetric vinylogous aldol reaction for the direct  $\gamma$ -functionalization of unsaturated carbonyl compounds.



### Tool

A bifunctional primary amine-thiourea catalyst that can combine H-bond-directing activation of the electrophile with the dienamine activation of enones to ensure high levels of enantio- and regio-selectivity.<sup>1</sup>

## 2.1. Background

The principle of vinylogy, originally defined by Fuson<sup>2</sup> as the electronic transmission through the conjugated  $\pi$ -system of poly-unsaturated carbonyl compounds, is at the basis of the dienamine activation mode. Using this strategy, the potential of the HOMO-raising activation approach (enamine catalysis) for the direct asymmetric  $\alpha$ -functionalization of carbonyl compounds could be extended to positions remote from the carbonyl moiety.

The first success in the design of direct vinylogous processes was achieved in 2006 by Jørgensen and co-workers.<sup>3</sup> In particular, they reported the enantioselective  $\gamma$ -amination of  $\alpha,\beta$ -unsaturated aldehydes proceeding via dienamine activation (Figure 1a). The diaryl prolinol trimethylsilyl ether catalyst (**S**-**1**), together with benzoic acid, effectively generated the transient electron-rich dienamine **3** after condensation with enal **1**. It was demonstrated that the reaction proceeds *via* a [4+2] cycloaddition pathway with the *cis* isomer of **3** intercepting the diethyl azodicarboxylate **2**, which acts as the dienophile. This gave origin to the cyclic amination

<sup>1</sup> The work discussed in this chapter has been published, see: D. Bastida, Y. Liu, X. Tian, E. Escudero-Adán, P. Melchiorre, Asymmetric Vinylogous Aldol Reaction via H-Bond-Directing Dienamine Catalysis. *Org. Lett.* **2013**, *15*, 220. Experimental part developed together with Dr. Yankai Liu.

<sup>2</sup> R. C. Fuson, The Principle of Vinylogy. *Chem. Rev.* **1935**, *16*, 1

<sup>3</sup> S. Bertelsen, M. Marigo, S. Brandes, P. Dinér, K. A. Jørgensen, Dienamine Catalysis: Organocatalytic Asymmetric  $\gamma$ -Amination of  $\alpha,\beta$ -Unsaturated Aldehydes. *J. Am. Chem. Soc.* **2006**, *128*, 12973.



intermediate **4** that opened up and hydrolyzed under the reaction conditions, leading to the final product **5** and the free catalyst (S)-**1**. This peculiar mechanism was congruent with the stereochemical outcome of the process. In addition, when 2-pentenal **7** was reacted with *N*-methylmaleimide **6** in the presence of the chiral aminocatalyst **1**, the tricyclic structure **8** was readily isolated (Figure 1b), further supporting a Diels-Alder type pathway. The cycloadduct **8** was incapable of eliminating the aminocatalyst **1**, thus representing a dead-end in a possible catalytic cycle.

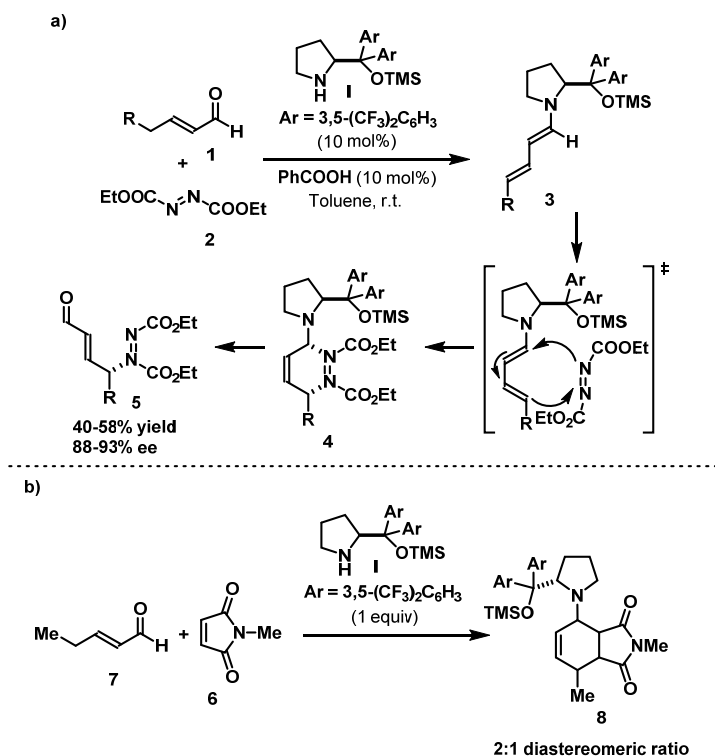


**Figure 1.** a) The first example of dienamine activation: the asymmetric  $\gamma$ -amination of  $\alpha,\beta$ -unsaturated aldehydes.<sup>3</sup> TMS= trimethylsilyl. b) Evidence for a [4+2]-cycloaddition pathway

The investigation from the Jørgensen group highlighted the promising synthetic potential of dienamine activation to provide a general synthetic technology for designing stereoselective vinylogous reactions. From a synthetic perspective, vinylogous processes represent an efficient approach to generating functionalized building blocks with high levels of structural complexity.

In spite of its potential, the approach initially found limited applications. This was probably because the  $\gamma$ -amination of unsaturated aldehydes **1** followed a [4+2] cycloaddition path (Figure 1), instead of a more general nucleophilic addition pathway. Moreover, initial studies suggested

that chiral secondary amines, such as proline and its derivatives, activated  $\gamma$ -enolizable unsaturated aldehydes toward the formation of the dienamine intermediate, but generally promoted  $\alpha$ -site selective alkylation *via* an enamine pathway in the presence of suitable electrophiles (Figure 2).<sup>4</sup>

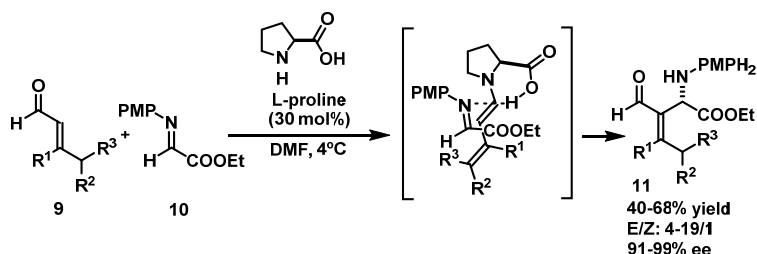


**Figure 2.**  $\alpha$ -Selectivity vs  $\gamma$ -selectivity of a Mannich-type reaction for the preparation of enantiomerically enriched aza-Morita-Baylis-Hillman-Type products. PMP: para-methoxy phenyl.

The chemistry community soon recognized the potential of dienamine activation. However, the peculiar Diels–Alder mechanism of the initial  $\gamma$ -amination chemistry and the difficult control of the site selectivity meant that the strategy found rapid applications in cycloaddition processes exclusively.  $\gamma$ -Site selective transformation based on dienamine activation remained limited to few exceptions due to the many challenges offered by this activation mode (Figure 3).<sup>5,6</sup>

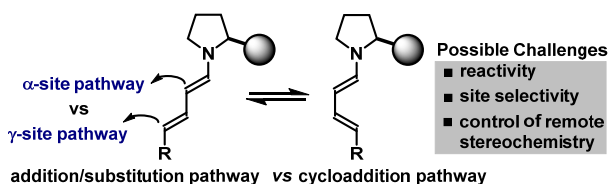


**Figure 3.** Designing vinylogous processes by means of dienamine activation: challenges to be addressed; The grey circle represents the chiral catalyst scaffold.

The first use of dienamine activation in a direct nucleophilic  $\gamma$ -addition was successfully reported by the Christmann group in 2008, as a single isolated example within the framework of a [4+2] type reaction of  $\alpha,\beta$ -unsaturated aldehydes (Figure 4).<sup>7</sup> The transient formation of the

<sup>4</sup> a) N. Utsumi, H. Zhang, F. Tanaka, C. F. Barbas III, A Way to Highly Enantiomerically Enriched aza-Morita-Baylis-Hillman-Type Products. *Angew. Chem. Int. Ed.* **2007**, *46*, 1878; b) J. Stiller, E. Marqués-López, R. P. Herrera, R. Fröhlich, C. Strhmann, M. Christmann, Enantioselective  $\alpha$ - and  $\gamma$ -Alkylation of  $\alpha,\beta$ -Unsaturated Aldehydes Using Dienamine Activation. *Org. Lett.* **2011**, *13*, 70.

<sup>5</sup> I. D. Jurberg I. Chatterjee, R. Tannert, P. Melchiorre, When Asymmetric Aminocatalysis Meets the Vinylogy Principle, *Chem. Comm*, **2013**, *49*, 4869.

<sup>6</sup> H. Jiang, Ł. Albrecht, K. A. Jørgensen, Aminocatalytic Remote Functionalization Strategies. *Chem. Sci.*, **2013**, *4*, 2287.

<sup>7</sup> R. M. de Figueiredo, R. Fröhlich, M. Christmann, Amine-Catalyzed Cyclizations of Tethered  $\alpha,\beta$ -Unsaturated Carbonyl Compounds. *Angew. Chem. Int. Ed.* **2008**, *47*, 1450.

dienamine **13**, formed after the condensation of the dienal **12** and aminocatalyst **II**, initiated a rapid intramolecular Diels-Alder process to obtain **14**, which underwent catalyst elimination in order to form the thermodynamically more stable conjugated bicyclic structure **15** with high stereocontrol (Figure 4a). On the other side, replacing one of the aldehydic functions in **12** with a keto moiety and using **16** as the substrate induced a change in the reaction manifold. Instead of the expected cycloaddition path, a vinylogous Michael addition was observed, leading to product **17** (Figure 4b).

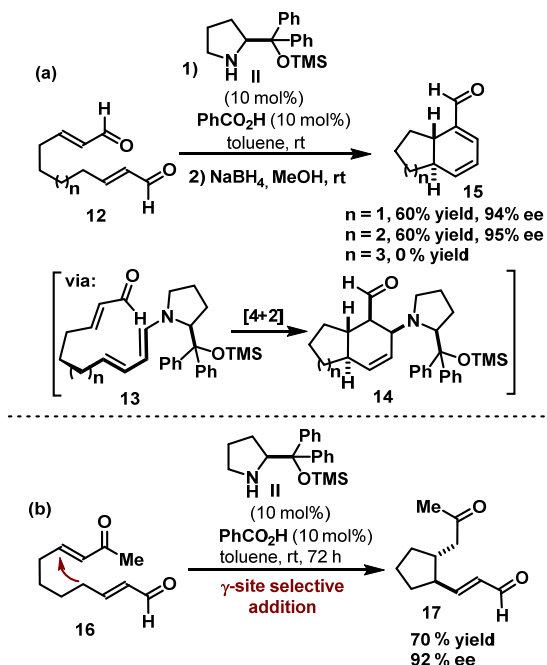


**Figure 4.** (a) The intramolecular Diels-Alder reaction of dienals under dienamine activation. (b) The first example of an intramolecular aminocatalytic vinylogous nucleophilic addition. TMS: trimethylsilyl.

Another example of dienamine activation in the context of vinylogous nucleophilic addition reaction was reported by Woggon and co-workers in 2008 as a key step for the synthesis of  $\alpha$ -Tocopherol (Figure 5).<sup>8</sup> This expedient route began by reacting *ortho*-hydroxy aldehyde **18** with the  $\beta$ -methyl substituted enal **19** to afford the tricyclic product **21**, which after 4 synthetic steps was converted into  $\alpha$ -Tocopherol **22**. This report provided a powerful annulation strategy while also demonstrating the potential of dienamine activation to streamline the total synthesis of natural compounds. In this approach, the direct vinylogous aldol reaction was featured at the

<sup>8</sup> K. Liu, A. Chougnnet, W.-D. Woggon, A Short Route to  $\alpha$ -Tocopherol. *Angew. Chem. Int. Ed.*, **2008**, *47*, 5827.

beginning of a cascade sequence followed by an intramolecular *oxa*-Michael cyclization. This cyclization step provided the driving force of the cascade sequence.

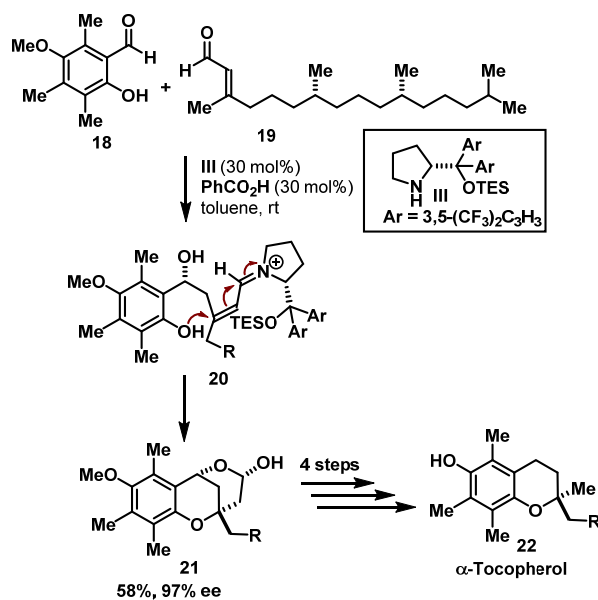


**Figure 5.** Dienamine-driven reaction sequence for the total synthesis of  $\alpha$ -Tocopherol. TES: triethylsilyl.

In 2010, our research group reported the first discrete, intermolecular, vinyllogous addition using the dienamine activation of unmodified  $\alpha,\beta$ -unsaturated carbonyl compounds.<sup>9</sup> It was demonstrated that the aminocatalyst 9-amino cupreine derivative **IV** could promote the direct, vinyllogous Michael addition of  $\beta$ -substituted cyclohexenone derivatives **23** to nitroalkenes **24** proceeding under dienamine activation (Figure 6a). Key to developing the chemistry was the unique potential of the *cinchona*-derived amine **IV** to easily condense with an enone substrate to form the iminium ion intermediate, while then coaxing the preferential formation of the *exo*-cyclic extended dienamine **C** over the *endo* isomer **B** or the cross-conjugated dienamine **A** (Figure 6b).<sup>10</sup> The transmission of the HOMO-raising effect through the transiently generated cyclic dienamine **C** allowed for intermolecular vinyllogous Michael additions to take place with high levels of selectivity. Exploitation of the unique ability of catalyst **IV** (in combination with an

<sup>9</sup> G. Bencivenni, P. Galzerano, A. Mazzanti, G. Bartoli, P. Melchiorre, Direct Asymmetric Vinyllogous Michael Addition of Cyclic Enones to Nitroalkenes Via Dienamine Catalysis. *Proc. Natl. Acad. Sci. U.S.A.* **2010**, *107*, 20642.

<sup>10</sup> The regiocontrolled formation of the extended dienamine **C** finds support in related enolization studies demonstrating that, under certain conditions, the selective formation of the thermodynamic *exo*-cyclic enolate is strongly favoured, see: S. Saito, M. Shiozawa, M. Ito, H. Yamamoto. Conceptually New Directed Aldol Condensation using Aluminum tris(2,6-diphenylphenoxide). *J. Am. Chem. Soc.*, **1998**, *120*, 813.

acidic co-catalyst) to perturb the iminium-dienamine equilibrium, taken together with thermodynamic factors, which govern the regioselective formation of the *exo* cyclic dienamine intermediate **C**, resulted in an exclusive  $\gamma$ -site selective pathway. Importantly, chiral secondary amines, in presence of the same reagent combination, induced the formation of the cross-conjugated dienamine **A**, leading to the product corresponding to the Diels-Alder pathway.<sup>11</sup>

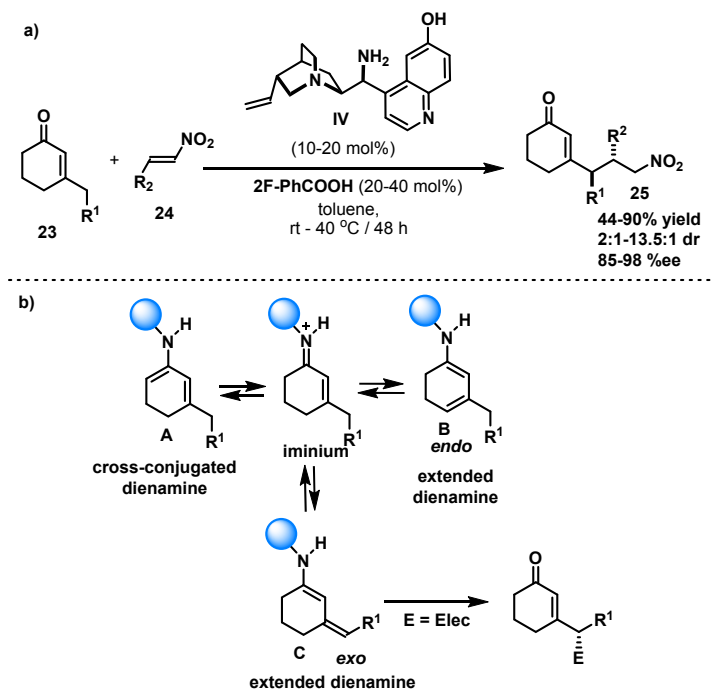


**Figure 6.** a) Dienamine-promoted vinylogous intermolecular Michael additions; b) Possible dienamine intermediates; The blue circle represents the chiral catalyst scaffold.

More recently, an alternative strategy aimed at increasing the scope of remote functionalizations of carbonyl compounds was introduced, demonstrating that the presence of hydrogen-bond (H-bond) directing groups within the chiral aminocatalysts could be beneficial. The idea of using the bifunctional amine-H-bond-directing catalyst was to simultaneously activate both the enal **26** (*via* dienamine formation) and the electrophile, such as nitro olefins **27**, (*via* H-bonding interactions). This ensured the control over the trajectory of the approaching electrophile to the  $\beta$ - $\gamma$  double bond of the dienamine (Figure 7).<sup>12, 13</sup>

<sup>11</sup> D.-Q. Xu, A.-B. Xia, S.-P. Luo, J. Tang, S. Zhang, J.-R. Jiang, Z.-Y. Xu. In Situ Enamine Activation in Aqueous Salt Solutions: Highly Efficient Asymmetric Organocatalytic Diels-Alder Reaction of Cyclohexenones with Nitroolefins. *Angew. Chem. Int. Ed.* **2009**, *48*, 3821.

<sup>12</sup> Ł. Albrecht, G. Dickmeiss, F. C. Acosta, C. Rodríguez-Escrib, R. L. Davis, K. A. Jørgensen, Asymmetric Organocatalytic Formal [2 + 2]-Cycloadditions via Bifunctional H-Bond Directing Dienamine Catalysis. *J. Am. Chem. Soc.* **2012**, *134*, 2543.

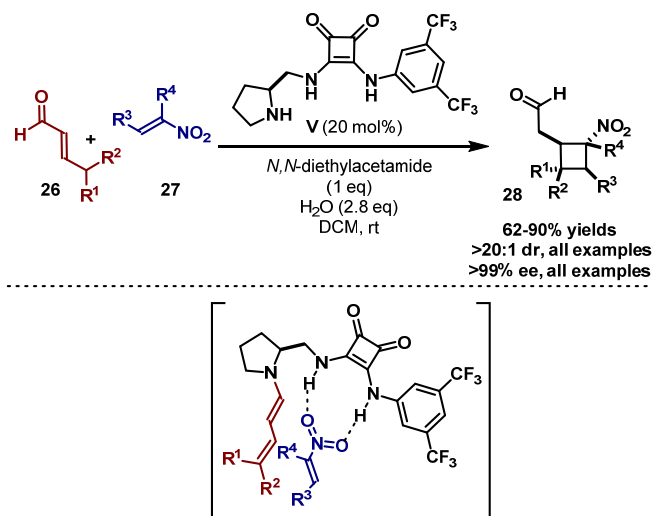


**Figure 7.** The aminocatalytic H-bond-directed dienamine strategy introduced by Jørgensen.

## 2.2. Asymmetric Direct Vinylogous Aldol Reaction

The main objective of this research project was to develop an enantioselective intermolecular vinylogous aldol reaction *via* a dienamine intermediate. We selected the combination of the readily available 3-substituted cyclohexanones **23** and  $\alpha$ -keto esters **29** as a starting point for our investigation (Figure 8). This choice was motivated by our previous report on vinylogous reactivity where cinchona-based primary amine **IV** was found to promote vinylogous nucleophilicity exclusively at  $\gamma$ -*exo* position of the dienamine resulting from substrate **23** (Figure 6a).<sup>9</sup> Successfully realized, this catalytic method would contribute the first example of a direct vinylogous aldol reaction *via* dienamine activation of enolizable enones.

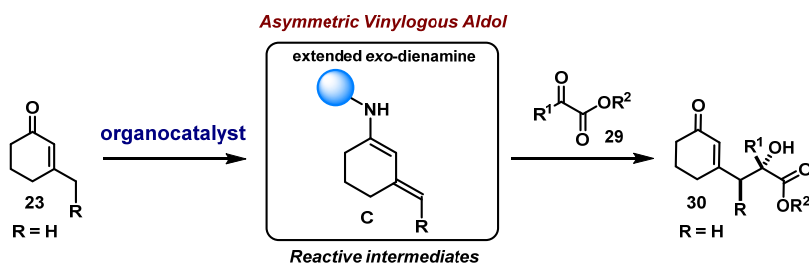


**Figure 8.** The design plan for developing a direct vinylogous aldol reaction using dienamine activation of cyclic enones; The blue circle represents the chiral catalyst scaffold.

<sup>13</sup> Ł. Albrecht, G. Dickmeiss, C. F. Weise, C. Rodriguez-Esrich, K. A. Jørgensen, Dienamine-Mediated Inverse-Electron-Demand Hetero-Diels–Alder Reaction by Using an Enantioselective H-Bond-Directing Strategy. *Angew. Chem. Int. Ed.* **2012**, *51*, 13109.

### 2.2.1. Precedents of Asymmetric Vinylogous Aldol Reaction

The vinylogous aldol reaction provides a powerful way to construct  $\delta$ -hydroxylated  $\alpha,\beta$ -unsaturated carbonyls. Many biologically active compounds, such as polyketides, contain this motif in their structures.<sup>14</sup> Asymmetric vinylogous aldol reactions have found a broad application for construction of polyketides or polyols skeletons in the total synthesis of natural products.<sup>15</sup> The vinylogous aldol chemistry was first developed by Mukaiyama in 1975,<sup>16</sup> who demonstrated that extended silyl enol ethers (namely 1-trimethylsiloxy-1,3-butadiene) reacted with aldehydes at their remote position when using  $\text{TiCl}_4$  as the Lewis acid. Extensive studies on the vinylogous Mukaiyama aldol reaction were based on the use of Lewis acidic metals, such as boron, titanium and copper, to activate the electrophilic carbonyl group.<sup>17</sup> More recently, an organocatalytic stereoselective vinylogous Mukaiyama aldol reaction has been realized. The first example was reported by Rawal and co-workers (Figure 9).<sup>18</sup> In this transformation, TADDOL **VI** ( $\alpha,\alpha,\alpha',\alpha'$ -tetraaryl-1,3-dioxolane-4,5-dimethanol) promotes the enantioselective vinylogous Mukaiyama aldol reaction by acting as a hydrogen bond donor to activate the electrophilic aldehyde **32**.

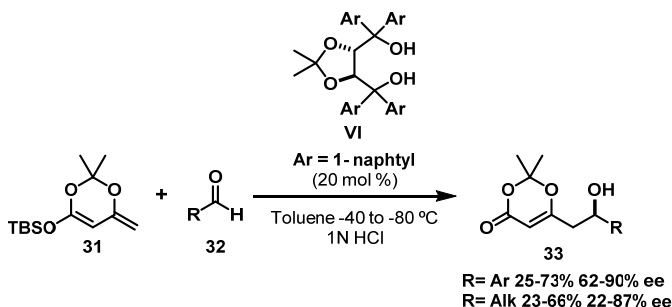


**Figure 9.** The first hydrogen bond-catalyzed asymmetric vinylogous Mukaiyama reaction.

One of the most powerful examples in this context has been published by List and co-workers.<sup>19</sup> Acyclic dienes **34** and aldehydes **32** were used for the organocatalytic vinylogous Mukaiyama aldol reaction in presence of disulfonimide catalyst **VII**. This methodology was extended to include trienes **36** as the nucleophiles, accomplishing the bis-vinylogous Mukaiyama aldol reaction with high selectivity for the  $\epsilon$  position (Figure 10).

<sup>14</sup> J. Krtiger E. M. Carreira, Convergent Synthesis of the Amphotericin Polyol Subunit Employing Asymmetric Dienolate Addition Reactions. *Tetrahedron Lett.* **1998**, *39*, 7013.

<sup>15</sup> S. E. Denmark, S. Fujimori, Total Synthesis of RK-397. *J. Am. Chem. Soc.* **2005**, *127*, 8971.

<sup>16</sup> T. Mukaiyama, A. Ishida, A Convenient Method for the Preparation of  $\delta$ -Alkoxy- $\alpha,\beta$ -Unsaturated Aldehydes by Reaction of Acetals with 1-Trimethylsiloxy-1,3-Butadiene. *Chem. Lett.* **1975**, *4*, 319.

<sup>17</sup> G. Casiraghi, L. Battistini, C. Curti, G. Rassu, F. Zanardi, The Vinylogous Aldol and Related Addition Reactions: Ten Years of Progress, *Chem. Rev.*, **2011**, *111*, 3076.

<sup>18</sup> V. B. Gondi, M. Gravel, V. H. Rawal, Hydrogen Bond Catalyzed Enantioselective Vinylogous Mukaiyama Aldol Reaction. *Org. Lett.*, **2005**, *7*, 5657

<sup>19</sup> L. Ratjen, P. García-García, F. Lay, M. E. Beck, B. List, Disulfonimide-Catalyzed Asymmetric Vinylogous and Bisvinylogous Mukaiyama Aldol Reactions. *Angew. Chem. Int. Ed.* **2011**, *50*, 754.

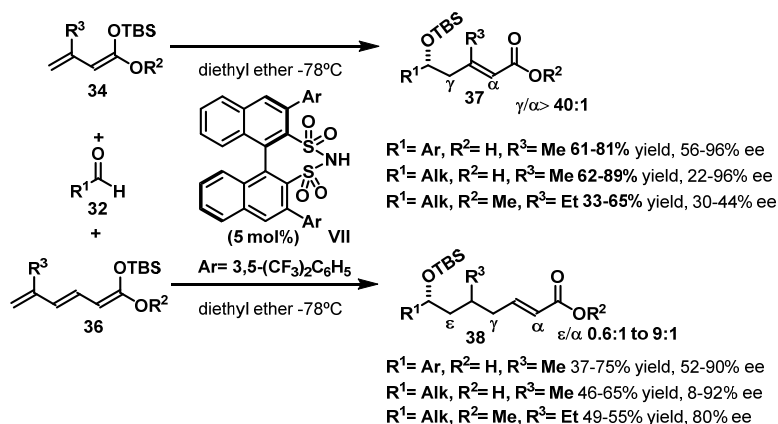


**Figure 10.** The chiral Brønsted acid-catalyzed vinyllogous Mukayama aldol and bis-vinyllogous Mukaiyama aldol reaction.

All the precedent stereoselective strategies, however, relied upon the use of preformed silyl-based nucleophiles.

### 2.2.2. Our Strategy: Results and Discussion

The strategy to design a direct vinyllogous aldol reaction was based on our previous experience, when we used 9-amino cupreine derivative **IV** to activate β-substituted cyclohexenone derivatives **23** toward vinyllogous reactivity (Figure 6a). We selected the combination of the commercially available β-methyl cyclohexenone **23** and α-keto ester **29** as a model for the vinyllogous aldol reaction (Figure 11).

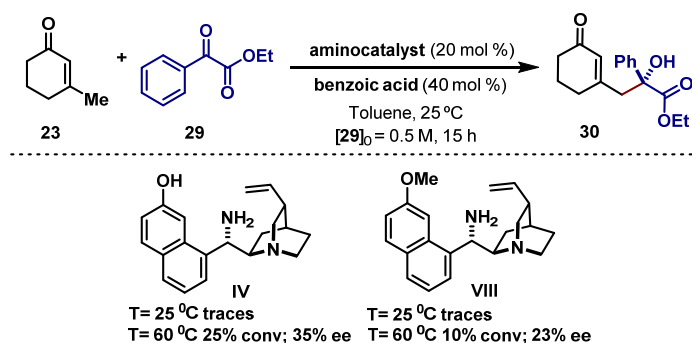


**Figure 11.** Exploratory studies on the enantioselective vinyllogous aldol reaction using 3-methyl cyclohexenone **23** and α-keto esters **29**. <sup>a</sup> Reactions carried out using 2 equivalents of **23** on a 0,05 mmol scale. <sup>b</sup> Conversions determined by <sup>1</sup>H NMR analysis of the crude mixture <sup>c</sup> Enantiomeric excess (ee) values were determined by HPLC analysis on commercially available chiral stationary phases.



We first tested the reaction conditions previously employed to realize the vinylogous Michael transformation,<sup>9</sup> using 20 mol% of the quinine derivative **IV** and benzoic acid as the acid co-catalyst (40 mol%). The acid was needed to aid the iminium ion formation, which is the precursor of the dienamine. Despite extensive efforts, we have not succeeded in translating the cyclic enone/cinchona-based catalyst system to the vinylogous aldol process. Catalysts **IV** and **VIII** led to only trace formation of the desired product **30** at room temperature. Increasing the temperature to 60 °C, low conversions and low ee's were obtained (Figure 10). These results suggested that the dienamine was not nucleophilic enough to attack the  $\alpha$ -keto esters **29**.

The quest for a more stereoselective and reactive system prompted us to consider a different strategy. We wondered if the application of chiral bifunctional H-bond-directing amine catalysts could provide a suitable solution. A bifunctional primary amine-thiourea catalyst, which can combine H-bond-directing activation of the  $\alpha$ -ketoester **29** and dienamine catalysis, might result in the simultaneous dual activation of the two reacting partners while positioning them in a proper three-dimensional molecular assembly.

We began our investigations by preparing and testing a wide variety of bifunctional primary amine H-bond donors, aimed at the dual activation of the two reacting partners. The results are reported in Figure 12.

The Jacobsen-type thiourea **IX** did not provide appreciable results, neither did catalyst **X**, derived from 1,1'-binaphthyl-2,2'-diamine. Interestingly, both cyclohexane diamine and diphenyl ethyl diamine (dphen) scaffolds afforded complete  $\gamma$ -site selectivity. Dphen was recognized as being a superior chiral scaffold comparing the results of catalysts **XI** and **XII**. The presence of an additional stereocontrol element on the thiourea moiety (catalysts **XII** and **XIII**) led to slightly improved enantiomeric excess without changing the sense of the absolute configuration. Further modifications of the thiourea moiety, by introducing more electron withdrawing (EWG) non-chiral substituents, demonstrated the crucial importance of the acidity of the protons on the corresponding thiourea. As more EWG the substituents were, more enantio-discrimination was observed (catalysts **XV** < **XVI** < **XVII** < **XVIII**). Catalyst **XVIII** provided a moderate reactivity along with a high level of enantiocontrol (89% ee). We further confirmed a direct relation between the acidity of the H-bond directing moiety and the level of the enantiocontrol, since replacing the thiourea moiety for the less acidic urea catalyst **XIX** provided a significantly lower stereocontrol (68% ee). With these results in hand, we selected catalyst **XVIII** for further screenings of the reaction parameters.

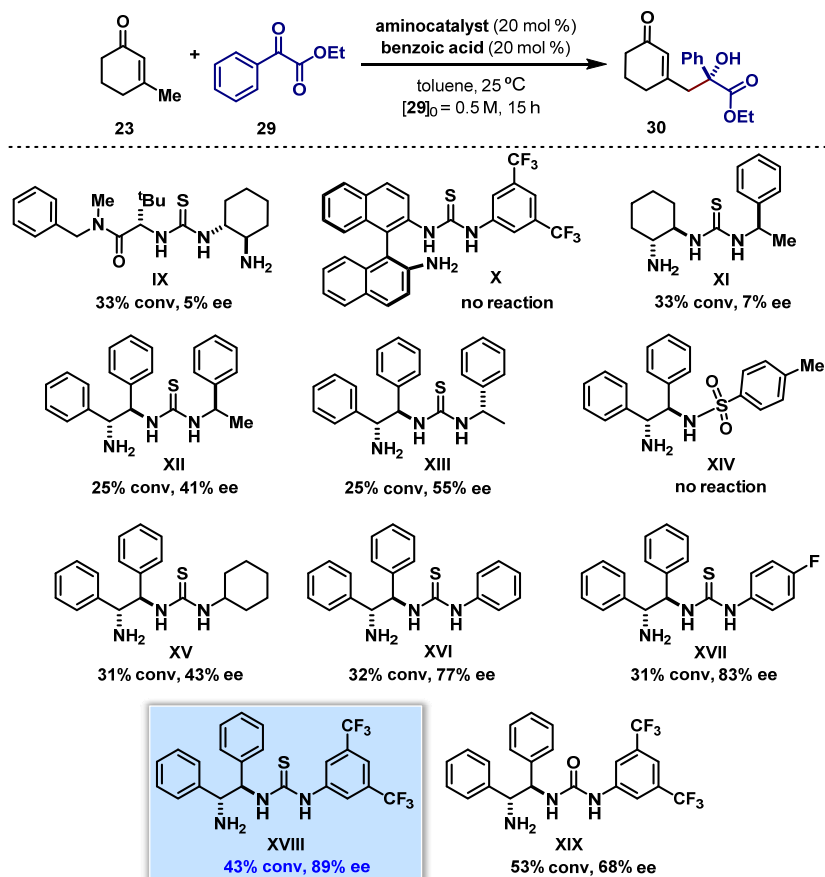
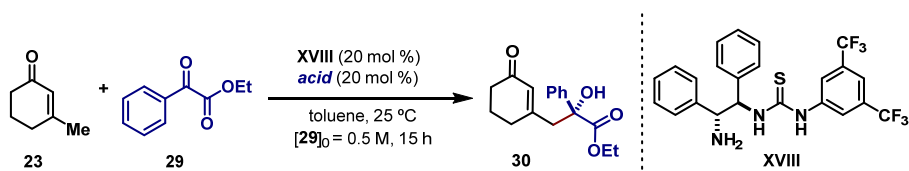


**Figure 12.** Bifunctional catalyst screening for the enantioselective vinylogous aldol reaction of 3-methylcyclohexenone **23** and  $\alpha$ -keto ester **29**. <sup>a</sup> Reactions carried out using 2 equivalents of **23** on a 0,05 mmol scale. <sup>b</sup> Conversions determined by <sup>1</sup>H NMR analysis of the crude mixture <sup>c</sup> Enantiomeric excess (ee) values were determined by HPLC analysis on commercially available chiral stationary phases.

Various acid co-catalysts were tested. As shown in Table 1, the nature of the acidic additive strongly affected the yields and ee's of the reaction. Strong acids, such as TFA or 2,6-CF<sub>3</sub>-benzoic acid, completely inhibited the transformation (entries 2 and 10). The use of less acidic benzoic acid derivatives did not alter the results (entry 3-9). The presence of pivalic acid led to almost identical reactivity. The use of *N*-protected chiral amino acids displayed a moderate matched/mismatched effect (entries 12 and 13) but, in the best case, the results were not better than using benzoic acid (entry 1). The absence of an acid co-catalyst led to a dramatic loss of enantiocontrol in the transformation (entry 15). Benzoic acid was thus selected for further optimization.

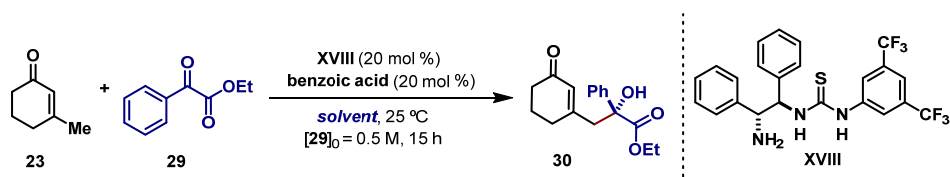
**Table 1.** Acid screening for the vinylogous aldol reaction.<sup>a</sup>



entry	acid	conversion (%) <sup>b</sup>	ee (%) <sup>c</sup>
1	Benzoic acid	43	89
2	TFA	<5	-
3	<i>p</i> -NO <sub>2</sub> -benzoic acid	37	79
4	2,6-OMe-benzoic acid	32	89
5	2,4,6-Me-benzoic acid	43	87
6	2F-benzoic acid	26	90
7	2-OH-benzoic acid	<10	90
8	1-Naphthoic acid	56	82
9	Biphenyl-2-carboxylic	54	83
10	2,6-CF <sub>3</sub> -benzoic acid	0	-
11	Pivalic acid	40	86
12	N-Boc- <i>L</i> -Valine	27	91
13	N-Boc- <i>D</i> -Valine	51	83
14	N-Boc- <i>D</i> -PheAlanine	42	83
15	None	24	44

<sup>a</sup> Reactions carried out using 2 equivalents of **23** on a 0,05 mmol scale. <sup>b</sup> Conversions determined by <sup>1</sup>H NMR analysis of the crude mixture by integration of the signals of the unreacted ketoester **29**. <sup>c</sup> Enantiomeric excess (ee) values were determined by HPLC analysis on commercially available chiral stationary phases. TFA: Trifluoroacetic acid, Boc: *tert*-butyloxycarbonyl.

We then evaluated the effect of the reaction media. The solvent screening is summarized in Table 2. These experiments identified toluene as the best reaction solvent (entry 1), which was selected for additional investigations.

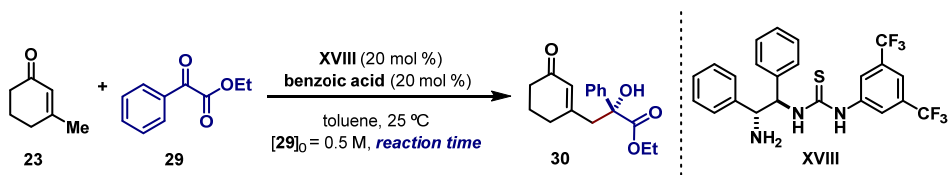
**Table 2.** Solvent screening for the vinylogous aldol reaction.<sup>a</sup>


entry	solvent	conversion (%) <sup>b</sup>	ee (%) <sup>c</sup>
1	Toluene	43	89
2	CHCl <sub>3</sub>	19	89
3	THF	61	69
4	DCM	27	87
5	CH <sub>3</sub> CN	19	79
6	EtOAc	22	87
7	Xilene	45	87
8	MTBE	40	81
9	Hexane	60	85

<sup>a</sup> Reactions carried out using 2 equivalents of **23** on a 0,05 mmol scale, <sup>b</sup> Conversions determined by <sup>1</sup>H NMR of the crude mixture by integration of the signals of the unreacted ketoester **29**. <sup>c</sup> Enantiomeric excess (ee) values were determined by HPLC analysis on commercially available chiral stationary phases. MTBE: methyl *tert*-butyl ether, THF: tetrahydrofuran, DCM: dichloromethane, CHCl<sub>3</sub>: chloroform, CH<sub>3</sub>CN: acetonitrile, EtOAc: ethyl acetate.

Having reached a satisfactory level of stereocontrol, our main focus was on improving the chemical yield of the transformation. Simply prolonging the reaction time to obtain higher conversion proved unsuccessful, since the reaction reached a standstill at approximately 60% conversion (entries 2-4, Table 3). In addition, the enantiomeric purity of the product **30** was observed to be slightly eroded during the course of the reaction. These observations prompted us to consider a possible reversible aldol addition pathway as responsible for the racemization.

**Table 3.** Effect of the reaction time on the optical purity of the vinylogous aldol product.<sup>a</sup>



Entry	Time (hours)	Conversion (%) <sup>b</sup>	ee (%) <sup>c</sup>
1	16	43	89
2	24	58	87
3	36	58	86
4	48	58	83

<sup>a</sup> Reactions carried out using 2 equivalents of **23** on a 0,05 mmol scale. <sup>b</sup> Conversions determined by <sup>1</sup>H NMR analysis of the crude mixture by integration of the signals of the unreacted ketoester **29**. <sup>c</sup> Enantiomeric excess (ee) values were determined by HPLC analysis on commercially available chiral stationary phases.

In order to confirm a possible retro-aldol pathway, the isolated enantioenriched adduct **30** was stirred in the presence of the catalytic salt (**XVIII** + benzoic acid) in toluene at ambient temperature for 24 hours. A similar ratio of the starting enone **23** and the  $\alpha$ -ketoester **29** was detected (Figure 13) compared to the catalytic reaction. This result, taken together with the decreasing of the ee observed over the time, proved that the aldol process at room temperature is reversible.

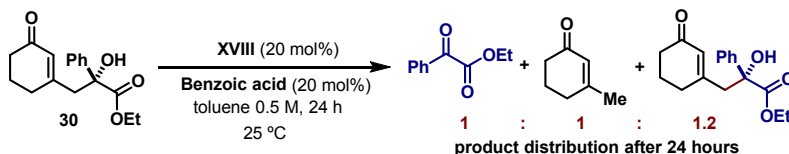
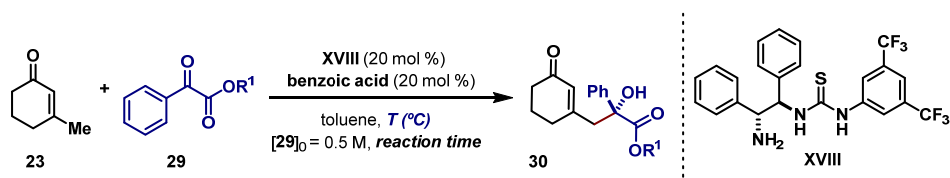


**Figure 13.** Control experiment confirming a retro-aldol pathway.

By further optimizing the reaction parameters, we found that the substituents on the  $\alpha$ -keto-ester moiety and the reaction temperature had a positive impact on the outcome of transformation (Table 4). By decreasing the temperature to 4 °C and using the benzyl ester **29e** (entry 12), the enantioselectivity was preserved over the time while the conversion of the starting material increased.

**Table 4.** Reaction optimization: Temperature and ester substituent effects.<sup>a</sup>

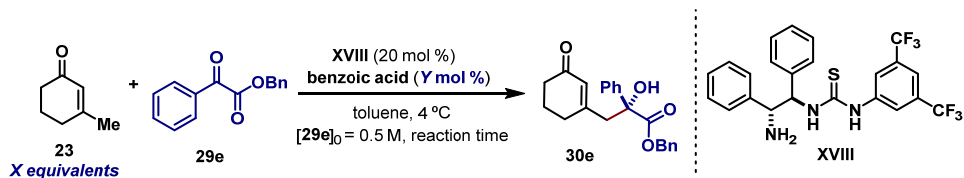


entry	$R^1$	time (hours)	temperature	<b>30</b>	conversion (%) <sup>b</sup>	ee (%) <sup>c</sup>
1	Ethyl	24	RT	<b>30a</b>	58	87
2	<i>tert</i> -Butyl	48	RT	<b>30b</b>	59	70
3	Methyl	24	RT	<b>30c</b>	44	81
4	<i>iso</i> -Propyl	24	RT	<b>30d</b>	38	68
5	Benzyl	24	RT	<b>30e</b>	65	84
6	Ethyl	48	0°C	<b>30a</b>	36	94
7	<i>tert</i> -Butyl	72	0°C	<b>30b</b>	32	94
8	Methyl	48	0°C	<b>30c</b>	28	94
9	<i>iso</i> -Propyl	48	0°C	<b>30d</b>	37	93
10	Benzyl	48	0°C	<b>30e</b>	36	93
11	Ethyl	48	4°C	<b>30a</b>	56	88
12	Benzyl	48	4°C	<b>30e</b>	56	89

<sup>a</sup> Reactions carried out using 2 equivalents of **23** on a 0,05 mmol scale, <sup>b</sup> Conversions determined by <sup>1</sup>H NMR of the crude mixture by integration of the signals of the unreacted ketoester **29**. <sup>c</sup> Enantiomeric excess (ee) values were determined by HPLC analysis on commercially available chiral stationary phases.

With the new reaction conditions (4 °C and  $R^1 = \text{Bn}$ ), we studied the effect of the stoichiometry, varying the equivalents of the ketone and the acid co-catalyst, with the idea to favor the forward aldol process in the equilibrium (Table 5). To our delight, excellent levels of conversion were achieved using 5 equivalents of **23** and 50 mol % of benzoic acid co-catalyst, while maintaining a high enantiocontrol (entry 9). The effect of the concentration was also tested, which clarified that 0.5 M was optimal for both yield and enantiocontrol (results not shown).

**Table 5.** Optimizing the amounts of ketone **23** and benzoic acid.<sup>a</sup>

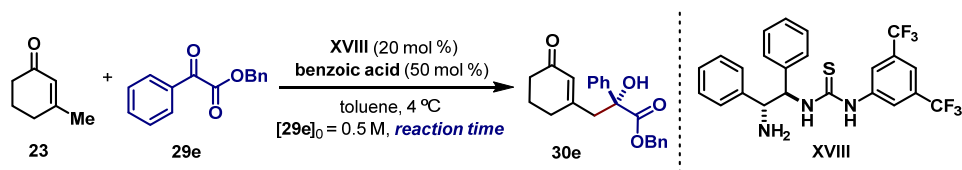


entry	<b>23</b> (X equiv.)	BA (Y mol%)	conversion (%) <sup>b</sup>	ee (%) <sup>c</sup>
1	2	20	56	89
2	2	30	63	89
3	2	40	62	89
4	2	50	53	90
5	3	50	65	90
6	5	20	92	84
7	5	30	84	88
8	5	40	90	89
9	5	50	72 <sup>d</sup>	92

<sup>a</sup> Reactions carried out on a 0,05 mmol scale. <sup>b</sup> Conversions determined by <sup>1</sup>H NMR analysis of the crude mixture by integration of the signals of the unreacted ketoester **29**. <sup>c</sup> Enantiomeric excess (ee) values were determined by HPLC analysis on commercially available chiral stationary phases. <sup>d</sup> Yield of the isolated product **29e**. BA = benzoic acid.

After finding the optimal reaction conditions, the effect of the time was re-examined (Table 6). Gratifyingly, it was observed that the level of stereoinduction remained constant throughout the reaction while the chemical yield increased.

**Table 6.** Effect of the reaction time on the enantiomeric purity of the vinylogous aldol product under the optimized conditions.<sup>a</sup>

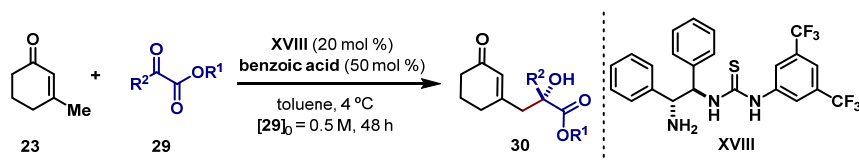


entry	reaction time	conversion (%) <sup>b</sup>	ee (%) <sup>c</sup>
1	5	30	92
2	15	58	92
3	24	69	92
4	30	77	92
5	48	82 (72) <sup>d</sup>	92

<sup>a</sup> Reactions carried out on a 0,05 mmol scale. <sup>b</sup> Conversions determined by <sup>1</sup>H NMR of the crude mixture by integration of the signals of the unreacted ketoester 29. <sup>c</sup> Enantiomeric excess (ee) values were determined by HPLC analysis on commercially available chiral stationary phases. <sup>d</sup> Yield of the isolated product 29e.

With the appropriate conditions in hands, we examined the scope of the asymmetric organocatalytic vinylogous aldol reaction on differently substituted α-keto esters (Table 6). The size of the ester moiety did not alter the stereochemical outcome of the reaction. The corresponding aldol adducts (entry 1-5) were produced with similar enantiomeric purity and chemical yield (ee ranging from 88% to 94%). Different substitution patterns were well-tolerated for α-keto ester derivatives 29, regardless of their position on the phenyl ring (entries 6-12). The presence of an electron-donating group or of a hetero-aromatic moiety partially affected the efficiency of the catalytic system (entries 13 and 14). Aliphatic α-keto esters proved to be competent electrophiles of the vinylogous aldol reaction, providing the corresponding aldol adducts 30q-t with synthetically useful results (entries 16-19).



**Table 7.** Scope of the asymmetric vinylogous aldol reaction.<sup>a</sup>

entry	R <sup>1</sup>	R <sup>2</sup>	30	yield (%) <sup>b</sup>	ee (%) <sup>c</sup>
1	Bn,	C <sub>6</sub> H <sub>5</sub>	<b>30b</b>	72	92
2	Me	C <sub>6</sub> H <sub>5</sub>	<b>30c</b>	68	90
3	<i>i</i> -Pr	C <sub>6</sub> H <sub>5</sub>	<b>30d</b>	65	88
4	<i>t</i> -Bu	C <sub>6</sub> H <sub>5</sub>	<b>30e</b>	65	90
5	Anth	C <sub>6</sub> H <sub>5</sub>	<b>30f</b>	80	94
6	Bn	4-Br-C <sub>6</sub> H <sub>4</sub>	<b>30g</b>	68	88
7	Bn	4-Cl- C <sub>6</sub> H <sub>4</sub>	<b>30h</b>	89	88
8	Bn	4-I- C <sub>6</sub> H <sub>4</sub>	<b>30i</b>	77	90
9	Bn	4-F- C <sub>6</sub> H <sub>4</sub>	<b>30j</b>	73	85
10	Bn	2-F- C <sub>6</sub> H <sub>4</sub>	<b>30k</b>	91	82
11	Bn	2-F,4-Br- C <sub>6</sub> H <sub>3</sub>	<b>30l</b>	87	80
12	Bn	4-Me- C <sub>6</sub> H <sub>4</sub>	<b>30m</b>	65	87
13	Bn	4-MeO- C <sub>6</sub> H <sub>4</sub>	<b>30n</b>	32	87
14	Bn	2-thiophenyl	<b>30o</b>	80	46
15	Anth	4-Cl- C <sub>6</sub> H <sub>4</sub>	<b>30p</b>	89	91
16	Bn	Methyl	<b>30q</b>	65	79
17	Et	Ph(CH <sub>2</sub> ) <sub>2</sub>	<b>30r</b>	87	90
18	Et	<i>c</i> -C <sub>6</sub> H <sub>11</sub>	<b>30s</b>	71	83
19	Bn	(CH <sub>2</sub> ) <sub>2</sub> CO <sub>2</sub> Bn	<b>30t</b>	86	91

<sup>a</sup> Reactions carried out on a 0.1 mmol scale using 5 equiv of **23**. <sup>b</sup> Yield of the products **30** isolated after chromatographic purification. <sup>c</sup> Enantiomeric excess (ee) values were determined by HPLC analysis on commercially available chiral stationary phases. <sup>d</sup> Anth: anthracen-9-ylmethyl. The (*R*) absolute configuration for products **30h** and **30p** has been unambiguously inferred by X-ray crystallographic analysis, see the experimental section for details.

As a limitation of the system, modifications on the scaffold of the enone **23** or the use of aldol acceptors rather than  $\alpha$ -keto esters, resulted in a complete loss of reactivity. Some of the examples of unproductive substrates are depicted below (Figure 14).

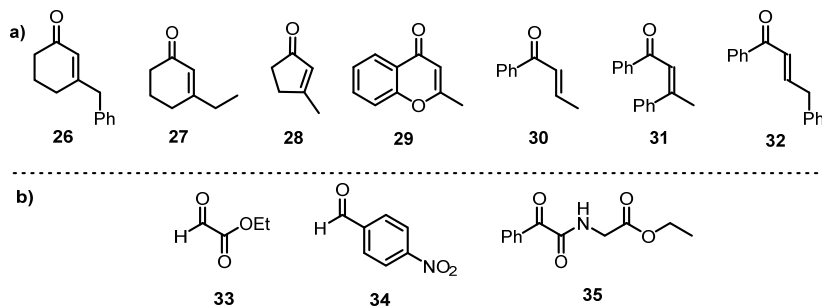


Figure 14. Failed substrates: a) enones; b) electrophiles.

### 2.2.3. Mechanistic Studies

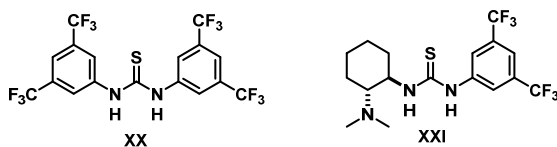
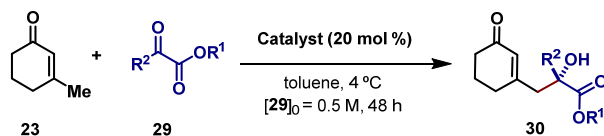
In order to rationalize the stereochemical outcome of the reaction and prove our hypothesis of a bifunctional mode of action, where the primary amine thiourea catalyst **XVIII** combines the H-bond activation of the  $\alpha$ -keto ester and the dienamine activation of the enone, we used two main approaches:

- Control experiments.
- Detection of reactive intermediates.

First, the examination of the role of each functional group of the catalyst was tested (Table 8). A base catalyzed pathway proceeding through an enolate intermediate was excluded, since triethylamine (entry 2) was not able to catalyze the model reaction. We also examined if the H-bond activation from the thiourea fragment was enough for driving the reaction. However, using the Schreiner thiourea **XX** as the catalyst, which is not adorned with the primary amino moiety primed for dienamine activation, the reactivity was completely suppressed (entry 1). This indicated that H-bonding alone could not promote the reaction. Replacing the primary amine in **XVIII** with the corresponding *N,N*-dimethyl tertiary amine (the Takemoto catalyst **D**,<sup>20</sup> entry 4) completely suppressed the reactivity. This is in agreement with a mechanistic scenario requiring the formation of a dienamine reactive intermediate.

<sup>20</sup> O. Tomotaka, Y. Hoashi, Y. Takemoto, Enantioselective Michael Reaction of Malonates to Nitroolefins Catalyzed by Bifunctional Organocatalysts. *J. Am. Chem. Soc.* **2003**, *125*, 12672.

**Table 8.** Control experiments



Entry	Catalyst	Conversion (%) <sup>b</sup>	ee(%) <sup>c</sup>
1	<b>XX</b>	<5%	-
2	<b>NEt<sub>3</sub></b>	<5%	-
3	<b>XXI</b>	<5%	-

<sup>a</sup> Reactions carried out on a 0.1 mmol scale using 5 equiv of **23**. <sup>b</sup> Conversions determined by <sup>1</sup>H NMR analysis of the crude mixture. <sup>c</sup> Enantiomeric excess (ee) values were determined by HPLC analysis on commercially available chiral stationary phases.

We next focused on the conformational analysis of the covalent intermediate actively involved in the stereo-defining step. We investigated spectroscopically the intermediate generated by direct condensation of 3-methyl 2-cyclohexen-1-one **23** with the catalyst **XVIII**. While the dienamine intermediate could not be detected, a mixture of *E* and *Z* imine were readily formed (Figure 15).

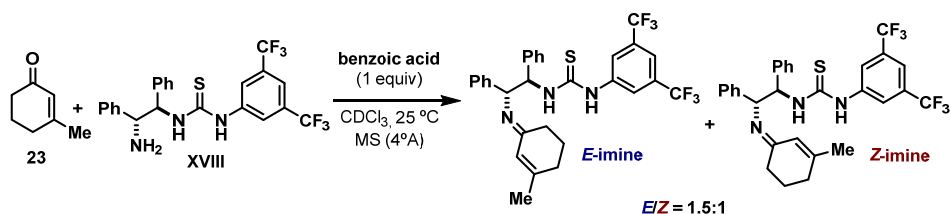


**Figure 15.** The imines distribution arising from the condensation of 3-methyl 2-cyclohexen-1-one **23** and the catalyst **XVIII**.

We used NMR spectroscopy to establish the presence of a H-bonding interaction between the thiourea moiety within the catalyst **XVIII** and the electrophilic  $\alpha$ -ketoester. We characterized the catalytic system made by combining the amine **XVIII** with 1 equiv of benzoic acid. This was done to mimic the reaction conditions, since the presence of the benzoic acid was needed to achieve stereoselectivity. The NMR spectroscopic studies of a catalyst **XVIII**/benzoic acid 1:1 mixture (Figure 16) revealed the formation of new molecular assembly, presumably as a result of the primary amine protonation (for complete characterization see experimental section). We note that a cooperative association of thiourea and a benzoic acid derivative has been reported.<sup>21</sup>

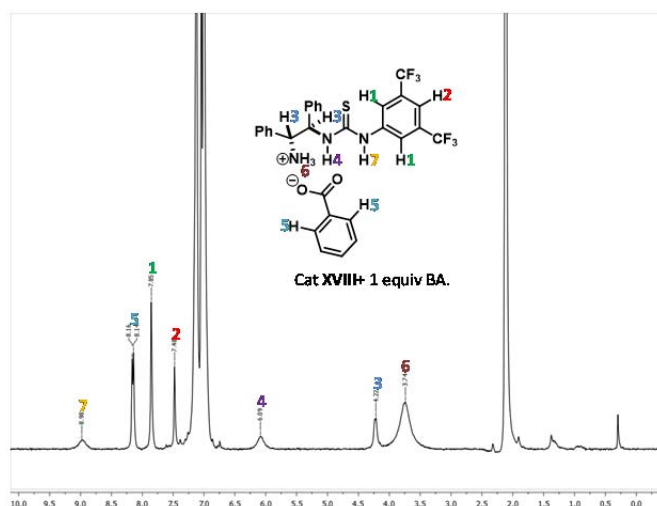


**Figure 16.** The  $^1\text{H}$  NMR spectrum of the amine **XVIII**-benzoic acid (1:1) complex in toluene  $d_8$ .

In order to demonstrate the activation of the electrophile by the thiourea moiety,  $^1\text{H}$  NMR titration studies of the catalytic system were conducted in toluene- $d_8$  with an increasing amount of the methyl  $\alpha$ -ketoester **29a** (Figure 17). The low-field shifts of the NH thiourea protons clearly indicated the H-bonding complexation with the  $\alpha$ -keto ester. In agreement with previous works,<sup>22</sup> our NMR studies revealed how the *ortho* proton of the 3,5-bis (trifluoro methyl)phenyl catalyst moiety, acting as an H-bond donor, also participated in the catalyst-substrate interaction.

<sup>21</sup> Z. Zhang, K. M. Lippert, H. Hausmann, M. Kotke, P.R. Schreiner, Cooperative Thiourea-Brønsted Acid Organocatalysis: Enantioselective Cyanosilylation of Aldehydes with TMSCN. *J. Org. Chem.* **2011**, *76*, 9764.

<sup>20</sup> A. Crespo-Peña, D. Monge, E. Martín-Zamora, E. Álvarez, R. Fernández, J. M Lassaletta. Asymmetric Formal Carbonyl-Ene Reactions of Formaldehyde *tert*-Butyl Hydrazone with  $\alpha$ -Keto Esters: Dual Activation by Bis-urea Catalysts. *J. Am. Chem. Soc.* **2012**, *134*, 12912.

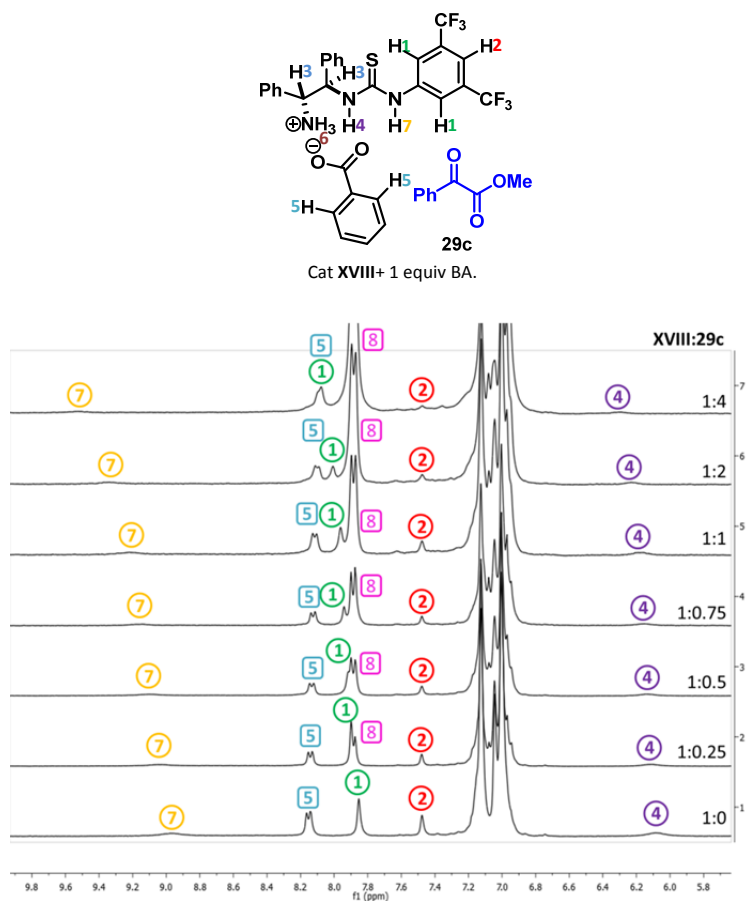


**Figure 17.**  $^1\text{H}$  NMR spectra of the 1:1 complex XVIII-BA (1:1 at 0.02 mmol in toluene  $d_8$ ) upon the addition of increasing amounts of  $\alpha$ -ketoester **29c** (ratio between the catalytic complex and **29c** specified in the y axis). BA = benzoic acid.

Further support for the proposed dual mode of activation was collected from mass spectrometry investigations.<sup>23</sup> As detailed in Figure 18, the ESI-MS spectrum in positive mode of the reaction mixture showed the presence of the imine precursor **D** at  $m/z$  576.1, and of the complex **E**  $m/z$  740.2, where both the reacting partners are brought together in close proximity.

<sup>23</sup> X. Jiang, L. Wang, M. Kai, L. Zhu, X. Yao, R. Wang, Asymmetric Inverse-Electron-Demand Hetero-Diels-Alder Reaction for the Construction of Bicyclic Skeletons with Multiple Stereocenters by Using a Bifunctional Organocatalytic Strategy: An Efficient Approach to Chiral Macrolides. *Chem. Eur. J.* **2012**, *18*, 11465.

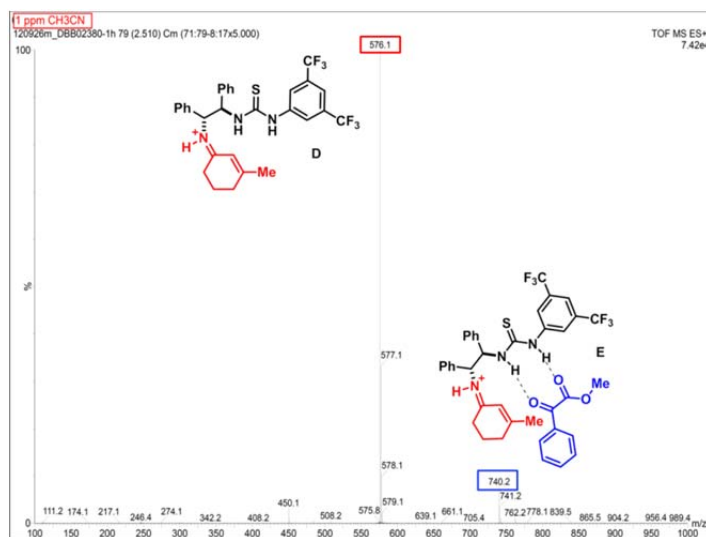


**Figure 18.** Detectable intermediates by ESI-MS analysis in positive mode of the catalytic vinyllogous aldol reaction of **23** and **29c**. The analyzed sample was collected 1 hour after the start of the reaction.

The analyzed sample was collected 5 minutes after the start of the reaction. A concomitant  $^1\text{H}$  NMR analysis did not show any detectable trace of the aldol product **30**, which would provide the same isotopic pattern of intermediate **E**. This fact confirmed the ability of catalyst **XVIII** to activate both the nucleophile and the electrophile. Interestingly, the dimer of the intermediate **D** has also been detected at  $m/z$  1151.4, as a result of a self-association of the thiourea moiety.<sup>24</sup>

On the basis of these observations, we propose a bifunctional mode of activation where the primary amine-thiourea catalyst **XVIII** combines the H-bond activation of the  $\alpha$ -keto ester and the dienamine activation of the enone. Figure 19 depicts a plausible catalytic machinery, which accounts for the observed stereochemical outcome. The relative spatial arrangement of the two reacting partners, as orchestrated by the bifunctional catalyst, determines the selective attack to the *Si*-face of the  $\alpha$ -keto ester.

<sup>24</sup> The self-aggregation is not an uncommon phenomenon for bifunctional thiourea-based catalysts, see for examples: a) H. B. Jang, H. S. Rho, J. S. Oh, E. H. Nam, S. E. Park, H. Y. Bae, C. E. Song, DOSY NMR for Monitoring Self-aggregation of Bifunctional Organocatalysts: Increasing Enantioselectivity with Decreasing Catalyst Concentration. *Org. Biomol. Chem.* **2010**, *8*, 3918; b) G. Tárkányi, P. Király, S. Varga, B. Vakulya and T. Soós, Edge-to-Face CH/ $\pi$  Aromatic Interaction and Molecular Self-Recognition in *epi*-Cinchona-Based Bifunctional Thiourea Organocatalysis. *Chem. Eur. J.* **2008**, *14*, 6078.

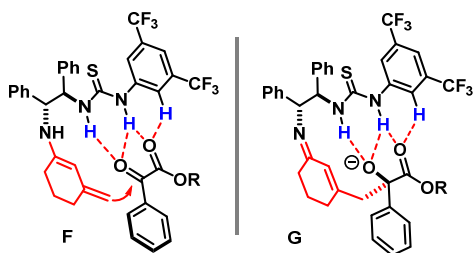


**Figure 19.** Possible ground-state association **F** and stabilization of the generating alkoxy anion **G**.

#### 2.2.4. Conclusions

We have developed a direct enantioselective catalytic vinylogous aldol reaction of an unmodified carbonyl compound. Key to the development of the chemistry was the design of a bifunctional primary amine-thiourea catalyst that can combine H-bond-directing activation and dienamine catalysis.

### 2.3. Experimental Section

#### 2.3.1. General Information

The NMR spectra were recorded at 400 MHz and 500 MHz for  $^1\text{H}$  or at 100 MHz and 125 MHz for  $^{13}\text{C}$ , respectively. The chemical shifts ( $\delta$ ) for  $^1\text{H}$  and  $^{13}\text{C}$  are given in ppm relative to residual signals of the solvents ( $\text{CHCl}_3$  @ 7.26 ppm  $^1\text{H}$  NMR, 77.16 ppm  $^{13}\text{C}$  NMR). Coupling constants are given in Hz. Carbon types were determined from DEPT  $^{13}\text{C}$  NMR experiments. When necessary,  $^1\text{H}$  and  $^{13}\text{C}$  signals were assigned by means of g-COSY, g-HSQC and g-HMBC 2D-NMR sequences. The following abbreviations are used to indicate the multiplicity: s, singlet; d, doublet; t, triplet; q, quartet; m, multiplet; bs, broad signal.

Mass spectra (high and low resolution) were obtained from the ICIQ High Resolution Mass Spectrometry Unit on a Bruker Maxis Impact (QTOF) or Waters Micromass LCT -Premier (TOF) in Electrospray Ionization (ESI) by direct infusion. X-ray data were obtained from the ICIQ X-Ray Unit using a Bruker-Nonius diffractometer equipped with an APPEX 2 4K CCD area detector. Optical rotations were measured on a Polarimeter Jasco P-1030 and are reported as follows:  $[\alpha]_D^{25}$  (c in g per 100 mL, solvent).

**The  $^1\text{H}$ ,  $^{13}\text{C}$  NMR spectra and the HPLC traces are available in the literature<sup>1</sup> and are not reported in the present thesis.**

**General Procedures.** All the reactions were set up under air and using freshly distilled solvents, without any precautions to exclude moisture, unless otherwise noted - *open air chemistry on the benchtop*. Chromatographic purification of products was accomplished using force-flow chromatography (FC) on silica gel (60-200 mesh). For thin layer chromatography (TLC) analysis throughout this work, Merck precoated TLC plates (silica gel 60 GF<sub>254</sub>, 0.25 mm) were used, using UV light as the visualizing agent and an acidic mixture of ceric ammonium molybdate

or basic aqueous potassium permanganate (KMnO<sub>4</sub>) as stain developing solutions. Organic solutions were concentrated under reduced pressure on a Büchi rotary evaporator.

**Determination of Enantiomeric Purity.** HPLC analyses on chiral stationary phase were performed on an Agilent 1200-series instrumentation. Daicel Chiralpak IA, IB or IC columns with *i*-PrOH/DCM/hexane as the eluent were used. HPLC traces were compared to racemic samples prepared using the racemic catalyst **XVIII** (20 mol%) in a 1:1 combination with benzoic acid. The reactions proceeded smoothly in toluene leading to racemic adducts **30**.

**Determination of Yield and Conversion in the Optimization Studies.** The conversion of the starting materials and the yield of products in the optimization studies related to the model reaction were determined by <sup>1</sup>H NMR spectroscopy using an internal standard in the crude reaction: 1,3,5-trimethoxybenzene: δ 6.10 ppm (s, 3H). Since in all instances the conversion of ketoester **23** was equal to the conversion of product, in some cases the conversion was determined by integration of the signals of the unreacted ketoester **29** in the <sup>1</sup>H NMR spectra. All yields refer to the yield of the isolated adducts **30**.

**Preparation of the starting materials.** Commercial grade reagents and solvents were purchased from Sigma Aldrich, Fluka, and Alfa Aesar and used as received. The bifunctional primary amine-thiourea catalyst (1*R*,2*R*)-**XVIII** was prepared from commercially available (1*R*,2*R*)-(+)-1,2-diphenyl-1,2-ethanediamine, according to literature precedents.<sup>25</sup> α-Keto esters **29c** and **29r** are commercially available, while **29a**, **29b**, **29d**, **29e**, **29f**, **29o**, **29q** **29t** were easily prepared from the commercially available ketoacid precursor.<sup>26</sup> α-Ketoesters (**29g**, **29h**, **29p**)<sup>27</sup> **29i**<sup>28</sup> were prepared from their ketoacid precursor, according to literature procedures. The preparations of ketoesters **29s**, **29m**, **29n**,<sup>29</sup> and **29j**, **29k**, **29l**<sup>30</sup> were reported in the literature. Enone **23** is commercially available.

<sup>25</sup> F. Yu, Z. Jin, H. Huang, T. Ye, X. Liang, J. Ye, A Highly Efficient Asymmetric Michael Addition of α,α-Disubstituted Aldehydes to Maleimides Catalyzed by Primary Amine Thiourea Salt. *Org. Biomol. Chem.*, **2010**, *8*, 4767.

<sup>26</sup> For the esterification procedure, see: N. Martin, X. Cheng, B. List, Organocatalytic Asymmetric Transferhydrogenation of β-Nitroacrylates: Accessing β<sup>2</sup>-Amino Acids. *J. Am. Chem. Soc.* **2008**, *130*, 13862.

<sup>27</sup> Z. Jin, L. Yang, S-J Liu, J. Wang, S. Li, H-Q Lin, D. C. Cheong Wan, C. Hu, Synthesis and Biological Evaluation of 3,6-diaryl-7H-thiazolo[3,2-b] [1,2,4]triazin-7-one Derivatives as Acetylcholinesterase Inhibitors. *Arch. Pharm. Res.* **2010**, *33*, 1641.

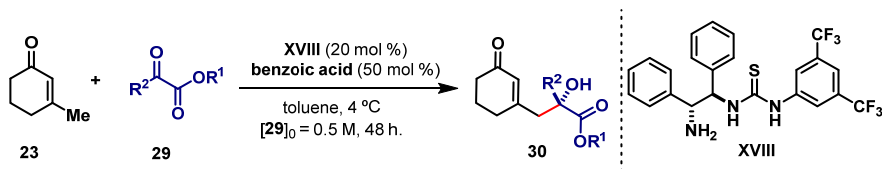
<sup>28</sup> J. Zhuang, C. Wang, F. Xie, W. Zhang, One-pot Efficient Synthesis of Aryl α-keto Esters From Aryl-ketones. *Tetrahedron*, **2009**, *65*, 9797.

<sup>29</sup> M. Hayashi, S. Nakamura, Catalytic Enantioselective Protonation of α-Oxygenated Ester Enolates Prepared through Phospha-Brook Rearrangement. *Angew. Chem. Int. Ed.* **2011**, *50*, 2249.

<sup>30</sup> A. Thorarensen, C. J Ruble, J. F. Fisher, D. L. Romero, T. J. Beauchamp, J. M. Northuis, Antibacterial Benzoic Acid Derivatives. WO 2004018428 A1.

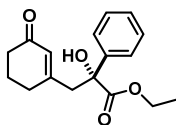


### 2.3.2. General Procedure for the Vinylogous Aldol Reaction.

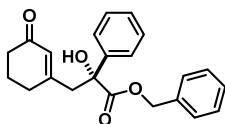


All the reactions were carried out in toluene (synthesis grade, >99%), without any precaution to exclude air and moisture (open air chemistry on the benchtop). An ordinary vial equipped with a Teflon-coated stir bar and a plastic screw cap was charged with 1-(1*R*,2*R*)-2-amino-1,2-diphenylethyl)-3-(3,5-bis(trifluoromethyl) phenyl)thiourea **XVIII** (0.02 mmol, 9.6 mg, 20 mol%). Then, benzoic acid (BA, 0.05 mmol, 6 mg, 50 mol%) and toluene (0.2 mL) were added and the resulting solution was stirred at ambient temperature for 10 minutes to allow the catalyst salt formation. The reaction was started by the sequential addition of the 3-methylcyclohex-2-enone **23** (0.5 mmol, 55 mg, 5 eq) and the ketoester derivative **29** (0.1 mmol). The vial was sealed and immersed in an acetone bath (thermostated at 4°C). After 48 hours stirring, the crude mixture was diluted with Et<sub>2</sub>O and the reaction quenched with NaHCO<sub>3(aq)</sub> saturated. The organic phase was dried over Na<sub>2</sub>SO<sub>4</sub>, and filtered. Solvent was removed under reduced pressure and the aldol product **30** isolated by flash column chromatography.

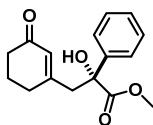
#### (*R*)-ethyl 2-hydroxy-3-(3-oxocyclohex-1-en-1-yl)-2-phenylpropanoate, (**30a**)



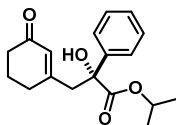
The reaction was carried out following the general procedure. The crude product was purified by flash column chromatography (4:1 hexane:EtOAc) to afford the title compound (20.1 mg, 70% yield, 90% ee) as a colorless oil. The enantiomeric excess was determined by HPLC analysis on a Daicel Chiralpak IC column, (70:20:10 hexane:<sup>i</sup>PrOH:DCM), flow rate 0.8 mL/min, λ = 254 nm: τ<sub>major</sub> = 16.8 min, τ<sub>minor</sub> = 16.0 min; HRMS *calcd* for (C<sub>17</sub>H<sub>20</sub>O<sub>4</sub>+Na): 311.1254, found 311.1254, [α]<sub>D</sub><sup>25</sup> = -5.2 (c = 0.43, CHCl<sub>3</sub>). <sup>1</sup>H NMR (400 MHz, CDCl<sub>3</sub>): 7.66-7.58 (m, 2H), 7.43-7.28 (m, 3H), 5.91 (s, 1H), 4.28 (qd, J = 7.1, 3.7 Hz, 2H), 3.87 (s, 1H), 3.15 (d, J = 13.8 Hz, 1H), 2.92 (d, J = 13.8 Hz, 1H), 2.50-2.23 (m, 4H), 2.02-1.85 (m, 2H), 1.32 (t, J = 7.1 Hz, 3H). <sup>13</sup>C NMR (100 MHz, CDCl<sub>3</sub>): 199.6, 174.2, 160.9, 141.2, 129.4, 128.4, 128.1, 125.3, 78.2, 63.0, 47.4, 37.2, 31.3, 22.8, 14.1.

**(R)-benzyl 2-hydroxy-3-(3-oxocyclohex-1-en-1-yl)-2-phenylpropanoate, (30b)**

The reaction was carried out following the general procedure to furnish the crude product, which was purified by flash column chromatography (4:1 hexane: EtOAc) to afford the title compound (25 mg, 72% yield, 89% ee) as a colorless oil. The enantiomeric excess was determined by HPLC analysis on a Daicel Chiralpak IA column, (80:20 hexane: <sup>1</sup>PrOH) flow rate 0.8 mL/min,  $\lambda = 254$  nm:  $\tau_{\text{major}} = 21.09$  min,  $\tau_{\text{minor}} = 22.07$  min; HRMS calcd for (C<sub>22</sub>H<sub>22</sub>O<sub>4</sub>+Na): 373.1410, found 373.1415 [ $\alpha$ ]<sub>D</sub><sup>rt</sup> = +4.5 (c = 0.38, CHCl<sub>3</sub>). <sup>1</sup>H NMR (400 MHz, CDCl<sub>3</sub>):  $\delta$  7.58-7.56 (m, 2H), 7.36-7.26 (m, 8H), 5.86 (s, 1H), 5.20 (s, 2H), 3.81 (s, 1H), 3.11 (d, J = 13.9 Hz, 1H), 2.91 (d, J = 13.9 Hz, 1H), 2.28-2.24 (m, 4H), 1.88-1.82 (m, 2H) ppm. <sup>13</sup>C NMR (100 MHz, CDCl<sub>3</sub>):  $\delta$  199.6, 174.0, 160.6, 140.9, 134.4, 129.4, 128.7, 128.7, 128.5, 128.4, 128.2, 125.3, 78.2, 68.6, 47.2, 37.2, 31.1, 22.7.

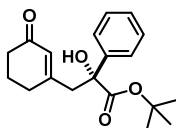
**(R)-methyl 2-hydroxy-3-(3-oxocyclohex-1-en-1-yl)-2-phenylpropanoate, (30c)**

The reaction was carried out following the general procedure to furnish the crude product, which was purified by flash column chromatography (4:1 hexane: EtOAc) to afford the title compound (19 mg, 68% yield, 90% ee) as a colorless oil. The enantiomeric excess was determined by HPLC analysis on a Daicel Chiralpak IA column, (90:10 hexane: <sup>1</sup>PrOH) flow rate 0.8 mL/min,  $\lambda = 254$  nm:  $\tau_{\text{major}} = 22.68$  min,  $\tau_{\text{minor}} = 29.51$  min; HRMS calcd for (C<sub>16</sub>H<sub>18</sub>O<sub>4</sub>+Na): 297.1097, found 297.1100 [ $\alpha$ ]<sub>D</sub><sup>rt</sup> = +3.3 (c = 0.29, CHCl<sub>3</sub>). <sup>1</sup>H NMR (400 MHz, CDCl<sub>3</sub>): 7.67-7.54 (m, 2H), 7.42-7.30 (m, 3H), 5.89 (s, 1H), 3.83 (s, 3H), 3.16 (d, J = 14.2 Hz, 1H), 2.93 (d, J = 14.2 Hz, 1H), 2.56-2.19 (m, 4H), 2.12-1.77 (m, 2H). <sup>13</sup>C NMR (100 MHz, CDCl<sub>3</sub>): 199.9, 174.8, 161.1, 141.1, 129.5, 128.6, 128.3, 125.4, 78.6, 53.7, 47.5, 37.4, 31.4, 22.9.

**(R)-isopropyl 2-hydroxy-3-(3-oxocyclohex-1-en-1-yl)-2-phenylpropanoate, (30d)**

The reaction was carried out following the general procedure to furnish the crude product, which was purified by flash column chromatography (4:1 hexane: EtOAc) to afford the title compound (19.6 mg, 65% yield, 88% ee) as a colorless oil. The enantiomeric excess was determined by HPLC analysis on a Daicel Chiralpak IA column, (90:10 hexane: <sup>1</sup>PrOH) flow rate 0.8 mL/min,  $\lambda = 254$  nm:  $\tau_{\text{major}} = 14.49$  min,  $\tau_{\text{minor}} = 17.87$  min; HRMS calcd for (C<sub>18</sub>H<sub>22</sub>O<sub>4</sub>+Na): 325.1410, found 325.1414, [ $\alpha$ ]<sub>D</sub><sup>rt</sup> = -5.5 (c = 1.05, CHCl<sub>3</sub>). <sup>1</sup>H NMR (400 MHz, CDCl<sub>3</sub>):  $\delta$  7.61-7.57 (m, 2H), 7.38-7.33 (m, 2H), 7.32-7.27 (m, 1H), 5.91 (s, 1H), 5.09 (hept, J = 6.3 Hz, 1H), 3.09 (d, J = 13.9 Hz, 1H), 2.89 (d, J = 13.9 Hz, 1H), 2.45-2.23 (m, 4H), 1.99-1.83 (m, 2H), 1.31 (d, J = 6.3 Hz, 3H), 1.21 (d, J = 6.3 Hz, 3H). <sup>13</sup>C NMR (100 MHz, CDCl<sub>3</sub>):  $\delta$  199.6, 173.7, 161.0, 141.4, 129.4, 128.3, 128.0, 125.2, 78.0, 71.3, 47.3, 37.3, 31.2, 22.8, 21.7, 21.5.

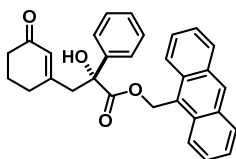
**(R)-tert-butyl 2-hydroxy-3-(3-oxocyclohex-1-en-1-yl)-2-phenylpropanoate, (30e)**



The reaction was carried out following the general procedure to furnish the crude product, which was purified by flash column chromatography (4:1 hexane: EtOAc) to afford the title compound (20.6 mg, 65% yield, 90% ee) as a colorless oil. The enantiomeric excess was determined by HPLC analysis on

a Daicel Chiralpak IC column, (80:20 hexane: <sup>i</sup>PrOH) flow rate 0.8 mL/min,  $\lambda = 254$  nm:  $\tau_{\text{major}} = 12.75$  min,  $\tau_{\text{minor}} = 11.94$  min; HRMS calcd for (C<sub>19</sub>H<sub>24</sub>O<sub>4</sub>+Na): 339.1567, found 339.1569,  $[\alpha]_{\text{D}}^{\text{rt}} = -24.3$  (c = 0.32, CHCl<sub>3</sub>). <sup>1</sup>H NMR (500 MHz, CDCl<sub>3</sub>):  $\delta$  7.61-7.57 (m, 2H), 7.38-7.33 (m, 2H), 7.32-7.27 (m, 1H), 5.93 (s, 1H), 3.92 (s, 1H), 3.07 (d, J = 13.8 Hz, 1H), 2.85 (d, J = 13.8 Hz, 1H), 2.40 (td, J = 5.3, 2.5 Hz, 1H), 2.39-2.21 (m, 3H), 2.04-1.77 (m, 2H), 1.44 (s, 9H). <sup>13</sup>C NMR (125 MHz, CDCl<sub>3</sub>):  $\delta$  199.6, 173.2, 161.3, 141.7, 129.4, 128.3, 127.9, 125.3, 84.2, 78.1, 47.4, 37.3, 31.2, 27.80, 22.8.

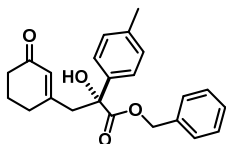
**(R)-anthracen-9-ylmethyl 2-hydroxy-3-(3-oxocyclohex-1-en-1-yl)-2-phenylpropanoate, (30f)**



The reaction was carried out following the general procedure to furnish the crude product, which was purified by flash column chromatography (4:1 hexane: EtOAc) to afford the title compound (36 mg, 80% yield, 94% ee) as a colorless oil. The enantiomeric excess was determined by HPLC analysis on a Daicel Chiralpak IA column, (90:10

hexane: <sup>i</sup>PrOH) flow rate 0.8 mL/min,  $\lambda = 254$  nm:  $\tau_{\text{major}} = 35.00$  min,  $\tau_{\text{minor}} = 27.04$  min; HRMS calcd for (C<sub>30</sub>H<sub>26</sub>O<sub>4</sub>+Na): 473.1723, found 473.1725,  $[\alpha]_{\text{D}}^{\text{rt}} = -33.8$  (c = 0.74, CHCl<sub>3</sub>). <sup>1</sup>H NMR (400 MHz, CDCl<sub>3</sub>)  $\delta$  8.57 (s, 1H), 8.18 (d, J = 8.5 Hz, 2H), 8.07 (d, J = 7.7 Hz, 2H), 7.66-7.46 (m, 6H), 7.32-7.20 (m, 3H), 6.35 (d, J = 12.5 Hz, 1H), 6.12 (d, J = 12.5 Hz, 1H), 5.82 (s, 1H), 2.98 (d, J = 14.1 Hz, 1H), 2.78 (d, J = 14.1 Hz, 1H), 2.24-2.02 (m, 4H), 1.85-1.60 (m, 2H). <sup>13</sup>C NMR (100 MHz, CDCl<sub>3</sub>)  $\delta$  199.4, 174.5, 160.5, 141.0, 131.3, 131.1, 129.8, 129.2, 129.1, 128.4, 128.1, 127.0, 125.3, 124.5, 123.5, 78.3, 61.3, 47.1, 37.1, 30.9, 22.6.

**(R)-benzyl 2-hydroxy-3-(3-oxocyclohex-1-en-1-yl)-2-(p-tolyl)propanoate, (30m)**

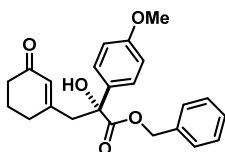


The reaction was carried out following the general procedure to furnish the crude product, which was purified by flash column chromatography (6:1 hexane: EtOAc) to afford the title compound (24.2 mg, 66% yield, 87% ee) as a colorless oil. The enantiomeric excess

was determined by HPLC analysis on a Daicel Chiralpak IC column, (70:30 hexane: <sup>i</sup>PrOH) flow rate 0.8 mL/min,  $\lambda = 254$  nm:  $\tau_{\text{major}} = 56.05$  min,  $\tau_{\text{minor}} = 28.57$  min; HRMS calcd for (C<sub>23</sub>H<sub>24</sub>O<sub>4</sub>+Na): 387.1567, found 387.1570,  $[\alpha]_{\text{D}}^{\text{rt}} = +2.8$  (c = 0.36, CHCl<sub>3</sub>). <sup>1</sup>H NMR (500 MHz, CDCl<sub>3</sub>):  $\delta$  7.47 (d, J = 8.3 Hz, 2H), 7.42-7.34 (m, 2H), 7.34-7.26 (m, 3H), 7.24-7.13 (m, 2H), 5.88 (s, 1H), 5.25-5.18 (m, 2H), 3.79 (bs, 1H), 3.11 (d, J = 13.9 Hz, 1H), 2.92 (d, J = 14.3 Hz, 1H), 2.36 (s, 3H), 2.34-2.20 (m, 4H), 1.96 – 1.81 (m, 2H). <sup>13</sup>C NMR (125 MHz, CDCl<sub>3</sub>):  $\delta$  199.6, 174.2, 160.7,

138.1, 138.0, 134.5, 129.4, 129.1, 128.8, 128.7, 128.5, 125.2, 78.2, 68.5, 47.3, 37.2, 31.1, 22.7, 21.0.

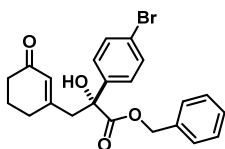
**(R)-benzyl 2-hydroxy-2-(4-methoxyphenyl)-3-(3-oxocyclohex-1-en-1-yl)propanoate, (30n)**



The reaction was carried out following the general procedure to furnish the crude product, which was purified by flash column chromatography (6:1 hexane: EtOAc) to afford the title compound (12.1 mg, 32% yield, 87% ee) as a colorless oil. The enantiomeric excess was determined by HPLC analysis on a Daicel Chiralpak IC column,

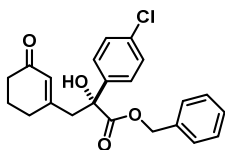
(70:30 hexane:<sup>i</sup>PrOH) flow rate 0.8 mL/min,  $\lambda = 254$  nm:  $\tau_{\text{major}} = 77.00$  min,  $\tau_{\text{minor}} = 39.72$  min; HRMS *calcd* for (C<sub>23</sub>H<sub>24</sub>O<sub>5</sub>+Na): 403.1516, found 403.1515,  $[\alpha]_{\text{D}}^{25} = +6.1$  ( $c = 0.56$ , CHCl<sub>3</sub>). <sup>1</sup>H NMR (500 MHz, CDCl<sub>3</sub>):  $\delta$  7.50-7.44 (m, 2H), 7.38-7.33 (m, 3H), 7.31-7.24 (m, 2H), 6.91-6.82 (m, 2H), 5.86 (s, 1H), 5.19 (s, 2H), 3.80 (s, 3H), 3.07 (d,  $J = 13.9$  Hz, 1H), 2.89 (d,  $J = 13.9$  Hz, 1H), 2.40-2.19 (m, 4H), 1.95-1.75 (m, 2H). <sup>13</sup>C NMR (125 MHz, CDCl<sub>3</sub>):  $\delta$  199.6, 174.2, 160.8, 159.4, 134.5, 133.0, 130.1, 129.4, 128.7, 128.5, 126.6, 113.7, 77.9, 68.5, 55.3, 47.3, 37.2, 31.1, 22.7.

**(R)-benzyl 2-(4-bromophenyl)-2-hydroxy-3-(3-oxocyclohex-1-en-1-yl)propanoate, (30g)**



The reaction was carried out following the general procedure to furnish the crude product, which was purified by flash column chromatography (6:1 hexane: EtOAc) to afford the title compound (29 mg, 68% yield, 88% ee) as a pale yellow oil. The enantiomeric excess was determined by HPLC analysis on a Daicel Chiralpak IC column, (70:30 hexane: <sup>i</sup>PrOH) flow rate 0.8 mL/min,  $\lambda = 254$  nm:  $\tau_{\text{major}} = 39.15$  min,  $\tau_{\text{minor}} = 21.59$  min; HRMS *calcd* for (C<sub>22</sub>H<sub>21</sub>BrO<sub>4</sub>+Na): 451.0515, found 451.0514  $[\alpha]_{\text{D}}^{25} = +15.6$  ( $c = 1.16$ , CHCl<sub>3</sub>). <sup>1</sup>H NMR (400 MHz, CDCl<sub>3</sub>):  $\delta$  7.48 (s, 4H), 7.45-7.32 (m, 3H), 7.36-7.23 (m, 2H), 5.87 (s, 1H), 5.22 (s, 2H), 3.89 (s, 1H), 3.08 (d,  $J = 13.9$  Hz, 1H), 2.88 (d,  $J = 13.9$  Hz, 1H), 2.39-2.12 (m, 4H), 1.97-1.77 (m, 2H). <sup>13</sup>C NMR (100 MHz, CDCl<sub>3</sub>):  $\delta$  199.4, 173.6, 160.0, 140.0, 134.2, 131.5, 129.6, 128.9, 128.8, 128.6, 127.3, 122.5, 77.9, 68.9, 47.3, 37.2, 31.1, 22.7.

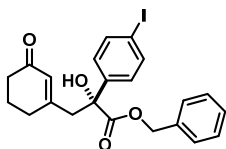
**(R)-benzyl 2-(4-chlorophenyl)-2-hydroxy-3-(3-oxocyclohex-1-en-1-yl)propanoate (30h)**



The reaction was carried out following the general procedure to furnish the crude product, which was purified by flash column chromatography (6:1 hexane: EtOAc) afforded the title compound (33.7 mg, 89% yield, 88% ee) as a yellowish solid. The enantiomeric excess was determined by HPLC analysis on a Daicel Chiralpak IC column, (70:30 hexane: <sup>i</sup>PrOH) flow rate 0.8 mL/min,  $\lambda = 254$  nm:  $\tau_{\text{major}} = 37.37$  min,  $\tau_{\text{minor}} = 20.52$  min; HRMS *calcd* for (C<sub>22</sub>H<sub>21</sub>ClO<sub>4</sub>+Na): 407.1021, found 407.1022,  $[\alpha]_{\text{D}}^{25} = +9.8$  ( $c = 0.88$ , CHCl<sub>3</sub>). <sup>1</sup>H NMR (500 MHz, CDCl<sub>3</sub>):  $\delta$  7.57-7.50 (m, 2H), 7.41-7.37 (m, 3H), 7.36-7.31 (m, 2H), 7.31-7.27 (m, 2H), 5.87 (s, 1H), 5.22 (s, 2H), 3.89 (bs, 1H), 3.09 (d,  $J = 13.9$  Hz, 1H), 2.89 (d,  $J = 13.9$  Hz, 1H), 2.54-2.15 (m, 4H),

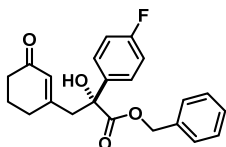
1.99-1.76 (m, 2H).  $^{13}\text{C}$  NMR (125 MHz,  $\text{CDCl}_3$ ):  $\delta$  199.5, 173.7, 160.2, 139.4, 134.3, 131.4, 129.5, 129.0, 128.8, 128.6, 128.5, 126.9, 77.9, 68.9, 47.3, 37.2, 31.1, 22.7.

**(R)-benzyl 2-hydroxy-2-(4-iodophenyl)-3-(3-oxocyclohex-1-en-1-yl)propanoate, (30i)**



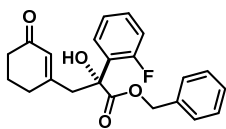
The reaction was carried out following the general procedure to furnish the crude product, which was purified by flash column chromatography (6:1 hexane: EtOAc) to afford the title compound (36.5 mg, 77% yield, 90% ee) as a pale yellow oil. The enantiomeric excess was determined by HPLC analysis on a Daicel Chiralpak IB column, (90:10 hexane:  $^i\text{PrOH}$ ) flow rate 0.8 mL/min,  $\lambda = 254$  nm:  $\tau_{\text{major}} = 20.06$  min,  $\tau_{\text{minor}} = 21.40$  min; HRMS *calcd* for ( $\text{C}_{22}\text{H}_{21}\text{IO}_4+\text{Na}$ ): 499.0377, found 499.0371,  $[\alpha]_{\text{D}}^{25} = +17.6$  ( $c = 0.38$ ,  $\text{CHCl}_3$ ).  $^1\text{H}$  NMR (300 MHz,  $\text{CDCl}_3$ ):  $\delta$  7.66 (d,  $J = 8.6$  Hz, 2H), 7.38-7.24 (m, 7H), 5.84 (s, 1H), 5.19 (s, 2H), 3.05 (d,  $J = 13.9$  Hz, 1H), 2.85 (d,  $J = 13.9$  Hz, 1H), 2.25 (dt,  $J = 10.3, 6.0$  Hz, 4H), 2.00-1.68 (m, 2H).  $^{13}\text{C}$  NMR (75 MHz,  $\text{CDCl}_3$ ):  $\delta$  199.6, 173.7, 160.2, 140.9, 137.6, 134.4, 129.7, 129.1, 128.9, 128.8, 127.6, 94.3, 77.6, 69.1, 47.3, 37.3, 31.3, 22.8.

**(R)-benzyl 2-(4-fluorophenyl)-2-hydroxy-3-(3-oxocyclohex-1-en-1-yl)propanoate, (30j)**



The reaction was carried out following the general procedure to furnish the crude product, which was purified by flash column chromatography (4:1 hexane: EtOAc) to afford the title compound (25.6 mg, 73% yield, 85% ee) as a colorless oil. The enantiomeric excess was determined by HPLC analysis on a Daicel Chiralpak IC column, (70:30 hexane:  $^i\text{PrOH}$ ) flow rate 0.8 mL/min,  $\lambda = 254$  nm:  $\tau_{\text{major}} = 36.95$  min,  $\tau_{\text{minor}} = 20.06$  min; HRMS *calcd* for ( $\text{C}_{22}\text{H}_{21}\text{FO}_4+\text{Na}$ ): 391.1316, found 391.1320,  $[\alpha]_{\text{D}}^{25} = +2.5$  ( $c = 1.09$ ,  $\text{CHCl}_3$ ).  $^1\text{H}$  NMR (400 MHz,  $\text{CDCl}_3$ ):  $\delta$  7.63-7.53 (m, 2H), 7.43-7.34 (m, 3H), 7.32-7.24 (m, 2H), 7.09-6.99 (m, 2H), 5.87 (s, 1H), 5.22 (s, 2H), 3.90 (s, 1H), 3.09 (d,  $J = 13.9$  Hz, 1H), 2.90 (d,  $J = 13.9$  Hz, 1H), 2.36-2.21 (m, 4H), 1.94-1.82 (m, 2H).  $^{13}\text{C}$  NMR (100 MHz,  $\text{CDCl}_3$ ):  $\delta$  199.5, 173.8, 162.5 (d,  $J = 247.5$  Hz), 160.3, 136.7, 134.3, 129.5, 128.9, 128.8, 128.6, 127.3 (d,  $J = 8.2$  Hz), 115.2 (d,  $J = 21.5$  Hz), 77.9, 68.7, 47.43, 37.2, 31.1, 22.7.  $^{19}\text{F}$  NMR (376 MHz,  $\text{CDCl}_3$ ):  $\delta$  -114.31 (tt,  $J = 8.5, 5.2$  Hz).

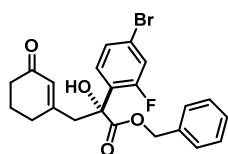
**(R)-benzyl 2-(2-fluorophenyl)-2-hydroxy-3-(3-oxocyclohex-1-en-1-yl)propanoate, (30k)**



The reaction was carried out following the general procedure to furnish the crude product, which was purified by flash column chromatography (4:1 hexane: EtOAc) to afford the title compound (33.5 mg, 91% yield, 82% ee) as a colorless oil. The enantiomeric excess was determined by HPLC analysis on a Daicel Chiralpak IC column, (70:30 hexane:  $^i\text{PrOH}$ ) flow rate 0.8 mL/min,  $\lambda = 254$  nm:  $\tau_{\text{major}} = 29.92$  min,  $\tau_{\text{minor}} = 22.22$  min; HRMS *calcd* for ( $\text{C}_{22}\text{H}_{21}\text{FO}_4+\text{Na}$ ): 391.1316, found 391.1318,  $[\alpha]_{\text{D}}^{25} = +4.2$  ( $c = 0.98$ ,  $\text{CHCl}_3$ ).  $^1\text{H}$  NMR (500 MHz,  $\text{CDCl}_3$ ):  $\delta$  7.54 (td,  $J = 7.9, 1.8$  Hz, 1H), 7.39-7.28 (m, 4H), 7.31 - 7.23 (m, 2H), 7.16 (td,  $J = 7.6, 1.3$

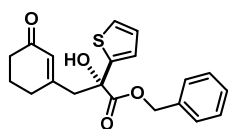
Hz, 1H), 7.05 (ddd,  $J = 11.8, 8.2, 1.2$  Hz, 1H), 5.86 (s, 1H), 5.22 (s, 2H), 3.85 (bs, 1H), 3.35-3.02 (m, 2H), 2.39-2.23 (m, 4H), 1.99-1.75 (m, 2H).  $^{13}\text{C}$  NMR (100 MHz,  $\text{CDCl}_3$ ):  $\delta$  199.5, 173.4, 160.4, 159.9 (d,  $J = 248.1$  Hz), 134.6, 130.4 (d,  $J = 8.7$  Hz), 129.69, 128.6, 128.6, 128.3, 128.2, 127.3 (d,  $J = 3.5$  Hz), 124.2 (d,  $J = 3.4$  Hz), 116.3 (d,  $J = 22.9$  Hz), 76.5 (d,  $J = 1.9$  Hz), 68.4, 44.7 (d,  $J = 3.3$  Hz), 37.2, 31.1, 22.8.  $^{19}\text{F}$  NMR (376 MHz,  $\text{CDCl}_3$ ):  $\delta$  -111.75 (ddt,  $J = 12.3, 8.2, 4.3$  Hz).

**(R)-benzyl 2-(4-bromo-2-fluorophenyl)-2-hydroxy-3-(3-oxocyclohex-1-en-1-yl)propanoate, (30l).**



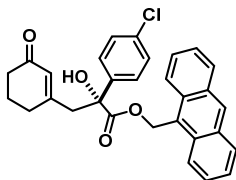
The reaction was carried out following the general procedure to furnish the crude product, which was purified by flash column chromatography (4:1 hexane: EtOAc) to afford the title compound (39 mg, 87% yield, 80% ee) as a colorless oil. The enantiomeric excess was determined by HPLC analysis on a Daicel Chiralpak IC column, (60:30:10 hexane:  $i$ PrOH: DCM) flow rate 0.8 mL/min,  $\lambda = 254$  nm:  $\tau_{\text{major}} = 14.07$  min,  $\tau_{\text{minor}} = 10.84$  min; HRMS *calcd* for ( $\text{C}_{22}\text{H}_{20}\text{BrFO}_4 + \text{Na}$ ): 469.0421, found 469.0416,  $[\alpha]_{\text{D}}^{25} = +8.1$  ( $c = 1.3$ ,  $\text{CHCl}_3$ ).  $^1\text{H}$  NMR (500 MHz,  $\text{CDCl}_3$ ):  $\delta$  7.44 (t,  $J = 8.4$  Hz, 1H), 7.39-7.34 (m, 3H), 7.33-7.20 (m, 4H), 5.85 (s, 1H), 5.21 (s, 2H), 3.90 (bs, 1H), 3.13 (q,  $J = 13.7$  Hz, 2H), 2.35-2.23 (m, 4H), 1.93-1.79 (m, 2H).  $^{13}\text{C}$  NMR (125 MHz,  $\text{CDCl}_3$ ):  $\delta$  199.4, 173.0, 159.9, 159.5 (d,  $J = 253.1$  Hz), 134.3, 129.8, 128.8, 128.8, 128.7, 128.4, 127.6 (d,  $J = 3.5$  Hz), 127.4 (d,  $J = 12.3$  Hz), 122.9 (d,  $J = 9.9$  Hz), 119.9 (d,  $J = 26.4$  Hz), 76.3 (d,  $J = 2.4$  Hz), 68.7, 44.7, 37.2, 31.1, 22.7.  $^{19}\text{F}$  NMR (376 MHz,  $\text{CDCl}_3$ ):  $\delta$  -108.52 (dd,  $J = 10.8, 8.5$  Hz).

**(S)-benzyl 2-hydroxy-3-(3-oxocyclohex-1-en-1-yl)-2-(thiophen-2-yl)propanoate (30o)**



The reaction was carried out following the general procedure to furnish the crude product, which was purified by flash column chromatography (4:1 hexane: EtOAc) to afford the title compound (28.5 mg, 80% yield, 46% ee) as a colorless oil. The enantiomeric excess was determined by HPLC analysis on a Daicel Chiralpak IC column, (60:30:10 hexane:  $i$ PrOH: DCM) flow rate 0.8 mL/min,  $\lambda = 254$  nm:  $\tau_{\text{major}} = 27.74$  min,  $\tau_{\text{minor}} = 13.28$  min; HRMS *calcd* for ( $\text{C}_{20}\text{H}_{20}\text{O}_4\text{S} + \text{Na}$ ): 379.0975, found 379.0977,  $[\alpha]_{\text{D}}^{25} = +2.1$  ( $c = 0.66$ ,  $\text{CHCl}_3$ ).  $^1\text{H}$  NMR (500 MHz,  $\text{CDCl}_3$ ):  $\delta$  7.41-7.33 (m, 3H), 7.35-7.28 (m, 2H), 7.24 (dd,  $J = 5.1, 1.2$  Hz, 1H), 7.07 (dd,  $J = 3.6, 1.2$  Hz, 1H), 6.96 (dd,  $J = 5.1, 3.6$  Hz, 1H), 5.85 (s, 1H), 5.28-5.18 (m, 2H), 4.14 (bs, 1H), 3.06 (d,  $J = 13.8$  Hz, 1H), 2.95 (d,  $J = 14.2$  Hz, 1H), 2.37-2.21 (m, 4H), 1.91-1.82 (m, 2H).  $^{13}\text{C}$  NMR (125 MHz,  $\text{CDCl}_3$ ):  $\delta$  199.5, 173.1, 159.8, 145.8, 134.3, 129.5, 128.9, 128.8, 128.6, 127.2, 125.4, 124.5, 77.2, 69.0, 48.6, 37.2, 31.0, 22.7.

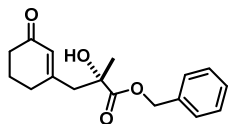
**(R)-anthracen-9-ylmethyl 2-(4-chlorophenyl)-2-hydroxy-3-(3-oxocyclohex-1-en-1-yl)propanoate, (30p).**



The reaction was carried out following the general procedure to furnish the crude product, which was purified by flash column chromatography (4:1 hexane: EtOAc) to afford the title compound (43 mg, 89% yield, 91% ee) as a white solid. The enantiomeric excess was determined by HPLC analysis on a Daicel Chiralpak IA column, (85:15

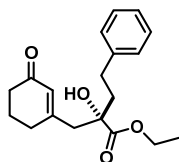
hexane: *i*PrOH) flow rate 0.8 mL/min,  $\lambda = 254$  nm:  $\tau_{\text{major}} = 25.03$  min,  $\tau_{\text{minor}} = 20.75$  min; HRMS *calcd* for (C<sub>30</sub>H<sub>25</sub>ClO<sub>4</sub>+Na): 507.1334, found 507.1340,  $[\alpha]_{\text{D}}^{25} = -17.0$  (c = 2.2, CHCl<sub>3</sub>). <sup>1</sup>H NMR (500 MHz, CDCl<sub>3</sub>):  $\delta$  8.56 (s, 1H), 8.10 (dd, J = 36.6, 8.9 Hz, 4H), 7.62-7.46 (m, 4H), 7.43-7.36 (m, 2H), 7.20-7.11 (m, 2H), 6.32 (d, J = 12.6 Hz, 1H), 6.14 (d, J = 12.5 Hz, 1H), 5.79 (s, 1H), 2.92 (d, J = 14.1 Hz, 1H), 2.72 (d, J = 14.1 Hz, 1H), 2.36-1.99 (m, 4H), 1.83-1.61 (m, 2H). <sup>13</sup>C NMR (125 MHz, CDCl<sub>3</sub>):  $\delta$  199.4, 174.1, 160.1, 139.5, 134.1, 131.3, 131.0, 129.9, 129.3, 129.2, 128.4, 127.1, 126.9, 125.3, 124.3, 123.4, 78.0, 61.6, 47.1, 37.1, 31.0, 22.6.

**(S)-benzyl 2-hydroxy-2-methyl-3-(3-oxocyclohex-1-en-1-yl)propanoate, (30q)**

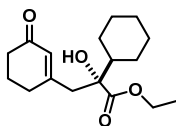


The reaction was carried out following the general procedure to furnish the crude product, which was purified by flash column chromatography (4:1 hexane: EtOAc) to afford the title compound (18.6 mg, 65% yield, 79% ee) as a colorless oil. The enantiomeric

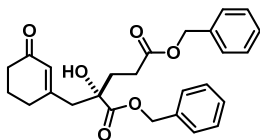
excess was determined by HPLC analysis on a Daicel Chiralpak IC column, (70:30 hexane: *i*PrOH) flow rate 0.8 mL/min,  $\lambda = 254$  nm:  $\tau_{\text{major}} = 45.29$  min,  $\tau_{\text{minor}} = 29.62$  min; HRMS *calcd* for (C<sub>17</sub>H<sub>20</sub>O<sub>4</sub>+Na): 311.1254, found 311.1254,  $[\alpha]_{\text{D}}^{25} = -2.8$  (c = 0.48, CHCl<sub>3</sub>). <sup>1</sup>H NMR (400 MHz, CDCl<sub>3</sub>):  $\delta$  7.47-7.33 (m, 5H), 5.86 (s, 1H), 5.29-5.16 (m, 2H), 3.27 (s, 1H), 2.68 (d, J = 13.4 Hz, 1H), 2.59 (d, J = 13.9 Hz, 1H), 2.46-2.16 (m, 4H), 1.91 (dt, J = 7.5, 6.1 Hz, 2H), 1.49 (s, 3H). <sup>13</sup>C NMR (100 MHz, CDCl<sub>3</sub>):  $\delta$  199.5, 176.0, 160.8, 134.7, 129.2, 128.8, 128.8, 128.6, 74.7, 68.1, 47.7, 37.2, 31.0, 26.9, 22.8.

**(S)-ethyl 2-hydroxy-2-((3-oxocyclohex-1-en-1-yl)methyl)-4-phenylbutanoate, (30r)**

The reaction was carried out following the general procedure to furnish the crude product, which was purified by flash column chromatography (4:1 hexane: EtOAc) to afford the title compound (27.5 mg, 87% yield, 90% ee) as a colorless oil. The enantiomeric excess was determined by HPLC analysis on a Daicel Chiralpak IC column, (70:30 hexane: *i*PrOH) flow rate 0.8 mL/min,  $\lambda = 254$  nm:  $\tau_{\text{major}} = 32.334$  min  $\tau_{\text{minor}} = 26.801$  min, HRMS *calcd* for (C<sub>19</sub>H<sub>24</sub>O<sub>4</sub>+Na): 339.1567, found 339.1569 [ $\alpha$ ]<sub>D</sub><sup>25</sup> = -17.9 (*c* = 0.76, CHCl<sub>3</sub>). <sup>1</sup>H NMR (400 MHz, CDCl<sub>3</sub>):  $\delta$  7.35-7.27 (m, 2H), 7.25-7.14 (m, 3H), 5.87 (s, 1H), 4.21 (q, *J* = 7.2, Hz, 2H), 3.50 (bs, 1H), 2.82 (ddd, *J* = 13.5, 11.2, 5.2 Hz, 1H), 2.73-2.59 (m, 2H), 2.56-2.40 (m, 2H), 2.40-2.26 (m, 3H), 2.21-1.88 (m, 4H), 1.33 (t, *J* = 7.2, Hz, 3H). <sup>13</sup>C NMR (100 MHz, CDCl<sub>3</sub>):  $\delta$  199.7, 175.6, 161.2, 141.2, 129.3, 128.6, 128.6, 126.2, 77.5, 62.7, 47.5, 41.7, 37.4, 31.3, 30.0, 23.0, 14.4.

**(R)-benzyl 2-cyclohexyl-2-hydroxy-3-(3-oxocyclohex-1-en-1-yl)propanoate, (30s)**

The reaction was carried out following the general procedure to furnish the crude product, which was purified by flash column chromatography (6:1 hexane:EtOAc) to afford the title compound (20.9 mg, 71% yield, 83% ee) as a colorless oil. The enantiomeric excess was determined by HPLC analysis on a Daicel Chiralpak IC column, (60:30:10 hexane:*i*PrOH:DCM) flow rate 0.8 mL/min,  $\lambda = 254$  nm:  $\tau_{\text{major}} = 20.18$  min,  $\tau_{\text{minor}} = 16.81$  min; HRMS *calcd* for (C<sub>17</sub>H<sub>26</sub>O<sub>4</sub>+Na): 317.1723, found 317.1725, [ $\alpha$ ]<sub>D</sub><sup>25</sup> = -1.5 (*c* = 0.15, CHCl<sub>3</sub>). <sup>1</sup>H NMR (500 MHz, CDCl<sub>3</sub>):  $\delta$  5.83 (s, 1H), 4.39-3.90 (m, 2H), 3.23 (s, 1H), 2.70 (d, *J* = 13.1 Hz, 1H), 2.53 (d, *J* = 13.0 Hz, 1H), 2.57-2.46 (m, 1H), 2.31 (t, *J* = 6.7 Hz, 2H), 2.28-2.18 (m, 1H), 2.06-1.61 (m, 7H), 1.42-1.02 (m, 9H). <sup>13</sup>C NMR (125 MHz, CDCl<sub>3</sub>):  $\delta$  199.8, 175.9, 162.7, 129.0, 80.6, 62.4, 46.2, 44.7, 37.4, 31.3, 27.5, 26.4, 25.9, 23.0, 14.4.

**(S)-dibenzyl 2-hydroxy-2-((3-oxocyclohex-1-en-1-yl)methyl)pentanedioate, (30t)**

The reaction was carried out following the general procedure to furnish the crude product, which was purified by flash column chromatography (3:1 hexane: EtOAc) to afford the title compound (37.6 mg, 86% yield, 91% ee) as a colorless oil. The enantiomeric excess was determined by HPLC analysis on a Daicel Chiralpak IC column, (60:30:10 hexane: *i*PrOH: DCM) flow rate 0.8 mL/min,  $\lambda = 254$  nm:  $\tau_{\text{major}} = 53.99$  min,  $\tau_{\text{minor}} = 22.74$  min; HRMS *calcd* for (C<sub>26</sub>H<sub>28</sub>O<sub>6</sub>+Na): 459.1778, found 459.1775, [ $\alpha$ ]<sub>D</sub><sup>25</sup> = -2.98 (*c* = 0.79, CHCl<sub>3</sub>). <sup>1</sup>H NMR (400 MHz, CDCl<sub>3</sub>):  $\delta$  7.44-7.28 (m, 10H), 5.81 (s, 1H), 5.23-5.10 (m, 2H), 5.09 (s, 2H), 3.41 (s, 1H), 2.60 (q, *J* = 13.5 Hz, 2H), 2.55-2.40 (m, 1H), 2.39-2.24 (m, 3H), 2.24-2.01 (m, 4H), 1.91-1.80 (m, 2H). <sup>13</sup>C NMR (100 MHz, CDCl<sub>3</sub>):  $\delta$  199.4, 175.0, 172.7, 160.3, 135.8, 134.5, 129.3, 129.0, 128.9, 128.8, 128.6, 128.3, 128.2, 76.8, 68.4, 66.5, 46.9, 37.2, 34.5, 31.0, 28.6, 22.7.



### 2.3.3. Single Crystal X-ray Diffraction Data for Compounds **30h** and **30p**.

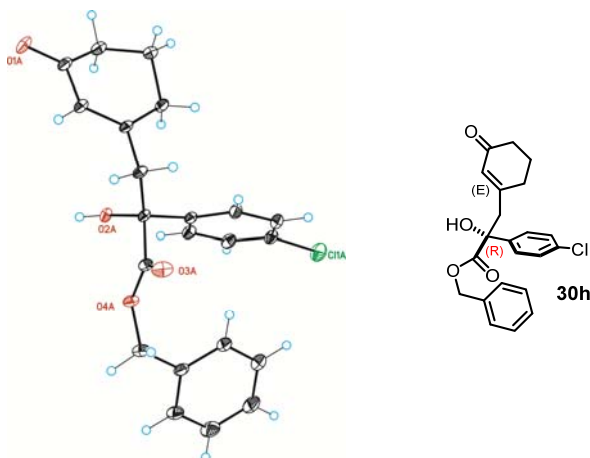
**Data Collection.** Measurements were made on a Bruker-Nonius diffractometer equipped with an APPEX 2 4K CCD area detector, a FR591 rotating anode with Mo<sub>Kα</sub> radiation, Montel mirrors and a Cryostream Plus low temperature device ( $T = -173\text{ }^{\circ}\text{C}$ ). Full-sphere data collection was used  $\omega$  and  $\varphi$  scans.

Programs used: Data collection Apex2 V2010 7.0 (Bruker-Nonius 2008), data reduction Saint + Version 7.60A (Bruker AXS 2008) and absorption correction SADABS.

**Structure Solution.** SIR2007 program was used.<sup>31</sup>

**Structure Refinement.** SHELXTL-97.<sup>32</sup>

X-ray structure determinations: Crystals of **30h** were obtained by slow evaporation of a Hexane/DCM/Et<sub>2</sub>O mixture (98:1:1) at room temperature. The measured crystals were stable under atmosphere conditions; nevertheless they were prepared under inert conditions immersed in perfluoropolyether as protecting oil for manipulation.

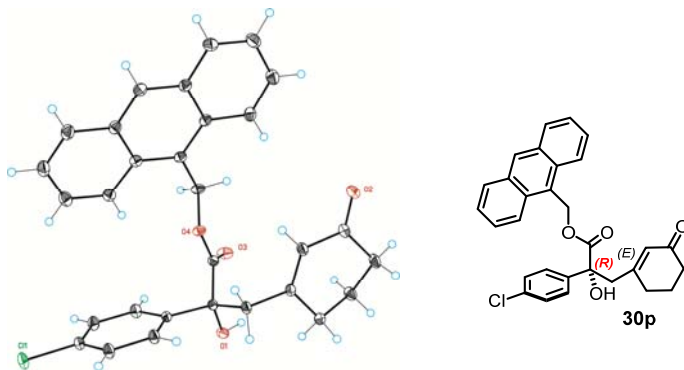


Crystal data for **30h** at 100(2) K: **CCDC 912144**

X-ray structure determinations: Crystals of **30p** were obtained by slow evaporation of a hexane/Et<sub>2</sub>O mixture at room temperature. The measured crystals were stable under atmosphere conditions; nevertheless they were prepared under inert conditions immersed in perfluoropolyether as protecting oil for manipulation.

<sup>31</sup> R. Caliandro, B. Carrozzini, G. L. Cascarano, L. De Caro, C. Giacovazzo, D. Siliqi, Advances in *ab initio* Protein Phasing by Patterson Deconvolution Techniques. *J. Appl. Cryst.* **2007**, *40*, 883.

<sup>32</sup> G.M. Sheldrick, A Short History of SHELX. *Acta Cryst.* **2008**, *A64*, 112.



Crystal data for **30p** at 100(2) K: **CCDC 912145**

### 2.3.4. Intermediate Characterization: NMR Spectroscopic Studies

The imine was achieved under anhydrous conditions (using Schlenk technique) by mixing an equimolar amount of the catalyst **XVIII** (1 equivalent, 0.1 mmol, 48 mg), benzoic acid (**BA**) (1 equivalent, 0.1 mmol 12 mg) and **23** (1 equivalent, 0.1 mmol 11 mg) in presence of freshly activated molecular sieves (4Å) directly in deuterated solvent ( $[23]_0 = 0.5$  M). After the complete disappearance of the enone, the reaction was filtered through a 0.2  $\mu\text{m}$  PTFE filter directly into the NMR tube. After dilution (till approximately 0.2-0.3M) with the same deuterated solvent the sample was analyzed by NMR spectroscopy.

Characterization of the imine adduct in deuterated chloroform. In this solvent two different conformers were found in solution with a ratio of 1.5:1 (Figure 19 to Figure 23).

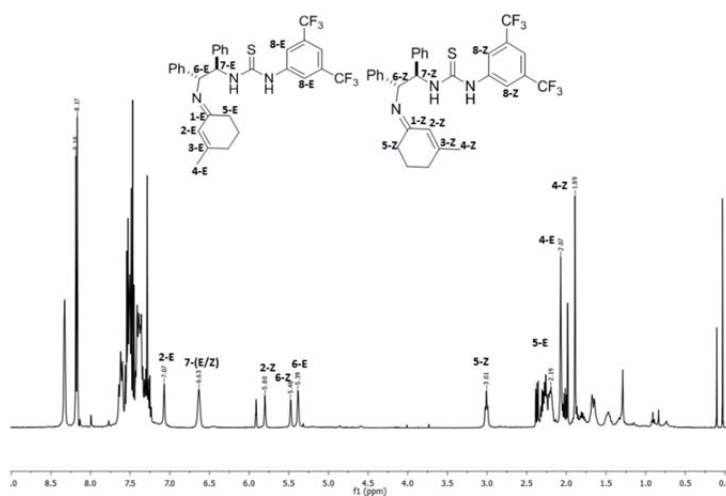


Figure 19.  $^1\text{H}$ NMR of the imine derived from **23** and catalyst **XVIII** in  $\text{CDCl}_3$ .

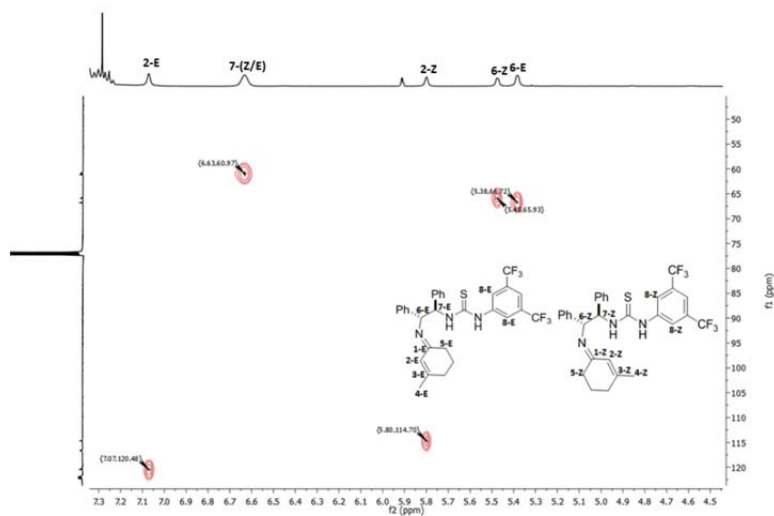


Figure 20. HSQC experiment in  $\text{CDCl}_3$ .  $^1\text{H}$ - $^{13}\text{C}$  short distance correlations of most relevant peaks.

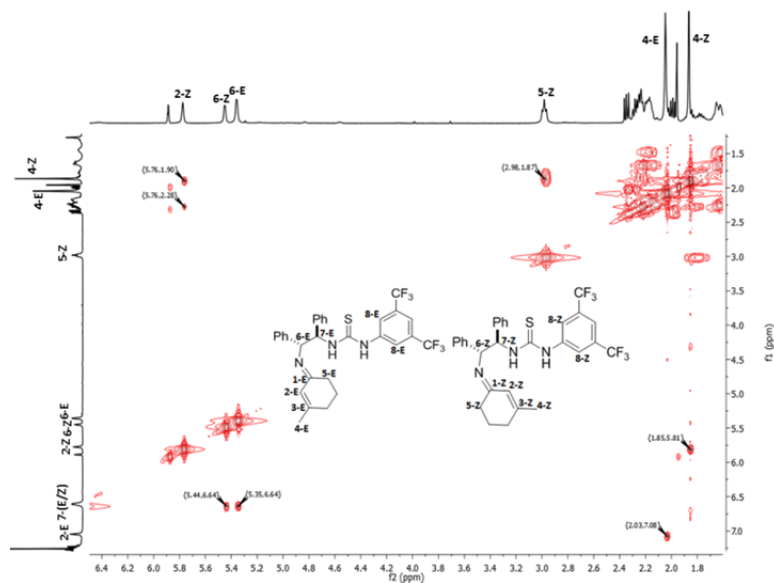
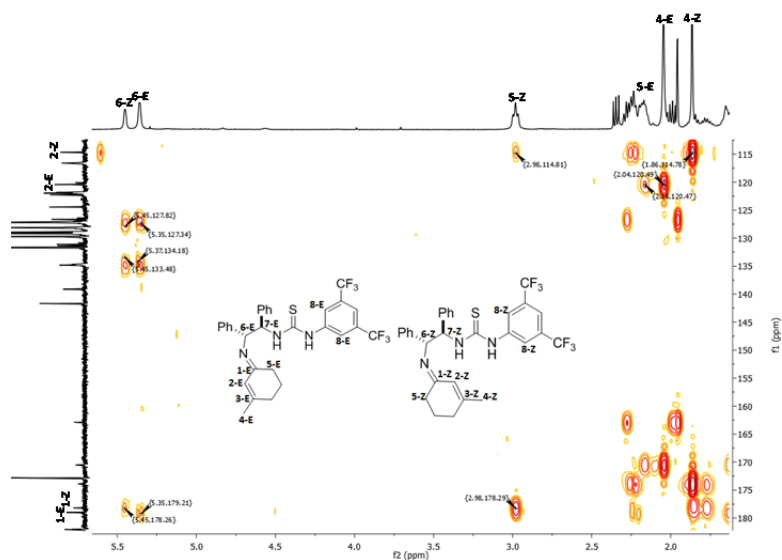
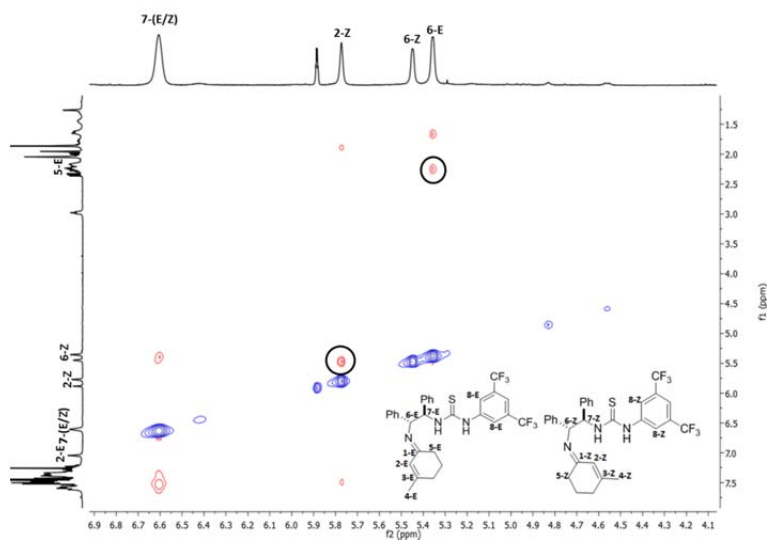


Figure 21. COSY experiment in  $\text{CDCl}_3$ . The most diagnostic cross peaks for the **Z** isomer [H(6Z)-H(7Z), H(2Z)-H(4Z), H(5Z)-H(4Z)] and for the **E** isomer [H(2E)-H(4E), H(6E)-H(7E)] are shown.



**Figure 22.** HMBC experiment in  $\text{CDCl}_3$ .  $^1\text{H}$ - $^{13}\text{C}$  large distance correlations of most relevant peaks: [H(6Z)-C(1Z), C(2Z)-H(5Z), C(2Z)-H(4Z)] for the **Z-isomer**; [H(6E)-C(1E), C(2E)-H(5E), C(2E)-H(4E)] for the **E-isomer**.



**Figure 23.** NOESY experiment in  $\text{CDCl}_3$ : the most diagnostic signals are highlighted. Strong nuclear Overhauser effects are shown between H-(2Z) and H-(6Z), while in the E-isomer shows a cross peak between H-(2E) and H-(5E) but no cross peaks between H-(2E) and H-(6E).

Characterization of the catalytic system made by combining the amine **XVIII** with 1 equiv of benzoic acid. The NMR spectroscopic studies of a catalyst **XVIII**/benzoic acid 1:1 mixture are detailed below (Figure 24 to Figure 27).

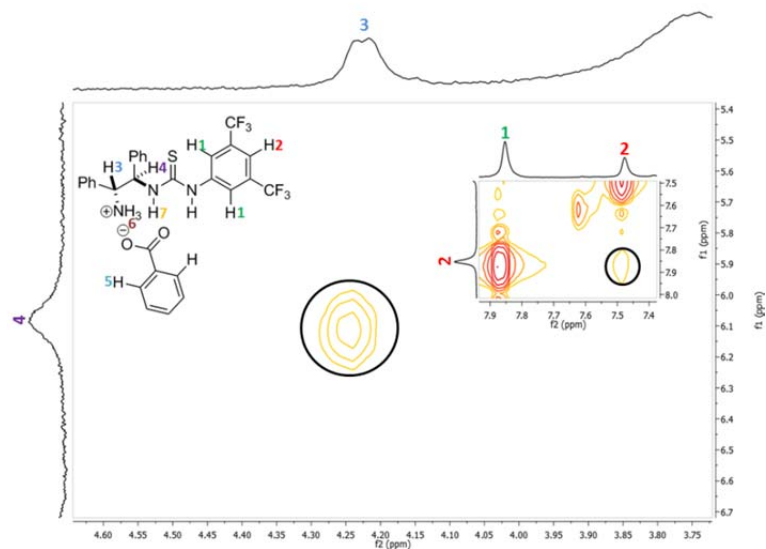


**Figure 24.** Section of the COSY experiment for **XVIII** and BA (1:1 at 0.02 mmol in toluene  $d_8$ ).

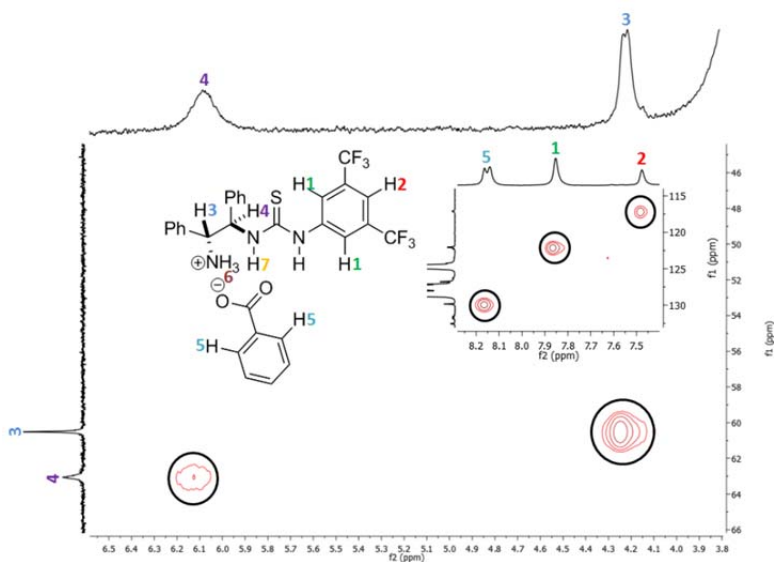


**Figure 25.** Section of the HSQC correlation studies for **XVIII** and BA (1:1 at 0.02 mmol in toluene  $d_8$ ). The most diagnostic cross peaks are shown.

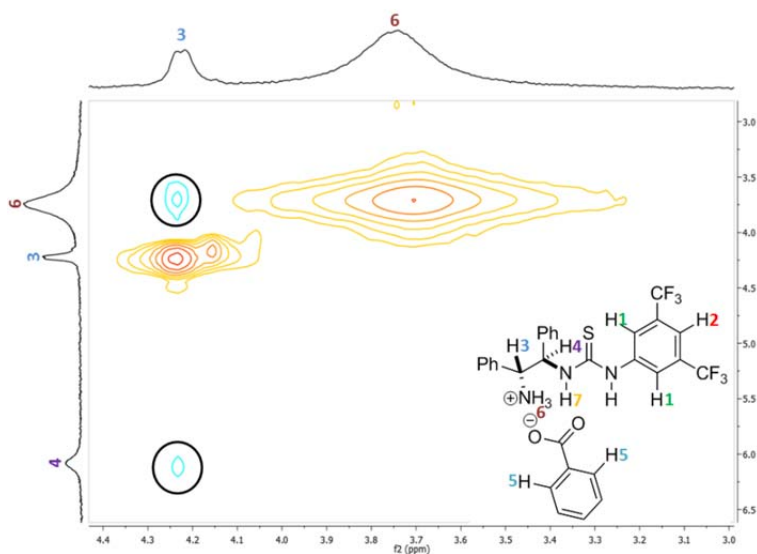


Figure 26. Section of the NOESY spectra for XVIII and BA (1:1 at 0.02 mmol in toluene  $d_8$ ).

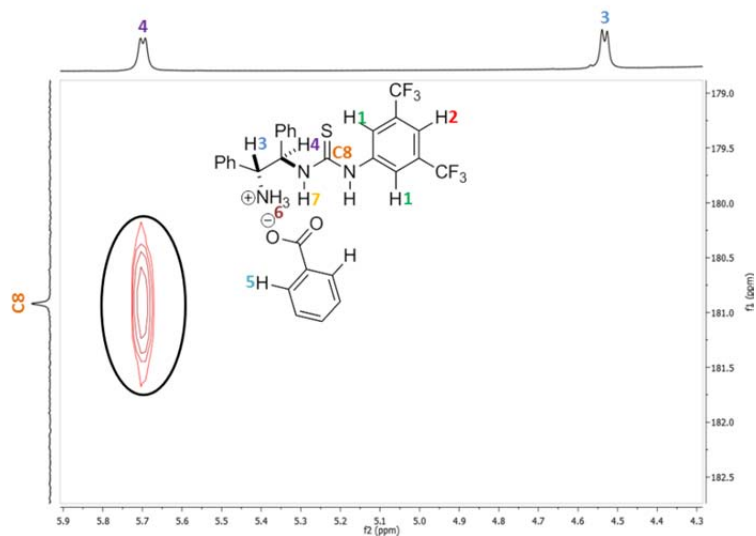


Figure 27. Section of the HMBC correlation studies for XVIII and BA (1:1 at 0.02 mmol in DMSO  $d_6$ ).

UNIVERSITAT ROVIRA I VIRGILI  
NOVEL ENANTIOSELECTIVE AMINOCATALYTIC PROCESSES BY MEANS OF VINYLLOGOUS  
REACTIVITY AND PHOTOREDOX CATALYSIS  
David Bastida Borrell

## Chapter III

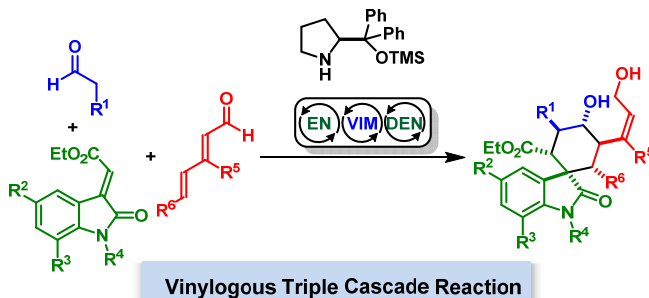
# Vinylogous Organocatalytic Triple Cascade Reaction: Forging Six Stereocenters in Complex Spiro-Oxindolic Cyclohexanes

### Target

Expand the potential of organocascade catalysis by including vinylogous reactivity as a design principle for realizing unprecedented asymmetric domino reactions.

### Tool

Merging the potential of aminocatalytic cascade reactions to generate high degrees of architectural and stereochemical complexity and the ability of vinylogous reactivity to forge remote stereocenters.<sup>1</sup>



### 3.1. Background

The efficient synthesis of stereochemically dense complex organic molecules that mimics the complexity and structural diversity of natural products is one of the most important targets for organic chemists. Asymmetric cascade reactions has been one of the strategy used for rapidly increasing structural and stereochemical complexity in the synthesis of target molecules, such as pharmaceuticals or natural products.<sup>2</sup> A domino reaction is a process in which two or more bond-forming events occur under the same reaction conditions. All the reagents and

<sup>1</sup> The work discussed in this chapter has been published, see: I. Chatterjee, D. Bastida, P. Melchiorre, Vinylogous Organocatalytic Triple Cascade Reaction: Forging Six Stereocenters in Complex Spiro-Oxindolic Cyclohexanes. *Adv. Synth. Catal.* **2013**, 355, 3124. Experimental part developed together with Dr. Indranil Chatterjee.

<sup>2</sup> K. C. Nicolaou, D. J. Edmonds, P. G. Bulger, Cascade Reactions in Total Synthesis. *Angew. Chem. Int. Ed.* **2006**, 45, 7134.



catalysts are added at the outset of the process to undergo a chemical transformation whose product becomes the substrate for the next step, and so on, until a product stable under the reaction conditions is reached.<sup>3</sup> These processes avoid time-consuming and costly protection and de-protection steps as well as the isolation of reaction intermediates. In addition, they are considered green chemical transformations because of the minimal waste generation. In the last decade, exploration of asymmetric catalyzed cascade reactions by employing a single catalyst capable of promoting each single step has gained attention. Aminocatalysts are particularly favorable when used in this context, because of the possibility of integrating orthogonal activation modes of carbonyl compounds (enamine and iminium ion catalysis) into more elaborate reaction sequences.<sup>4</sup>

In addition to creating multiple stereocentres in a one-step process, the combination of multiple asymmetric transformations in a cascade sequence also imparts increased enantiomeric excess to the final product when compared to the corresponding discrete transformations. The *Horeau* principle<sup>5</sup> provides the mathematical foundation for the rationalization of the enantioenrichment observed in tandem reactions (Figure 1).

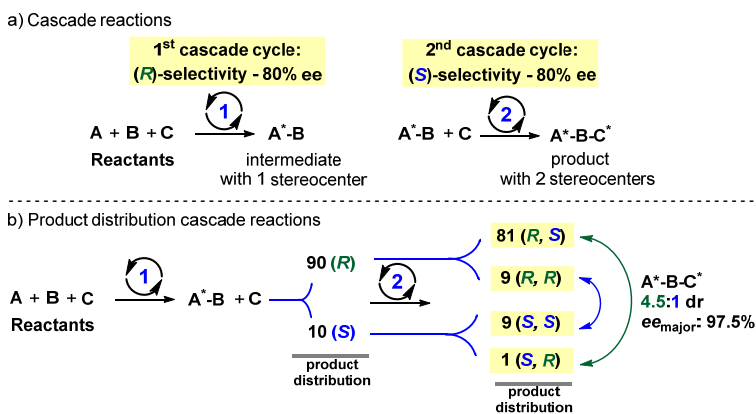


**Figure 1.** Schematic explanation of the *Horeau* principle and the product enantio-enrichment within the cascade reactions. The system is simplified in that possible matched/mismatched interactions (substrate vs catalyst control) in the second step of the tandem process would likely lead to a different product distribution.

<sup>3</sup> a) L. F. Tietze, U. Beifuss. Sequential Transformations in Organic Chemistry: A Synthetic Strategy with a Future. *Angew. Chem. Int. Ed.* **1993**, *32*, 131. b) L. F. Tietze, Domino Reactions in Organic Synthesis. *Chem. Rev.* **1996**, *96*, 115.

<sup>4</sup> C. M. R. Volla, I. Atodiresei, M. Rueping, Catalytic C-C Bond-Forming Multi-Component Cascade or Domino Reactions: Pushing the Boundaries of Complexity in Asymmetric Organocatalysis. *Chem. Rev.* **2014**, *114*, 2390.

<sup>5</sup> J. P. Vigneron, M. Dhaenens, A. Horeau. Nouvelle Methode Pour Porter au Maximum la Purete Optique d'un Produit Partiellement Dedouble sans l'Aide d'Aucune Substance Chirale. *Tetrahedron*, **1973**, *29*, 1055.

In the model example above, simple calculations reveal that cascade sequences can provide the major diastereomer with exquisite levels of enantiocontrol despite combining catalytic cycles that might be only moderately selective (e.g. 80% ee + 80% ee = 97.5% ee). This powerful tool is broadly used for building up molecular complexity with high levels of optical purity.

### 3.1.1. Amine-Catalyzed Cascade Reactions

Aminocatalytic cascade reactions are based on the conjugate addition of a nucleophile to an  $\alpha,\beta$ -unsaturated aldehyde or ketone followed by the  $\alpha$ -functionalization of the resulting saturated carbonyl compound. These  $\alpha,\beta$ -unsaturated carbonyl substrates are first activated through an iminium ion to facilitate the conjugate addition. The resulting enamine can then react with electrophiles affording the double-substituted products forging two new stereocenters (Figure 2).<sup>6</sup> In this well-defined sequence, the catalyst has an active role in both steps, initially forming the activated iminium ion species and later the electron-rich enamine intermediate. The main reactivity issue to be addressed lies in the identification of a nucleophilic and an electrophilic substrate that can coexist under the reaction conditions without interacting with each other through competitive coupling.

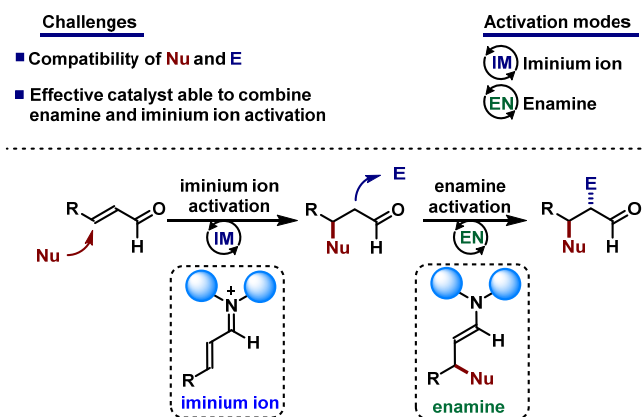


**Figure 2.** The concept of iminium-enamine activation for cascade reaction. The blue circle represents the chiral catalyst scaffold.

In 2005, nearly at the same time, three research groups introduced the iminium-enamine activation concept.<sup>7</sup> The group of MacMillan reported that a large variety of electron-rich

<sup>6</sup> D. Enders, C. Grondal, M. R. M. Hüttl. Asymmetric Organocatalytic Cascade Reactions. *Angew. Chem. Int. Ed.* **2007**, *52*, 1570.

<sup>7</sup> a) J. W. Yang, M. T. Hechavarría Fonseca, B. List, Catalytic Asymmetric Reductive Michael Cyclization. *J. Am. Chem. Soc.* **2005**, *127*, 15036. b) Y. Huang, A. M. Walji, C. H. Larsen, D. W. C. MacMillan, Enantioselective Organo-Cascade Catalysis. *J. Am. Chem. Soc.* **2005**, *127*, 15051. c) M. Marigo, T. Schulte, J. Franzén, K. A. Jørgensen, Asymmetric Multicomponent Domino Reactions and Highly Enantioselective Conjugated Addition of Thiols to  $\alpha,\beta$ -Unsaturated Aldehydes. *J. Am. Chem. Soc.* **2005**, *127*, 15710.

heteroaromatics can undergo conjugate addition with enals **1** catalyzed by the imidazolidinone catalyst **I**. The resulting enamine is then reacting with electrophilic halogen source **2** (Figure 3).<sup>7b</sup>

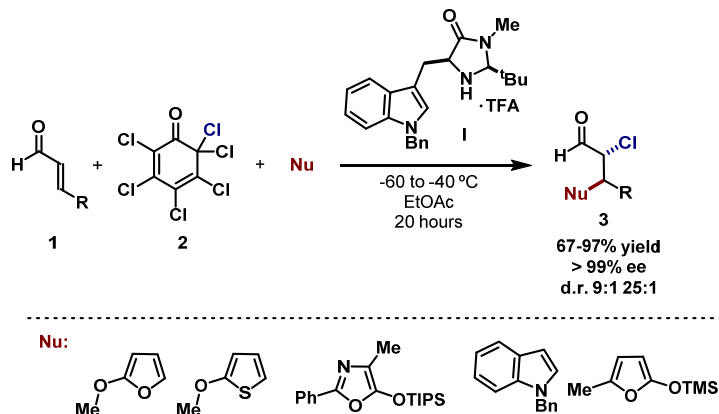


**Figure 3.** MacMillan example of iminium-enamine activation for cascade reaction.

The group of Jørgensen reported a conjugated nucleophilic addition-electrophilic amination reaction that gives access to 1,2-aminothiol derivatives with high levels of enantiocontrol in a single pot operation (Figure 4).<sup>7c</sup> The soft thiol nucleophile **5** reacts with the iminium ion intermediate formed after condensation of catalyst **II** and enal **1**. This step is followed by the addition of the nitrogen-centered electrophile **4** to the enamine intermediate. The highly functionalized oxazolidinones **6** were obtained by in situ reduction and cyclization.

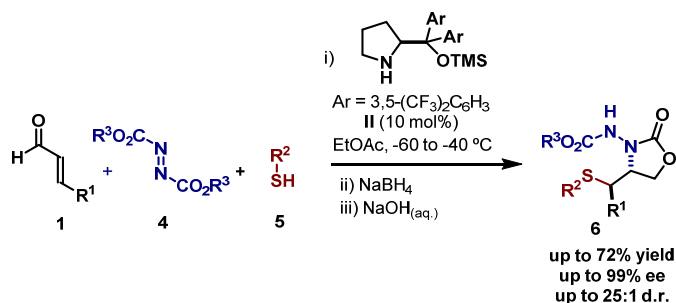


**Figure 4.** The Jørgensen approach to iminium ion-enamine cascade reaction.

One of the most impressive examples of asymmetric organocascade reactions was published by Enders and co-workers,<sup>8</sup> who designed a triple cascade reaction for the construction of tetrasubstituted cyclohexene carbaldehydes (Figure 5). The cascade sequence involves an enamine/iminium/enamine sequence proceeding through a Michael/Michael/aldol

<sup>8</sup> D. Enders, M. R. M. Hüttl, C. Grondal, G. Raabe. Control of Four Stereocentres in a Triple Cascade Organocatalytic Reaction. *Nature*, **2006**, *441*, 861.

condensation for the formation of three new carbon-carbon bonds and four stereogenic centers with high chemoselectivity and regioselectivity, and complete enantioselectivity. The *O*-TMS diphenyl prolinol catalyst **III** first controls a Michael addition of aliphatic aldehydes **7** to nitrostyrene derivatives **8**. In the second step, the chiral amine catalyzes the conjugate addition of the nitroalkane intermediate **A** to  $\alpha,\beta$ -unsaturated aldehydes **9**. The last step is an aldol reaction, where the less hindered aldehyde acts as a nucleophile, followed by elimination of water. The highly functionalized products **10** are obtained in essentially enantiopure form in a single operation.

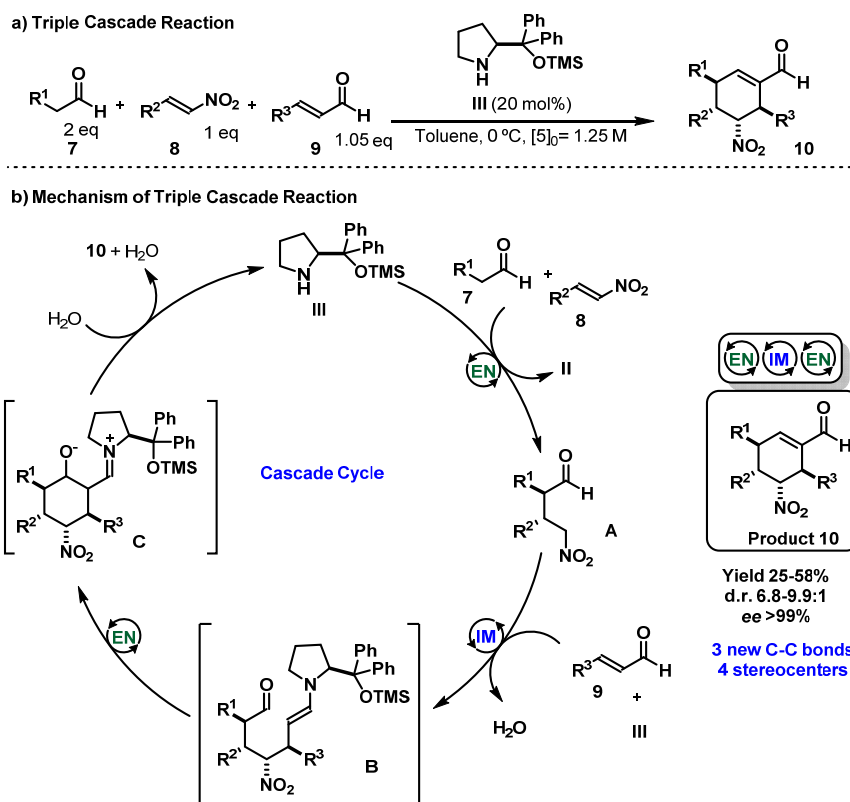


**Figure 5.** a) The asymmetric organocatalytic triple cascade developed by Enders and b) the proposed catalytic cycle.

### 3.1.2. Cascade Reactions and the Vinylogy Principle

As discussed above, progress within the field of organocascade catalysis has mainly been boosted by the ability of chiral secondary amines to integrate enamine and iminium ion catalysis into more elaborate reaction sequences. The iminium ion/enamine strategy has been extensively applied to access  $\alpha$ - and  $\beta$ -functionalized carbonyl chiral building blocks. The main

objective of this project was to expand the potential of organocatalytic cascade reactions by including vinylogous reactivity as a new design principle for realizing unprecedented asymmetric domino reactions. Our motivation was that translating the enamine/iminium ion technique into a vinylogous reactivity pattern could provide a direct entry into enantio-enriched  $\delta$ - and  $\gamma$ -functionalized chiral carbonyls while preserving an  $\alpha,\beta$ -unsaturated system (Figure 6).

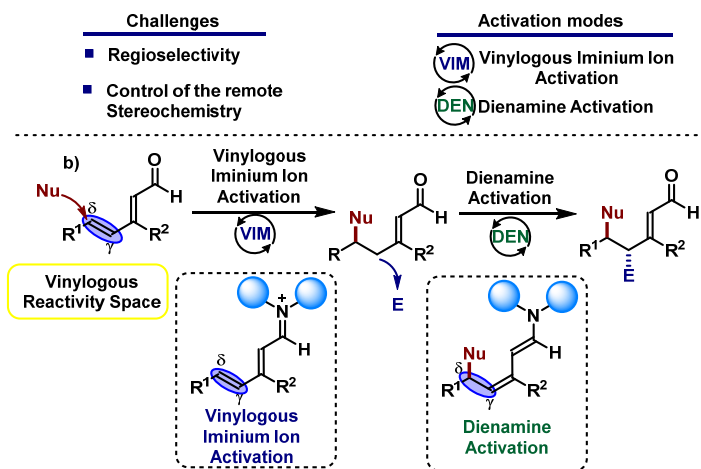


**Figure 6.** Design plan for the design of an organocatalytic vinylogous cascade: 1,6 addition/ $\gamma$ -functionalization driven by vinylogous iminium ion/dienamine activation.

One of the challenges to address is that the chiral catalyst is far away from the reactive center, thus complicating an effective shielding of one of the prochiral faces of the vinylogous iminium ion intermediate, which is a requirement to obtain high stereocontrol. On the other hand, the catalyst will have to ensure exclusive  $\delta$ -selectivity in the 1,6-addition. Nucleophilic conjugate additions to  $\alpha,\beta,\gamma,\delta$ -diunsaturated carbonyl compounds are complicated by the presence of three possible competing pathways, since 1,2-, 1,4-, and 1,6-addition manifolds are all feasible (Figure 7).

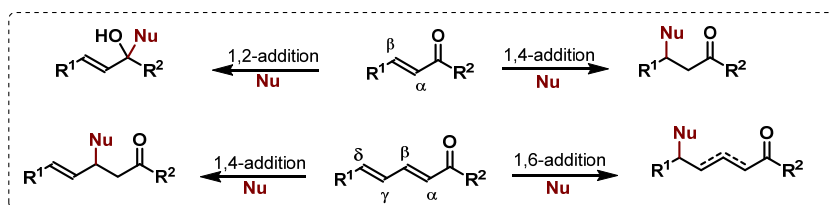


**Figure 7.** Possible pathways for the nucleophilic additions to unsaturated carbonyl systems.

Channeling the reaction toward 1,6-addition manifold is far from easy: a chemist can rely on three main factors to achieve site-selectivity, including steric effects, electronic effects, and the

nature of the nucleophile used. All of these effects may predominate and control the course of the reaction.<sup>9</sup> Experimental and computational studies have shown that organocatalytic 1,4-addition is generally favored against 1,6-addition manifolds.<sup>10</sup> However, some strategies from the realm of both asymmetric metal- and organo-catalysis have recently been reported to address this issue.<sup>11</sup>

### 3.1.3. Organocatalytic Asymmetric 1,6-Conjugate Additions

Transition-metal catalysts have been extensively used in asymmetric 1,6-conjugate addition.<sup>12</sup> In particular rhodium<sup>13</sup> and copper<sup>14</sup> based catalysts have found useful applications. In contrast, asymmetric organocatalytic 1,6-conjugate additions has remained far less developed, although recent studies have demonstrated that organocatalysis can provide useful alternatives for the design of enantio- and regio-selective 1,6-addition reactions.<sup>15</sup>

In 2007, Jørgensen and co-workers reported the first example of an organocatalytic asymmetric addition of  $\beta$ -keto esters **11** and benzophenone imines **14** to  $\alpha,\beta,\gamma,\delta$ -diunsaturated ketones **12** (Figure 8). They obtained complete  $\delta$ -site selective<sup>16</sup> using *Cinchona* alkaloid-based phase transfer catalysts **IV** and **V**. The exclusive formation of the 1,6-addition product can be ascribed to the high reactivity of the terminal olefin in **12**. The *E*-stereochemistry of the “non-conjugated” double bond within the products (**13**, **15**) derived from a kinetic protonation of the extended enolate, transiently generated upon the 1,6-addition of **11** to the dienone **12**.

<sup>9</sup> J. W. Ralls, Unsymmetrical 1,6-Additions to Conjugated Systems. *Chem. Rev.* **1959**, *59*, 329.

<sup>10</sup> Y. Hayashi, D. Okamura, S. Umemiya, T. Uchamaru, Organocatalytic 1,4-Addition Reaction of  $\alpha,\beta,\gamma,\delta$ -Diunsaturated Aldehydes versus 1,6-Addition Reaction. *Chem. Cat. Chem.* **2012**, *4*, 959. b) A. T. Biju. Organocatalytic Asymmetric 1,6-Addition Reactions. *Chem. Cat. Chem.* **2011**, *3*, 1847.

<sup>11</sup> For aminocatalytic 1,6-addition reactions published after the completion of this work, see: a) P. H. Poulsen, K. S. Feu, B. M. Paz, F. Jensen, and K. A. Jørgensen, Organocatalytic Asymmetric 1,6-Addition/1,4-Addition Sequence to 2,4-Dienals for the Synthesis of Chiral Chromans. *Angew. Chem. Int. Ed.* **2015**, *54*, 8203. b) M. Silvi, I. Chatterjee, Y. Liu, P. Melchiorre, Controlling the Molecular Topology of Vinylogous Iminium Ions by Logical Substrate Design: Highly Regio- and Stereoselective Aminocatalytic 1,6-Addition to Linear 2,4-Dienals. *Angew. Chem. Int. Ed.* **2013**, *52*, 10780. c) R. C. da Silva, I. Chatterjee, E. Escudero-Adán, M. W. Paixao, P. Melchiorre, Synthesis of Cyclopropane Spirooxindoles by means of a Vinylogous Organocatalytic Cascade. *Asian J. Org. Chem.* **2014**, *3*, 466.

<sup>12</sup> E. M. P. Silva, A. M. S. Silva. 1,6-Conjugate Addition of Nucleophiles to  $\alpha,\beta,\gamma,\delta$ -Diunsaturated Systems. *Synthesis*, **2012**, *44*, 3109.

<sup>13</sup> T. Hayashi, S. Yamamoto, N. Tokunaga, Rhodium-Catalyzed Asymmetric 1,6-Addition of Aryl Zinc Reagents to Dienones. *Angew. Chem. Int. Ed.* **2005**, *44*, 4224.

<sup>14</sup> T. den Hartog, S. R. Harutyunyan, D. Font, A. J. Minnaard, B. L. Feringa, Catalytic Enantioselective 1,6-Conjugate Addition of Grignard Reagents to Linear Dienoates. *Angew. Chem. Int. Ed.* **2008**, *47*, 398, b) H. Hénon, M. Mauduit, A. Alexakis. Regiodivergent 1,4 versus 1,6 Asymmetric Copper-Catalyzed Conjugate Addition. *Angew. Chem. Int. Ed.* **2008**, *47*, 9122.

<sup>15</sup> For reviews see: a) A. C. Csáký, G. de la Herrán, M. C. Murcia. Conjugate Addition Reactions of Carbon Nucleophiles to Electron-Deficient Dienes. *Chem. Soc. Rev.* **2010**, *39*, 4080. b) E. M. P. Silva, A. M. S. Silva. 1,6-Conjugate Addition of Nucleophiles to  $\alpha,\beta,\gamma,\delta$ -Diunsaturated Systems, *Synthesis*, **2012**, *44*, 3109.

<sup>16</sup> L. Bernardi, J. López-Cantarero, B. Niess, K. A. Jørgensen, Organocatalytic Asymmetric 1,6-Additions of  $\alpha$ -ketoesters and Glycine Imine, *J. Am. Chem. Soc.* **2007**, *129*, 5772.

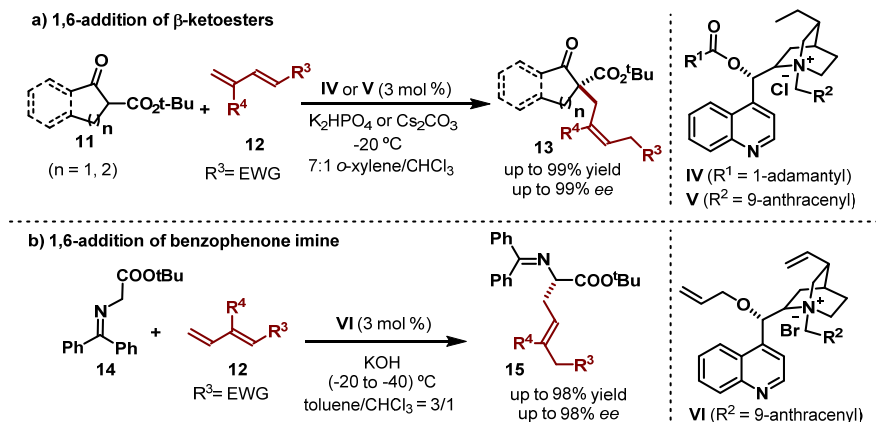


**Figure 8.** Enantioselective organocatalytic 1,6-addition of a) cyclic  $\beta$ -ketoesters and b) benzophenone imines to activated dienes.

An interesting example of enamine-mediated 1,6-addition was published in 2011 by Alexakis and co-workers (Figure 9).<sup>17</sup> The key to success was the appropriate design of butadiene **16**, bearing two electron-withdrawing sulfonyl groups. The sulfonyl group in the  $\alpha$ -position of **16** is not able to induce 1,4-enamine addition to vinyl derivatives. This lack of reactivity toward the beta carbon has set the stage for designing a 1,6-conjugate addition, by exploiting the delocalizing ability of a second sulfonyl group. (*R*)-diphenyl prolinol silyl ether **VII** serves to generate the enamine nucleophilic partner from aliphatic aldehydes **17**, which then reacts with the sulfonyl diene **16** to afford the 1,6-addition product (Figure 9b). The 1,6-conjugate addition intermediate was not observed since it cyclized spontaneously to form the cyclohexadiene **18** in excellent yield and selectivity.

<sup>17</sup> J. J. Murphy, A. Quintard, P. McArdle, A. Alexakis, J. C. Stephens. Asymmetric Organocatalytic 1,6-Conjugate Addition of Aldehydes to Dienic Sulfones. *Angew. Chem. Int. Ed.* **2011**, *50*, 5095.

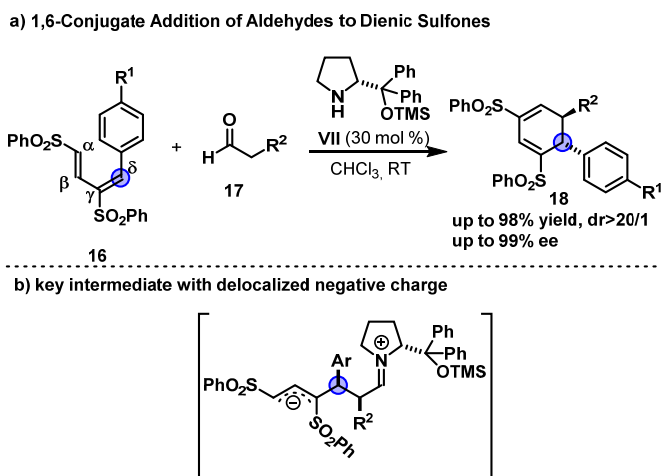


**Figure 9.** Asymmetric Organocatalytic 1,6-Conjugate Addition of Aldehydes to Dienic Sulfones.

All strategies discussed above relied on the ability of the chiral catalyst to effectively activate the nucleophilic component of the reaction, to then drive a stereocontrolled 1,6-addition to a polyunsaturated acceptor. In 2012, our research group published the asymmetric catalytic 1,6-addition of thiols to cyclic dienones (Figure 10).<sup>18</sup> This strategy exploits the activation of the dienone acceptor to obtain a remote functionalization. Upon selective condensation with a *cinchona* primary amine catalyst **VII**, the conjugated  $\pi$ -system of 2,4-dienones **20** forms a reactive vinylogous iminium ion which effectively activates the electrophilic partner toward asymmetric organocatalytic 1,6-additions. This transformation proceeds with high stereocontrol and good  $\delta$ -site selectivity due to the inherent steric bias of the  $\beta$ -substituent, which prevents a 1,4-addition manifold. This study demonstrated the importance of a steering group at the  $\beta$ -position of the dienone to secure high regioselectivity.

<sup>18</sup> X. Tian, Y. Liu, P. Melchiorre, Aminocatalytic Enantioselective 1,6-Additions of Alkyl Thiols to Cyclic Dienones: Vinylogous Iminium Ion Activation. *Angew. Chem. Int. Ed.* **2012**, 51, 6439.



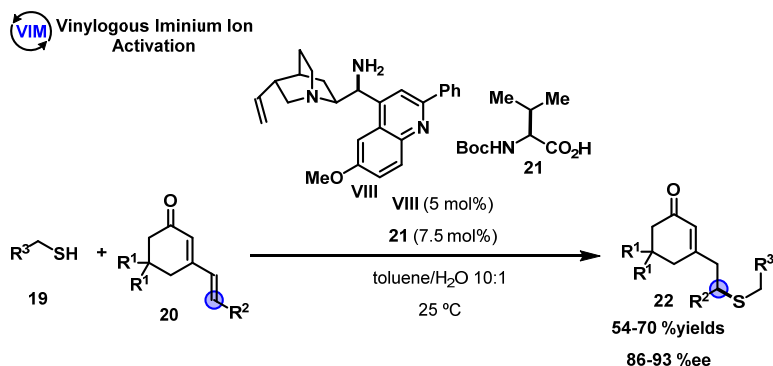


**Figure 10.** Enantioselective 1,6-addition of thiols to dienones through vinylogous iminium ion activation.

During the development of the current studies, an interesting example of vinylogous iminium ion-mediated 1,6-addition was published by Jørgensen and co-workers. They used a linear, geometrically unbiased 2,4-dienals **24** for developing an aminocatalytic asymmetric 1,6-addition (Figure 11).<sup>19</sup>

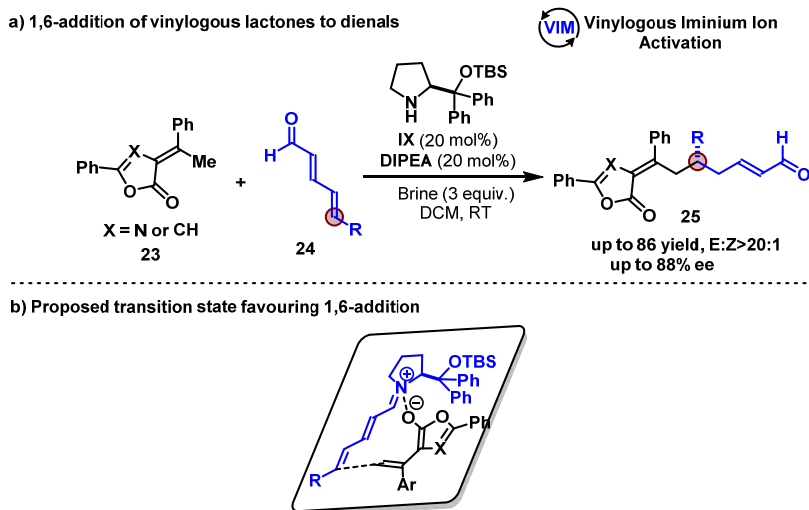


**Figure 11.** 1,6-addition of methyl-substituted vinylogous lactones **20** to linear 2,4-dienals.  
 DIPEA: N,N-Diisopropylethylamina

<sup>19</sup> L. Dell'Amico, Ł. Albrecht, T. Naicker, P. H. Poulsen, K. A. Jørgensen, Beyond Classical Reactivity Patterns: Shifting from 1,4- to 1,6-Additions in Regio- and Enantioselective Organocatalyzed Vinylogous Reactions of Olefinic Lactones with Enals and 2,4-Dienals. *J. Am. Chem. Soc.* **2013**, *135*, 8063.

In order to rationalize the high level of  $\delta$ -site- and stereo-selectivity, an electrostatic interaction between the negatively charged oxygen atom of the transiently generated dienolate species and the positively charged nitrogen atom of the iminium ion intermediate was proposed (Figure 11b).

### 3.2. Results and Discussion

As mentioned before, our objective was to expand the potential of organocascade catalysis by including vinyllogous reactivity as a new design principle. Our group recently used the ability of a chiral amine to stereochemically bias intermediary cyclic vinyllogous iminium ion intermediates, generated upon condensation with cyclic dienones (Figure 10). Clearly, the synthetic potential of the approach is limited by the need for a cyclic substrate. In addition, a careful design of the substrates was needed, since the first step of the tandem reaction must generate a multifunctional intermediate able to successively undergo an intramolecular process (Figure 12a).<sup>20</sup> We reasoned that the use of a linear  $\alpha,\beta,\gamma,\delta$ -unsaturated carbonyl compound would provide a much more flexible tool for designing more complicated and synthetically relevant vinyllogous cascade reactions, based on intermolecular and stereoselective bond-forming events (Figure 12b). However, the successful realization of this plan is far from easy since controlling the  $\delta$ -site and stereo-selectivity in the 1,6-addition reactions of linear substrates poses more than a conundrum though.

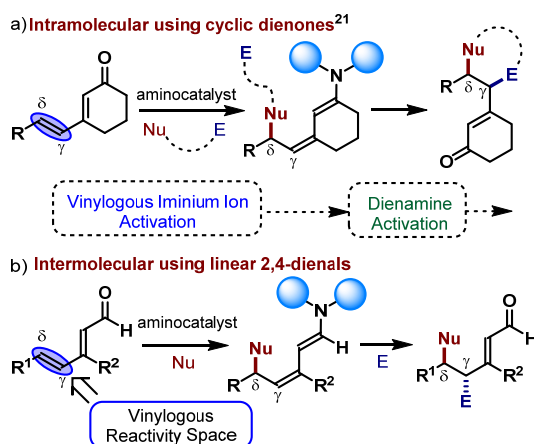


**Figure 12.** Design plan for vinyllogous organocascade catalysis: 1,6-addition/ $\gamma$ -functionalization sequence driven by vinyllogous iminium ion/dienamine activation. a) Precedent approach: two-component reaction using cyclic dienones; the second step is an *intramolecular* event. b) Present plan: multicomponent reaction with linear 2,4-dienals, where two *intermolecular* and stereoselective bond-forming events are combined.

<sup>20</sup> X. Tian, P. Melchiorre, Control of Remote Stereochemistry in the Synthesis of Spirocyclic Oxindoles: Vinyllogous Organocascade Catalysis. *Angew. Chem. Int. Ed.* **2013**, *52*, 5360.

Based on our previous studies,<sup>21</sup> and on the Enders' triple cascade reaction,<sup>Error! Bookmark not defined.</sup> we envisioned the possibility of using linear  $\alpha,\beta,\gamma,\delta$ -unsaturated aldehydes in a triple *vinylogous* cascade sequence. In our initial experiments, we examined the combination of propanal **26**, the Michael acceptor **27**, and the (2*E*,4*E*)-5-phenylpenta-2,4-dienal **28** (Figure 13). The commercially available diphenyl prolinol silylether catalyst **III**<sup>22</sup> was selected because of its established ability to efficiently promote triple cascade reactions. Unfortunately, the cascade sequence proceeded with complete  $\beta$  selectivity, affording the product **29** exclusively. This result is consonant with the established catalytic profile of amine **III**, which is not generally able to induce a 1,6-addition manifold when activating unbiased dienals of type **28**.<sup>10</sup>

#### Vinylogous Triple Cascade Reaction<sup>a</sup>

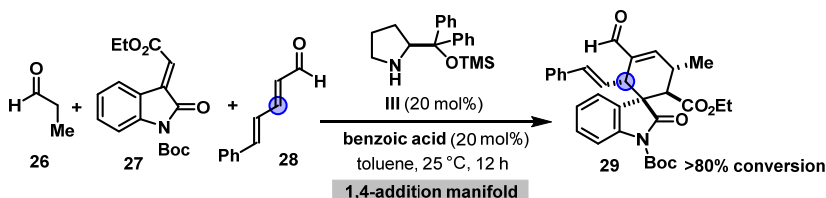


**Figure 13.** Initial attempts on vinylogous triple cascade: the unbiased linear 2,4-dienal **25** is not a competent substrate. <sup>a</sup>Reaction performed on a 0.05 mmol scale. Both conversion and diastereomeric ratios (dr) were determined by <sup>1</sup>H NMR analysis of the crude reaction mixture. All the substrates (**23:24:25**) added at the outset of the reaction.

We next considered the possibility of structurally modifying the substrate scaffold of the 2,4-dienal **28** so as to channel the process toward a selective 1,6-addition manifold. The inherent steric bias of a  $\beta$ -substituent on the dienal **28** could provide a suitable control element for securing  $\delta$ -site selectivity by suppressing the competing 1,4-addition path. The results shown in Figure 14 validate the feasibility of this idea. Introducing a phenyl moiety at the  $\beta$ -position of the enal **30** completely switched the site selectivity toward the desired 1,6-addition driven by vinylogous iminium ion activation. The cyclohexane spirooxindole **31**, bearing six contiguous stereogenic centers, was formed with complete regioselectivity and enantiocontrol (Figure 14).

<sup>21</sup> C. Cassani, X. Tian, E. Escudero-Adan, P. Melchiorre. Multiple Approaches to Enantiopure Spirocyclic Benzofuranones Using Organocatalytic Cascade Reactions, *Chem. Commun.* **2011**, 47, 233.

<sup>22</sup> J. Franzén, M. Marigo, D. Fielenbach, T. C. Wabnitz, A. Kjærsgaard, and K. A. Jørgensen, A General Organocatalyst for Direct  $\alpha$ -Functionalization of Aldehydes: Stereoselective C–C, C–N, C–F, C–Br, and C–S Bond-Forming Reactions. Scope and Mechanistic Insights, *J. Am. Chem. Soc.*, **2005**, 127, 18296.

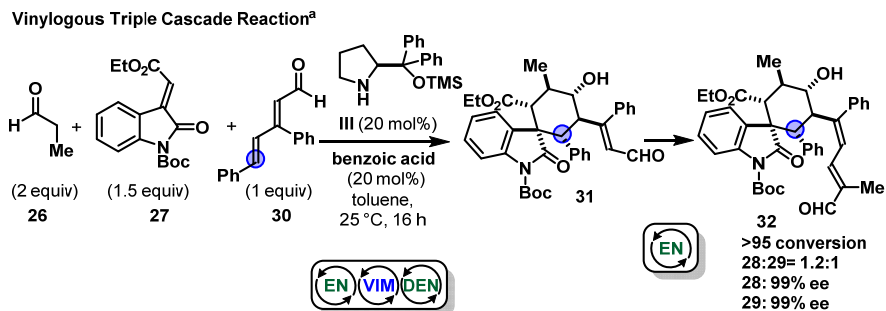


**Figure 14.** The  $\beta$ -substituted dienal **30** directs the key 1,6-addition reaction toward an exclusive  $\delta$ -site selective pathway. <sup>a</sup>Reaction performed on a 0.05 mmol scale. Both conversion and diastereomeric ratios (dr) were determined by <sup>1</sup>H NMR analysis of the crude reaction mixture. All the substrates (**26:27:30**) added at the outset of the reaction.

Although simple from an experimental point of view, the process is based on a complicated catalytic machinery, which is largely based on vinylogous reactivity. An enamine-catalyzed Michael addition of the aldehyde **26** to the acceptor **27** leads to the transient formation of the nucleophilic intermediate **D** (Figure 15). **D** can then engage in the  $\gamma$ -site selective intermolecular 1,6-addition, upon vinylogous iminium ion activation of the  $\beta$ -substituted 2,4-dienal **30**, to forge the spiro-stereocenter. The transient formation of a nucleophilic dienamine **E** drives an intramolecular vinylogous aldolization to provide the final cyclohexane product **31**. Unfortunately, further reactivity takes place under the reaction conditions, and a mixture of products **31** and **32** was obtained. Specifically, the cascade product **31** undergoes a further aldol condensation with **26** to obtain **32** as a single enantiomer.

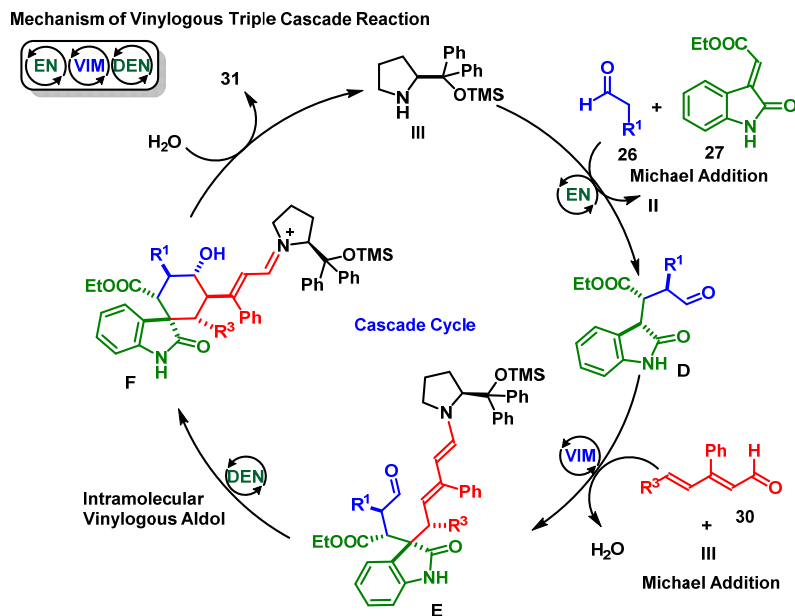


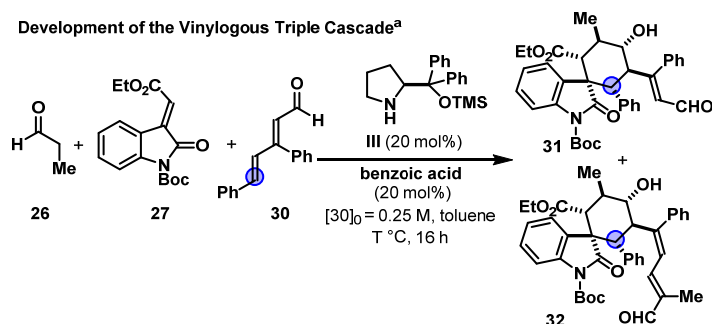
**Figure 15.** Mechanism of Vinylogous Triple Cascade Reaction: Enamine/Vinylogous iminium ion/Dienamine sequence.

In order to obtain the cascade adduct **28** as the single product, we investigated the classical reaction parameters. Screening of solvents or dilution effect did not bring about any improvement (results not presented). We then focused on the stoichiometry of the reaction (Table 1). We found that an excess of propanal induced the preferential formation of product **32** (entry 2), but not as a single product. When we reversed the stoichiometry of the process, using 1 equivalent of propanal and 1.5 equivalents of **27** (entry 3), a **31/32** ratio of 2:1 was obtained. All the experiments conducted to date were run adding all the substrates at the outset of the reaction. We surmised that a sequential addition of the reagents could represent a solution to the complex chemoselectivity issue inherent to the particular substrate combinations of the triple vinylogous cascade.<sup>23</sup> Sequentially adding the last component, namely the linear α,β,γ,δ-unsaturated aldehyde **30**, after 15 minutes ensured a high degree of propanal **26** consumption in

<sup>23</sup> This scenario provides an additional illustration that achieving a high degree of chemoselectivity is one of the greatest difficulties in designing effective cascade processes. Implementing a cascade reaction requires careful consideration of the compatibility of the transiently formed intermediates and the substrates, which should not undergo alternative irreversible reactions to form by-products. Chemoselectivity lies at the heart of modern organic chemistry. For an inspiring conspectus on the topic, see: a) R. A. Shenvi, D. P. O'Malley, P. S. Baran, Chemoselectivity: The Mother of Invention in Total Synthesis. *Acc. Chem. Res.* **2009**, *42*, 530. For an overview on how to achieve chemoselectivity in aminocatalytic domino strategies, see: b) M. Marigo, P. Melchiorre, Chemoselectivity in Asymmetric Aminocatalysis. *ChemCatChem*, **2010**, *2*, 621.

the first enamine-based Michael reaction with **27**, resulting in a perfect control of the product distribution: only the cascade adduct **31** was formed as a 2:1 diastereomeric pair (99% ee). Lowering the reaction temperature down to 0 °C inferred a much higher level of diastereoselectivity (10:1 dr, 99% ee, entry 5), demonstrating the potential of the triple vinylogous cascade to stereoselectively provide direct and rapid access to one out of the 64 possible stereoisomers of **31**. Last, we examined the effect of the acid co-catalyst, finding that the reaction outcome was not modified (entry 6). These conditions - toluene at 0 °C and avoiding the presence of the acid co-catalyst - were selected to test the scope of the vinylogous domino reactions.

**Table 1.** Development of the vinylogous triple organocascade.<sup>a</sup>



entry	26 : 27 : 30	T [°C]	31/32	conv [%] <sup>b</sup>	dr <b>31</b> <sup>b</sup>	ee <sup>c</sup>
1 <sup>d</sup>	2 : 1.5 : 1	25	1.2/1	>95	-	99
2 <sup>d</sup>	4 : 1.5 : 1	25	1/1.35	>95	-	99
3 <sup>d</sup>	1 : 1.5 : 1	25	2/1	>95	-	99
4 <sup>e</sup>	1 : 1.2 : 1	25	100/0	>95	2:1	99
5 <sup>f</sup>	1 : 1.2 : 1	0	100/0	>95 (74) <sup>h</sup>	10:1	99
6 <sup>f,g</sup>	1 : 1.2 : 1	0	100/0	>95 (75) <sup>h</sup>	10:1	99

<sup>a</sup>Reaction performed on a 0.05 mmol scale. b) Both conversion and diastereomeric ratios (dr) were determined by <sup>1</sup>H NMR analysis of the crude reaction mixture. c) Ee value of the major diastereomer of the product **31** determined by HPLC analysis on chiral stationary phases. In all instances, the ee value of the product **31** was 99%. d) All substrates (**26:27:30**) added at the outset of the reaction e) The 2,4-dienal **30** was added after 15 min. f) The 2,4-dienal **30** was added after 60 min. g) The reaction was run in the absence of benzoic acid. h) Yield of the isolated pure major diastereoisomer of **31**.

However, before evaluating the substrate scope, we noted the presence of other species when attempting to isolate the desired compound **31** as a single diastereoisomer. Specifically, the cyclized adduct **33** was generated upon acetal formation, as driven by the reversible condensation of the secondary alcohol with the aldehyde within the cyclohexane moiety (Figure 16). The presence of such equilibrating species (**31** and **33**) did not allow to obtain a clean NMR analysis and to easily isolate the products. In addition, the analysis to determine the enantiomeric excess by chiral HPLC was not reliable (because of the broad signals observed). We decided to further functionalize the product **31** to overcome this equilibration event.

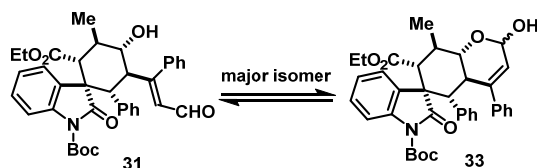


**Figure 16.** Acetal equilibrium of the cascade product **31** under the reaction conditions.

All attempts to oxidize compound **33** to obtain the corresponding lactone were unsuccessful and we decided to further reduce the aldehyde functionality within **31** to the corresponding alcohol **34** (Figure 17).

*in-situ* Reduction of triple cascade product **31**<sup>a</sup>

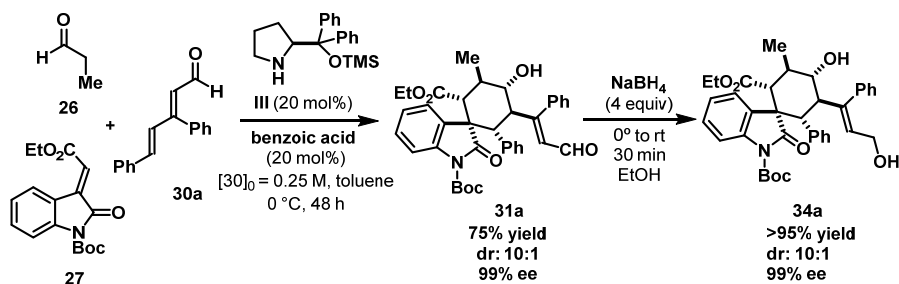


**Figure 17.** In-situ reduction of the aldehyde **28**, a) Reaction performed on a 0.05 mmol scale; after completion of the triple cascade, 4 equivalents of sodium borohydride were added.

Reduction of the crude mixture in a one pot operation with sodium borohydride provided the corresponding alcohol **34** in a quantitative yield containing a valuable spiro-oxindolic cyclohexane ring with 6 contiguous stereocenters with high d.r. and complete enantiomeric purity. With a stable final product in hand, we examined the scope of the transformation evaluating a variety of dienals, aldehydes, and oxindoles substrates (Figure 18).

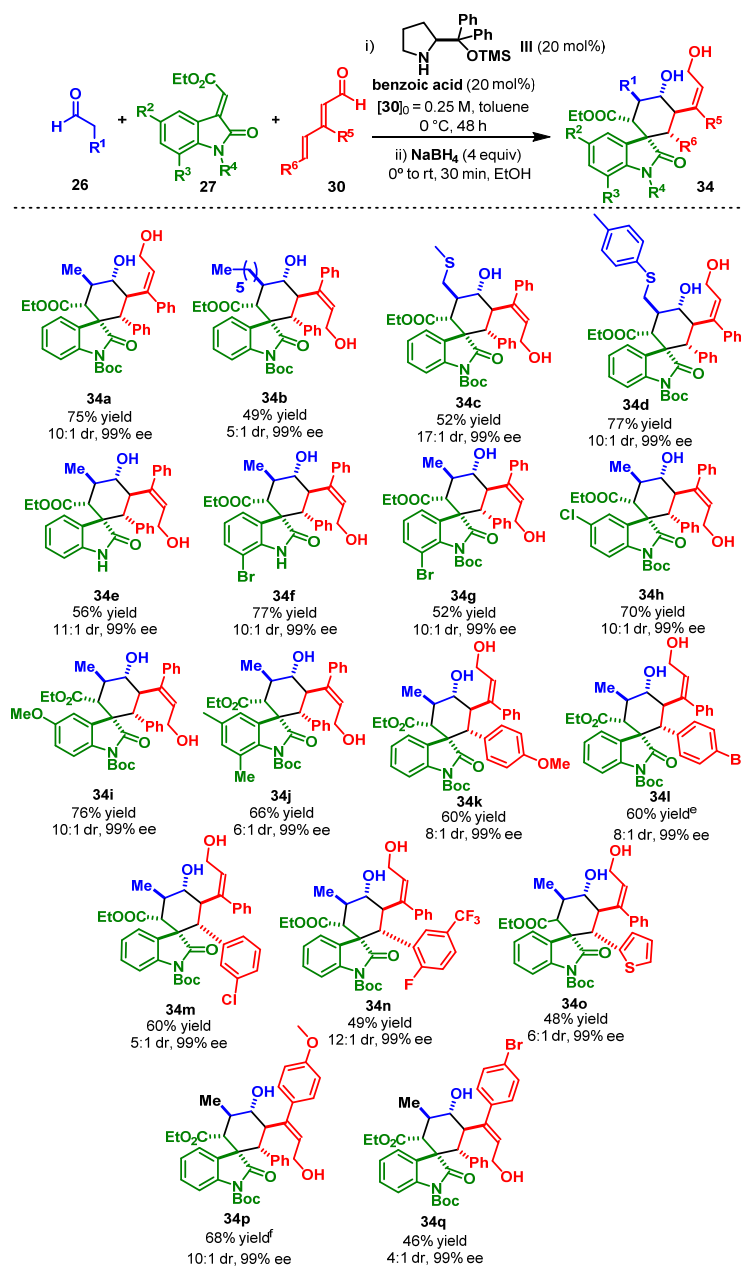


**Figure 18. Scope of the Vinylogous Triple Cascade**, a) Reactions performed on a 0.1 mmol scale using a 1:1:1:1 ratio of **26:27:30** and toluene as the solvent at  $0^\circ\text{C}$ . The 2,4-dienal **30** was added after 60 min. b) Yield of the isolated major diastereoisomer of product **34** after chromatographic purification on silica gel. c) Diastereomeric ratios (dr) were determined by  $^1\text{H}$  NMR analysis of the crude reaction mixture. d) Ee value of the major diastereomer of product **34**, as determined by HPLC analysis on chiral stationary phases. e) Yield given on the mixture of the two diastereoisomers of **34l**. f) 1 mmol scale reaction.



The fact that the residues R<sup>1</sup>–R<sup>6</sup> of the precursors **26**, **27** and **30** can be varied demonstrates the high flexibility of the approach. The substituent R<sup>1</sup> of the aldehyde **26** can bear simple alkyl chain as well as valuable functional groups (products **34b**, **34c**, and **34d**). A wide range of oxindole derivatives **27** with different substituents at the C5 and C7 positions are compatible with the catalytic system (products **34g**, **34h**, **34i**, and **34j**). The use of *N*-unprotected **27** (R<sup>4</sup> = H, products **34e**, **34f**) preserved the stereoselectivity of the process. As a limitation of the system, the cascade product **34** could not be obtained when replacing the carboethoxy group in **27** with a *p*-nitro-phenyl group or a keto moiety. As for the  $\delta$ -position of the dialenal substrate **30**, different substitution patterns at the aromatic moiety were well-tolerated, regardless of their electronic properties and position on the phenyl ring (products **34k**, **34l**, **34m**, and **34n**). A heteroaryl framework can be included in the final product, as shown for the thiophenyl-substituted adduct **34o**. The  $\beta$ -aryl substituent can be varied as well (products **34p**, **34q**). However, all efforts to introduce alkyl groups in R<sup>5</sup> or R<sup>6</sup> were unsuccessful and need further optimization. On the other side, in order to test the method as suitable for synthetically useful purpose, product **34p** was isolated with high yield and selectivity when the reaction was performed on a 1mmol scale reaction.

We further extended the synthetic applicability of the triple cascade reaction using benzofuranones as starting material, using the acceptor **35** instead of compounds **27** (Figure 19). The desired product **36** was obtained in a high yield and diastereomeric excess and complete enantiocontrol.

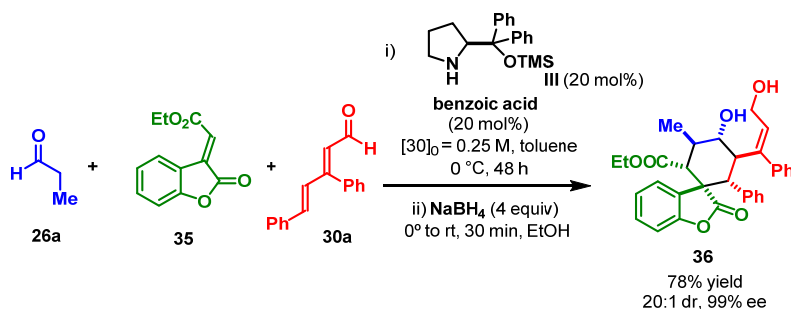


**Figure 19.** Preparation of spiro-cyclic benzofuranones. Reaction performed on a 0.1 mmol scale using a 1:1.2:1 ratio of **26a**:**35**:**23a** and toluene as the solvent at 0 °C. The 2,4-dienal **30a** was added after 60 min. Yield of the isolated major diastereoisomer of product **33** after chromatographic purification on silica gel. Diastereomeric ratios (dr) were determined by <sup>1</sup>H NMR analysis of the crude reaction mixture. Ee value of the major diastereomer of product **36**, as determined by HPLC analysis on chiral stationary phases.

The relative configuration of the adduct **34a** has been determined by nuclear Overhauser enhancement (nOe) spectroscopy. First of all we fully characterized the NMR signals of the proton (Figure 20, for further details on the characterization see the experimental part).

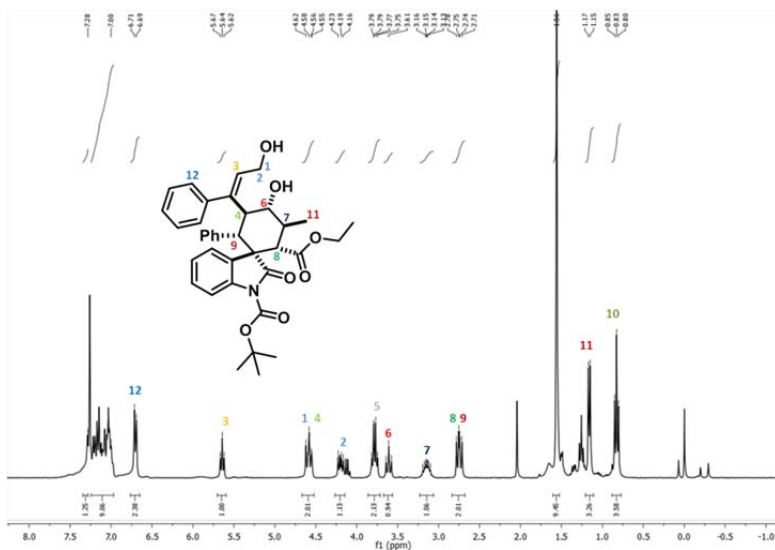


Figure 20. <sup>1</sup>H NMR spectrum of the major diastereoisomer of **34a** in CDCl<sub>3</sub>.

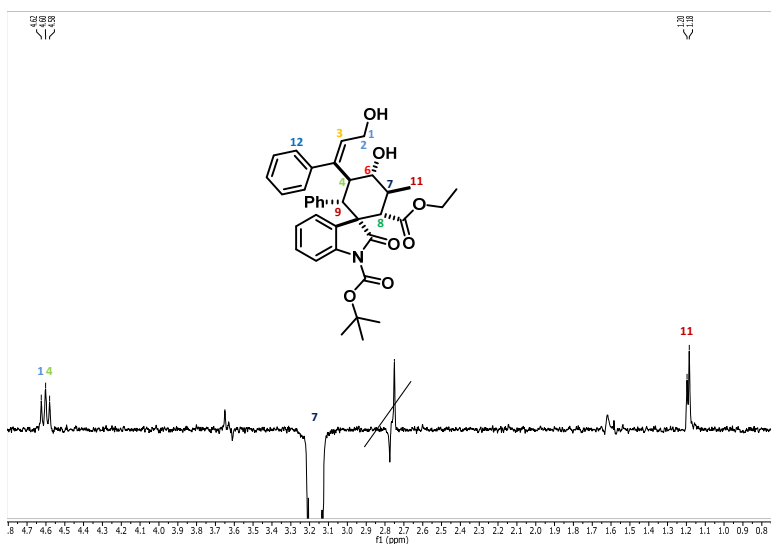
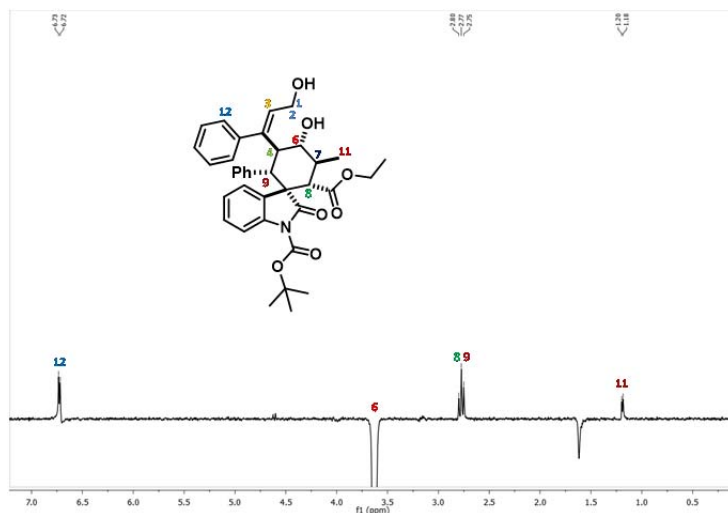
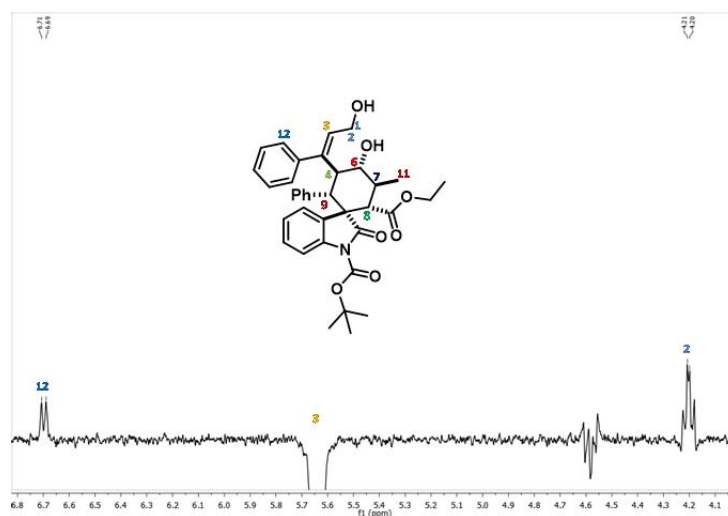


Figure 21. NOE experiment in CDCl<sub>3</sub>: Strong nuclear Overhauser effects are evident when H-7 is selectively irradiated at 3.14 ppm. This correlation indicates that (H-4, H-7) are in a *cis* relative spatial arrangement.



**Figure 22.** NOE experiment in  $\text{CDCl}_3$ : Strong nuclear Overhauser effects are evident when **H-6** was selectively irradiated at 3.6 ppm. This correlation indicates that (**H-6**, **H-8**, **H-9**) are in a *cis* relative spatial arrangement. The nOe observed with (**H-12**) requires a short distance between (**H-6**, **H-12**)



**Figure 23.** NOE experiment in  $\text{CDCl}_3$ : Strong nuclear Overhauser effects are evident when **H-3** was selectively irradiated at 5.64 ppm. This correlation (**H-12**, **H-3**) reveals a *E*-geometry of the double bond.

The absolute configuration of the major diastereoisomer of **34a** was unambiguously determined by anomalous dispersion X-ray crystallographic analysis. X-ray structure of **34e** was obtained from a triple cascade reaction conducted by using the catalyst (*R*)-III so as to afford the enantiomeric product *ent*-**34e**. This data are in agreement with the relative configuration as inferred by the NMR spectroscopic studies (Figure 21, 22 and 23)

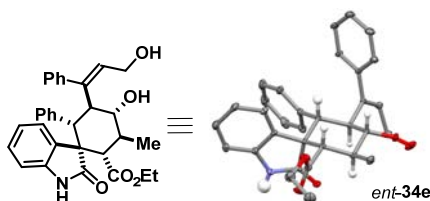


Figure 24. X-ray structure of *ent*-**34e**

Looking at the structure of product **34**, we can easily recognize the presence of functional groups amenable to further transformations. In particular, the presence of an  $\alpha,\beta$ -unsaturated system provides the stimulating possibility of rapidly increasing the stereochemical and structural complexity of the adducts. Performing a simple epoxidation of the enantiopure **34a** (*meta*-chloroperoxybenzoic acid, *m*CPBA in DCM) quantitatively afforded the corresponding epoxide with a 8:1 diastereomeric ratio (Figure 25). Simple separation by flash chromatography allowed access to the enantiomerically pure major isomer **37a**, with full control over eight contiguous stereogenic centers.

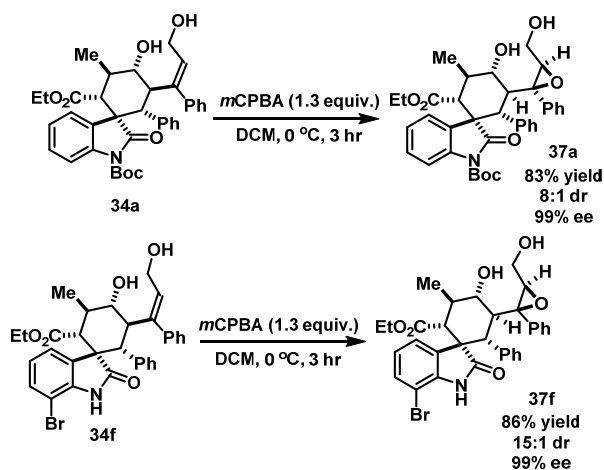


Figure 25. Synthetic manipulation of the cascade product. The stereochemistry of compound **37f** was unambiguously determined by anomalous dispersion X-ray crystallographic analysis (see experimental part).

### 3.2.1. Conclusions

In summary, we have developed an aminocatalytic triple vinylogous cascade reaction, yielding valuable spiro-oxindolic cyclohexane derivatives. The three component domino process proceeds by way of an amino-catalyzed Michael addition/1,6-addition/vinylogous aldolization sequence which combines two intermolecular and one intramolecular bond-forming events while forging six contiguous stereogenic centers with high fidelity. Key to this study was the ability to control the d-site-selectivity of an asymmetric 1,6-addition to linear 2,4-dienals, which was achieved by positioning a directing group within the  $\beta$ -dienal architecture.

### 3.3. Experimental Section

The spectra were recorded at 400 MHz and 500 MHz for  $^1\text{H}$  NMR or at 100 MHz and 125 MHz for  $^{13}\text{C}$  NMR. The chemical shifts ( $\delta$ ) for  $^1\text{H}$  and  $^{13}\text{C}$  are given in ppm relative to residual signals of the solvents ( $\text{CHCl}_3$  @ 7.26 ppm  $^1\text{H}$  NMR, 77.0 ppm  $^{13}\text{C}$  NMR). Coupling constants are given in Hz. Carbon types were determined from DEPT  $^{13}\text{C}$  NMR experiments. When necessary,  $^1\text{H}$  and  $^{13}\text{C}$  signals were assigned by means of g-COSY, g-HSQC and g-HMBC 2D-NMR sequences. The following abbreviations are used to indicate the multiplicity: s, singlet; d, doublet; t, triplet; q, quartet; qn, quintet; m, multiplet; bs, broad signal. High-resolution mass spectra (HRMS) were obtained from the ICIQ High Resolution Mass Spectrometry Unit on Waters GCT gas chromatograph coupled time-of-flight mass spectrometer (GC/MS-TOF) with electron ionization (EI). X-ray data were obtained from the ICIQ X-Ray Unit using a Bruker-Nonius diffractometer equipped with an APPEX 2 4K CCD area detector. Optical rotations are reported as follows:  $[\alpha]_{\text{D}}^{25}$  (c in g per 100 mL, solvent).

***The  $^1\text{H}$ ,  $^{13}\text{C}$  NMR spectra and the HPLC traces are available in the literature<sup>1</sup> and are not reported in the present thesis.***

**General Procedures.** All the catalytic reactions were set up under air and using HPLC grade solvents, without any precautions to exclude moisture, unless otherwise noted - *open air chemistry on the benchtop*. Chromatographic purification of products was accomplished using force-flow chromatography (FC) on silica gel (35-70 mesh). For thin layer chromatography (TLC) analysis throughout this work, Merck precoated TLC plates (silica gel 60 GF<sub>254</sub>, 0.25 mm) were used, using UV light as the visualizing agent and an acidic mixture of ceric ammonium molybdate or basic aqueous potassium permanganate ( $\text{KMnO}_4$ ), and heat as developing agents. Organic solutions were concentrated under reduced pressure on a Büchi rotary evaporator.

**Determination of Diastereomeric Ratios:** The diastereomeric ratio for the products **31** obtained from the vinylogous triple cascade reactions followed by in situ  $\text{NaBH}_4$  reduction to the corresponding alcohols (data detailed in Figure 17, 18, 19 and 25) was determined by  $^1\text{H}$  NMR analysis of the crude reaction mixture.

**Determination of Enantiomeric Purity:** HPLC analysis on chiral stationary phase was performed on an Agilent 1200-series instrumentation. Daicel Chiralpak AD-H, IA, IB or IC columns with EtOH/hexane/DCM as the eluent were used. HPLC traces were compared to racemic samples prepared by mixture of two enantiomeric final products obtained using (*S*) and (*R*) catalysts.

**Determination of Yield and Conversion in the Optimization Studies:** The conversion of the starting materials and the yield of product in the optimization studies related to the model reaction depicted in Table 1 were determined by  $^1\text{H}$  NMR spectroscopy by adding an internal standard to the crude reaction mixture: 1,3,5-trimethoxybenzene:  $\delta$  6.10 ppm (s, 3H). Since in all instances the conversion of the ( $\alpha,\beta,\gamma,\delta$ )-unsaturated aldehyde **30** was equal to the NMR yield of the triple cascade products, in some cases the conversion of the products **31** and **32** (and their relative ratio) was determined by integration of the signals of the unreacted ( $\alpha,\beta,\gamma,\delta$ )-unsaturated aldehyde **30** and the cascade products in the  $^1\text{H}$  NMR spectra: ( $\alpha,\beta,\gamma,\delta$ )-unsaturated aldehyde **30**:  $\delta$  10.3 (dd), 9.45 ppm (dd); cascade product **31**:  $\delta$  10.4 (dd), 9.2 (dd) ppm, and cascade product **32**:  $\delta$  9.1 (s).

**Materials.** Commercial grade reagents and solvents were purchased from Sigma Aldrich, TCI, and Alfa Aesar and used as received without further purification; when necessary, they were purified as recommended.<sup>24</sup> The chiral secondary amine catalyst **III** is commercially available (Aldrich); it was purified by flash column chromatography prior to use and stored at 4°C under argon to avoid undesired desilylation that would affect the catalytic potential of the amine.

---

<sup>24</sup> Armarengo, W. L. F.; Perrin, D. D. In *Purification of Laboratory Chemicals*, 4th ed.; Butterworth Heinemann: Oxford, 1996.

### 3.3.1. Preparation of the Linear 2,4-dienals **30**

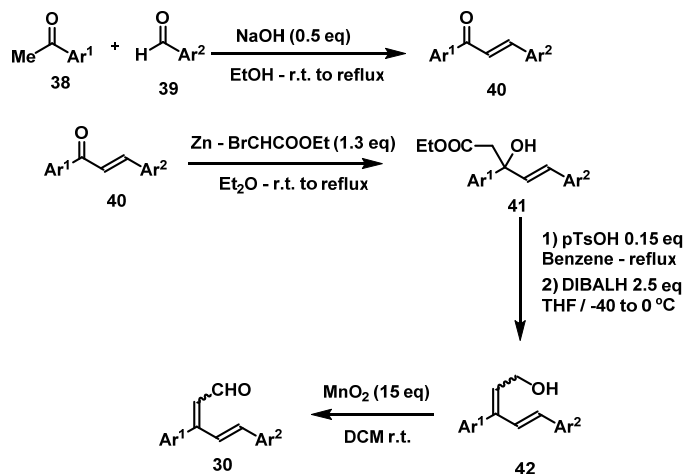


Figure 26. Synthetic route to synthesize  $\beta$ -substituted enals **27**

**General procedure:** The aromatic aldehyde **39** (1.1 equiv) was slowly added to a solution of aromatic ketone **38** (1 M in EtOH). Then a 10% aqueous solution of NaOH (0.5 eq) was added dropwise over a period of 5 minutes. The reaction was stirred overnight until full conversion of the ketone **35** was achieved, as determined by <sup>1</sup>H NMR analysis of the crude mixture. When needed, warming up the reaction to reflux (1-2 h) allowed obtaining full conversion. The pH of the aqueous solution was then adjusted to  $\approx 4$  by slowly adding a 1M HCl solution. The mixture was diluted with water (30 mL for each mmol of starting ketone **38**) and extracted 3 times with diethyl ether (20 mL for each mmol of starting ketone **38**). The organic layers were combined and washed with a saturated solution of sodium bicarbonate and brine. After drying over sodium sulphate, solvents were removed under vacuum affording the crude condensation products **40**.

Freshly activated zinc in pellets was kept in a dry flask under argon atmosphere. For complete activation of the zinc, traces of iodine and 4 mL of dry diethyl ether were added and the solution stirred until decolouration occurred. Then, ethyl bromoacetate (1.1 eq) and a solution of crude condensation product **40** (1.5 M in dry diethyl ether) were added under vigorous stirring. The reaction was refluxed until complete consumption of the starting material was achieved, as judged by TLC analysis (90 min approximately). The reaction mixture was then filtered and diluted with diethyl ether (10 mL for each mmol of **40**), washed with 1 M aqueous solution of HCl, saturated with a solution of sodium bicarbonate and finally with brine. After drying over sodium sulphate, the organic layers were removed under vacuum affording the crude compounds **41**, which were purified through flash chromatography on silica gel

(Hexane/EtOAc 99:1 – 95:5 as the eluent). All the products **41** were obtained with an overall yield over two steps of 60 – 80%.

**General procedure for preparing compounds 42.** The alcohol **41** was dissolved in benzene (0.2 M solution) and heated up to reflux. *p*-Toluensulfonic acid (0.15 eq) was added all at once to the boiling mixture. The reaction was stirred until complete consumption of the starting material, as judged by TLC analysis (approximately 30 minutes). A saturated solution of sodium bicarbonate served to quench the reaction (20 mL for each mmol of **41**) and the mixture was extracted three times with diethyl ether (10 mL). The organic layers were collected, washed with brine (10 mL) and dried over sodium sulphate. Quick chromatographic purification (hexane:EtOAc 99:1- 97:3) afforded the crude elimination product as an oil, which was employed in the next step without further purification. The crude elimination product was placed in a dry flask and dissolved in dry THF (0.2 M solution) or toluene. The solution was then cold to -40°C and 2.5 eq of DIBAL-H (1 M solution in hexanes) was added dropwise over a period of 20 minutes. The reaction was then stirred for further 60 minutes at 0 °C. A saturated solution of Rochelle's salt in water (10 mL for each mmol of the starting material) was then carefully added dropwise at 0 °C in order to quench the reaction. The mixture was stirred 2 h at room temperature and then extracted 3 times with diethyl ether. The combined organic layers were washed with brine and dried over sodium sulphate. Removal of the solvent under vacuum and purification through flash chromatography on silica gel (hexanes/EtOAc 95:5 to 80:20 as the eluent) afforded the compound **42** as a colourless oil. All the products **42** were obtained with an overall yield over two steps of 40 – 60%.

**Preparation of 2,4-dienals 30:** Compound **42** was dissolved in dry DCM (0.1 M solution) under an argon atmosphere. Then, activated MnO<sub>2</sub> (15 eq) was added to the solution and the reaction stirred until complete consumption of the starting material, as determined by TLC analysis (generally 16 hours). The reaction mixture was then filtered through a pad of Celite and solvents were removed in vacuo to afford the crude product. Purification by flash chromatography on silica gel (Hexanes/EtOAc 90:10) afforded the enals **30** as a mixture of geometrical isomers. The yield of the oxidation was ranging from 90 to 99%.



### 3.3.2. Preparation of 3-olefinic Oxindoles 24.

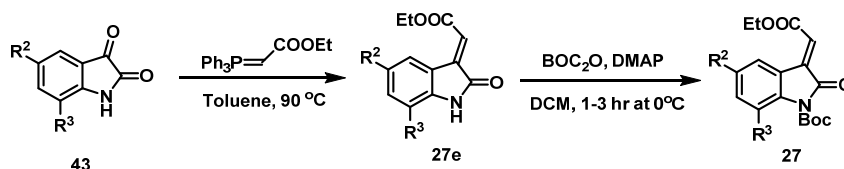
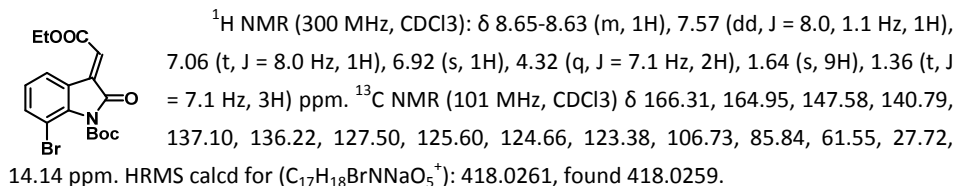


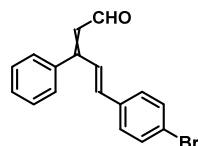
Figure 27. Synthetic pathway for the synthesis of 3-olefinic oxindoles.

Commercially available isatin **43** derivatives were mixed with Wittig reagents (1.1 equiv.) in toluene and the reaction mixtures were heated up to 90 °C for 30 min. After cooling, the mixture was filtered through a pad of silica and solvent was evaporated to have the crude Wittig product. The crude product was dissolved in DCM and mixed with 4-(dimethylamino)pyridine (10-20 mol%). The reaction mixture was cooled down to 0 °C and di-*tert*-butyl-dicarbonate (1.1 equiv.) was added to the reaction mixture. The reaction was monitored by TLC. The solvent was removed under reduced pressure and the crude reaction mixture was purified by FC to yield the 3-olefinic oxindoles **27**.<sup>25</sup>

*tert*-butyl (E)-7-bromo-3-(2-ethoxy-2-oxoethylidene)-2-oxoindoline-1-carboxylate (**27g**).



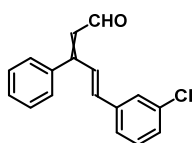
(4E)-5-(4-methoxyphenyl)-3-phenylpenta-2,4-dienal **30k** obtained as a mixture of isomers (2.3:1): <sup>1</sup>H NMR (500 MHz, CDCl<sub>3</sub>)<sub>(major)</sub>: δ 10.27 (d, *J* = 7.5 Hz, 1H), 7.66 (d, *J* = 15.8 Hz, 1H), 7.52-7.45 (m, 5H), 7.42-7.33 (m, 2H), 6.93 (m, 2H), 6.89 (m, 1H), 6.77 (d, *J* = 15.8 Hz, 1H), 6.15 (d, *J* = 7.6 Hz, 1H), 3.87 (s, 3H) ppm. <sup>13</sup>C NMR (126 MHz, CDCl<sub>3</sub>)<sub>(mixture)</sub>: δ 193.6, 190.6, 160.8, 160.7, 160.5, 158.7, 141.2, 139.9, 139.3, 134.9, 129.9, 129.5, 129.1, 129.0, 128.9, 128.8, 128.6, 128.6, 128.5, 128.5, 128.3, 127.1, 121.0, 114.4, 114.3, 55.4, 55.4 ppm. HRMS calcd for (C<sub>18</sub>H<sub>16</sub>NaO<sub>2</sub><sup>+</sup>): 287.1043, found 287.1049.



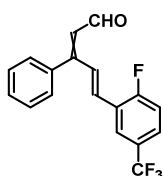
(4E)-5-(4-bromophenyl)-3-phenylpenta-2,4-dienal **30l** obtained as a mixture of isomers (1:3.7): <sup>1</sup>H NMR (400 MHz, CDCl<sub>3</sub>)<sub>(mixture)</sub>: δ 9.44 (d, *J* = 8.2 Hz, 1H), 7.5-7.46 (m, 5H), 7.33- 7.31 (m, 2H), 7.29-7.27 (m, 2H), 7.11 (d, *J* = 16.5 Hz, 1H), 6.53 (d, *J* = 15.9 Hz, 1H), 6.25 (d, *J* = 8.2 Hz, 1H)

<sup>25</sup> Halskov, K. S.; Johansen, T. K.; Davis, R. L.; Steurer, M.; Jensen, F.; Jørgensen, K. A. *J. Am. Chem. Soc.* **2012**, *134*, 12943.

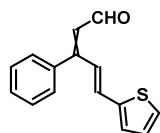
ppm.  $^{13}\text{C}$  NMR (126 MHz,  $\text{CDCl}_3$ )<sub>(mixture)</sub>:  $\delta$   $^{13}\text{C}$  NMR (126 MHz,  $\text{CDCl}_3$ )  $\delta$  193.5, 190.4, 159.5, 140.0, 138.7, 134.7, 134.4, 132.1, 132.0, 131.3, 130.1, 129.8, 129.7, 129.0, 128.9, 128.8, 128.7, 128.5, 128.0, 124.0, 123.5, 123.5 ppm. HRMS *calcd* for  $(\text{C}_{17}\text{H}_{13}\text{BrNaO}^+)$ : 335.0042, found 335.0047.



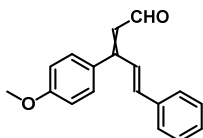
(4E)-5-(3-chlorophenyl)-3-phenylpenta-2,4-dienal **30m** was obtained as a mixture of isomers (2.1:1):  $^1\text{H}$  NMR (400 MHz,  $\text{CDCl}_3$ )<sub>(major)</sub>:  $\delta$  10.27 (d,  $J = 7.4$  Hz, 1H), 7.76 (d,  $J = 15.9$  Hz, 1H), 7.54-7.26 (m, 9H), 6.75 (d,  $J = 15.9$  Hz, 1H), 6.23 (d,  $J = 7.4$  Hz, 1H) ppm.  $^{13}\text{C}$  NMR (101 MHz,  $\text{CDCl}_3$ )<sub>(mixture)</sub>:  $\delta$  193.5, 190.4, 159.3, 157.5, 139.7, 138.7, 138.4, 137.7, 137.6, 135.0, 134.9, 134.4, 132.0, 130.3, 130.1, 130.0, 129.8, 129.8, 129.3, 129.2, 129.1, 128.7, 128.5, 128.5, 128.5, 128.2, 127.3, 127.3, 125.6, 124.7. HRMS *calcd* for  $(\text{C}_{17}\text{H}_{13}\text{ClNaO}^+)$ : 291.0547, found 291.0548



(4E)-5-(2-fluoro-5-(trifluoromethyl)phenyl)-3-phenylpenta-2,4-dienal **30n** was obtained as a mixture of isomers (21:1):  $^1\text{H}$  NMR (400 MHz,  $\text{CDCl}_3$ )<sub>(major)</sub>:  $\delta$  10.26 (d,  $J = 7.4$  Hz, 1H), 7.87 (dd,  $J = 16.1, 0.8$  Hz, 1H), 7.63-7.55 (m, 1H), 7.82 (dd,  $J = 6.7, 2.3$  Hz, 1H), 7.52-7.42 (m, 5H), 7.26-7.16 (m, 1H), 6.90 (d,  $J = 16.1$  Hz, 1H), 6.26 (d,  $J = 7.5$  Hz, 1H) ppm.  $^{13}\text{C}$  NMR (101 MHz,  $\text{CDCl}_3$ )<sub>(major)</sub>:  $\delta$  190.4, 163.5, 157.2, 138.3, 132.1 (d,  $J = 2.2$  Hz), 129.9, 128.8, 128.8, 128.4, 127.8 (d,  $J = 6.7$  Hz), 127.7-127.3 (m), 125.8 (t,  $J = 3.9$  Hz), 124.9, 124.7 (d,  $J = 12.9$  Hz), 122.2, 116.9 (d,  $J = 23.6$  Hz). HRMS *calcd* for  $(\text{C}_{18}\text{H}_{12}\text{F}_4\text{NaO}^+)$ : 343.0716, found 343.0708.  $^{19}\text{F}$  NMR (376 MHz,  $\text{CDCl}_3$ )<sub>(major)</sub>:  $\delta$  -62.26, -110.53.

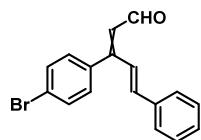


(4E)-3-phenyl-5-(thiophen-2-yl)penta-2,4-dienal **30o** was obtained as a mixture of isomers (4:3:1):  $^1\text{H}$  NMR (500 MHz,  $\text{CDCl}_3$ )<sub>(mixture of major's)</sub>:  $\delta$  10.26 (d,  $J = 7.6$  Hz, 1H), 9.40 (d,  $J = 8.3$  Hz, 1H), 7.60 (d,  $J = 15.6$  Hz, 1H), 7.51-7.39 (m, 9H), 7.37-7.29 (m, 3H), 7.10 (dt,  $J = 3.7, 0.8$  Hz, 1H), 7.06-7.00 (m, 2H), 7.00 (dd,  $J = 5.0, 3.6$  Hz, 1H), 6.93 (d,  $J = 15.6$  Hz, 1H), 6.89 (d,  $J = 15.6$  Hz, 1H), 6.70 (d,  $J = 15.6$  Hz, 1H), 6.21 (d,  $J = 8.4$  Hz, 1H), 6.09 (d,  $J = 7.6$  Hz, 1H) ppm.  $^{13}\text{C}$  NMR (126 MHz,  $\text{CDCl}_3$ )<sub>(mixture)</sub>:  $\delta$  193.4, 191.2, 190.2, 159.7, 157.8, 157.6, 141.4, 141.3, 140.6, 138.9, 134.5, 134.0, 132.7, 130.1, 130.0, 129.8, 129.6, 129.3, 129.3, 128.9, 128.8, 128.6, 128.6, 128.4, 128.4, 128.1, 128.1, 127.5, 127.5, 127.4, 127.3, 126.3, 122.5. HRMS *calcd* for  $(\text{C}_{15}\text{H}_{12}\text{NaOS}^+)$ : 263.0501, found 263.0506.



(4E)-3-(4-methoxyphenyl)-5-phenylpenta-2,4-dienal **30p** was obtained as a mixture of isomers (6:1):  $^1\text{H}$  NMR (500 MHz,  $\text{CDCl}_3$ )<sub>(major)</sub>:  $\delta$  10.18 (d,  $J = 7.7$  Hz, 1H), 7.60 (d,  $J = 15.9$  Hz, 1H), 7.51 (d,  $J = 7.1$  Hz, 2H), 7.44 (d,  $J = 8.9$  Hz, 2H), 7.42-7.33 (m, 3H), 6.96 (d,  $J = 8.9$  Hz, 2H), 6.85 (d,  $J$

= 15.9 Hz, 1H), 6.22 (d,  $J = 7.7$  Hz, 1H), 3.87 (s, 3H) ppm.  $^{13}\text{C}$  NMR (126 MHz,  $\text{CDCl}_3$ )<sub>(major)</sub>:  $\delta$  190.9, 161.2, 158.1, 141.2, 131.4, 131.2, 123.0, 129.4, 128.9, 127.4, 126.8, 123.5, 114.1, 55.4 ppm. HRMS *calcd* for  $(\text{C}_{18}\text{H}_{16}\text{NaO}_2)^+$ : 287.1043, found 287.1048.



(4E)-3-(4-bromophenyl)-5-phenylpenta-2,4-dienal **30q** as a mixture of isomers (2:1):  $^1\text{H}$  NMR (500 MHz,  $\text{CDCl}_3$ )<sub>(major)</sub>:  $\delta$  10.24 (d,  $J = 7.4$  Hz, 1H), 7.71 (d,  $J = 15.9$  Hz, 1H), 7.63 (d,  $J = 8.4$  Hz, 1H), 7.58 (d,  $J = 8.6$  Hz, 2H), 7.49 (d,  $J = 7.7$  Hz, 2H), 7.46-7.29 (m, 3H), 7.22 (d,  $J = 8.4$  Hz, 1H), 6.77 (d,  $J = 15.9$  Hz, 1H), 6.14 (d,  $J = 7.4$  Hz, 1H) ppm.  $^{13}\text{C}$  NMR (126 MHz,  $\text{CDCl}_3$ )<sub>(mixture)</sub>:  $\delta$  193.0, 190.4, 158.5, 156.9, 141.7, 140.3, 140.3, 137.9, 135.6, 135.6, 133.5, 131.9, 131.7, 131.4, 130.2, 130.1, 129.9, 129.6, 129.6, 129.0, 127.7, 127.5, 127.5, 124.0, 123.3, 122.8. HRMS *calcd* for  $(\text{C}_{17}\text{H}_{13}\text{BrNaO}^+)$ : 335.0042, found 335.0046.

### 3.3.3. General Procedure of the Triple Vinylogous Cascade Reactions.

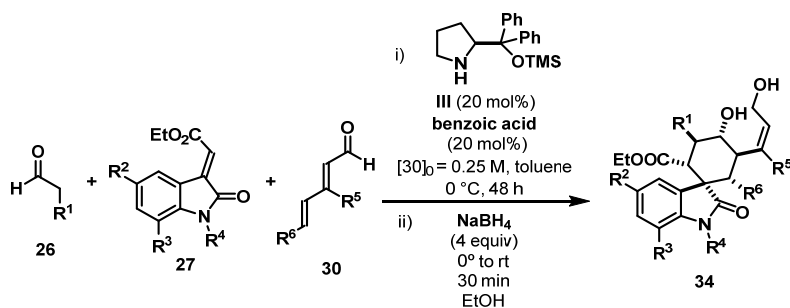


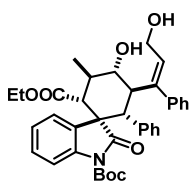
Figure 28. Triple vinylogous cascade reaction

All the reactions were carried out in toluene (synthesis grade, >99%), without any precaution to exclude air and moisture (open air chemistry on the benchtop). An ordinary vial equipped with a Teflon-coated stir bar and a plastic screw cap was charged with amine **II** (0.02 mmol, 6.5 mg, 20 mol %). Then toluene (0.4 mL, 0.25 M) and the oxindole-bearing substrate **27** (1.2 equiv., 0.12 mmol) were sequentially added. The reaction mixture was stirred in a cooling bath maintained at 0 °C for 5 minutes to let the mixture reaching a uniform temperature. The reaction was started by the addition of **26** (1 equiv., 0.1 mmol) and the reaction mixture was stirred at 0 °C for 1 hr. After that,  $\alpha,\beta,\gamma,\delta$ -unsaturated aldehyde **30** (1 equiv., 0.1 mmol) was added and the vial was sealed and immersed in the cooling bath again (maintained at 0 °C). Stirring was continued over 48 hr. The progress of the reaction was monitored by TLC and by  $^1\text{H}$  NMR analysis of the aliquot taken from the crude mixture. Upon completion of the reaction, the mixture (still at 0 °C) was diluted with 1.0 mL of EtOH; solid  $\text{NaBH}_4$  (0.4 mmol, 4 equiv) was added in one portion. Frothing occurs but is readily controllable through magnetic stirring of the solution. After 30 minutes, the mixture was quenched with few drops of water. Brine (5 mL) was

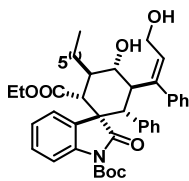
added and the resulting mixture extracted with DCM (3 × 10 mL). The combined organics were washed with brine (5 mL), dried over MgSO<sub>4</sub>, filtered and concentrated *in vacuo*. The crude mixture was analyzed by <sup>1</sup>H NMR spectroscopy to determine the *d.r.* (key signal of the olefinic proton) of the reaction. The product **34** was isolated by flash column chromatography.

### 3.3.4. Characterization of the Cascade Products

It is to be noted that the spectroscopic characterization of some of the cascade products **34** revealed a difficult integration for the aromatic protons. In some cases, the number of carbon atoms in the <sup>13</sup>C NMR analysis was not matching the expected number too. All the attempts to address these issues, by means of low temperature NMR spectroscopy and time resolving study (time delay during proton scan), have met with failure. However, the high-resolution mass spectra (HRMS) obtained for all the compounds and the X-ray crystallographic analysis of compound **34e** unambiguously supported the structural identity of the cascade products **34**.

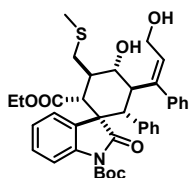


The reaction was carried out following the general procedure to furnish the crude product as a 10:1 mixture of diastereoisomers; *d.r.* determined by integration of <sup>1</sup>H NMR signal:  $\delta_{\text{major}}$  5.63 (t),  $\delta_{\text{minor}}$  5.47 ppm (t). The title compound **34a** was isolated by flash column chromatography (eluent hexane/ethyl acetate = 1.5/1) in 75% yield (45.8 mg) as a single diastereomer. The enantiomeric excess was determined to be 99% by HPLC analysis on a Daicel Chiralpak IC column: 67/30/3 hexane/DCM/EtOH, flow rate 0.8 mL/min,  $\lambda$  = 254 nm:  $\tau_{\text{Major}}$  = 56.9 min,  $\tau_{\text{Minor}}$  = 13.8 min.  $[\alpha]_{\text{D}}^{26} = +22.7$  (*c* = 0.68, CHCl<sub>3</sub>). HRMS *calcd* for (C<sub>37</sub>H<sub>41</sub>NNaO<sub>7</sub><sup>+</sup>): 634.2775, found 634.2779. <sup>1</sup>H NMR (300 MHz, CDCl<sub>3</sub>):  $\delta$  7.29-6.69 (m, 14H), 5.64 (t, *J* = 7.2 Hz, 1H), 4.62-4.55 (m, 2H), 4.20 (dd, *J* = 11.9, 7.0 Hz, 1H), 3.82-3.75 (m, 2H), 3.61 (t, *J* = 9.9 Hz, 1H), 3.19-3.10 (m, 1H), 2.77 (d, *J* = 8.3 Hz, 1H), 2.73 (d, *J* = 8.2 Hz, 1H), 1.56 (s, 9H), 1.16 (d, *J* = 6.5 Hz, 3H), 0.83 (t, *J* = 7.1 Hz, 3H) ppm. <sup>13</sup>C NMR (75 MHz, CDCl<sub>3</sub>):  $\delta$  175.0, 170.7, 148.5, 143.9, 140.6, 139.2, 135.4, 133.0, 128.9, 128.8, 128.3, 127.5, 127.1, 127.0, 123.7, 122.3, 114.4, 100.0, 83.7, 74.7, 60.6, 57.9, 57.1, 53.8, 53.3, 43.4, 35.4, 28.1, 16.2, 13.6 ppm.

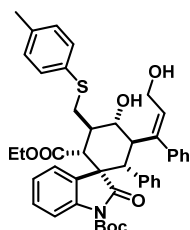


The reaction was carried out following the general procedure to furnish the crude product as a 5:1 mixture of diastereoisomers; *d.r.* determined by integration of <sup>1</sup>H NMR signal:  $\delta_{\text{major}}$  5.63 (t),  $\delta_{\text{minor}}$  5.50 ppm (t). The title compound **34b** was isolated by flash column chromatography (eluent hexane/ethyl acetate = 2.5/1) in 49% yield (33.5 mg) as a single diastereomer. The enantiomeric excess was determined to be 99% by HPLC analysis on a Daicel Chiralpak IC column: 67/30/3 hexane/DCM/EtOH, flow rate 0.8 mL/min,  $\lambda$  = 254 nm:  $\tau_{\text{Major}}$  = 35.2 min,  $\tau_{\text{Minor}}$  = 8.5 min.  $[\alpha]_{\text{D}}^{26} = +19.1$  (*c* = 1.15, CHCl<sub>3</sub>). HRMS *calcd* for (C<sub>42</sub>H<sub>51</sub>NNaO<sub>7</sub><sup>+</sup>): 704.3558, found 704.3552. <sup>1</sup>H NMR (500 MHz, CDCl<sub>3</sub>):  $\delta$  7.28-6.67 (m, 14H), 5.63 (t, *J* = 7.3 Hz, 1H), 4.6-4.55

(m, 2H), 4.20 (dd,  $J = 11.9, 6.9$  Hz, 1H), 3.81 (t,  $J = 10.1$  Hz, 1H), 3.76 (dd,  $J = 7.1, 1.4$  Hz, 2H), 3.17-3.11 (m, 1H), 2.90 (d,  $J = 12.1$  Hz, 1H), 2.72 (d,  $J = 12.0$  Hz, 1H), 1.80-1.73 (m, 1H), 1.56 (s, 9H), 1.48-1.43 (m, 1H), 1.34-1.25 (m, 8H), 0.88 (t,  $J = 6.8$  Hz, 3H), 0.82 (t,  $J = 7.1$  Hz, 3H) ppm.  $^{13}\text{C}$  NMR (126 MHz,  $\text{CDCl}_3$ )  $\delta$  175.0, 170.9, 148.5, 143.9, 140.7, 139.2, 135.4, 133.1, 128.8, 128.3, 127.5, 127.0, 127.0, 123.7, 122.4, 114.4, 83.6, 71.8, 60.5, 57.9, 54.9, 53.9, 53.2, 43.4, 39.4, 31.8, 30.0, 29.3, 28.1, 24.5, 22.7, 14.1, 13.5 ppm.

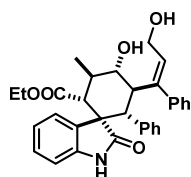


The reaction was carried out following the general procedure to furnish the crude product as a 17:1 mixture of diastereoisomers; d.r. determined by integration of  $^1\text{H}$  NMR signal:  $\delta_{\text{major}}$  5.65 (t),  $\delta_{\text{minor}}$  5.52 ppm (t). The title compound **34c** was isolated by flash column chromatography (eluent hexane/ethyl acetate = 2/1) in 52% yield (34.5 mg) as a single diastereomer. The enantiomeric excess was determined to be 99% by HPLC analysis on a Daicel Chiralpak IC column: 67/30/3 hexane/DCM/EtOH, flow rate 0.8 mL/min,  $\lambda = 254$  nm:  $\tau_{\text{Major}} = 26.0$  min,  $\tau_{\text{Minor}} = 12.7$  min.  $[\alpha]_{\text{D}}^{26} = +20.8$  ( $c = 0.65$ ,  $\text{CHCl}_3$ ). HRMS *calcd* for ( $\text{C}_{38}\text{H}_{43}\text{NNaO}_7\text{S}^+$ ): 680.2652, found 680.2653.  $^1\text{H}$  NMR (500 MHz,  $\text{CDCl}_3$ ):  $\delta$  7.33-6.99 (m, 12H), 6.70-6.69 (m, 2H), 5.65 (t,  $J = 7.3$  Hz, 1H), 4.62-4.56 (m, 2H), 4.16 (dd,  $J = 11.8, 6.9$  Hz, 1H), 4.03 (t,  $J = 9.9$  Hz, 1H), 3.78 (q,  $J = 7.1$  Hz, 2H), 3.45-3.39 (m, 1H), 3.09-3.03 (m, 2H), 2.75 (d,  $J = 12.0$  Hz, 1H), 2.68 (dd,  $J = 13.9, 4.3$  Hz, 1H), 2.24 (s, 3H), 1.56 (s, 9H), 0.82 (t,  $J = 7.1$  Hz, 3H) ppm.  $^{13}\text{C}$  NMR (126 MHz,  $\text{CDCl}_3$ ):  $\delta$  175.1, 170.5, 148.4, 143.7, 140.5, 139.2, 135.2, 133.0, 128.9, 128.6, 128.4, 127.5, 127.1, 127.1, 123.7, 122.5, 114.4, 83.7, 71.4, 60.8, 57.8, 53.8, 53.8, 52.9, 42.9, 39.6, 35.4, 28.1, 17.0, 13.5 ppm.

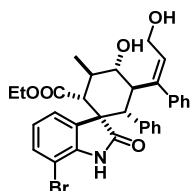


The reaction was carried out following the general procedure to furnish the crude product as a 6.3:1 mixture of diastereoisomers; d.r. determined by integration of  $^1\text{H}$  NMR signal:  $\delta_{\text{major}}$  5.59 (t),  $\delta_{\text{minor}}$  5.48 ppm (t). The title compound **34d** was isolated by flash column chromatography (eluent hexane/ethyl acetate = 1.5/1) in 42% yield (31 mg) as a single diastereomer. The enantiomeric excess was determined to be 99% by HPLC analysis on a Daicel Chiralpak IC column: 67/30/3 hexane/DCM/EtOH, flow rate 0.8 mL/min,  $\lambda = 254$  nm:  $\tau_{\text{Major}} = 52.3$  min,  $\tau_{\text{Minor}} = 11.9$  min.  $[\alpha]_{\text{D}}^{26} = +27.4$  ( $c = 0.65$ ,  $\text{CHCl}_3$ ). HRMS *calcd* for ( $\text{C}_{44}\text{H}_{47}\text{NNaO}_7\text{S}^+$ ): 756.2965, found 756.2966.  $^1\text{H}$  NMR (500 MHz,  $\text{CDCl}_3$ ):  $\delta$  7.47-7.44 (m, 2H), 7.32-7.28 (m, 1H), 7.24-7.12 (m, 9H), 7.07-6.98 (m, 4H), 6.52-6.50 (m, 2H), 5.59 (t,  $J = 7.4$  Hz, 1H), 4.56-4.50 (m, 2H), 4.11 (dd,  $J = 11.7, 7.0$  Hz, 1H), 4.04 (t,  $J = 10.0$  Hz, 1H), 3.78 (q,  $J = 7.1$  Hz, 2H), 3.61 (dd,  $J = 14.1, 4.0$  Hz, 1H), 3.53-3.47 (m, 1H), 3.23 (d,  $J = 11.9$  Hz, 1H), 3.05 (dd,  $J = 14.0, 3.2$  Hz, 1H), 2.72 (d,  $J = 12.0$  Hz, 1H), 2.35 (s, 3H), 1.55 (s, 9H), 0.81 (t,  $J = 7.1$  Hz, 3H) ppm.  $^{13}\text{C}$  NMR (126 MHz,  $\text{CDCl}_3$ ):  $\delta$  175.1, 170.4, 148.4, 143.3, 140.5, 139.3, 136.7, 135.2, 133.3,

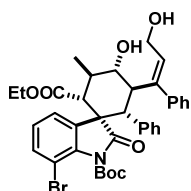
133.3, 130.8, 129.9, 129.9, 128.8, 128.7, 128.4, 127.5, 127.1, 127.0, 123.7, 122.5, 114.4, 83.7, 70.2, 60.9, 57.8, 53.7, 53.2, 52.9, 42.6, 40.4, 35.9, 28.1, 21.1, 13.5 ppm.



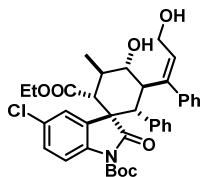
The reaction was carried out following the general procedure to furnish the crude product as a 11:1 mixture of diastereoisomers; d.r. determined by integration of  $^1\text{H}$  NMR signal:  $\delta_{\text{major}}$  5.64 (t),  $\delta_{\text{minor}}$  5.54 ppm (t). The title compound **34e** was isolated by flash column chromatography (eluent hexane/ethyl acetate = 1/1.2) in 56% yield (28.7 mg) as a single diastereomer. The enantiomeric excess was determined to be 99% by HPLC analysis on a Daicel Chiralpak IC column: 67/30/3 hexane/DCM/EtOH, flow rate 0.8 mL/min,  $\lambda = 254$  nm:  $\tau_{\text{Major}} = 114.4$  min,  $\tau_{\text{Minor}} = 105.7$  min.  $[\alpha]_{\text{D}}^{26} = +28.3$  ( $c = 0.5$ ,  $\text{CHCl}_3$ ). HRMS *calcd* for ( $\text{C}_{32}\text{H}_{33}\text{NNaO}_5^+$ ): 534.2251, found 534.2253.  $^1\text{H}$  NMR (300 MHz,  $\text{CDCl}_3$ ):  $\delta$  7.71 (s, 1H), 7.24- 6.65 (m, 13H), 6.39 (d,  $J = 7.7$  Hz, 1H), 5.63 (t,  $J = 7.2$  Hz, 1H), 4.82- 4.61 (m, 2H), 4.20 (dd,  $J = 12.0$ , 6.6 Hz, 1H), 3.77 (q,  $J = 7.2$ , 6.4 Hz, 2H), 3.61 (t,  $J = 9.9$  Hz, 1H), 3.26- 3.07 (m, 1H), 2.83 (d,  $J = 11.9$  Hz, 1H), 2.76 (d,  $J = 11.9$  Hz, 1H), 1.16 (d,  $J = 6.4$  Hz, 3H), 0.79 (t,  $J = 7.1$  Hz, 3H) ppm.  $^{13}\text{C}$  NMR (126 MHz,  $\text{CDCl}_3$ ):  $\delta$  178.9, 171.3, 143.7, 140.9, 140.2, 136.0, 133.0, 130.4, 129.0, 128.1, 127.4, 126.9, 126.8, 123.0, 121.7, 109.1, 74.9, 60.4, 58.0, 57.0, 54.4, 52.5, 43.3, 35.3, 16.3, 13.7.



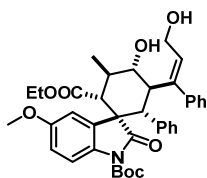
The reaction was carried out following the general procedure to furnish the crude product as a 10:1 mixture of diastereoisomers; d.r. determined by integration of  $^1\text{H}$  NMR signal:  $\delta_{\text{major}}$  5.64 (t),  $\delta_{\text{minor}}$  5.54 ppm (t). The title compound **34f** was isolated by flash column chromatography (eluent hexane/ethyl acetate = 1/2) in 77% yield (45 mg) as a single diastereomer. The enantiomeric excess was determined to be 99% by HPLC analysis on a Daicel Chiralpak IC column: 67/30/3 hexane/DCM/EtOH, flow rate 0.8 mL/min,  $\lambda = 254$  nm:  $\tau_{\text{Major}} = 86.8$  min,  $\tau_{\text{Minor}} = 55.0$  min.  $[\alpha]_{\text{D}}^{26} = +24.9$  ( $c = 0.85$ ,  $\text{CHCl}_3$ ). HRMS *calcd* for ( $\text{C}_{32}\text{H}_{32}\text{BrNNaO}_5^+$ ): 612.1356, found 612.1359.  $^1\text{H}$  NMR (500 MHz,  $\text{CDCl}_3$ ):  $\delta$  7.66 (s, 1H), 7.36-6.70 (m, 13H), 5.64 (dd,  $J = 7.7$ , 6.7 Hz, 1H), 4.72-4.63 (m, 2H), 4.19 (dd,  $J = 11.9$ , 6.7 Hz, 1H), 3.86-3.81 (m, 2H), 3.19-3.11 (m, 1H), 3.62 (t,  $J = 9.9$  Hz, 1H), 2.80 (d,  $J = 11.9$  Hz, 1H), 2.73 (d,  $J = 11.8$  Hz, 1H), 1.17 (d,  $J = 6.4$  Hz, 3H), 0.84 (t,  $J = 7.1$  Hz, 3H).ppm.  $^{13}\text{C}$  NMR (126 MHz,  $\text{CDCl}_3$ ):  $\delta$  177.5, 170.9, 143.8, 140.7, 139.7, 135.5, 133.1, 131.8, 130.8, 129.0, 127.5, 127.1, 126.9, 123.0, 121.9, 102.0, 74.7, 60.6, 57.9, 57.0, 55.9, 52.6, 43.2, 35.2, 16.2, 13.7 ppm.



The reaction was carried out following the general procedure to furnish the crude product as a 10:1 mixture of diastereoisomers; d.r. determined by integration of  $^1\text{H}$  NMR signal:  $\delta_{\text{major}}$  5.65 (t),  $\delta_{\text{minor}}$  5.47 ppm (t). The title compound **34g** was isolated by flash column chromatography (eluent hexane/ethyl acetate = 1.5/1) in 52% yield (36 mg) as a single diastereomer. The enantiomeric excess was determined to be 99% by HPLC analysis on a Daicel Chiralpak IC column: 67/30/3 hexane/DCM/EtOH, flow rate 0.8 mL/min,  $\lambda = 254$  nm:  $\tau_{\text{Major}} = 28.6$  min,  $\tau_{\text{Minor}} = 14.8$  min.  $[\alpha]_{\text{D}}^{26} = -13.5$  ( $c = 0.55$ ,  $\text{CHCl}_3$ ). HRMS *calcd* for  $(\text{C}_{37}\text{H}_{40}\text{BrNNaO}_7^+)$ : 712.1880, found 712.1878.  $^1\text{H}$  NMR (400 MHz,  $\text{CDCl}_3$ ):  $\delta$  7.28-6.67 (m, 13H), 5.65 (t,  $J = 7.3$  Hz, 1H), 4.62-4.56 (m, 2H), 4.20 (dd,  $J = 11.9, 7.0$  Hz, 1H), 3.87-3.78 (m, 2H), 3.60 (t,  $J = 9.9$  Hz, 1H), 3.08-3.01 (m, 1H), 2.78 (d,  $J = 12.0$  Hz, 1H), 2.67 (d,  $J = 11.9$  Hz, 1H), 1.56 (s, 9H), 1.14 (d,  $J = 6.5$  Hz, 3H), 0.88 (t,  $J = 7.1$  Hz, 3H) ppm.  $^{13}\text{C}$  NMR (101 MHz,  $\text{CDCl}_3$ ):  $\delta$  174.9, 170.1, 147.0, 143.8, 140.5, 138.2, 135.0, 133.1, 133.0, 132.4, 128.9, 127.5, 127.3, 127.1, 124.7, 121.6, 106.1, 84.7, 74.6, 60.9, 57.9, 57.5, 55.1, 52.9, 43.4, 35.4, 27.7, 16.1, 13.6 ppm.

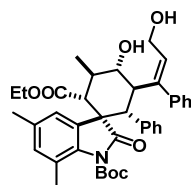


The reaction was carried out following the general procedure to furnish the crude product as a 10:1 mixture of diastereoisomers; d.r. determined by integration of  $^1\text{H}$  NMR signal:  $\delta_{\text{major}}$  5.64 (t),  $\delta_{\text{minor}}$  5.51 ppm (t). The title compound **34h** was isolated by flash column chromatography (eluent hexane/ethyl acetate = 1.5/1) in 70% yield (46 mg) as a single diastereomer. The enantiomeric excess was determined to be 99% by HPLC analysis on a Daicel Chiralpak IC column: 67/30/3 hexane/DCM/EtOH, flow rate 0.8 mL/min,  $\lambda = 254$  nm:  $\tau_{\text{Major}} = 49.2$  min,  $\tau_{\text{Minor}} = 11.6$  min.  $[\alpha]_{\text{D}}^{26} = +13.7$  ( $c = 0.5$ ,  $\text{CHCl}_3$ ). HRMS *calcd* for  $(\text{C}_{37}\text{H}_{40}\text{ClNNaO}_7^+)$ : 668.2386, found 668.2387.  $^1\text{H}$  NMR (400 MHz,  $\text{CDCl}_3$ ):  $\delta$  7.26-7.01 (m, 11H), 6.70-6.67 (m, 2H), 5.64 (t,  $J = 7.3$  Hz, 1H), 4.59-4.52 (m, 2H), 4.20 (dd,  $J = 11.9, 7.0$  Hz, 1H), 3.85-3.79 (m, 2H), 3.60 (t,  $J = 9.9$  Hz, 1H), 3.15-3.08 (m, 1H), 2.73 (d,  $J = 6.8$  Hz, 1H), 2.70 (d,  $J = 6.7$  Hz, 1H), 1.56 (s, 9H), 1.17 (d,  $J = 6.5$  Hz, 3H), 0.87 (t,  $J = 7.1$  Hz, 3H) ppm.  $^{13}\text{C}$  NMR (101 MHz,  $\text{CDCl}_3$ ):  $\delta$  174.3, 170.6, 148.3, 143.7, 140.4, 137.9, 135.1, 133.1, 130.9, 129.2, 128.8, 128.4, 127.6, 127.3, 127.2, 122.5, 115.8, 84.1, 74.6, 60.7, 57.9, 56.9, 54.0, 53.3, 43.3, 35.5, 28.1, 16.2, 13.7 ppm.

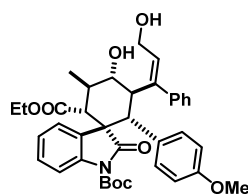


The reaction was carried out following the general procedure to furnish the crude product as a 10:1 mixture of diastereoisomers; d.r. determined by integration of  $^1\text{H}$  NMR signal:  $\delta_{\text{major}}$  5.63 (t),  $\delta_{\text{minor}}$  5.53 ppm (t). The title compound **34i** was isolated by flash column chromatography (eluent hexane/ethyl acetate = 1.5/1) in 76% yield (48.5 mg) as a single diastereomer. The enantiomeric excess was determined to be 99% by HPLC analysis on a Daicel Chiralpak IC column: 67/30/3 hexane/DCM/EtOH, flow rate 0.8

mL/min,  $\lambda = 254$  nm:  $\tau_{Major} = 67.6$  min,  $\tau_{Minor} = 15.2$  min.  $[\alpha]_D^{26} = +54.6$  (c = 0.8, CHCl<sub>3</sub>). HRMS *calcd* for (C<sub>38</sub>H<sub>43</sub>NNaO<sub>8</sub><sup>+</sup>): 664.2881, found 664.2883. <sup>1</sup>H NMR (500 MHz, CDCl<sub>3</sub>):  $\delta$  7.28-6.56 (m, 13H), 5.63 (t, *J* = 7.2 Hz, 1H), 4.62-4.56 (m, 2H), 4.16 (dd, *J* = 11.9, 6.8 Hz, 1H), 3.82-3.77 (m, 2H), 3.74 (s, 3H), 3.61 (t, *J* = 9.9 Hz, 1H), 3.1-3.11 (m, 1H), 2.73 (d, *J* = 11.9 Hz, 1H), 2.69 (d, *J* = 11.9 Hz, 1H), 1.55 (s, 9H) 1.15 (d, *J* = 6.5 Hz, 3H), 0.85 (t, *J* = 7.1 Hz, 3H) ppm. <sup>13</sup>C NMR (126 MHz, CDCl<sub>3</sub>)  $\delta$  175.2, 170.7, 156.4, 148.5, 143.9, 140.7, 135.4, 133.0, 132.7, 130.3, 128.9, 127.5, 127.0, 127.0, 115.4, 112.7, 109.0, 83.5, 74.7, 60.5, 57.8, 57.1, 55.8, 54.2, 53.4, 43.4, 35.5, 28.1, 16.2, 13.6 ppm.



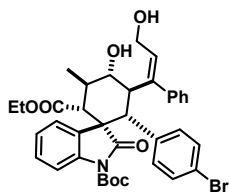
The reaction was carried out following the general procedure to furnish the crude product as a 6:1 mixture of diastereoisomers; d.r. determined by integration of <sup>1</sup>H NMR signal:  $\delta_{major}$  5.63 (t),  $\delta_{minor}$  5.49 ppm (t). The title compound **34j** was isolated by flash column chromatography (eluent hexane/ethyl acetate = 1.5/1) in 66% yield (43 mg) as a single diastereomer. The enantiomeric excess was determined to be 99% by HPLC analysis on a Daicel Chiralpak IC column: 67/30/3 hexane/DCM/EtOH, flow rate 0.8 mL/min,  $\lambda = 254$  nm:  $\tau_{Major} = 52.8$  min,  $\tau_{Minor} = 13.6$  min.  $[\alpha]_D^{26} = +44.8$  (c = 1.15, CHCl<sub>3</sub>). HRMS *calcd* for (C<sub>39</sub>H<sub>45</sub>NNaO<sub>7</sub><sup>+</sup>): 662.3088, found 662.3095. <sup>1</sup>H NMR (500 MHz, CDCl<sub>3</sub>):  $\delta$  7.28-6.65 (m, 12H), 5.63 (t, *J* = 7.3 Hz, 1H), 4.62-4.57 (m, 2H), 4.20 (dd, *J* = 11.9, 6.9 Hz, 1H), 3.84-3.74 (m, 2H), 3.59 (t, *J* = 9.9 Hz, 1H), 3.09-3.03 (m, 1H), 2.77 (d, *J* = 11.9 Hz, 1H), 2.66 (d, *J* = 11.9 Hz, 1H), 2.23 (s, 3H), 1.84 (s, 3H), 1.55 (s, 9H), 1.13 (d, *J* = 6.5 Hz, 3H), 0.83 (t, *J* = 7.1 Hz, 3H) ppm. <sup>13</sup>C NMR (126 MHz, CDCl<sub>3</sub>)  $\delta$  175.7, 170.5, 148.5, 144.0, 140.7, 135.6, 135.6, 133.1, 133.0, 131.7, 129.8, 128.9, 127.5, 127.0, 126.9, 122.7, 120.6, 83.7, 74.8, 60.5, 57.9, 57.5, 54.5, 52.9, 43.5, 35.4, 27.8, 20.9, 19.1, 16.2, 13.5 ppm.



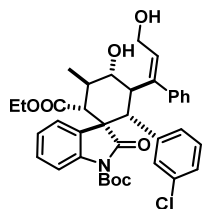
The reaction was carried out following the general procedure to furnish the crude product as a 8:1 mixture of diastereoisomers; d.r. determined by integration of <sup>1</sup>H NMR signal:  $\delta_{major}$  5.65 (t),  $\delta_{minor}$  5.48 ppm (t). The title compound **34k** was isolated by flash column chromatography (eluent hexane/ethyl acetate = 1.5/1) in 60% yield (32.3 mg) as a single diastereomer. The enantiomeric excess was determined to be 99% by HPLC analysis on a Daicel Chiralpak IC column: 67/30/3 hexane/DCM/EtOH, flow rate 0.8 mL/min,  $\lambda = 254$  nm:  $\tau_{Major} = 52.3$  min,  $\tau_{Minor} = 14.5$  min.  $[\alpha]_D^{26} = 19$  (c = 1.7, CHCl<sub>3</sub>). HRMS *calcd* for (C<sub>38</sub>H<sub>43</sub>NNaO<sub>8</sub><sup>+</sup>): 664.2881, found 664.2896. <sup>1</sup>H NMR (400 MHz, CDCl<sub>3</sub>):  $\delta$  7.31-6.72 (m, 13H), 5.64 (t, *J* = 7.3 Hz, 1H), 4.61-4.51 (m, 2H), 4.18 (dd, *J* = 11.9, 6.9 Hz, 1H), 3.77 (qd, *J* = 7.1, 1.5 Hz, 2H), 3.65 (s, 3H), 3.59 (t, *J* = 9.9 Hz, 1H), 3.16-3.08 (m, 1H), 2.70 (d, *J* = 11.8 Hz, 2H), 1.57 (s, 9H), 1.14 (d, *J* = 6.5 Hz, 3H), 0.82 (t, *J* = 7.1 Hz, 3H) ppm. <sup>13</sup>C NMR (126 MHz, CDCl<sub>3</sub>)  $\delta$  175.3, 170.8, 158.4, 148.5, 144.0, 140.7, 139.2, 132.9, 129.0, 128.9, 128.3,



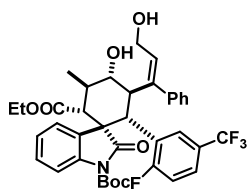
127.5, 127.4, 127.0, 123.7, 122.3, 114.5, 83.7, 74.7, 60.5, 57.8, 57.1, 55.0, 54.0, 52.4, 43.6, 35.4, 28.1, 16.2, 13.6 ppm.



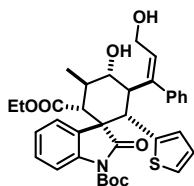
The reaction was carried out following the general procedure to furnish the crude product as a 2:1 mixture of diastereoisomers; d.r. determined by integration of  $^1\text{H}$  NMR signal:  $\delta_{\text{major}}$  5.69 (t),  $\delta_{\text{minor}}$  5.49 ppm (t). The title compound **34l** was isolated by flash column chromatography (eluent hexane/ethyl acetate = 1.2/1) in 61% yield (42 mg) as a mixture of both diastereomer. The enantiomeric excess was determined to be 99% by HPLC analysis on a Daicel Chiralpak IC column: 67/30/3 hexane/DCM/EtOH, flow rate 0.8 mL/min,  $\lambda = 254$  nm:  $\tau_{\text{Major}} = 52.6$  min,  $\tau_{\text{Minor}} = 13.2$  min.  $[\alpha]_{\text{D}}^{26} = -30.2$  ( $c = 0.43$ ,  $\text{CHCl}_3$ ). HRMS *calcd* for ( $\text{C}_{37}\text{H}_{40}\text{BrNNaO}_7^+$ ): 712.1880, found 712.1893.  $^1\text{H}$  NMR (400 MHz,  $\text{CDCl}_3$ ) (of major diastereomer):  $\delta$  7.29-7.01 (m, 11H), 6.71- 6.69 (m, 2H), 5.67 (t,  $J = 7.2$  Hz, 1H), 4.59-4.52 (m, 2H), 4.18 (dd,  $J = 11.9$ , 6.9 Hz, 1H), 3.81-3.76 (m, 2H), 3.62 (t,  $J = 9.9$  Hz, 1H), 3.15-3.08 (m, 1H), 2.72 (d,  $J = 11.9$  Hz, 2H), 1.57 (s, 9H), 1.16 (d,  $J = 6.5$  Hz, 3H), 0.83 (t,  $J = 7.1$  Hz, 3H) ppm.  $^{13}\text{C}$  NMR (126 MHz,  $\text{CDCl}_3$ )  $\delta$  175.1, 170.6, 148.2, 143.6, 140.4, 139.1, 134.6, 133.1, 128.7, 128.6, 128.5, 127.6, 127.2, 123.9, 122.2, 121.1, 114.7, 84.0, 74.7, 60.6, 57.8, 57.1, 53.7, 52.7, 43.2, 35.5, 28.1, 16.1, 13.6 ppm.



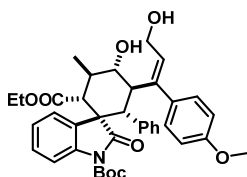
The reaction was carried out following the general procedure to furnish the crude product as a 5:1 mixture of diastereoisomers; d.r. determined by integration of  $^1\text{H}$  NMR signal:  $\delta_{\text{major}}$  5.68 (t),  $\delta_{\text{minor}}$  5.47 ppm (t). The title compound **34m** was isolated by flash column chromatography (eluent hexane/ethyl acetate = 1.5/1) in 60% yield (38.8 mg) as a single diastereomer. The enantiomeric excess was determined to be 99% by HPLC analysis on a Daicel Chiralpak IC column: 67/30/3 hexane/DCM/EtOH, flow rate 0.8 mL/min,  $\lambda = 254$  nm:  $\tau_{\text{Major}} = 46.7$  min,  $\tau_{\text{Minor}} = 11.7$  min  $[\alpha]_{\text{D}}^{26} = 11.4$  ( $c = 1.02$ ,  $\text{CHCl}_3$ ). HRMS *calcd* for ( $\text{C}_{37}\text{H}_{40}\text{ClNNaO}_7^+$ ): 668.2386, found 668.2400.  $^1\text{H}$  NMR (400 MHz,  $\text{CDCl}_3$ ):  $\delta$  7.35-6.69 (m, 13H), 5.68 (t,  $J = 7.2$  Hz, 1H), 4.60-4.52 (m, 2H), 4.26-4.15 (m, 1H), 3.81-3.75 (m, 2H), 3.63 (t,  $J = 9.8$  Hz, 1H), 3.15-3.08 (m, 1H), 2.73 (d,  $J = 11.9$  Hz, 2H), 1.59 (s, 9H), 1.16 (d,  $J = 6.5$  Hz, 3H), 0.83 (t,  $J = 7.1$  Hz, 3H) ppm.  $^{13}\text{C}$  NMR (101 MHz,  $\text{CDCl}_3$ )  $\delta$  170.6, 143.5, 140.4, 139.1, 137.7, 133.3, 128.7, 128.6, 128.4, 127.6, 127.6, 127.2, 127.2, 123.9, 122.2, 114.5, 84.0, 74.7, 60.6, 57.8, 57.2, 53.6, 53.0, 43.2, 35.5, 28.1, 16.1, 13.6 ppm.



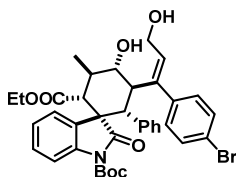
The reaction was carried out following the general procedure to furnish the crude product as a 11.5:1 mixture of diastereoisomers; d.r. determined by integration of  $^1\text{H}$  NMR signal:  $\delta_{\text{major}}$  5.70 (t),  $\delta_{\text{minor}}$  5.60 ppm (t). The title compound **34n** was isolated by flash column chromatography (eluent hexane/ethyl acetate = 2/1) in 49% yield (34.4 mg) as a single diastereomer. The enantiomeric excess was determined to be 99% by HPLC analysis on a Daicel Chiralpak IC column: 67/30/3 hexane/DCM/EtOH, flow rate 0.8 mL/min,  $\lambda = 254$  nm:  $\tau_{\text{Major}} = 14.7$  min,  $\tau_{\text{Minor}} = 8.3$  min.  $[\alpha]_{\text{D}}^{26} = +20.3$  ( $c = 1.65$ ,  $\text{CHCl}_3$ ). HRMS *calcd* for  $(\text{C}_{38}\text{H}_{39}\text{F}_4\text{NNaO}_7^+)$ : 720.2555, found 720.2582.  $^1\text{H}$  NMR (400 MHz,  $\text{CDCl}_3$ ):  $\delta$  7.57-7.55 (m, 1H), 7.40-7.38 (m, 1H), 7.30-7.27 (m, 1H), 7.24-7.22 (m, 1H), 7.18-7.14 (m, 3H), 7.09-7.05 (m, 1H), 7.01-6.98 (m, 1H), 6.67-6.65 (m, 2H), 6.56 (t,  $J = 8.9$  Hz, 1H), 5.70 (t,  $J = 7.2$  Hz, 1H), 4.72-4.67 (m, 1H), 4.55 (dd,  $J = 12.0$ , 7.5 Hz, 1H), 4.17 (dd,  $J = 12.1$ , 6.8 Hz, 1H), 3.78 (q,  $J = 7.1$  Hz, 2H), 3.72 (t,  $J = 9.8$  Hz, 1H), 3.40 (d,  $J = 12.1$  Hz, 1H), 3.13-3.06 (m, 1H), 2.80 (d,  $J = 11.9$  Hz, 1H), 1.59 (s, 9H), 1.17 (d,  $J = 6.4$  Hz, 3H), 0.84 (t,  $J = 7.1$  Hz, 3H) ppm.  $^{13}\text{C}$  NMR (101 MHz,  $\text{CDCl}_3$ )  $\delta$   $^{13}\text{C}$  NMR (126 MHz,  $\text{CDCl}_3$ )  $\delta$  174.6, 170.3, 148.7, 143.4, 140.1, 138.9, 133.4, 128.8, 128.2, 127.8, 127.4, 127.3, 127.1, 126.7-126.6 (m), 126.2 (m), 125.3 (d,  $J = 15.4$  Hz), 124.7, 123.7, 123.3 (d,  $J = 3.6$  Hz), 115.1 (d,  $J = 25.5$  Hz), 113.9, 100.0, 84.4, 74.9, 60.7, 57.9, 57.5, 53.3, 43.2, 43.2, 35.7, 27.9, 16.1, 13.5 ppm.  $^{19}\text{F}$  NMR (376 MHz,  $\text{CDCl}_3$ )  $\delta$  -61.98, -108.53 ppm.



The reaction was carried out following the general procedure to furnish the crude product as a 6:1 mixture of diastereoisomers; d.r. determined by integration of  $^1\text{H}$  NMR signal:  $\delta_{\text{major}}$  5.73 (t),  $\delta_{\text{minor}}$  5.58 ppm (t). The title compound **34o** was isolated by flash column chromatography (eluent hexane/ethyl acetate = 1.5/1) in 48% yield (29.9 mg) as a single diastereomer. The enantiomeric excess was determined to be 99% by HPLC analysis on a Daicel Chiralpak IC column: 67/30/3 hexane/DCM/EtOH, flow rate 0.8 mL/min,  $\lambda = 254$  nm:  $\tau_{\text{Major}} = 63.0$  min,  $\tau_{\text{Minor}} = 14.0$  min.  $[\alpha]_{\text{D}}^{26} = +20.9$  ( $c = 0.32$ ,  $\text{CHCl}_3$ ). HRMS *calcd* for  $(\text{C}_{35}\text{H}_{39}\text{NNaO}_7\text{S}^+)$ : 640.2339, found 640.2349.  $^1\text{H}$  NMR (300 MHz,  $\text{CDCl}_3$ ):  $\delta$  7.44-7.40 (m, 1H), 7.25-7.06 (m, 6H), 6.93-6.91 (m, 1H), 6.85-6.82 (m, 2H), 6.64-6.62 (m, 1H), 6.33-6.32 (m, 1H), 5.73 (t,  $J = 7.3$  Hz, 1H), 4.63-4.46 (m, 2H), 4.22 (dd,  $J = 11.9$ , 7.0 Hz, 1H), 3.78 (q,  $J = 7.1$  Hz, 2H), 3.52 (t,  $J = 9.9$  Hz, 1H), 3.13-3.03 (m, 2H), 2.67 (d,  $J = 11.9$  Hz, 1H), 1.57 (s, 9H), 1.13 (d,  $J = 6.4$  Hz, 3H), 0.83 (t,  $J = 7.1$  Hz, 3H) ppm.  $^{13}\text{C}$  NMR (75 MHz,  $\text{CDCl}_3$ )  $\delta$  174.8, 170.6, 148.6, 143.8, 140.3, 139.7, 138.2, 133.2, 129.1, 128.9, 128.6, 127.6, 127.1, 126.8, 125.5, 124.3, 124.0, 122.1, 114.6, 83.8, 74.4, 60.6, 57.9, 57.0, 54.1, 48.4, 45.0, 35.1, 28.1, 16.1, 13.6 ppm.



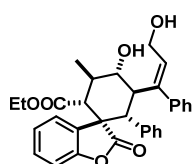
The reaction was carried out on a 1 mmol scale. An ordinary vial equipped with a Teflon-coated stir bar and a plastic screw cap was charged with amine **A** (0.2 mmol, 65 mg, 20 mol %). Then toluene (4 mL, 0.25 M) and the oxindole-bearing substrate **27** (1.2 equiv., 380 mg, 1.2 mmol) were sequentially added. The reaction mixture was stirred in a cooling bath maintained at 0 °C for 5 minutes to let the mixture reaching a uniform temperature. The reaction was started by the addition of propanal **26** (1 equiv., 72  $\mu$ L 1 mmol) and the reaction mixture was stirred at 0 °C for 1 hr. After that, the  $\alpha,\beta,\gamma,\delta$ -unsaturated aldehyde **30p** (1 equiv., 264.3 mg, 1 mmol) was added and the vial was sealed and immersed in the cooling bath again (maintained at 0 °C). Stirring was continued over 48 hr. The progress of the reaction was monitored by TLC and by  $^1\text{H}$  NMR analysis of the aliquot taken from the crude mixture. After 48 hr, the mixture (still at 0 °C) was diluted with 5.0 mL of EtOH; solid  $\text{NaBH}_4$  (4 mmol, 152 mg, 4 equiv) was added in one portion to furnish, after reduction, the crude product **34p** as a 10:1 mixture of diastereoisomers; d.r. determined by integration of  $^1\text{H}$  NMR signal:  $\delta_{\text{major}}$  5.62 (t),  $\delta_{\text{minor}}$  5.47 ppm (t). The title compound **34p** was isolated by flash column chromatography (eluent hexane/ethyl acetate = 1/1) in 69% yield (430 mg) as a single diastereomer. The enantiomeric excess was determined to be 99% by HPLC analysis on a Daicel Chiralpak IC column: 67/30/3 hexane/DCM/EtOH, flow rate 0.8 mL/min,  $\lambda$  = 254 nm:  $\tau_{\text{Major}}$  = 71.5 min,  $\tau_{\text{Minor}}$  = 18.7 min.  $[\alpha]_{\text{D}}^{26}$  = -12.2 ( $c$  = 1.2,  $\text{CHCl}_3$ ). HRMS *calcd* for ( $\text{C}_{38}\text{H}_{43}\text{NNaO}_8^+$ ): 664.2881, found 664.2887.  $^1\text{H}$  NMR (400 MHz,  $\text{CDCl}_3$ ):  $\delta$  7.29-6.61 (m, 13H), 5.62 (t,  $J$  = 7.3 Hz, 1H), 4.59-4.51 (m, 2H), 4.20-4.15 (m, 1H), 3.81-3.74 (m, 2H), 3.78 (s, 3H), 3.59 (t,  $J$  = 9.9 Hz, 1H), 3.17-3.10 (m, 1H), 2.75 (dd,  $J$  = 13.2, 11.9 Hz, 2H), 1.56 (s, 9H) 1.16 (d,  $J$  = 6.5 Hz, 3H), 0.83 (t,  $J$  = 7.1 Hz, 3H), ppm.  $^{13}\text{C}$  NMR (126 MHz,  $\text{CDCl}_3$ ):  $\delta$  175.1, 170.8, 158.6, 148.5, 143.5, 139.2, 135.5, 133.0, 132.9, 130.0, 128.9, 128.3, 127.0, 123.7, 122.3, 114.4, 112.8, 83.7, 74.7, 60.6, 57.9, 57.2, 55.2, 53.8, 53.3, 43.5, 35.4, 28.1, 16.2, 13.6 ppm.



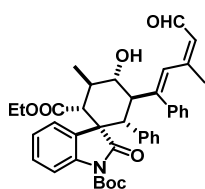
The reaction was carried out following the general procedure to furnish the crude product as a 4:1 mixture of diastereoisomers; d.r. determined by integration of  $^1\text{H}$  NMR signal:  $\delta_{\text{major}}$  5.62 (t),  $\delta_{\text{minor}}$  5.55 ppm (t). The title compound **34q** was isolated by flash column chromatography (eluent hexane/ethyl acetate = 1.5/1) in 46% yield (32.1 mg) as a single diastereomer. The enantiomeric excess was determined to be 99% by HPLC analysis on a Daicel Chiralpak IC column: 67/30/3 hexane/DCM/EtOH, flow rate 0.8 mL/min,  $\lambda$  = 254 nm:  $\tau_{\text{Major}}$  = 51.0 min,  $\tau_{\text{Minor}}$  = 17.2 min.  $[\alpha]_{\text{D}}^{26}$  = -45.9 ( $c$  = 0.69,  $\text{CHCl}_3$ ). HRMS *calcd* for ( $\text{C}_{37}\text{H}_{40}\text{BrNNaO}_7^+$ ): 712.1880, found 712.1884.  $^1\text{H}$  NMR (500 MHz,  $\text{CDCl}_3$ ):  $\delta$  7.29-7.01 (m, 11H), 6.71- 6.69 (m, 2H), 5.61 (t,  $J$  = 7.2 Hz, 1H), 4.62- 4.56 (m, 2H), 4.19 (dd,  $J$  = 11.8, 6.9 Hz, 1H), 3.82- 3.76 (m, 2H), 3.52 (t,  $J$  = 9.9 Hz, 1H), 3.15-3.10 (m, 1H), 2.72 (d,  $J$  = 11.9 Hz, 1H), 2.69 (d,  $J$  = 12.0 Hz, 1H), 1.56 (s, 9H), 1.16 (d,  $J$  = 6.5 Hz, 3H), 0.83 (t,  $J$  = 7.1 Hz, 3H) ppm.  $^{13}\text{C}$  NMR (126 MHz,  $\text{CDCl}_3$ )  $\delta$  175.1, 170.7, 148.4, 143.1, 139.5, 135.2, 133.1,

130.6, 128.7, 128.4, 127.2, 123.8, 122.3, 121.2, 114.5, 83.8, 74.7, 60.6, 57.8, 57.1, 53.8, 53.3, 43.2, 35.6, 28.1, 16.1, 13.6 ppm.

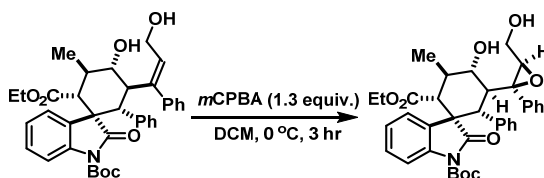
The reaction was carried out following the general procedure to furnish the crude product



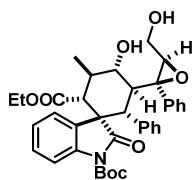
as a 19:1 mixture of diastereoisomers; d.r. determined by integration of  $^1\text{H}$  NMR signal:  $\delta_{\text{major}}$  5.66 (t),  $\delta_{\text{minor}}$  5.52 ppm (t). The title compound **36** was isolated by flash column chromatography (eluent hexane/ethyl acetate = 1.5/1) in 78% yield (40 mg) as a single diastereomer. The enantiomeric excess was determined to be 99% by HPLC analysis on a Daicel Chiralpak IC column: 67/30/3 hexane/DCM/EtOH, flow rate 0.8 mL/min,  $\lambda = 254$  nm:  $\tau_{\text{Major}} = 96.3$  min,  $\tau_{\text{Minor}} = 54.4$  min.  $[\alpha]_{\text{D}}^{26} = +87.9$  ( $c = 1.2$ ,  $\text{CHCl}_3$ ). HRMS *calcd* for  $(\text{C}_{32}\text{H}_{32}\text{NaO}_6)^+$ : 532.2091, found 532.2091.  $^1\text{H}$  NMR (400 MHz,  $\text{CDCl}_3$ ):  $\delta$  7.29-6.63 (m, 14H), 5.66 (t,  $J = 7.3$  Hz, 1H), 4.50-4.61 (m, 2H), 4.20 (dd,  $J = 11.9$ , 6.8 Hz, 1H), 3.85-3.78 (m, 2H), 3.65 (t,  $J = 9.9$  Hz, 1H), 3.04-2.94 (m, 1H), 2.83 (d,  $J = 12.0$  Hz, 1H), 2.77 (d,  $J = 11.9$  Hz, 1H), 1.19 (d,  $J = 6.4$  Hz, 3H), 0.84 (t,  $J = 7.1$  Hz, 3H) ppm.  $^{13}\text{C}$  NMR (75 MHz,  $\text{CDCl}_3$ ):  $\delta$  175.8, 170.7, 152.5, 143.6, 140.4, 135.3, 133.1, 129.0, 128.8, 128.4, 127.5, 127.3, 127.1, 123.6, 122.9, 110.2, 74.5, 60.9, 57.9, 57.1, 54.2, 52.3, 43.5, 35.7, 16.1, 13.6 ppm.



(Compound **32**). The enantiomeric excess was determined to be 99% by HPLC analysis on a Daicel Chiralpak IA column: 97/3 hexane/ $i$ PrOH, flow rate 0.8 mL/min,  $\lambda = 254$  nm:  $\tau_{\text{Major}} = 43.6$  min,  $\tau_{\text{Minor}} = 30.0$  min. HRMS *calcd* for  $(\text{C}_{40}\text{H}_{43}\text{NNaO}_7)^+$ : 672.2932, found 672.2933.  $^1\text{H}$  NMR (500 MHz,  $\text{CDCl}_3$ ):  $\delta$  9.06 (s, 1H), 7.48-7.46 (m, 1H), 7.39-7.37 (m, 4H), 7.34-7.32 (m, 1H), 7.20-7.13 (m, 7H), 6.98-6.96 (m, 1H), 6.53-6.51 (m, 1H), 6.31 (dd,  $J = 11.5$ , 1.0 Hz, 1H), 4.43 (dd,  $J = 12.8$ , 2.1 Hz, 1H), 3.91-3.90 (m, 1H), 3.85-3.79 (m, 2H), 3.73 (d,  $J = 12.3$  Hz, 1H), 3.47 (d,  $J = 12.0$  Hz, 1H), 3.26-3.22 (m, 1H), 1.66 (d,  $J = 1.3$  Hz, 3H), 1.55 (s, 9H), 1.06 (d,  $J = 6.9$  Hz, 3H), 0.86 (t,  $J = 7.2$  Hz, 3H) ppm.  $^{13}\text{C}$  NMR (126 MHz,  $\text{CDCl}_3$ ):  $\delta$  194.9, 171.8, 151.3, 145.1, 139.5, 139.3, 137.5, 136.4, 128.7, 128.6, 128.6, 128.4, 128.3, 127.0, 126.8, 125.6, 124.0, 122.5, 114.5, 83.6, 71.1, 60.5, 54.1, 51.6, 48.9, 48.2, 33.0, 28.1, 16.5, 13.7, 9.4 ppm.

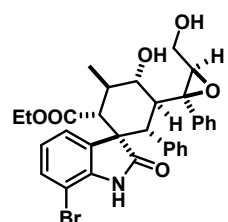
3.3.5. General Procedure for the Epoxidation of Compounds **34**.Figure 29. Epoxidation of product **34**

Allylic alcohol **34a** (25.3 mg, 0.041 mmol), as obtained following the general procedure for the vinylogous triple cascade, was placed in a round bottom flask and dissolved in DCM (0.2 mL) at 0 °C. *meta*-Chloroperoxybenzoic acid (*m*CPBA, 1.3 equiv., 0.054 mmol) was added and the reaction mixture stirred for 3 hr. Then the reaction was diluted with 10 mL of DCM and washed with NaHCO<sub>3</sub> solution (2 times) and brine. The organic phase was dried over Na<sub>2</sub>SO<sub>4</sub> and filtered. Solvent was evaporated *in vacuo* and the crude reaction mixture purified by flash column chromatography on silica gel.



The reaction furnished the crude product as a 8:1 mixture of diastereoisomers; d.r. determined by integration of <sup>1</sup>H NMR signal: δ<sub>major</sub> 6.13 (d), δ<sub>minor</sub> 6.30 ppm (d). The title compound **37a** was isolated by flash column chromatography (eluent hexane/ethyl acetate = 2/1) in 83% yield (21.3 mg) as a single diastereomer. The enantiomeric excess was determined to be 99% by HPLC analysis on a Daicel Chiralpak IC column: 67/30/3 hexane/DCM/EtOH, flow rate 0.8 mL/min, λ = 254 nm: τ<sub>Major</sub> = 115.7 min, τ<sub>Minor</sub> = 31.8 min. [α]<sub>D</sub><sup>26</sup> = -23.6 (c = 0.41, CHCl<sub>3</sub>). HRMS *calcd* for (C<sub>37</sub>H<sub>41</sub>NNaO<sub>8</sub><sup>+</sup>): 650.2724, found 650.2724. <sup>1</sup>H NMR (500 MHz, CDCl<sub>3</sub>): δ 7.34-7.31 (m, 2H), 7.28-7.27 (m, 3H), 7.22-7.20 (m, 1H), 7.11-7.08 (m, 1H), 7.05-7.01 (m, 3H), 7.0-6.94 (m, 2H), 6.83 (t, *J* = 7.7 Hz, 1H), 6.12 (d, *J* = 7.8 Hz, 1H), 4.57 (bs, 1H), 3.97 (t, *J* = 9.5 Hz, 1H), 3.91-3.83 (m, 2H), 3.78-3.72 (m, 2H), 3.40-3.33 (m, 1H), 3.20-3.12 (m, 1H), 2.87 (dd, *J* = 7.0, 4.2 Hz, 1H), 2.58 (d, *J* = 12.1 Hz, 1H), 2.49 (d, *J* = 11.7 Hz, 1H), 1.58 (s, 9H), 1.13 (d, *J* = 6.4 Hz, 3H), 0.80 (t, *J* = 7.1 Hz, 3H) ppm. <sup>13</sup>C NMR (101 MHz, CDCl<sub>3</sub>): δ 174.8, 170.6, 148.6, 139.2, 134.8, 133.3, 129.0, 128.5, 128.4, 128.4, 127.9, 127.7, 127.6, 127.1, 126.9, 123.8, 122.1, 114.4, 83.8, 75.8, 63.1, 60.9, 60.6, 56.7, 53.6, 52.7, 42.3, 34.1, 29.7, 28.1, 15.9, 13.6 ppm.

The epoxidation furnished the crude product as a 15:1 mixture of diastereoisomers; d.r.



determined by integration of  $^1\text{H}$  NMR signal:  $\delta_{\text{major}}$  6.20 (d),  $\delta_{\text{minor}}$  6.30 ppm (d). The title compound **37f** was isolated by flash column chromatography (eluent hexane/ethyl acetate = 1/1) in 86% yield (32 mg) as a single diastereomer.  $[\alpha]_{\text{D}}^{26} = -48.1$  ( $c = 0.30$ ,  $\text{CHCl}_3$ ).  $^1\text{H}$  NMR (400 MHz,  $\text{CDCl}_3$ ):  $\delta$  7.70 (s, 1H), 7.50-7.49 (m, 1H), 7.36-7.26 (m, 4H), 7.17-7.03 (m, 4H), 6.93-6.87 (m, 2H), 6.78 (t,  $J = 7.8$  Hz, 1H), 6.19 (d,  $J = 7.2$  Hz, 1H), 4.03-3.91 (m, 3H), 3.85-3.79 (m, 2H), 3.57-3.48 (m, 1H), 3.21-3.14 (m, 1H), 2.91 (dd,  $J = 6.7, 4.2$  Hz, 1H), 2.61 (d,  $J = 12.0$  Hz, 1H), 2.53 (d,  $J = 12.1$  Hz, 1H), 1.16 (d,  $J = 6.4$  Hz, 3H), 0.83 (t,  $J = 7.1$  Hz, 3H) ppm.  $^{13}\text{C}$  NMR (101 MHz,  $\text{CDCl}_3$ ):  $\delta$  176.7, 170.6, 139.5, 134.7, 133.3, 131.2, 130.8, 129.7, 129.0, 128.5, 128.0, 127.7, 127.1, 126.9, 123.0, 121.8, 101.9, 77.2, 75.7, 60.9, 60.6, 56.4, 55.6, 52.1, 34.0, 29.7, 15.9, 13.6 ppm.

The stereochemistry of compound **37f** was unambiguously determined by anomalous dispersion X-ray crystallographic analysis.

### 3.3.6. NMR Conformational Studies

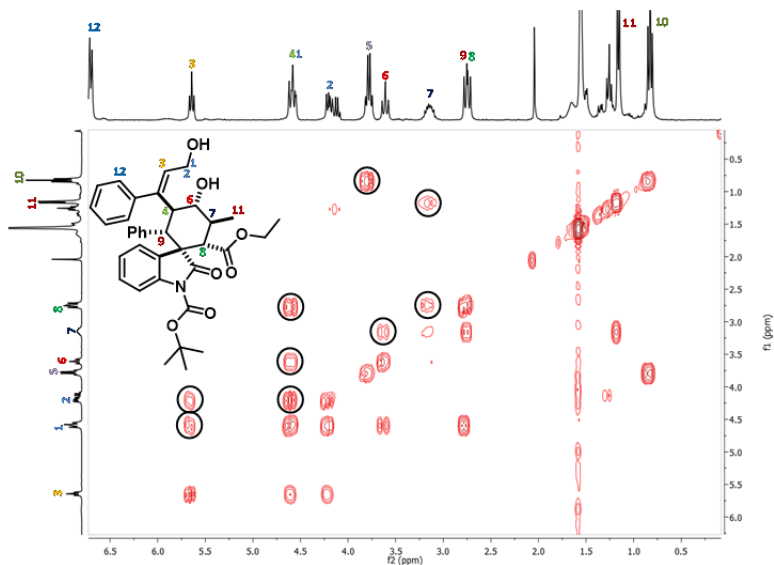
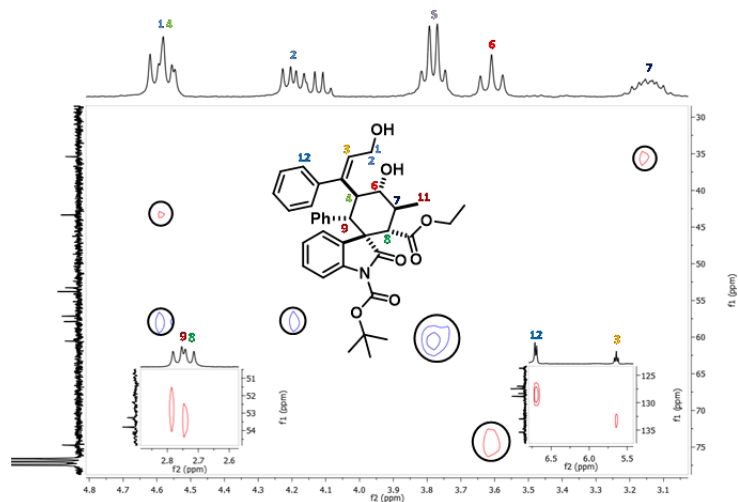


Figure 30. Cosy spectra of the major diastereoisomer of **34a** in  $\text{CDCl}_3$ .



**Figure 31.** HSQC spectra of the major diastereoisomer of **34** in  $\text{CDCl}_3$ . (blue signals represent  $\text{CH}_2$ , red signals CH).

### 3.3.7. Single Crystal X-Ray Diffraction Data

X-ray structure determinations: Crystals of *ent*-**34e** were obtained by slow evaporation of a Hexane/EtOAc mixture (3:1) at room temperature and the crystals of **37f** were obtained by evaporation of Hexane/DCM/Chloroform. The measured crystals were stable under atmosphere conditions; nevertheless they were prepared under inert conditions immersed in perfluoropolyether as protecting oil for manipulation.

Data Collection. Measurements were made on a Bruker-Nonius diffractometer equipped with an APPEX 2 4K CCD area detector, a FR591 rotating anode with MoK $\alpha$  radiation, Montel mirrors and a Cryostream Plus low temperature device ( $T = -173\text{ }^\circ\text{C}$ ). Full-sphere data collection was used  $\omega$  and  $\phi$  scans.

Programs used: Data collection Apex2 V2010 7.0 (Bruker-Nonius 2008), data reduction Saint + Version 7.60A (Bruker AXS 2008) and absorption correction SADABS.

Structure Solution. SIR2007 program was used.<sup>26</sup>

Structure Refinement. SHELXTL-97.<sup>27</sup>

<sup>26</sup>R. Caliandro, B. Carrozzini, G. L. Cascarano, L. De Caro, C. Giacovazzo, D. Siliqi, Advances in *ab initio* Protein Phasing by Patterson Deconvolution Techniques. *J. Appl. Cryst.* **2007**, *40*, 883.

<sup>27</sup>G. M. Sheldrick, A Short History of SHELX. *Acta Cryst.* **2008**, *A64*, 112.

Crystal data for *ent*-**34e** at 100(2) K: **CCDC 950227**

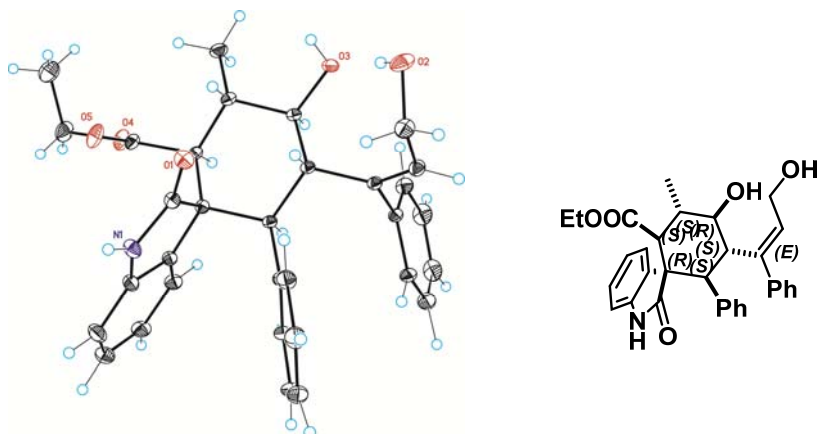


**Figure 32.** Crystal data and structure refinement for CCDC 950227.

Although product *ent*-**34e** does not bear any heavy atom, the data obtained from anomalous dispersion X-ray crystallographic analysis of the single crystal were good enough to unambiguously determine the absolute configuration of the molecule.<sup>28,29</sup>

Crystal data for **37f** at 100(2) K: **CCDC 956658**

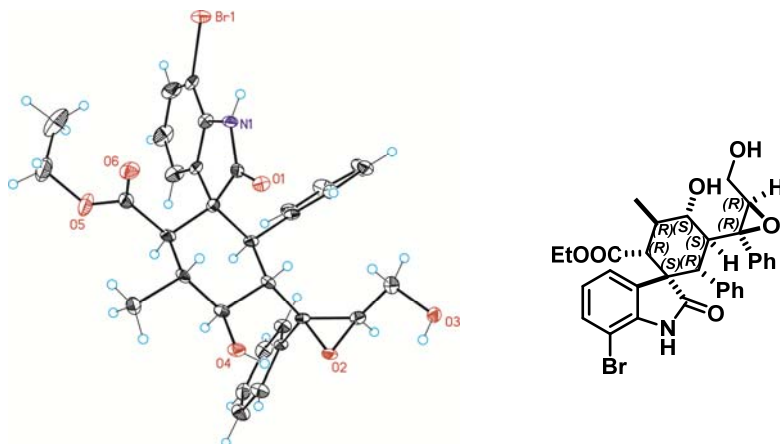


**Figure 33.** Crystal data and structure refinement for CCDC 956658.

<sup>28</sup> R.W.W. Hooft, L.H. Straver, A.L. Spek, *J. Appl. Cryst.*, **2008**, 41, 96.

<sup>29</sup> S. Parsons, H.D. Flack, *Acta Cryst.* **2004**, A60, s61



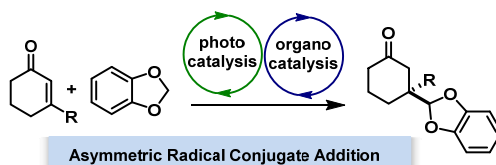
UNIVERSITAT ROVIRA I VIRGILI  
NOVEL ENANTIOSELECTIVE AMINOCATALYTIC PROCESSES BY MEANS OF VINYLLOGOUS  
REACTIVITY AND PHOTOREDOX CATALYSIS  
David Bastida Borrell

## Chapter IV

# Photochemical Enantioselective $\beta$ -Alkylation of Enones by Means of Iminium Ion Activation

### Target

Developing an enantioselective radical conjugate addition of enones by trapping photochemically generated carbon-centered radicals using iminium ion activation.



### Tool

Merging the ability of iminium ion catalysis to activate  $\alpha,\beta$ -unsaturated ketones with the tendency of light-activated polyoxometalate catalysts to generate carbon-centered radicals under mild conditions.<sup>1</sup>

### 4.1. The Project Idea, the Precedents and the Challenges Behind

The conception of this research project arose from our desire to use the iminium ion activation of enones **1** to trap nucleophilic radicals. The general idea, as detailed in Figure 1, was to couple the electrophilic iminium ion intermediate **2**, transiently generated upon condensation of **1** with a chiral aminocatalyst, and the nucleophilic radical intermediates **4**, generated by means of photoredox activation of alkanes **3**. Successfully developed, this system would contribute the first method for conducting asymmetric radical conjugate additions by means of iminium ion catalysis. The general iminium ion activation mode, which has found extensive applications in polar pathways,<sup>2</sup> has never been used before for trapping photochemically generated open-shell intermediates.

<sup>1</sup> The work discussed in this chapter has not been published as of 01-Nov-2015 Experimental part developed together with Dr. John J. Murphy. Project conducted in collaboration with Professor Maurizio Fagnoni, University of Pavia - Italy.

<sup>2</sup> G. Lelais, D. W. C. MacMillan, *Modern Strategies in Organic Catalysis: the Advent and Development of Iminium Activation*, *Aldrichim. Acta*, 2006, **39**, 79.

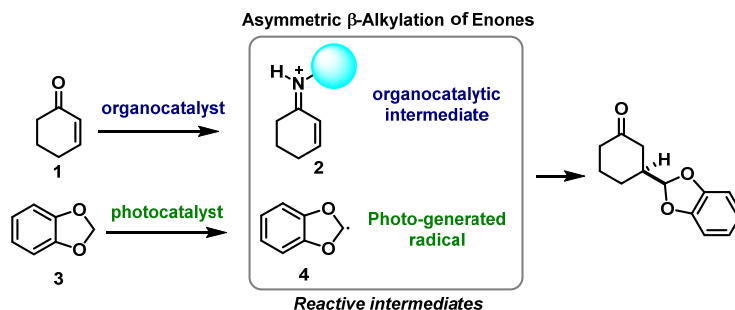


**Figure 1. Combining Organo- and Photo-catalysis.** Design plan for developing an organocatalytic photochemical radical conjugate addition; the blue circle represents the chiral organocatalyst fragment.

Many challenges can be anticipated for making this process enantioselective:

- 1) Chiral iminium ions have never been used to successfully trap radicals in a stereoselective fashion.
- 2) Establish reaction conditions compatible with both the organocatalytic and the photoredox catalytic regime.
- 3) Tendency of the photogenerated, highly reactive carbon centered radical **4** to racemically add to enones of type **1** without the need of any iminium ion activation (*background reaction*).
- 4) An additional difficulty may arise from the fact that the addition of a reactive carbon-centered radical to a carbon-carbon double bond is generally exothermic because a  $\pi$  bond is replaced by a  $\sigma$  bond.<sup>3</sup> Therefore, and according to Hammond's postulate,<sup>4</sup> the transition state is early, that is, the cleavage of the  $\pi$  bond and the formation of the  $\sigma$  bond are far from being complete in the transition structure. This brings about a more loosely transition state, which makes it difficult for the chiral catalyst to control the stereoselectivity of the radical conjugate addition. This means that the aminocatalyst would need to induce a better diastereotopic face discrimination of the iminium ion than in related conjugate additions of closed shell substrates.

Sparse methodologies have been already reported for the enantioselective conjugate additions of nucleophilic carbon-centered alkyl radicals to electrophilic acceptor olefins.

<sup>3</sup> a) H. Fischer, L. Radom, Factors Controlling the Addition of Carbon-Centered Radicals to Alkenes—An Experimental and Theoretical Perspective, *Angew. Chem. Int. Ed.* **2001**, *40*, 1340. b) B. Giese, Syntheses with Radicals - C-C Bond Formation via Organotin and Organomercury Compounds, *Angew. Chem. Int. Ed. Engl.* **1985**, *24*, 553.

<sup>4</sup> G. S. Hammond, A Correlation of Reaction Rates, *J. Am. Chem. Soc.* **1955**, *77*, 334.

Pioneering work by Sibi and Porter described the use of a chiral Lewis acid, which could be used catalytically, to activate alkene towards radical traps, leading to a stereoselective  $\beta$ -functionalization (Figure 2). In this approach, the alkyl radicals were generated from alkyl iodides by means of a combination of  $\text{Et}_3\text{B}/\text{O}_2$  and  $\text{Bu}_3\text{SnH}$ .<sup>5</sup>

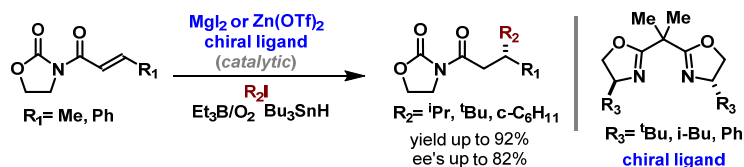


**Figure 2.** The first chiral Lewis acid-catalyzed enantioselective radical conjugate addition

This methodology provided the first example of a catalytic system able to induce enantioselectivity in alkyl radical conjugate additions. The addition of the radical took place at the less hindered alkene face, as dictated by the steric shielding abilities of the chiral Lewis acid. The different rate between the catalyzed reaction and the background racemic process was crucial to achieve good levels of enantiomeric excess.

Recently, and during the development of this research project, Yoon and co-workers reported the enantioselective conjugate addition of photochemically generated  $\alpha$ -amino radicals **7** to  $\alpha,\beta$ -unsaturated acyl pyrazolidinones **6** using a dual-catalyst protocol that combined a metal photoredox catalyst with a chiral Lewis acid catalyst (Figure 3).<sup>6</sup> The Lewis acid/chiral ligand complex dictated the enantioselectivity of the radical conjugate addition, while the  $\alpha$ -amino radicals **7** was generated *via* an oxidation of the silylamine **5** by the excited state of the photocatalyst ( $\text{Ru}(\text{bpy})_3^{2+*}$ ). Upon formation of the radical cation of **5**, a facile fragmentation afforded the  $\alpha$ -amino radical **7**.<sup>7</sup> A significant background reaction was observed, suggesting that the rate acceleration provided by the chiral Lewis acid catalyst had to be considerable in order to overtake the rate of the racemic process, thus securing the observed high level of enantioselectivity.

<sup>5</sup> M. P. Sibi, J. Ji, J. H. Wu, S. Gürtler, N. A. Porter, Chiral Lewis Acid Catalysis in Radicals Reactions: Enantioselective Conjugate Radical Additions, *J. Am. Chem. Soc.* **1996**, *118*, 9200.

<sup>6</sup> L. Ruiz Espelt, I. S. McPherson, E. M. Wiesnsch, T. Yoon. Enantioselective Conjugate Additions of  $\alpha$ -Amino Radicals via Cooperative Photoredox and Lewis Acid Catalysis, *J. Am. Chem. Soc.*, **2015**, *137*, 2452.

<sup>7</sup> X. Zhang, S.-R. Yeh, S. Hong, J. M. Freccero, A. Albini, D. E. Falvey, P. S. Mariano., Dynamics of  $\alpha$ -CH Deprotonation and  $\alpha$ -Desilylation Reactions of Tertiary Amine Cation Radicals, *J. Am. Chem. Soc.* **1994**, *116*, 4211.

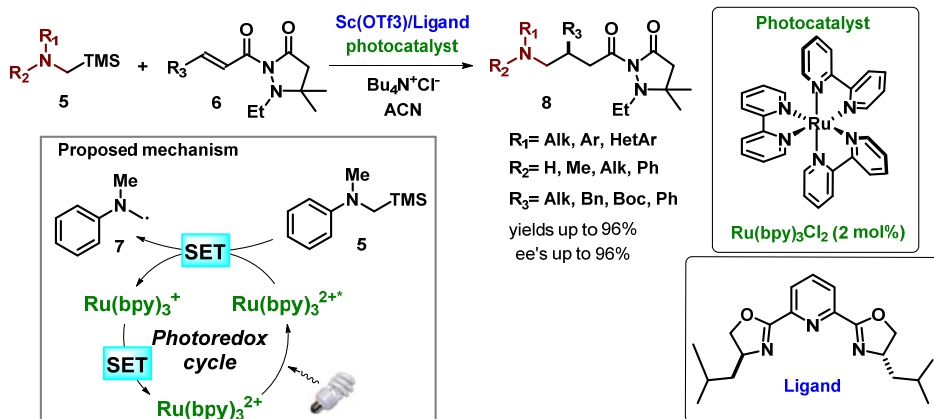


**Figure 3.** Lewis acid-catalyzed asymmetric conjugate addition of photochemically generated radicals; ACN: acetonitrile; SET: single electron transfer. The second SET event, which restores the  $\text{Ru}^{2+}$  catalyst while reducing the  $\alpha$ -carbonyl radical generated upon radical conjugate addition, is not shown.

From this literature overview, it is apparent that few effective catalytic methods exist for realizing enantioselective radical conjugate additions to activated alkenes. This justified our interest in developing a new catalytic strategy by capitalizing upon the iminium ion activation of enones. We sought to approach the conjugate addition to transiently generated chiral iminium ions using an alternative strategy to access open shell species, which had previously not been used in asymmetric transformations. To this end, we identified tetrabutylammonium decatungstate (TBADT)<sup>8,9</sup> as a powerful photoredox catalyst for generating, under mild conditions and from simple precursors, nucleophilic carbon-centered radicals that can undergo conjugate additions to electron deficient alkenes. In this context, Fagnoni and Albini have recently used the light-activated TBADT photoredox catalyst to generate radicals **4** (see Figure 1) from benzodioxole **3**, which could easily add to  $\alpha,\beta$ -unsaturated carbonyl compounds in a racemic fashion.<sup>10</sup> Our target was to make this process catalytic and enantioselective, using the iminium ion activation of enones as the enabling strategy to achieve stereocontrol.

Successfully developed, this strategy would expand the scope of enantioselective conjugate addition reactions promoted by asymmetric aminocatalysis. Until now, this type of transformation was restricted to polar reactivities (Michael reactions), using nucleophiles bearing easily deprotonable carbon atoms (*i.e.* rather acidic C-H bonds).<sup>11</sup>

<sup>8</sup> C. L. Hill, Introduction of Functionality into Unactivated Carbon-Hydrogen Bonds. Catalytic Generation and Nonconventional Utilization of Organic Radicals, *Synlett*, **1995**, 127.

<sup>9</sup> C. Tanielian, Decatungstate photocatalysis, *Coord. Chem. Rev.* **1998**, 178, 1165

<sup>10</sup> D. Ravelli, A. Albini, M. Fagnoni, Smooth Photocatalytic Preparation of 2-Substituted 1,3-Benzodioxoles, *Chem. Eur. J.* **2011**, 17, 572.

<sup>11</sup> B. List, *Science of Synthesis, Asymmetric Organocatalysis 1 - Lewis Base and Acid Catalysis*, **2012**, Georg Thieme Verlag KG, Stuttgart-New York.

## 4.2. Generating Carbon-Centered Radicals using Photoredox Catalysis.

The most common method for the generation of radicals involves the homolytic cleavage of a covalent bond by the application of energy in the form of heat, light, or *via* intermolecular electron transfer. The majority of covalent bonds require extremely harsh conditions to be cleaved such as high energy radiation or high temperatures. In order to circumvent this problem, radical initiators have become the option choice for organic chemists. Radical initiators are molecules with low bond dissociation energies (BDE) that can produce radicals under mild conditions and promote radical reactions. Examples of radical initiators are: azo compounds like azobisisobutyronitrile (AIBN), peroxides like benzoyl peroxide (BPO), organometallic compounds like triethylborane (Et<sub>3</sub>B), and inorganic compounds like samarium iodide (SmI<sub>2</sub>). Radical initiators have to be stable at room temperature while thermally decomposing to afford radicals under mild conditions (relatively low temperature).<sup>12</sup>

More recently, photoredox catalysis has emerged as a convenient and mild methodology to produce radical intermediates.<sup>15</sup> This approach relies on the ability of visible light-absorbing metal complexes or organic dyes to get excited after low energy photon absorption, and to readily engage in an array of redox processes to generate radicals from organic substrates.<sup>13</sup>

In this vein, the light-activated TBADT offers the possibility of generating radicals under mild conditions. To better detail the mode of action of TBADT, it can be useful to remind some basic concepts of photochemistry and photoredox catalysis. This will help us to explain the special features of TBADT.

## 4.3. Principles of Photochemistry and Photoredox Catalysis

Photochemistry is the branch of chemistry which describes the interactions between molecules and photons of visible or ultraviolet light (UV) and the subsequent processes of the excited state. The inability of many organic compounds to absorb light in the visible region has limited application of photochemical methodologies to the use of more high-energy-light sources. The advent of photoredox catalysts, such as Ru(bpy)<sub>3</sub><sup>2+</sup>,<sup>14</sup> which can absorb visible light, has rapidly broadened the potential application of photochemistry.<sup>15</sup> Photoredox catalysts have the ability to absorb energy from photons. This event promotes an electron from the HOMO orbital to a higher energy electronic configuration, thus generating an electronically excited state of the photocatalyst (Figure 4, transition 1). These photoexcited species have a different

<sup>12</sup> P. Renaud, M. Sibi, *Radicals in Organic Synthesis*, **2001**, WILEY-VCH Verlag GmbH, D-69469, Weinheim, Germany.

<sup>13</sup> D. M. Schultz, T. P. Yoon, Solar Synthesis: Prospects in Visible Light Photocatalysis, *Science*, **2014**, *343*, 1239176.

<sup>14</sup> A. Juris, V. Balzani, F. Barigelletti, S. Campagna, P. Belser, A. von Zelewsky, Ru(II) Polypyridine Complexes: Photophysics, Photochemistry, Electrochemistry, and Chemiluminescence, *Coord. Chem. Rev.* **1988**, *84*, 85.

<sup>15</sup> C. K. Prier, D. A. Rankic, D. W. C. MacMillan, Visible Light Photoredox Catalysis with Transition Metal Complexes: Applications in Organic Synthesis, *Chem. Rev.* **2013**, *113*, 5322.

electronic structure than the ground state molecule. An electronically excited state has a high energy content due to the arrangement of the electrons in the molecular orbitals, and therefore could undergo deactivation within a short period of time. Two main deactivation pathways are possible: intramolecular or intermolecular processes.

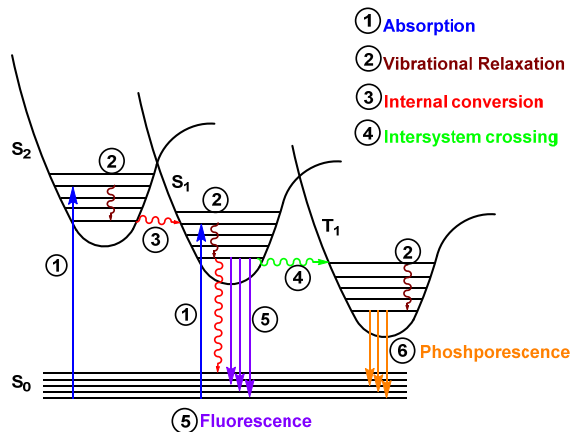


**Figure 4.** Relaxation processes of excited states represented in the Jablonski diagram.<sup>16</sup>

#### 4.3.1. Intramolecular photophysical processes of the excited state.

Relaxation of excited states by intramolecular processes is conveniently represented by the Jablonski diagram (Figure 4).<sup>16</sup> Radiation-less transitions are represented as wavy arrows. Vibrational relaxation (transition 2) takes place between a vibrationally excited state ( $v>0$ ) and the  $v=0$ . Internal conversion (transition 3) is the relaxation of a high energy excited states ( $S_2$ ,  $S_3$ ,...) to the lowest one in energy ( $S_1$ ) and is usually faster than other processes. Intersystem crossing (transition 4) is also a radiation-less transition. It is a spin forbidden transition between isoenergetic states of different multiplicity ( $S_1$  to  $T_1$ , transition 4).

On the other side, radiative transitions (photon emission) take place when the excited molecule relaxes to the ground state. They are represented in Figure 4 as straight arrows. Fluorescence (transition 5) involves the radiative transition between  $S_1$  and the ground state, while phosphorescence (transition 6) involves photon emission associated to the transition between the excited state  $T_1$  and the ground state. This transition is spin forbidden and thus this process is much slower than fluorescence.

#### 4.3.2. Intermolecular photophysical processes of the excited state.

When an exogenous molecule increases the rate of deactivation of an electronically excited state, this molecule is called “quencher”. An electronically excited state of a molecule may interact with another ground state molecule in three different ways.

<sup>16</sup> B. Wardle, *Principles and Applications of Photochemistry*, 2009, John Wiley & Sons Ltd., UK.

1. *Energy transfer* occurs when an excited state of one molecule (the donor  $D^*$ ) is quenched by transferring energy to the ground state of another molecule (the acceptor  $B$ ). After the quenching process occurs, the excited state  $B^*$  is generated while the  $D$  singlet ground state is recovered (Figure 5A).

As mentioned before, the absorption of a photon can promote an electron to a higher energy level electronic configuration. In this way, a molecule may become an electron donor (reducing agent) and/or a better electron acceptor (oxidizing agent), depending on how the excited state reacts with the quencher (Q). This is known as *photoinduced electron transfer* (PET) and, as such, is described by the following dichotomy (Figures 5B, 5C)

2. Oxidative quenching occurs when the excited state  $D^*$  acts as an electron donor (oxidative electron transfer) reducing the quencher  $M_1$  (usually an electron poor organic molecule).
3. Reductive quenching occurs when the excited state  $A^*$  acts as an electron acceptor (reductive electron transfer), oxidizing the quencher  $M_2$  (usually an electron poor organic molecule).

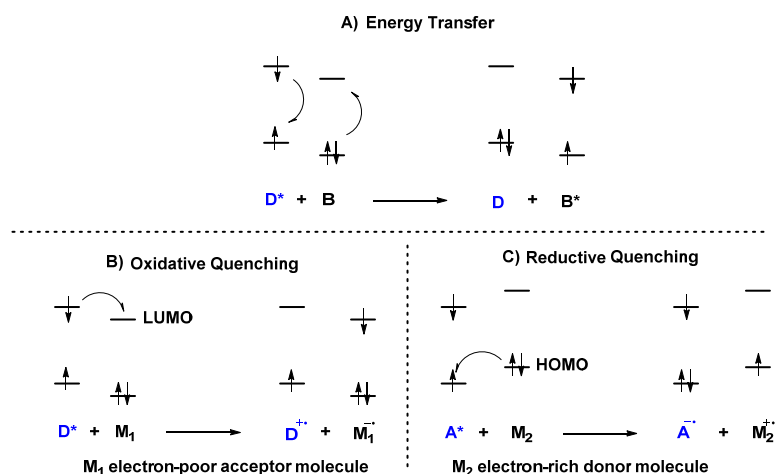


**Figure 5.** A) Energy transfer quenching. B) Oxidative quenching of excited state. C) Reductive quenching of excited state.

The photoinduced electron transfer is a key process to promote a redox reaction catalyzed by light. It allows the reduction or the oxidation of a substrate, whose product could undergo subsequent chemical transformations. The most studied one-electron photoredox catalysts, which can absorb visible light and promote chemical transformations via PET, are ruthenium- and iridium-based complexes (Figure 6). In particular, polypyridyl complexes are the most



employed in organic chemistry.<sup>17</sup> Absorption of photons in the high-energy visible region (454 and 375 nm for Ru and Ir, respectively) promotes a metal-to-ligand electronic transition (MLCT) leading to the formation of stable, long lifetime ( $\tau$ ) triplet states *via* intersystem crossing ( $\tau = 1100$  and 1900 ns for Ru and Ir, respectively).

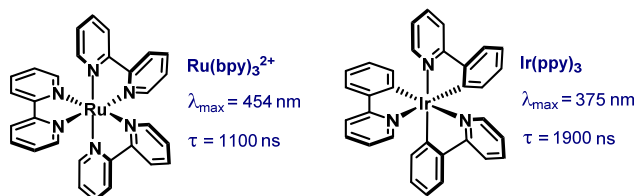


Figure 6. Polypyridyl complexes of ruthenium and iridium: Ru(bpy)<sub>3</sub><sup>2+</sup> and Ir(ppy)<sub>3</sub>

#### 4.3.3. Photoinduced Proton-Coupled Electron Transfer and Hydrogen Atom.

Proton coupled electron transfer (PCET) consists of a single chemical reaction step involving concerted transfer of both a proton and an electron between two molecules. If one of the reaction partners is an excited state of a molecule generated by absorption of light, we call this process photoinduced PCET.<sup>18</sup> Hydrogen atom transfer (HAT) is considered to be a subclass of PCET, in which the proton and electron start in the same orbital and move together in a concerted fashion to the final orbital.<sup>19</sup> Historically, HAT reactions have been catalyzed by p-block centered radicals such as (<sup>t</sup>BuO<sup>•</sup>), which were thermally generated. In more recent times, transition metal complexes or polyoxometalates, such as TBADT, equipped with protonatable or deprotonable ligands, have been recognized as superior catalysts for HAT reactions.<sup>18b</sup>

PCET reactions involving the transfer of one electron and one proton can be described in terms of the four electronic states (Figure 7).<sup>20</sup> In the initial state, the electron and proton are on their donors, while in the final state the electron and proton are on their acceptors. The other two states correspond to either only the proton or only the electron being transferred (Figure 7, blue species).<sup>21</sup>  $\Delta G$  values for PCET are often more favorable than  $\Delta G$ s for competing initial ET or PT. This is because, when electrons and protons react in concerted fashion, charged high-energy intermediates (Figure 7, blue species) are avoided, allowing the overall chemical reaction to occur with lower activation barriers.<sup>18</sup>

<sup>17</sup> J. W. Tucker, C. R. J. Stephenson, Shining Light on Photoredox Catalysis: Theory and Synthetic Applications, *J. Org. Chem.* **2012**, *77*, 1617.

<sup>18</sup> a) O. S. Wenger, Proton-Coupled Electron Transfer with Photoexcited Metal Complexes, *Acc. Chem. Res.* **2013**, *46*, 1517. b) O. S. Wenger, Proton-coupled Electron Transfer with Photoexcited Ruthenium (II), Rhenium(I), and Iridium(III) Complexes, *Coord. Chem. Rev.* **2015**, *282*, 150.

<sup>19</sup> M. Hang, V. Huynh, T. J. Meyer, Proton-Coupled Electron Transfer, *Chem. Rev.* **2007**, *107*, 5004.

<sup>20</sup> J. M. Mayer, Proton-Coupled Electron Transfer: A Reaction Chemist's View, *Annu. Rev. Phys. Chem.* **2004**, *55*, 363.

<sup>21</sup> S. Hammes-Schiffer, Proton-Coupled Electron Transfer: Moving Together and Charging Forward, *J. Am. Chem. Soc.* **2015**, *137*, 8860.

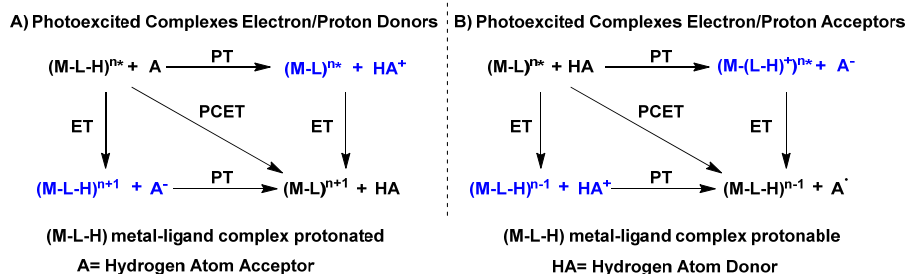


Figure 7. Metal complexes suitable for PCET and possible pathways for photoexcited PCET reaction.<sup>208</sup>

#### 4.4. Polyoxometalates and TBADT as Photoredox Catalysts

Polyoxometalate (POM) ions have recently found increasing applications in radical generation, acting as photoredox catalysts. POM's are metal oxygen clusters that exhibit a variety of properties and they have been used in many different fields, including materials,<sup>22</sup> catalysis,<sup>23</sup> and medicine.<sup>24</sup> One of the privileged polyoxometalate photocatalysts is tetrabutylammonium decatungstate (NBu<sub>4</sub>(W<sub>10</sub>O<sub>32</sub>), or TBADT).<sup>25</sup> NBu<sub>4</sub>(W<sub>10</sub>O<sub>32</sub>) is a cluster of tungsten with oxo ligands, which is highly soluble in acetonitrile. After absorption within the UV region ( $\lambda_{max}$  = 323 nm), a ligand-to-metal charge transfer (LMCT) occurs, leading to the formation of a short lived excited state of (W<sub>10</sub>O<sub>32</sub>)<sup>4-</sup>.<sup>26</sup> After a rapid decay of the excited state, a so called "relaxed excited state" is formed which is known colloquially as wO. This relaxed excited state exhibits a lifetime of around 85 nanoseconds and is not quenched by O<sub>2</sub>.<sup>27</sup> Although this species has not yet been fully characterized, wO is presumed to be the active species involved in the photocatalytic cycle of TBADT (Figure 8). While the ground state of the TBADT is inactive in redox processes, the strong oxidizing features of wO (with potentials estimated from 2.26 to 2.61 V vs SCE),<sup>9</sup> allow the use of TBADT as a photocatalyst for many reactions. TBADT has been particularly exploited for its ability to homolytically abstract a hydrogen atom (HAT) from a wide range of alkanes, like cyclohexane (BDE<sub>CH</sub> = 99.5 Kcal/mol, Figure 9a).<sup>28</sup>

<sup>22</sup> E. Coronado, C. J. Gómez-García, Polyoxometalate-Based Molecular Materials, *Chem. Rev.* **1998**, *98*, 273.

<sup>23</sup> I. V. Kozhevnikov, Catalysis by Heteropoly Acids and Multicomponent Polyoxometalates in Liquid-Phase Reactions, *Chem. Rev.* **1998**, *98*, 171.

<sup>24</sup> J. T. Rhule, C. L. Hill, D. A. Judd, R. F. Schinazi, Polyoxometalates in Medicine, *Chem. Rev.* **1998**, *98*, 327.

<sup>25</sup> M. Fagnoni, D. Dondi, D. Ravelli A. Albinì, Photocatalysis for the Formation of the C-C Bond, *Chem. Rev.* **2007**, *107*, 2725.

<sup>26</sup> I. Texier, J. A. Delaire, C. Giannotti, Reactivity of the Charge Transfer Excited State of Sodium Decatungstate at the Nanosecond Time Scale, *Phys. Chem. Phys. Chem.* **2000**, *2*, 1205

<sup>27</sup> C. Tanielian, C. Schweitzer, R. Seghrouchni, M. Esch, R. Mechin, Polyoxometalate Sensitization in Mechanistic Studies of Photochemical Reactions: The Decatungstate Anion as a Reference Sensitizer for Photoinduced Free Radical Oxygenations of Organic compounds, *Photochem. Photobiol. Sci.* **2003**, *2*, 297.

<sup>28</sup> Y.-R. Luo, *Handbook of Bond Dissociation Energies in Organic Compounds*, **2003**, CRC Press LLC, Boca Raton.

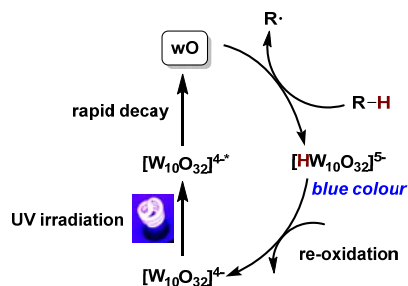


**Figure 8.** Photocatalytic cycle of TBADT (tetrabutylammonium decatungstate).

After HAT takes place, an alkyl radical and the reduced form of the photocatalyst ( $HW_{10}O_{32})^{4-}$  are generated. The reduced form features a strong blue color, and is characterized by high re-oxidation potential which can result in practical problems in re-generating the photocatalyst and achieving turnover. Different re-oxidation pathways of  $(HW_{10}O_{32})^{4-}$  are possible. The oxidation potential has been electrochemically determined to be  $-1.30$  V (vs SCE) in DMF,<sup>29</sup> and it is known that molecular  $O_2$  can act as an oxidant. In many cases, the product generated from radical addition is proposed to be the responsible for the oxidation of the reduced form of the tungstate, a mechanistic aspect which will be further detailed below.

It is known that  $wO$  can be quenched by organic molecules *via* two different quenching pathways, which provide alternative methods to generate radical species (Figure 9). While hydrogen atom transfer from cyclohexane **9** leads to the formation of the protonated reduced form of the decatungstate  $(HW_{10}O_{32})^{4-}$  and to the cyclohexane radical **12** (Figure 9a), an electron transfer can take place when a molecule with low oxidation potential (such as **14**) is used (Figure 9b). This process leads to the formation of the reduced form of the decatungstate  $(W_{10}O_{32})^{5-}$  and to the radical cation **17**.

<sup>29</sup> A. Chemseddine, C. Sanchez, J. Livage, J. P. Launay, M. Fournier, Electrochemical and Photochemical Reduction of Decatungstate: a Reinvestigation, *Inorg. Chem.* **1984**, *23*, 2609.

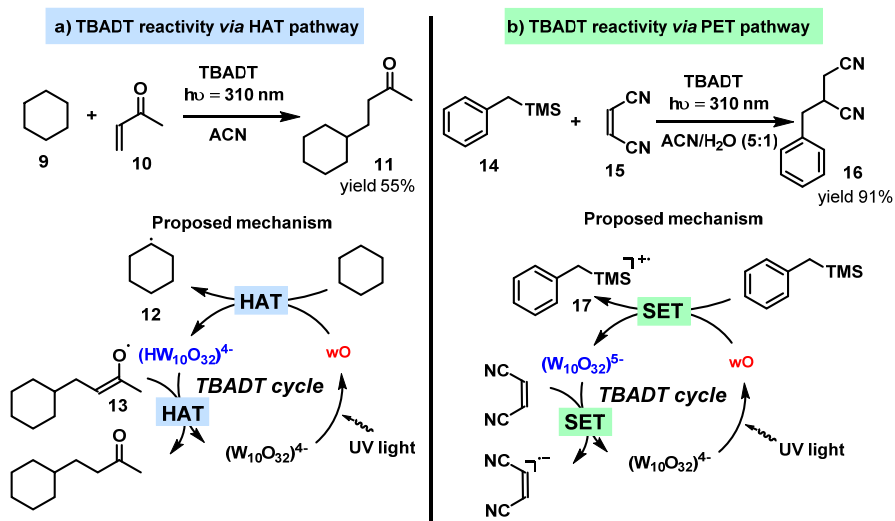


**Figure 9.** Mechanisms of radical generation available to wO, the active form of the photoexcited TBADT.

#### 4.5. Research Project and Initial Trials

Our strategy for the development of an organocatalytic, light-triggered asymmetric radical conjugate addition protocol was based on the synergistic combination of two catalytic cycles: the use of primary amine catalysts to generate iminium ion species **2** upon condensation with cyclohexenone **1**, and the use of TBADT that, upon light excitation and *via* a HAT pathway, generates the radical **4** from the benzodioxole **3** (Figure 10).

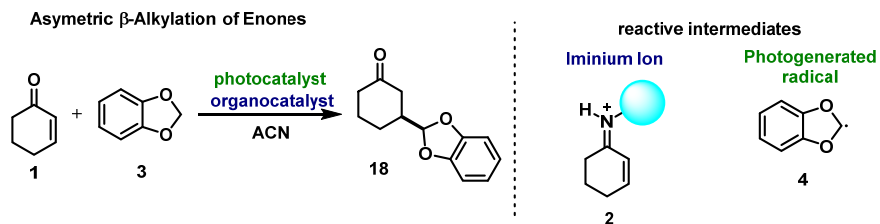


**Figure 10.** The model reaction and the key reactive intermediates. The blue circle represents the chiral organocatalyst fragment.

The coupling of cyclohexenone **1** and benzodioxole **3** was reported in racemic fashion by Fagnoni and co-workers (Figure 11).<sup>10</sup>

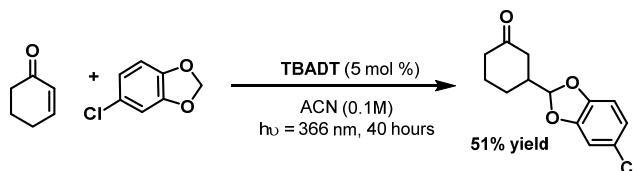


**Figure 11.** Precedent showing the feasibility of the transformation using TBADT.<sup>10</sup>

Our main concern was that the nucleophilic carbon-centered radical **4**, photogenerated *in situ*, could react with either of the two electrophilic species in the reaction media, *i.e.* the enone **1** (background racemic pathway) and the chiral iminium ion **2** (stereoselective pathway). Initially, cyclohex-2-en-1-one **1** and 1,3-benzodioxole **2** were chosen as partners for the first explorations, in the presence of a variety of chiral primary amines as organocatalyst (20 mol%),<sup>30</sup> benzoic acid as the acid co-catalyst (40 mol%, the acid was needed to aid the iminium ion formation) and TBADT as the photocatalyst (5 mol%) in acetonitrile (Figure 12). Commercially available black lights bulbs (BLB,  $\lambda_{\text{max}} = 366 \text{ nm}$ ) were used to irradiate the reaction mixture.

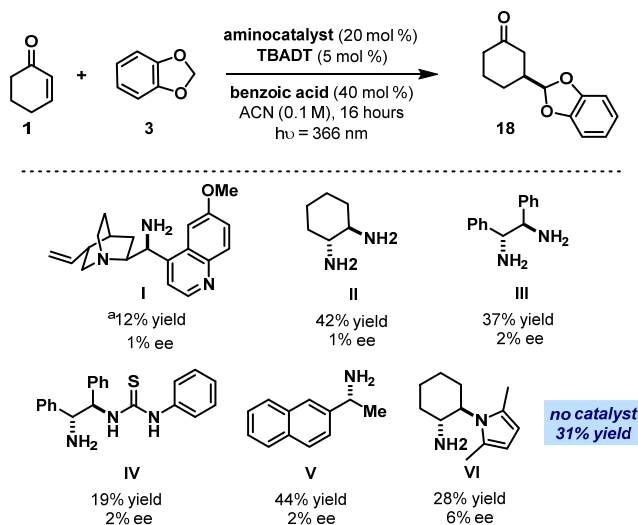


**Figure 12.** Initial attempts to perform the enantioselective radical addition to cyclohexenone **1**.<sup>b</sup> Reactions conducted under irradiation of 2 x 15 W black-light bulbs positioned 5 cm away from the reaction vessel, using 3 equivalents of **3** on a 0,1 mmol scale,  $[1]_0 = 0,1 \text{ M}$  in acetonitrile (ACN). Yields determined by <sup>1</sup>H NMR analysis of the crude mixture using trichloroethylene (TCE) as the internal standard. Enantiomeric excess (ee) values determined by HPLC analysis on chiral stationary phases. <sup>a</sup>40 mol % of TFA was used instead of benzoic acid.

<sup>30</sup> The choice of the organocatalysts was motivated by the fact that less sterically encumbered primary amines are readily prone to form an iminium ion upon condensation with enones. Secondary amine catalysts are less effective for enone activation, mainly for steric reasons.

Unfortunately, while all the trials led to reasonable yields, almost racemic products were obtained. We thought the low stereocontrol to be directly related to the presence of a fast, racemic background reaction, which was outcompeting the asymmetric organocatalytic regime. This was confirmed by the experiment conducted under the same conditions as detailed in Figure 12, but in the absence of any chiral organocatalyst and benzoic acid, which gave the product **18** with a chemical yield as high as 31%.

To attenuate this issue, we decided to modify the substrate in order to suppress the background reaction as much as possible. In this vein, we tested some blank reactions (without aminocatalyst) using different enones, which were designed with the aim of being less prone toward radical conjugate addition from the carbon centered radical **4** (generated from **3**). This was achieved by introducing an electron donating group (EDG) within the enone, so as to raise the energy level of the LUMO, or by introducing more hindered substituents at the  $\beta$  position, which should reduce the rate of the background reaction for steric reasons.

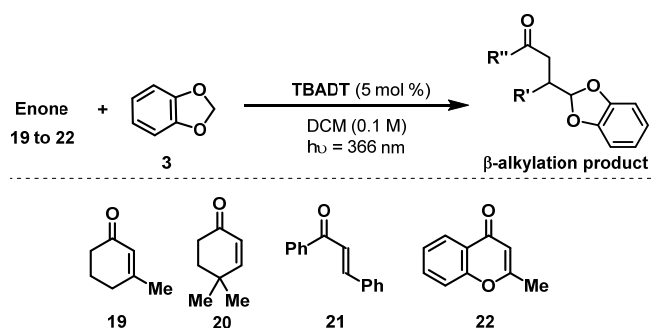


**Figure 13.** Substrates modification of enones to reduce the background reaction.

In the cases of enones **20** and **21**, a large amount of the  $\beta$ -alkylation products were detected, while **19** and **22** gave only traces (about 5% yield) of the radical conjugate addition adducts. For these enones could not “spontaneously” react with the nucleophilic radical, we expected that the more electrophilic, and hopefully stereoselective, iminium ion regime could dominate.

With this idea in mind, we investigated the reactivity of  $\beta$ -methyl cyclohexenone **19** in the presence of different chiral primary amine catalysts and benzoic acid<sup>31</sup> (Figure 14) in DCM (preferable solvent for aminocatalytic reactions). The cinchona-derived primary amine

<sup>31</sup> The acid co-catalyst aids the formation of the iminium ion by activating the carbonyl compound. The role of the acid co-catalyst could extend to its conjugated base, which is closely associated with the reacting iminium ion and may thus be directly implicated in shaping the transition structure of the iminium ion chemistry.

catalysts<sup>32</sup> (**I**, **VII**, and **VIII**) afforded only traces of the desired product **23** in racemic fashion. Interestingly, catalyst **VI**, adorned with a pyrrole ring, provided the most significant results, inducing a moderate level of stereocontrol albeit with a low reactivity (37% ee, 12% yield).

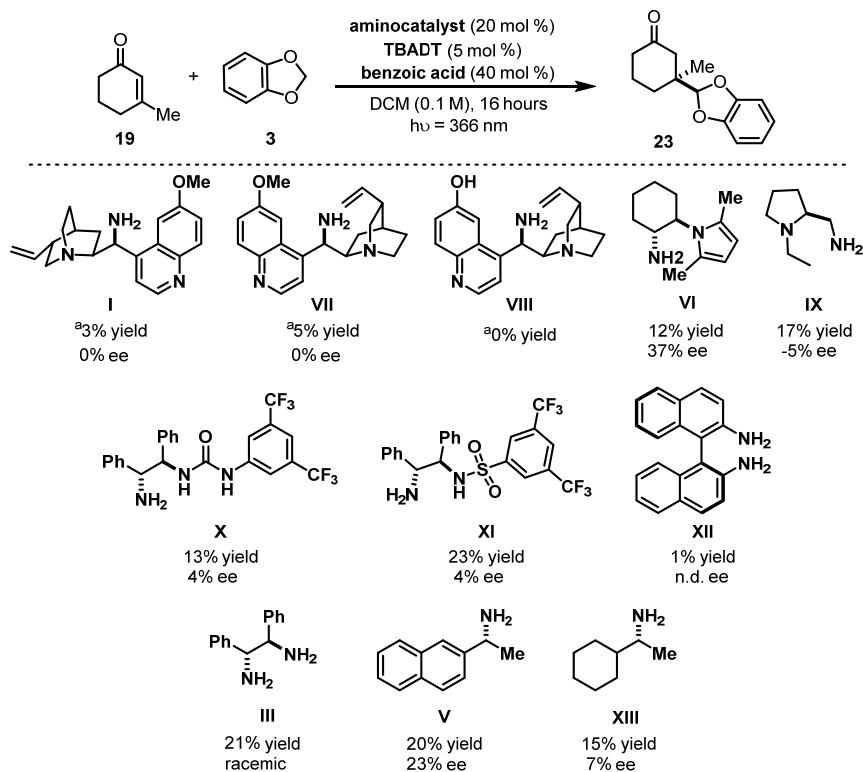


**Figure 14.** Initial catalyst screening using enone **19**. Reactions performed using 3 x 15 W blacklight irradiation positioned 5 cm away from the reaction vessel, 3 equivalents of **3** on a 0,1 mmol scale,  $[\mathbf{19}]_0 = 0,5 \text{ M}$  in dichloromethane (DCM) during 16 hours. Yield determined by  $^1\text{H}$  NMR analysis using trichloroethylene (TCE) as the internal standard. Enantiomeric excess (ee) values were determined by HPLC analysis on commercially available chiral stationary phases. n.d. not determined. <sup>a</sup>40 mol % of trifluoroacetic acid (TFA) was used instead of benzoic acid.

<sup>32</sup> P. Melchiorre, Cinchona-based Primary Amine Catalysis in the Asymmetric Functionalization of Carbonyl Compounds, *Angew. Chem. Int. Ed.* **2012**, *51*, 9748.

We wondered whether catalyst **VI** could be useful to promote the asymmetric radical addition to substrate **22** (Figure 15). However, no trace of the desired product was observed.

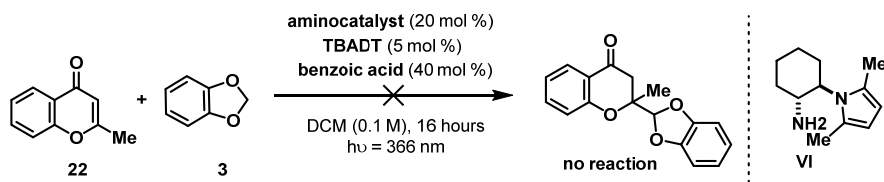


Figure 15. Asymmetric reaction using primary amine catalyst **VI** and enone **22**.

It is important to remark how introducing a substituent at the enone  $\beta$ -position not only reduced the racemic background radical addition. It also brings about an additional synthetic benefit in that the radical conjugate addition directly forges a quaternary carbon stereogenic center.

#### 4.6. Enantioselective $\beta$ -Quaternarization of Cyclic Enones.

The formation of quaternary carbon stereocenters represents a difficult target in asymmetric catalysis. Few methodologies are available for the enantioselective  $\beta$ -quaternarization of enones by means of catalytic and stereocontrolled conjugated additions.<sup>33</sup> A suitable strategy for addressing this problem capitalizes upon the generation of chiral organometallic nucleophiles and subsequent coupling with  $\beta,\beta$ -disubstituted enones. The group of Alexakis has pioneered this area by introducing a variety of enantioselective copper-catalyzed additions of various alkyl, alkenyl, and aryl aluminium compounds to cyclic enones in the presence of chiral phosphoramidite ligands.<sup>34</sup> Hoveyda has also reported the use of Cu/Ag-N-heterocyclic carbenes as effective chiral catalysts for the conjugate additions of alkyl- or arylzinc reagents to enones.<sup>35</sup> A recent example reported by Fletcher demonstrated that alkylmetal species, generated *in situ* from alkenes *via* hydrozirconation, can be used for copper-catalyzed asymmetric conjugate additions to  $\beta,\beta$ -disubstituted enones providing quaternary carbon stereocenters with high fidelity (Figure 16).<sup>36</sup>

<sup>33</sup> K. W. Quasdorf, L. E. Overman, Catalytic Enantioselective Synthesis of Quaternary Carbon Stereocentres, *Nature* **2014**, *516*, 181.

<sup>34</sup> a) M. Vuagnoux-d'Augustin, A. Alexakis, Copper-catalyzed Asymmetric Conjugate Addition of Trialkylaluminum Reagents to Trisubstituted Enones: Construction of Chiral Quaternary Centers, *Chem. Eur. J.* **2007**, *13*, 9647. b) D. Müller, A. Alexakis, Formation of Quaternary Stereogenic Centers by Copper Catalyzed Asymmetric Conjugate Addition Reactions of Alkenyl Aluminums to Trisubstituted Enones, *Chem. Eur. J.* **2013**, *19*, 15226. c) C. Hawner, K. Li, V. Cirriez, A. Alexakis, Copper-Catalyzed Asymmetric Conjugate Addition of Aryl Aluminum Reagents to Trisubstituted Enones: Construction of Aryl Substituted Quaternary Centers, *Angew. Chem. Int. Ed.* **2008**, *47*, 8211.

<sup>35</sup> K-S Lee, M. K. Brown, A. W. Hird, and A. H. Hoveyda, A Practical Method for Enantioselective Synthesis of All-Carbon Quaternary Stereogenic Centers through NHC-Cu-Catalyzed Conjugate Additions of Alkyl and Arylzinc Reagents to  $\beta$ -Substituted Cyclic Enones, *J. Am. Chem. Soc.* **2006**, *128*, 7182.

<sup>36</sup> M. Sidera, P. M. C. Roth, R. M. Maksymowicz, S. P. Fletcher, Formation of Quaternary Centers by Copper-Catalyzed Asymmetric Conjugate Addition of Alkylzirconium Reagents, *Angew. Chem. Int. Ed.* **2013**, *52*, 7995.



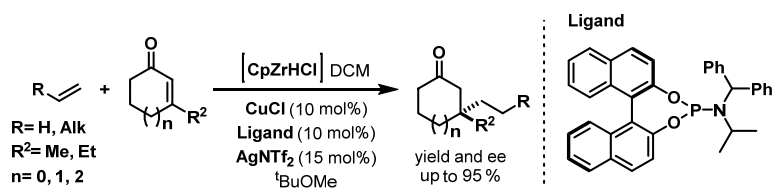


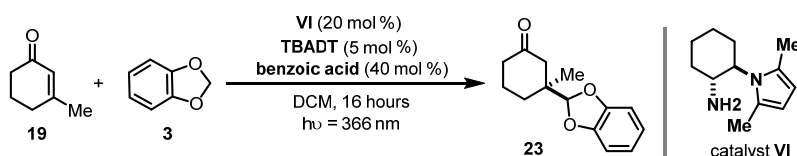
**Figure 16.** Formation of quaternary stereocenters by copper-catalyzed asymmetric conjugate addition of alkylzirconium reagents.

In contrast, iminium ion-mediated organocatalytic strategies for the quaternarization of cyclic and acyclic enones are restricted to the use of nucleophiles bearing readily enolizable carbon atoms, such as nitroalkanes.<sup>37</sup>

## 4.7. Results and Discussion

Initial trials identified catalyst **VI** as the best lead compound to obtain suitable levels of enantiocontrol in the model radical conjugate addition reaction with enone **19**. However, typical concentration values for the optimum TBADT catalyzed reactions (which generally require a high dilution) were not compatible with the conditions suitable for effective primary amine-iminium ion catalysis (which generally require concentrated systems). This is why we carefully evaluated concentration effects on the reaction (Table 1).

**Table 1.** Concentration effect using primary amine catalyst **VI**<sup>a</sup>



entry	concentration (M)	yield (%) <sup>b</sup>	ee (%) <sup>c</sup>
1	0.1	12	37
2	0.25	19	55
3	0.5	29	60
4	1	21	60

<sup>a</sup>Reactions carried out using 3 x 15 W black light irradiation and 3 equivalents of **3**. <sup>b</sup>Yield determined by <sup>1</sup>H NMR analysis of the crude reaction mixture using trichloroethylene (TCE) as an internal standard. <sup>c</sup>Enantiomeric excess determined by HPLC analysis.

<sup>37</sup> X. Gu, Y. Dai, T. Guo, A. Franchino, D. J. Dixon, J. Ye, A General, Scalable, Organocatalytic Nitro-Michael Addition to Enones: Enantioselective Access to All-Carbon Quaternary Stereocenters, *Org. Lett.* **2015**, *17*, 1505.

The use of a more concentrated reaction system ( $[\mathbf{19}]_0 = 0,5 \text{ M}$  in DCM, entry 3), provided an increase of both yield and enantiomeric excess.

We then investigated a variety of other chiral catalysts using DCM as the reaction medium (Figure 17), including bifunctional primary amines bearing a hydrogen bond donor functionality (sulfonamide and thiourea-derived catalysts **XIV**, **XV**, **XVI**, **XVII**, **XVIII**), which did not lead to any improvement. Catalysts having the diphenylethylamine (DPEN) chiral backbone and adorned with a 2,5 methyl-pyrrole moiety as the shielding group (catalysts **XIX**, **XX**, **XXI**) inferred lower enantioselectivity. Last, installing bulkier substituents at the 2,5-pyrrole ring positions (catalysts **XXII**, **XXIII**, **XXIV**) was detrimental.

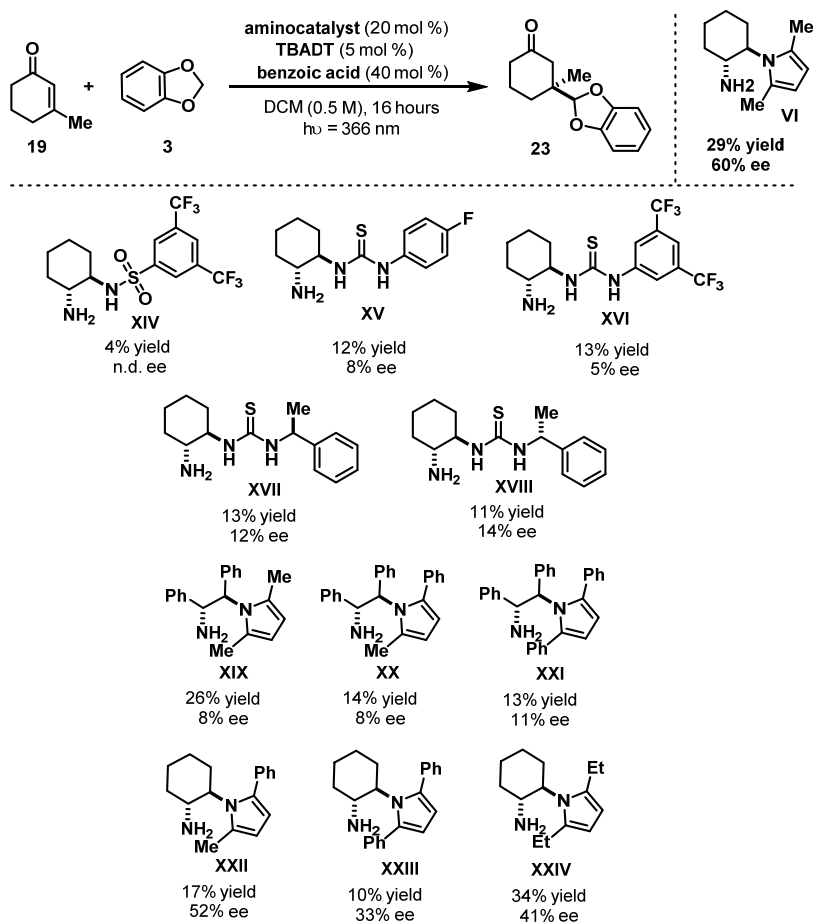


**Figure 17.** Screening of the 2<sup>nd</sup> generation catalyst. Reactions carried out using 3 x 15 W blacklight irradiation, 3 equivalents of **3** on a 0,1 mmol scale,  $[\mathbf{19}]_0 = 0,5 \text{ M}$  in DCM for 16 hours. Yield determined by  $^1\text{H}$  NMR analysis using trichloroethylene (TCE) as an internal standard. Enantiomeric excess (ee) values determined by HPLC analysis on commercially available chiral stationary phases. n.d. not determined.

At this point, we wondered whether the use of 2,5 substituted pyrrole catalysts bearing larger shielding groups could increase the level of stereocontrol (methyl-substituted catalyst **XIX**, ethyl-substituted catalyst **XXIV**, phenyl-substituted catalyst **XXIII**). However, the best stereoinduction was inferred by the catalyst bearing a methyl substituent.

Following the same conceptual line, we synthesized primary amine catalysts bearing larger shielding groups than pyrrole on the chiral scaffold (Figure 18).

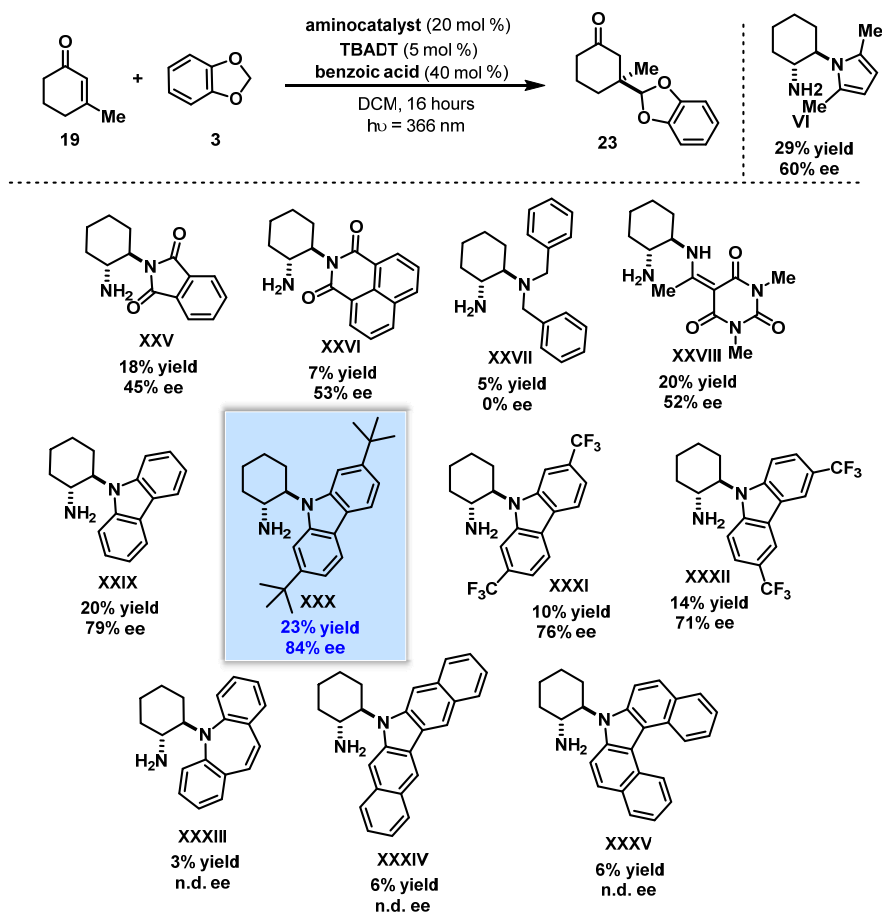
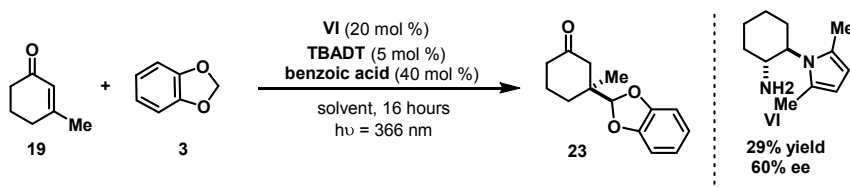


**Figure 18.** Screening the 3<sup>rd</sup> generation catalysts. Reactions performed using 3 x 15 W blacklight irradiation, 3 equivalents of **3** on a 0,1 mmol scale,  $[\mathbf{19}]_0 = 0,5 \text{ M}$  in DCM for 16 hours. Yield determined by  $^1\text{H}$  NMR analysis of the crude reaction mixture using trichloroethylene (TCE) as an internal standard.  $^c$ Enantiomeric Excess (ee) values determined by HPLC analysis on commercially available chiral stationary phases. n.d. not determined.

To our delight, replacing the pyrrole group of catalyst **VI** for a carbazole moiety (**XXIX**) improved the enantioselectivity up to 79% ee. The use of chiral primary amines with bulkier fused rings (catalysts **XXXIII**, **XXXIV**, **XXXV**) almost completely suppressed the asymmetric transformation. Gratifyingly, however, the stereocontrol was sensitive to catalyst structural modifications at the 3,6 or 2,7 positions of the carbazole moiety (catalysts **XXX**, **XXXI**, **XXXII**). Catalysts **XXIX** and **XXX** provided the best results (84% ee for the latter). However, the lengthy and difficult synthetic strategy used for the preparation of these catalysts did not allow us to obtain them in large amounts. While a new and more effective synthetic route (detailed in Section 4.7.2) to easily obtain the well-performing catalysts was investigated, optimization of the model reaction was continued with the simpler catalyst **VI**.

We evaluated the effects of the reaction media and additives on the model reaction catalyzed by **VI**, as detailed in Table 2. Not many solvents were suitable for the transformation, mainly because TBADT is poorly soluble in apolar solvents, such as toluene. Gratifyingly, the use of acetonitrile (entry 2) resulted in higher levels of enantiocontrol but at the expense of the reactivity. In order to improve the yield, additional additives were tested. It is known that the quantum yield of the TBADT photocatalyst, and therefore its effectiveness, is strongly related to the counter-ion of decatungstate. The addition of tetrabutylammonium bromide (TBAB) is known to further increase the quantum yield of the TBADT.<sup>9</sup> Pleasingly, using one equivalent of TBAB led to a doubling of the yield of the model transformation while maintaining the levels of enantiocontrol (entry 3).

**Table 2.** Screening of additives and solvents.<sup>a</sup>



entry	solvent	additive	yield (%) <sup>b</sup>	ee (%) <sup>c</sup>
1	DCM	-	29	60
2	ACN	-	17	69
3	ACN	TBAB (1 equiv)	38	70
4	ACN	TBAB (1equiv)/(10 mol%)RuO <sub>2</sub>	30	70

<sup>a</sup> Reactions carried out using 3 x 15 W black light irradiation, 3 equivalents of **3** on a 0,1 mmol scale, [19]<sub>0</sub> = 0,5 M in DCM. <sup>b</sup> Yield of **23** determined by <sup>1</sup>H NMR analysis using trichloroethylene (TCE) as an internal standard. <sup>c</sup> Enantiomeric excess (ee) values determined by HPLC analysis on commercially available chiral stationary phases.

In a different experiment, a catalytic amount of RuO<sub>2</sub> was used to facilitate photocatalyst turnover by means of oxidation (regenerating (W<sub>10</sub>O<sub>32</sub>)<sup>4-</sup> from the reduced (W<sub>10</sub>O<sub>32</sub>)<sup>5-</sup>), but unfortunately any improvement was observed (entry 4). Further screening of classical reaction parameters using amine catalyst **VI** in acetonitrile (e.g. stoichiometry, acid co-catalysts, etc.) did not further improve the yield or the enantiomeric excess of the model reaction (results not shown).

#### 4.7.1. Final Optimization Studies

Once the conditions in Table 2, entry 3 (acetonitrile, use of 1 equiv of TBAB, 20 mol% of catalyst **VI**) were identified, we decided to develop a robust synthetic route for making the chiral aminocatalyst, which allowed a flexible modification of the substitution patterns within the carbazole moiety.

#### 4.7.2. Synthetic route for the preparation of catalyst **XXIX** and analogous thereof

As mentioned before, catalyst **XXIX** was not available in large amount following our original synthetic procedure. After many synthetic plans, we have developed the following modular synthesis for accessing a variety of enantio-enriched chiral primary amine-carbazole catalyst derivatives. The retrosynthetic analysis is shown in (Figure 19). The key step is an enantioselective aza-Michael reaction of the carbazole **29A** and the nitro-alkene **28**.

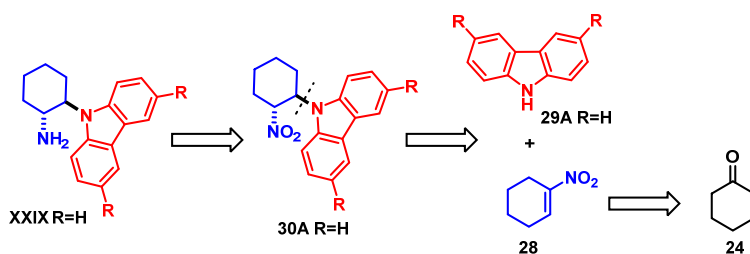


**Figure 19.** Retrosynthetic analysis for the preparation of catalyst **XXIX**-type derivatives.

Compound **28** was prepared from the ketone **24** in 4 steps with an overall yield of 25 % (Figure 20).

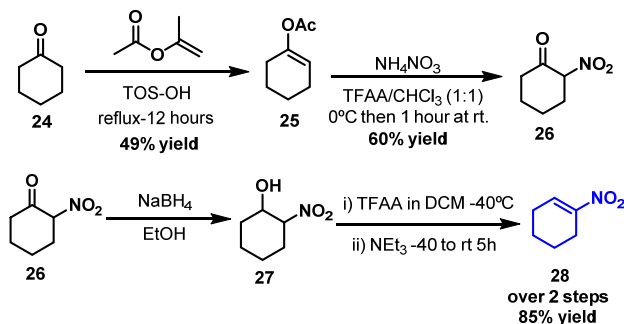


**Figure 20.** Synthetic route for preparation of the cyclic nitroalkene **28**. TosOH= Tosylic acid,  $\text{NH}_4\text{NO}_3$  = ammonium nitrate, TFAA = trifluoroacetic anhydride,  $\text{CHCl}_3$  = chloroform,  $\text{NaBH}_4$  = sodium borohydride, EtOH = ethanol, DCM = dichloromethane,  $\text{NEt}_3$  = triethylamine.

For the preparation of the enantioenriched compound **30**, an enantioselective aza-Michael reaction was developed using a stoichiometric amount of the chiral complexing agent **31** (Figure 21).<sup>38</sup> The key of success was the formation of a chiral organo-lithium intermediate that could induce enantioselectivity in the aza-Michael reaction (full experimental details are detailed within the experimental section).

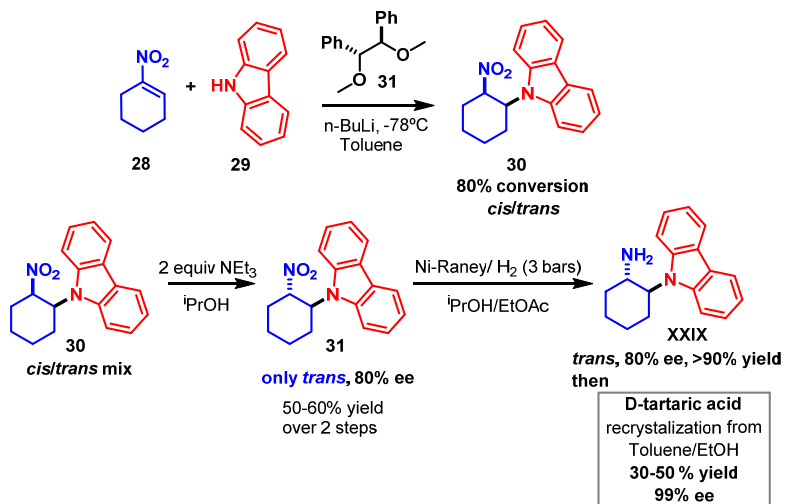


**Figure 21.** Synthetic route for preparation of catalyst **XXIX**. EtOH = ethanol, DCM = dichloromethane,  $\text{NEt}_3$  = triethylamine, *i*PrOH = isopropanol, EtOAc = ethyl acetate,  $n\text{-BuLi}$  = butyllithium.

<sup>38</sup> H. Doi, T. Sakai, M. Iguchi, K. Yamada, K. Tomioka, Chiral Ligand-Controlled Asymmetric Conjugate Addition of Lithium Amides to Enoates, *J. Am. Chem. Soc.* **2003**, *125*, 2886.

### 4.7.3. Light Source

In the initial studies, we used 3 normal blacklight bulbs (15 W), available in a household shop, as a source of light to irradiate the reaction mixture. Using this set up, it was not possible to control the intensity of the irradiation and the temperature of the reaction, influenced by the heat generated by the light source and dependent on the distance between the reaction vessel and the bulb. Since both the light intensity and the resulting reaction temperature have a direct influence on the reaction outcome, we tried to design a more reproducible and controllable photochemical set-up. In collaboration with José Luis León (the manager of mechanical workshop at ICIQ) and Dr. Javier Pérez Hernández (the manager of the Photophysics Unit at ICIQ), a more reproducible irradiation system was ideated, which allowed us to independently control all the desired parameters (*i.e.* light emission and reaction temperature). Firstly, a system that uses a single light emitting diode (LED) with the  $\lambda_{\max}$  centered at 355 nm was designed. This set-up assured a constant distance between the reaction vessel and the LED and a constant temperature (Figure 22, system 1). A second system used a single LED with  $\lambda_{\max}$  centered at 365 nm. In the latter case, the temperature was controlled by an internal water flow system connected to an electronic cryostat. This flow was connected to the aluminum holder of the reaction vials bearing the LED source (designed by the ICIQ services). Using this system, it was possible to precisely control the reaction temperature in a range between 40 to  $-20^{\circ}\text{C}$  (Figure 22, system 2). The two systems were connected to a power supplier, which controls the intensity of the emitting light. Technical details are explained in Appendix 2 of this Chapter.

A third system consisted of a strip of LED's with a  $\lambda_{\max}$  centered at 365 nm. The multitude of LED's (LED Stripe Set of 3m, with single LED every 4 cm) secured higher light irradiation to the reaction mixture. The addition of a fan was necessary to keep the temperature of the vessels below  $50^{\circ}\text{C}$  (Figure 22, system 3).

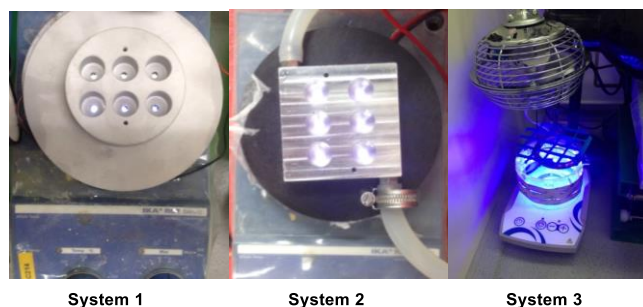
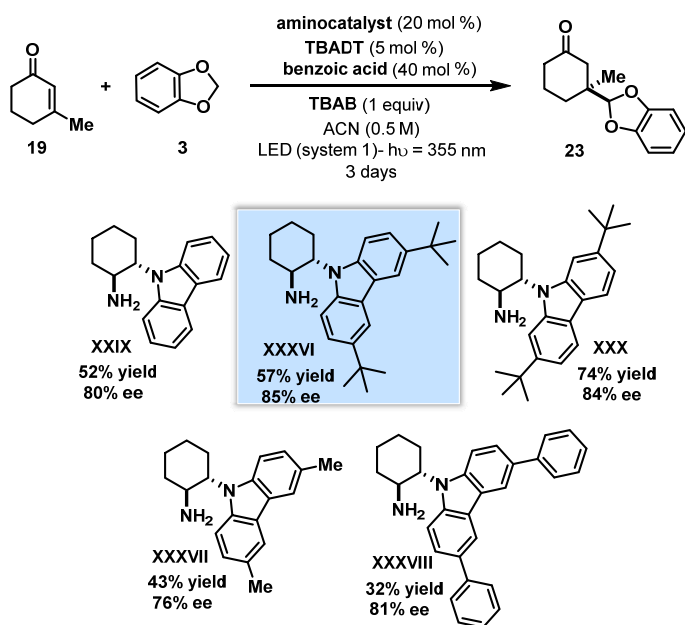


Figure 22. Different illumination devices: 355 nm and 366 nm LEDs setups.

#### 4.7.4. Further Optimization Studies.

With an effective synthetic route for accessing the carbazole-based aminocatalysts and a more reliable illumination system in hand, we started an additional cycle of optimization of the model reaction (Figure 23). We prepared some chiral catalysts bearing structural modifications at the 3,6 or 2,7 positions of the carbazole moiety, and they were tested against the conditions selected as optimal using catalyst **VI** (Table 2 - entry 3) and with the single LED system 1. Catalyst **XXIX** confirmed an interesting behavior (52% yield, 80% ee). Other primary amine catalysts were tested and catalyst **XXXVI**, bearing a sterically prominent *tert*-butyl substituent at the 3,6-positions of the carbazole moiety, provided better enantiocontrol (57% yield, 85% ee). Poorer selectivity was observed when smaller substituents than a *tert*-butyl group were placed at the 3,6-positions of the carbazole (catalysts **XXXVII**, **XXXVIII**). Similar results were obtained with catalyst **XXXVI** and catalyst **XXX** (the latter was not further investigated since the separation of the enantiomers was extremely difficult and required preparative HPLC approaches). Catalyst **XXXVI** was selected for further optimization studies.



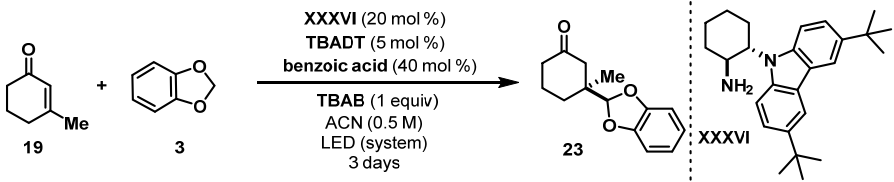
**Figure 23.** Modifications of the carbazole scaffold within the chiral aminocatalyst.

An extensive screening of light intensity and temperature revealed a dramatic effect in both yield and enantiomeric excess of the transformation (Table 3). The effect of the temperature was first tested using the irradiation system 1 as the light source, introducing the system in the fridge (entry 2) and the freezer (entry 3). While a small decrease of the reaction temperature lead to poorer yields and levels of enantiocontrol (entry 2), a larger decrease shut down the



process almost completely (entry 3). Using system 2, greater levels of yield along with similar levels of enantiocontrol were observed when increasing the temperature to 35 °C (entry 4). Prolonging the reaction time, synthetically useful yields with good enantiocontrol were obtained (entry 6). We further confirmed the necessity of higher temperature, since at 25 °C the reaction gave poorer yields and enantiocontrol (entry 5) compared to the same reaction performed at 35 °C (entry 6). Less enantiocontrol was observed using the high intensity irradiation system 3 (entry 7), a likely consequence of the magnified competition of the background reaction (entry 9), compared with the background process observed when using the illuminating system 2 (entry 8). On these bases, we decided to use the light illumination system 2 using 35°C as the reaction temperature for further studies. This system provided also a more reliable control of the reaction temperature.

**Table 3.** Screening of the temperature and irradiation systems.<sup>a</sup>

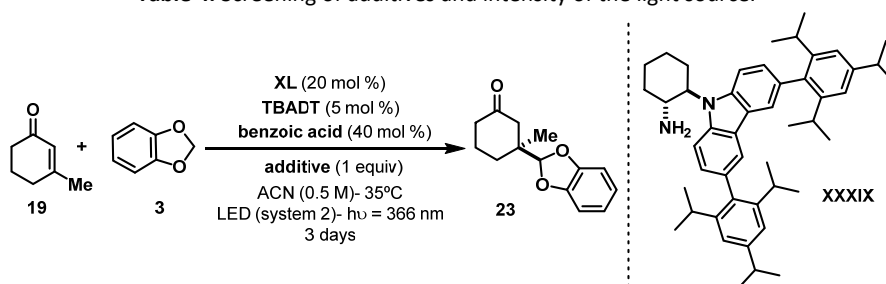


Entry	time (hours)	Light Source - Irradiance (W/cm <sup>2</sup> )	T (°C)	Aminocatalyst	yield (%) <sup>b</sup>	ee (%) <sup>c</sup>
1	18	System 1 - 11,25 W/cm <sup>2</sup>	25	yes	20	85
2	18	System 1 - 11,25 W/cm <sup>2</sup>	14	yes	15	82
3	18	System 1 - 11,25 W/cm <sup>2</sup>	0	yes	8	40
4	18	System 2 - 9,85 W/cm <sup>2</sup>	35	yes	46	82
5	72	System 2 - 9,85 W/cm <sup>2</sup>	25	yes	71	75
6	72	System 2 - 9,85 W/cm <sup>2</sup>	35	yes	89	80
7	72	System 3	30	yes	65	66
8	72	System 2 - 9,85 W/cm <sup>2</sup>	35	no	19	-
9	72	System 3	30	no	27	-

<sup>a</sup> Reactions carried out using 3 equivalents of **3** on a 0,1 mmol scale,  $[19]_0 = 0,5$  M in ACN. <sup>b</sup> Yield of **23** determined by <sup>1</sup>H NMR analysis using trichloroethylene (TCE) as an internal standard. <sup>c</sup> Enantiomeric excess (ee) values determined by HPLC analysis on commercially available chiral stationary phases.

To further increase the level of enantiocontrol (80% ee, entry 6), we synthesized a more sterically hindered primary amine catalyst, bearing bulkier groups than the *tert*-butyl at the 3,6 positions of the carbazole moiety. The (1*R*,2*R*)-2-(3,6-bis(2,4,6-triisopropylphenyl)-9H-carbazol-9-yl)cyclohexan-1-amine **XXXIX** was prepared following the synthetic route detailed in Figure 21 with some modifications, as detailed in Section 4.9.2 of this Chapter. We next focused on the fine tuning of the reaction parameters using the new catalyst **XXXIX** (Table 4). Direct comparison of conditions with entry 6 - Table 3 revealed a similar yield and higher levels of enantiocontrol when using **XXXIX** (88% ee, Table 4, entry 4). Different light intensities (applying different voltages to the light system 2) at shorter reaction times (40 hours) were tested, obtaining higher enantiomeric excess with less intensity (91% ee, entry 1). Unfortunately, this increased stereoselectivity was not maintained when conducting the reaction over a longer time (72 hours, entry 3). The counterion of tetrabutylammonium salt was again found to have a beneficial effect on the level of enantiocontrol, albeit the reduced reactivity required a 72 hour reaction time (entries 5 and 6).

**Table 4.** Screening of additives and intensity of the light source.<sup>a</sup>



Entry	Reaction Time (hours)	System 2 Irradiance (W/cm <sup>2</sup> )	Additive	yield (%)	ee (%)
1	40	7,30 W/cm <sup>2</sup>	TBAB	64	91
2	40	9,85 W/cm <sup>2</sup>	TBAB	86	89
3	72	7,30 W/cm <sup>2</sup>	TBAB	91	88
4	72	9,85 W/cm <sup>2</sup>	TBAB	94	88
5	72	9,85 W/cm <sup>2</sup>	TBAPF <sub>6</sub>	71	92
6	72	9,85 W/cm <sup>2</sup>	TBAPF <sub>4</sub>	75	93

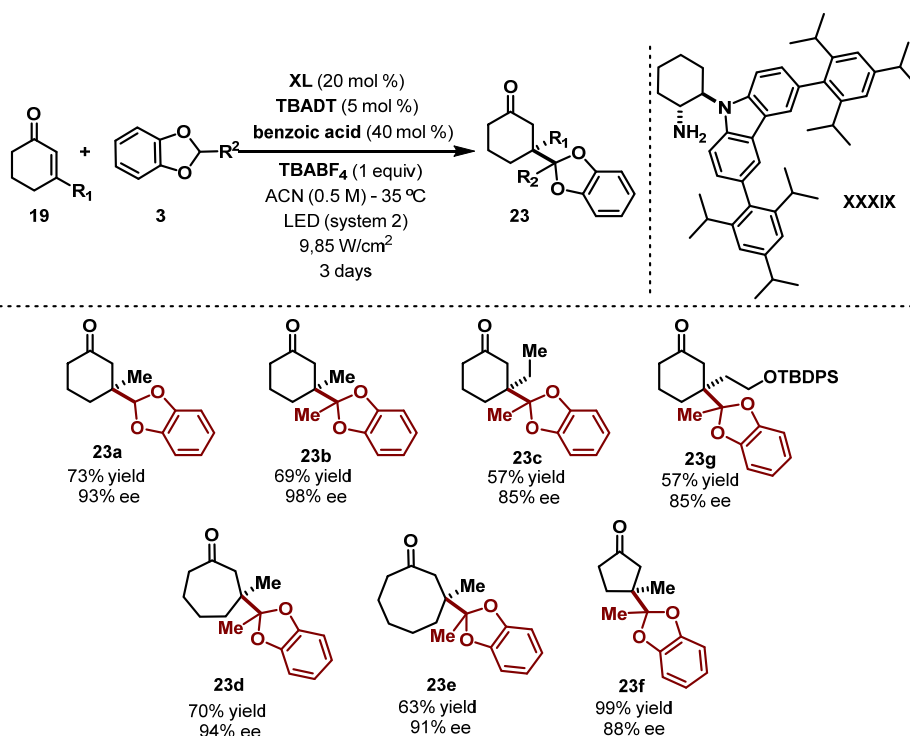
<sup>a</sup> Reactions carried out using 3 equivalents of **3** on a 0,1 mmol scale, [**19**]<sub>0</sub> = 0,5 M in ACN. <sup>b</sup> Yield of **23** determined by <sup>1</sup>H NMR analysis using trichloroethylene (TCE) as an internal standard.

<sup>c</sup> Enantiomeric excess (ee) values determined by HPLC analysis on commercially available chiral stationary phases.

After extensive and massive optimization studies, the following conditions were eventually selected to study the scope of the reaction: a power supplier at 18 V of applied voltage to control the emission intensity of the black LEDs within system 2 (irradiation of the single LED of 9.85 W/cm<sup>2</sup>), 3 equivalents of benzodioxole **3** in the presence of 1 equivalent of TBABF<sub>4</sub> salt as an additive, 20 mol% of the chiral primary amine catalyst **XXXIX**, 40 mol% of benzoic acid as co-catalyst, and 5 mol% of TBADT photocatalyst in ACN (0,5 M). The reactions were conducted for 72 hours at 35°C.

Exploring the scope of the transformation (Table 5), we observed how the presence of a methyl group at the R<sup>2</sup> position of benzodioxole **3** resulted in higher stereoselectivity (98% ee, product **23b**). A wide range of cyclic enones are compatible with the catalytic system, leading to the quaternarized products **23d**, **23e**, **23f**. The use of longer alkyl substituents within **19** (R<sub>1</sub> = Et, CH<sub>2</sub>CH<sub>2</sub>OTBDPS) preserved the levels of enantiocontrol of the transformation.

**Table 5.** Optimized conditions and scope of the enantioselective β-alkylation of enones by means of iminium ion trapping of photochemically generated radicals.<sup>a</sup>



<sup>a</sup> Reactions carried out using 3 equivalents of **3** on a 0,2 mmol scale, [**19**]<sub>0</sub> = 0,5 M in ACN. <sup>b</sup> Yield of the isolated product **23** after chromatographic purification on silica gel. <sup>c</sup> Enantiomeric excess (ee) values determined by HPLC analysis on commercially available chiral stationary phases. OTBDPS = tert-butyl(diphenyl) silyl ether.

## 4.8. ANNEX 1 - Synthetic Efforts Toward the Preparation of the Carbazole-Derived Organocatalysts

The preparation of the enantiopure chiral primary amine-carbazole catalyst **XXIX** and its derivatives with substituents at the 3,6 or 2,7 heteroaromatic position was one of the most challenging parts of the project. When attempting the synthesis of the organocatalysts, we faced two main hurdles when trying to:

- 1) Stereoselectively introduce the carbazole within the cyclohexane moiety.
- 2) Obtain the organocatalyst as a single enantiomer.

In order to summarize all the efforts devoted to this synthetic endeavor, this annex has been divided into 3 parts. Each part details a different key reaction used to introduce the carbazole moiety into the cyclohexane ring: *i*) an  $S_N2$  substitution, *ii*) a light mediated N-cyclohexyl substituted carbazole preparation, and *iii*) a Michael addition of a carbazole-based nucleophile.

### 4.8.1. Route 1: $S_N2$ Substitution

The first retrosynthetic route considered a possible  $S_N2$  reaction of the carbazole **29** or analogs with synthon **A** (Figure 24).

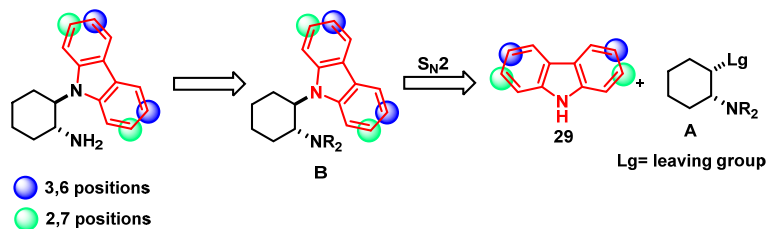
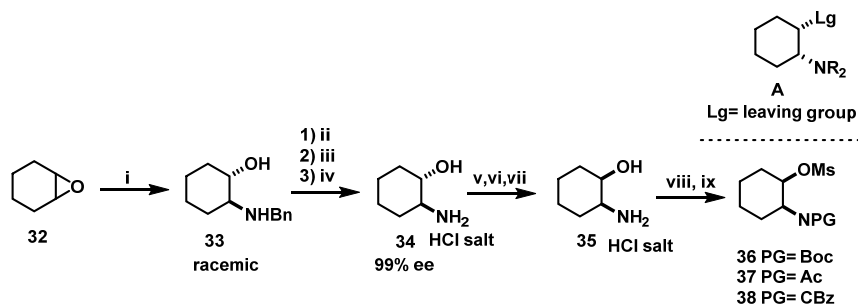


Figure 24. Retro-synthetic route 1 for the catalyst preparation.

Preparation of the enantiopure chiral synthon **A** (Figure 25) started with the ring opening of the cyclohexene oxide with benzyl amine to obtain the racemic aminoalcohol **33**. Salt recrystallization using *S*-mandelic acid as the chiral resolving agent, and reduction afforded the enantiopure *trans*-aminoalcohol **34**. Epimerization of the alcohol-bearing stereogenic center in **34** gave the enantiopure *cis* isomer **35**. After different amino protecting groups were installed, alcohol mesylation provided the protected aminoalcohols substrates **36**, **37**, and **38**.



**Figure 25.** Approach for the preparation of the synthon **A**: i)  $\text{BnNH}_2$ ,  $\text{H}_2\text{O}$ ,  $100\text{ }^\circ\text{C}$ ; ii) (*S*)-mandelic acid,  $\text{EtOAc}$ , recrystallization from ( $\text{EtOAc}/\text{EtOH}$ ).<sup>39</sup> iii)  $\text{NaOH}$ ; iv)  $\text{Pd/C}$ ,  $\text{H}_2$ ,  $\text{MeOH}$ ; then  $\text{HCl}$  gas. v)  $\text{Ac}_2\text{O}$ , ( $\text{Na}_2\text{CO}_3$  (10% aq. solution)/Acetone)  $0^\circ\text{C}$  then rt. vi)  $\text{SOCl}_2$ ,  $\text{CHCl}_3$ ,  $0\text{ }^\circ\text{C}$  then rt. vii)  $\text{HCl}$  (10% aq. solution), reflux.<sup>40</sup> viii) 36)  $\text{Boc}_2\text{O}$ ,  $\text{NEt}_3$ , 37)  $\text{Ac}_2\text{O}$ ,  $\text{NaOAc}$ ,  $\text{H}_2\text{O}$  38)  $\text{CbzCl}$ ,  $\text{NEt}_3$ ; ix)  $\text{MsCl}$ ,  $\text{NEt}_3$ .

On the other side, we prepared compound **41**, containing an azide as the amine precursor, starting from compound **39** and using imidazole-1-sulfonyl azide hydrochloride **40** as a diazo transfer reagent (Figure 26).<sup>41</sup>

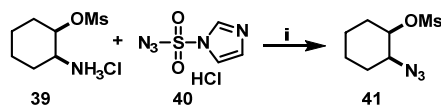


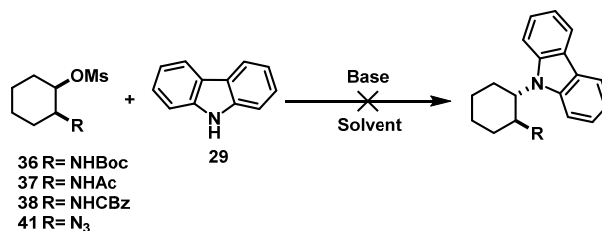
**Figure 26.** Approach for the preparation of the synthon **A**. i)  $\text{K}_2\text{CO}_3$ ,  $\text{CuSO}_4 \cdot 10\text{H}_2\text{O}$ ,  $\text{MeOH}$ , 80% yield.

With all these substrates at hand, we tested the feasibility of the  $\text{S}_{\text{N}}2$  reaction with carbazole **29** under different conditions (Table 6).

<sup>39</sup> I. Schiffrers, C. Bolm, Synthesis and Resolution of Racemic Trans-2-(*n*-benzyl)amino-1-cyclohexanol: Enantiomer Separation by Sequential use of (*R*)- and (*S*)-Mandelic Acid, *Org. synth.* **2008**, *85*, 106.

<sup>40</sup> S. E. Schaus, J. F. Larrow, E. N. Jacobsen, Practical Synthesis of Enantiopure Cyclic 1,2-Amino Alcohols via Catalytic Asymmetric Ring Opening of Meso Epoxides, *J. Org. Chem.* **1997**, *62*, 4197.

<sup>41</sup> E. D. Goddard-Borger, R. V. Stick, An Efficient, Inexpensive, and Shelf-Stable Diazotransfer Reagent: Imidazole-1-sulfonyl Azide Hydrochloride, *Org. Lett.*, **2007**, *9*, 3797.

**Table 6.** Conditions for the  $S_N2$ -type introduction of the carbazole.

Entry	Substrate	Conditions	Conversion
1 <sup>a</sup>	5	n-BuLi (1.05 equiv), THF, -78 °C to rt	RSM
2 <sup>a</sup>	5	n-BuLi (1.05 equiv), THF, (0 to 65) °C	RSM
3 <sup>a</sup>	5	NaH (1.2 equiv), DMF, 90 °C	Degradation
4 <sup>a</sup>	5	<sup>t</sup> BuOK (1.05 equiv), DMF, (55 to 110) °C	Degradation
5	5	K <sub>2</sub> CO <sub>3</sub> (2 equiv) DMSO, 18-crown-6, rt	RSM
6	5	Cs <sub>2</sub> CO <sub>3</sub> (2 equiv), Tol., 18-crown-6, 80 °C	RSM
8 <sup>a</sup>	6	n-BuLi (1.05 equiv), THF, (0 to 65) °C	RSM
9 <sup>a</sup>	7	n-BuLi (1.05 equiv), THF, (0 to 65) °C	RSM
10	8	KOH (5 equiv), DMSO	E2

<sup>a</sup>Upon stirring for 1 hour, a carbazole and base solution was added to a solution of the aminoalcohol derivative.

Unfortunately, we did not detect any trace of the desired carbazole substitution product. Failure to successfully develop route 1 required us to go back to the literature to plan another synthetic route in order to stereoselectively introduce the carbazole within the cyclohexane moiety.

#### 4.8.2. Route 2: Photoinduced, Copper-Catalyzed Couplings of Carbazoles.

We based our synthetic plan on the chemistry reported by Fu and Peters,<sup>42</sup> who described the photoinduced coupling of carbazoles with cyclic alkyl iodides catalyzed by copper. The following retrosynthetic route was envisaged (Figure 27).

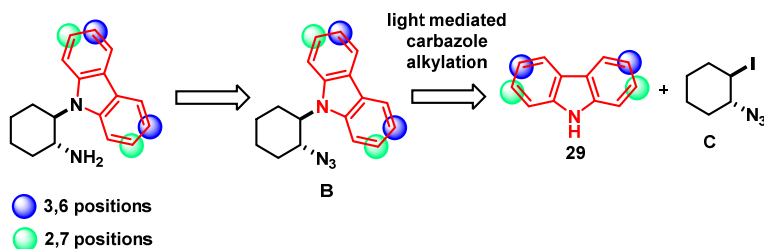


Figure 27. Light-triggered retro-synthetic route 2 for catalyst preparation.

We surmised that synthon **C** could be useful to obtain the catalyst precursor **B**. Our idea was based on the report by Fu and Peters, who described a diastereoselective alkylation of the chiral racemic substrate **42** with carbazole **29** under 100 W Hg lamp irradiation in the presence of a base and a copper catalyst to obtain **43** as a single diastereoisomer (Figure 28).<sup>42</sup>

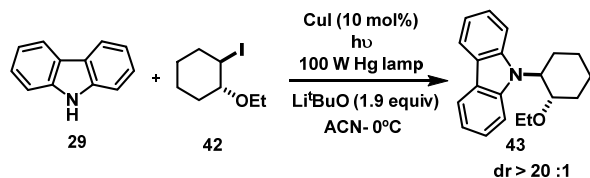


Figure 28. Precedent detailing a diastereoselective copper catalyzed carbazole N-alkylation reaction.<sup>42</sup>

To test this synthetic possibility, we synthesized compound **48** (Figure 29). Iodination of cyclohexanone **44** with N-iodosuccinimide under acidic conditions afforded compound **45**. After ketone reduction and mesylation of the resulting alcohol, compound **47** was isolated. Simple S<sub>N</sub>2 reaction using sodium azide afforded compound **48** as the pure *trans* isomer.

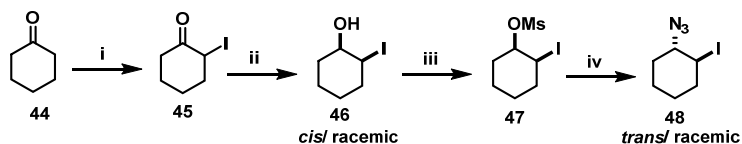
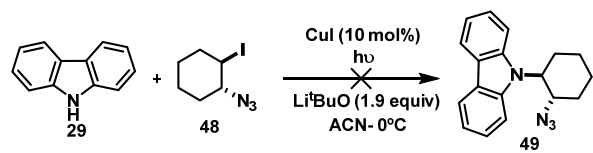


Figure 29. i) TosOH, NIS, DCM ii) NaBH<sub>4</sub>, MeOH, iii) MsCl, Et<sub>3</sub>N, iv) NaN<sub>3</sub>, DMF

<sup>42</sup> A. C. Bissember, R. J. Lundgren, S. E. Creutz, J. C. Peters, G. C. Fu, Transition-Metal-Catalyzed Alkylations of Amines with Alkyl Halides: Photoinduced, Copper-Catalyzed Couplings of Carbazoles, *Angew. Chem. Int. Ed.* **2013**, *52*, 5129.

We then tested the feasibility of the copper catalyzed carbazole N-alkylation reaction of substrate **48** (Table 7).

**Table 7.** Exploratory studies of the  $S_N2$ -type reaction for carbazole introduction



entry <sup>a</sup>	Light source	conversion
1	3 CFL bulbs	RSM
2	16 x 350nm photoreactor	RSM
3	Fiber Optic Mercury Lamp (50W)	RSM

<sup>a</sup> Reactions were carried out using freeze pump thaw technique in a schlenk tube to exclude traces of oxygen.

Different light sources were tested but unfortunately any trace of the product **49** was observed. We thus focused on another synthetic route in order to install the carbazole moiety.

#### 4.8.3. Preparation of Catalyst XXIX Using the Michael Addition as a Key Step.

Our last retrosynthetic plan was based on the introduction of the carbazole by means of a Michael addition using nitrocyclohexene **28** as the Michael acceptor (Figure 30). We anticipated that the nitro substituent within the cyclohexene would work as a suitable amine precursor while providing the electron withdrawing character required for an effective Michael addition to take place. The nucleophile in this synthetic sequence would be the deprotonated carbazole.

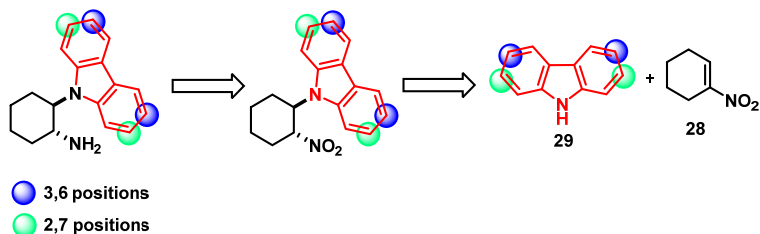
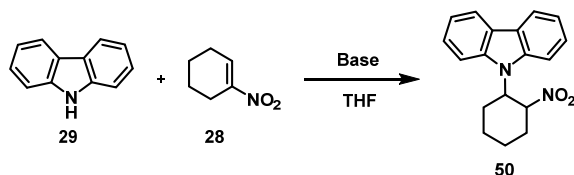


**Figure 30.** Retro-synthetic route 3 for catalyst preparation.

Compound **28** was commercially available but quite expensive. We designed a synthetic route to prepare it from easily available and cheap starting materials (details shown in Figure 20). With substrates **28** and **29** in hands, we explored the ability of different bases to effectively drive the Michael addition (Table 8).

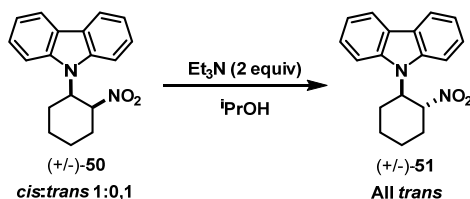


**Table 8.** Exploratory studies of the Michael addition for the carbazole introduction



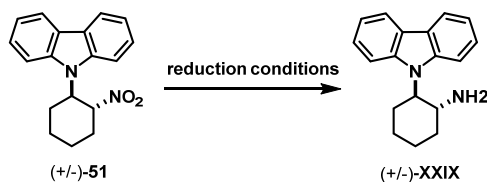
entry	conditions	conversion (%)
1	NaH (1 equiv)	65
2	BuLi (1equiv)	95

To our delight, conversion reached 95% when using BuLi as a base. Carbazole and the base were stirred for 1 h at 0° C before **28** was added. High yields of the *cis* isomer of **50** (10:1 *cis* to *trans* ratio) were obtained. Since the *trans* isomer was needed for our purposes, an epimerization reaction was attempted. Dissolving the *cis* isomer of **50** in <sup>i</sup>PrOH and stirring overnight in the presence of 2 equivalents of triethylamine under reflux conditions exclusively afforded the desired *trans* isomer **51** in quantitative yield (Figure 31).



**Figure 31.** Isomerization of *cis/trans* mixtures.

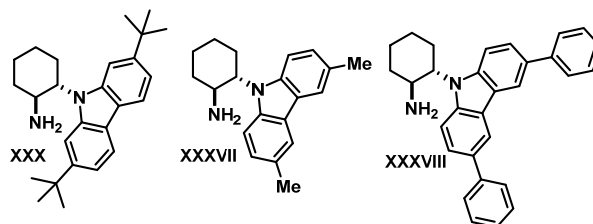
After many efforts, the synthetic precursor of the desired carbazole-based primary amine catalyst was obtained in high yields. Our main objective then became the development of a methodology for the reduction of the nitro group to the corresponding amine. In spite of the many methods available in the literature for this purpose, only the use of Raney nickel under hydrogen (2 bars) in <sup>i</sup>PrOH proved suitable for obtaining almost quantitative yield of the racemic catalyst **XXIX** (Table 9).

**Table 9.** Reaction conditions for the reduction of the nitro group.

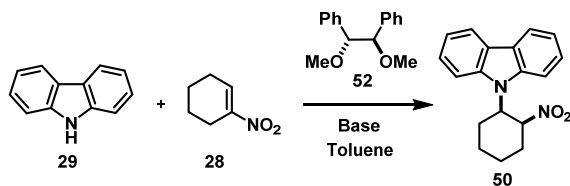
entry <sup>a</sup>	reaction conditions	conversion
1	Pd/C, 1 bar H <sub>2</sub>	RSM
2	Zn/HOAc	Less 5%
3 <sup>a</sup>	Raney Nickel, 2 bar H <sub>2</sub>	Full conversion

<sup>a</sup> Reactions were carried out using PARR Hydrogenator.

By using semi-preparative HPLC separation, available at the Chromatography Unit at ICIQ, both enantiomers of the racemic catalyst were resolved. Catalysts **XXXVII**, **XXXVIII**, and **XXX** (Figure 32) were obtained as a single enantiomer using this technique.

**Figure 32.** Catalysts obtained as a single enantiomer using semi-preparative HPLC separation.

However, in order to avoid this tedious and slow chromatographic resolution step, we focused on the development of an asymmetric aza-Michael reaction of carbazole **29** to the acceptor **28**. Tomioka and co-workers reported a conjugate addition reaction of lithium N-benzyltrimethylsilylamide with Michael acceptors controlled by an external chiral ligand.<sup>38</sup> Our strategy was based on this precedent. We hoped that the lithium N-carbazole, when treated with the external chiral Tomioka's ligand **52**, would provide a suitable chiral environment to induce enantioselectivity in the formation of the desired product **50** (Table 10). Using butyl lithium as the base at -78 °C and adding the ligand **52** after 1 hour provided the Michel addition product **50** in low enantiomeric excess (entry 1). When the deprotonation and the ligand coordination step took place sequentially at 0 °C and the Michael acceptor was added at -78 °C, practical levels of enantiocontrol were achieved (80 % ee, entry 2). When a bulkier base was used instead, both lower conversion and enantioselectivity were achieved (entry 3).

**Table 10.** Developing an enantioselective Michael addition of carbazole.

entry <sup>a</sup>	reaction conditions	temperature	conversion <sup>b</sup>	ee (%)
1	BuLi	-78 °C	>95%	55
2	BuLi	0°C then -78 °C	>95%	80
3	LDA	0°C then -78 °C	40%	40

<sup>a</sup> Reactions carried out using 1,1 equivalents of **28**, 1,3 equivalents of **52** and 1,05 equivalents of the base,  $[\mathbf{29}]_0 = 0,05$  M in toluene. <sup>b</sup> Conversions are determined by  $^1\text{H}$  NMR analysis. <sup>c</sup> Enantiomeric excess (ee) values were determined by HPLC analysis on commercially available chiral stationary phases after isomerization and reduction steps.

To our delight, this methodology was successfully applied to a variety of carbazole derivatives, providing an effective access to the target catalyst precursors. In order to obtain the enantiopure catalysts **XIX** and **XXXVI**, recrystallizations of the salts formed upon treatment with *D*-tartaric acid were required. Catalyst **XXXIX** required several recrystallizations of the corresponding menthyl-carbamate from boiling ethanol (further details are reported in the experimental section).

## 4.9. Experimental Section

The  $^1\text{H}$  and  $^{13}\text{C}$  NMR spectra were recorded at 400 MHz and 500 MHz or at 100 MHz and 125 MHz, respectively. The chemical shifts ( $\delta$ ) for  $^1\text{H}$  and  $^{13}\text{C}$  are given in ppm relative to residual signals of the solvents ( $\text{CHCl}_3$  @ 7.26 ppm  $^1\text{H}$  NMR, 77.0 ppm  $^{13}\text{C}$  NMR). Coupling constants are given in Hz. Carbon types were determined from DEPT  $^{13}\text{C}$  NMR experiments. When necessary,  $^1\text{H}$  and  $^{13}\text{C}$  signals were assigned by means of *g*-COSY, *g*-HSQC and *g*-HMBC 2D-NMR sequences. The following abbreviations are used to indicate the multiplicity: s, singlet; d, doublet; t, triplet; q, quartet; qn, quintet; m, multiplet; bs, broad signal.

High-resolution mass spectra (HRMS) were obtained from the ICIQ High Resolution Mass Spectrometry Unit on Waters GCT gas chromatograph coupled time-of-flight mass spectrometer (GC/MS-TOF) with electron ionization (EI). X-ray data were obtained from the ICIQ X-Ray Unit using a Bruker-Nonius diffractometer equipped with an APPEX 2 4K CCD area detector. Optical rotations are reported as follows:  $[\alpha]_D^{rt}$  (c in g per 100 mL, solvent).

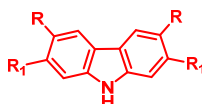
**General Procedures.** All the catalytic reactions were set up under argon and using HPLC grade solvents. The reaction mixture was degassed via vacuum evacuation (1 min) and backfilled with argon. This process was repeated four times. Chromatographic purification of products was accomplished using force-flow chromatography (FC) on silica gel (35-70 mesh). For thin layer chromatography (TLC) analysis throughout this work, Merck precoated TLC plates (silica gel 60 GF<sub>254</sub>, 0.25 mm) were used, using UV light as the visualizing agent and an acidic mixture of ceric ammonium molybdate or potassium permanganate (KMnO<sub>4</sub>), and heat as developing agents. Organic solutions were concentrated under reduced pressure on a Büchi rotary evaporator.

**Determination of Enantiomeric Purity:** HPLC analysis on chiral stationary phase was performed on an Agilent 1200-series instrumentation. Daicel Chiralpak AD-H, IA, IB or IC columns with iPrOH/hexane/DCM as the eluent were used. HPLC traces were compared to racemic samples prepared by performing the reaction with the racemic catalyst **XXIX**.

**Determination of the Yields in the Optimization Studies:** The yield of the product **23** in the optimization studies (Sections 4.5 and 4.7) were determined after diluting the crude in DCM (0.5 mL) and filtered through a plug of silica gel rinsed 3 times with (DCM:EtOAc, 1:1). The solutions were evaporated and an external standard was added, trichloroethylene:  $\delta$  6.55 ppm (s, 1H).

Commercial grade reagents and solvents were purchased from Sigma Aldrich, Fluka, and Alfa Aesar and used as received without further purification; when necessary, they were purified as recommended.<sup>43</sup>

#### 4.9.1. Preparation of Different Carbazole Compounds.



- 30A R=H, R<sub>1</sub>=H
- 30B R=<sup>t</sup>Bu, R<sub>1</sub>=H
- 30C R=H, R<sub>1</sub>=<sup>t</sup>Bu
- 30D R=Ph, R<sub>1</sub>=H
- 30E R=Me, R<sub>1</sub>=H
- 30F R=Br, R<sub>1</sub>=H
- 30G R=Trip, R<sub>1</sub>=H

**Figure 33.** The carbazole precursors prepared in this study

Compound **30A** was commercially available and was used without any further purification.

<sup>43</sup> W. L. F. Armarengo, D. D. Perrin, in *Purification of Laboratory Chemicals*, 4th ed.; Butterworth Heinemann: Oxford, 1996.

#### Preparation of carbazole **30B**:<sup>44</sup>

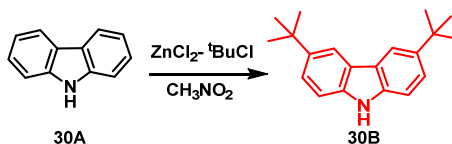


Figure 34. Synthetic scheme for the preparation of **30B**.

$\text{ZnCl}_2$  (16 g, 60 mmol) was charged into a three-necked flask fitted with an air-inlet, a glass stopper and a septum. The zinc(II) chloride was dried by heating under high vacuum. After cooling to room temperature, the reaction flask was back-filled with argon. 9-*H*-carbazole **30A** (6.6 g, 35 mmol) along with 200 mL of nitromethane were added. Neat 2-chloro-2-methylpropane (13 mL, 120 mmol) was added dropwise under stirring. The mixture was stirred at room temperature overnight and the reaction was then quenched by adding 100 mL of water. The product was extracted with  $\text{CH}_2\text{Cl}_2$  (3 x 60 mL). The organic layer was washed with  $\text{H}_2\text{O}$  (2 x 150 mL), dried with  $\text{MgSO}_4$ , and evaporated under vacuum to yield 6 g (60% yield) of a white solid. Spectral characterization matched with the literature data.<sup>44</sup>

#### Preparation of carbazole **30C**:

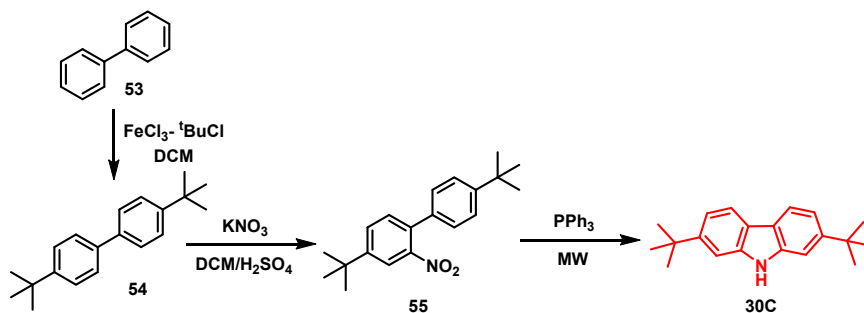


Figure 35. Synthetic route for the preparation of **30C**.

Compound **54** was prepared from commercially available biphenyl **53**, according to a reported procedure.<sup>45</sup> Preparation of compound **55**: solid  $\text{KNO}_3$  (7 g, 69.4 mmol) was stirred with concentrated sulfuric acid (4 mL) for 15 minutes at room temperature under an atmosphere of argon. The suspension was cooled in an ice-bath and 35 mL of dichloromethane was added. 4,4-di-*tert*-butylbiphenyl **54** (18.5 g, 69.4 mmol) in dichloromethane (175 mL) was added to the cold nitrating mixture. The reaction was stirred for 12 hours at room temperature before an

<sup>44</sup> Adapted from: Y. Liu, M. Nishiura, Y. Wang, Z. Hou,  $\pi$ -Conjugated Aromatic Enynes as a Single-Emitting Component for White Electroluminescence, *J. Am. Chem. Soc.* **2006**, *128*, 5592.

<sup>45</sup> R. Rathore, C. L. Burns, A Practical One-Pot Synthesis of Soluble Hexa-*peri*-hexabenzocoronene and Isolation of Its Cation-Radical Salt, *J. Org. Chem.* **2003**, *68*, 4071.

additional portion of  $\text{KNO}_3$  (0.7 g, 6.94 mmol) was added. When the reaction was complete, the mixture was poured into  $\text{H}_2\text{O}$  and extracted with dichloromethane (3 x 100 mL). The combined organic layers were washed with 1 N NaOH (2 x 100 mL) and brine, dried over  $\text{MgSO}_4$ , and concentrated. The product was purified by passing the crude mixture through a short plug of silica using hexane as eluent. A brilliant yellow solid was obtained after recrystallization from boiling ethanol, 9.6 g (44%).

Preparation of **30C**, from compound **55**, was completed following reported procedure and the spectral data are consonant with the literature.<sup>46</sup>

#### Preparation of carbazoles **30D**, **30E**, **30G**:

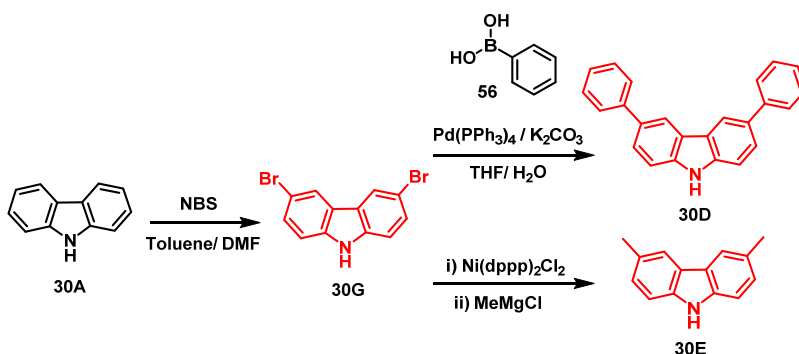


Figure 36. Synthetic route for the preparation of **30D**, **30E**, and **30G**.

Preparation of compound **30G**:<sup>47</sup> a mixture of carbazole **30A** (6.5 g, 39 mmol) in toluene (35 mL) was cooled down to 0 °C. A solution of *N*-bromosuccinimide (15 g, 84 mmol) in 100 mL of DMF was added dropwise over 30 minutes. Once the addition was finished, the reaction was stirred for an additional 30 minutes. The mixture was poured into iced  $\text{H}_2\text{O}$  (1 L) causing a yellow solid to precipitate. The precipitate was filtered and washed with cold MeOH (2 x 15 mL). The product was isolated by recrystallization from boiling ethanol to yield 5.2 g (41%) of an off-white solid.

Preparation of compound **30D**:<sup>48</sup> 3,6-dibromo-9H-carbazole **30G** (1.5 g, 4.65 mmol) and phenylboronic acid **56** (1.36 g, 11.2 mmol) were placed in a 250 mL three-necked flask equipped with a reflux condenser and diluted with 60 mL of THF. Then, a solution of potassium carbonate (6.4 g, 46.5 mmol), in 30 mL of  $\text{H}_2\text{O}$ , and tetrakis(triphenylphosphine)palladium (127 mg 0.11

<sup>46</sup> A. W. Freeman, M. Urvoy, M. E. Criswell, Triphenylphosphine-Mediated Reductive Cyclization of 2-Nitrotriphenyls: A Practical and Convenient Synthesis of Carbazoles, *J. Org. Chem.*, **2005**, *70*, 5014.

<sup>47</sup> Adapted from: C.-H. Ku, C.-H. Kuo, C.-Y. Chen, M.-K. Leungac, K.-H. Hsieh; PLED Devices Containing Triphenylamine-Derived Polyurethanes as Hole-Transporting Layers Exhibit High Current Efficiencies, *J. Mater. Chem.*, **2008**, *18*, 1296.

<sup>48</sup> Adapted from: BASF SE, (2010). *Polycyclic Compounds for Electronic Applications*. WO2010046259 (A1).

mmol) were added and the reaction was refluxed overnight. The reaction was allowed to reach room temperature and a 5% aqueous solution of NaCN was added. The mixture was returned to reflux for an additional 30 minutes. The reaction was then diluted with 100 mL of EtOAc and washed with brine, dried over MgSO<sub>4</sub>, and concentrated. The crude material was purified over silica gel (hexane: EtOAc 10:1 to 4:1) to yield 1.2 g (81% yield) of a white solid.

Preparation of compound **30E**:<sup>49</sup> 3,6-dibromo-9H-carbazole **30G** (1 g, 3.1 mmol) and [1,3-bis-(diphenylphosphino)propane]dichloronickel(II) (Ni(dppp)<sub>2</sub>Cl<sub>2</sub>) (98 mg, 0.17 mmol) were suspended in 60 mL of diethyl ether in a dried and argon flushed 250 mL three-necked flask equipped with a reflux condenser. To the suspension was added 3.13 mL of a 2.97 M CH<sub>3</sub>MgBr solution in diethyl ether (9.29 mmol) over a period of 20 min, yielding a brown clear solution. The reaction mixture was refluxed for 2 h, cooled to room temperature, and quenched with 10 mL of saturated aqueous NH<sub>4</sub>Cl solution. The organic phase was washed with 10 mL of saturated aqueous Na<sub>2</sub>CO<sub>3</sub> solution, and 10 mL of brine. The organic phases were combined and dried over MgSO<sub>4</sub>, and concentrated. The crude material was purified over silica gel (hexane: EtOAc 4:1) to yield 605 mg (43% yield) of a white solid.

#### Preparation of carbazole **30F** (Figure 37 in the next page):

Preparation of compound **57**: A solution of 3,6-dibromo-9H-carbazole **30G** (18.6 g, 57.7 mmol) in DMF (300 mL) was stirred at room temperature in a 500 mL round bottom flask. K<sub>2</sub>CO<sub>3</sub> (79g, 570 mmol) and benzyl bromide (17.2 mL, 144.4 mmol) were added and the reaction was stirred at room temperature overnight. After this time, 200 mL of H<sub>2</sub>O was added, and the mixture extracted with DCM (3 x 100 mL). The combined organic phases were washed with brine, dried over MgSO<sub>4</sub>, and concentrated. The product was recrystallized in boiling mixture of (hexane: DCM) to yield 16 g (67% yield) of a white solid. Spectral data matched with the reported literature.<sup>50</sup>

---

<sup>49</sup> M. Beyer, J. Fritscher, E. Feresin, O. Schiemann, Synthesis of Novel Aromatic Nitroxides as Potential DNA Intercalators. An EPR Spectroscopical and DFT Computational Study, *J. Org. Chem.* **2003**, *68*, 2209.

<sup>50</sup> J-F. Xing, W-Q. Chen, J. Gu, X-Z. Dong, N. Takeyasu, T. Tanaka, X-M. Duan, S. Kawata, Design of High Efficiency for Two-Photon Polymerization Initiator: Combination of Radical Stabilization and Large Two-Photon Cross-Section Achieved by N-Benzyl 3,6-bis(phenylethynyl)carbazole Derivatives, *J. Mater. Chem.*, **2007**, *17*, 1433.

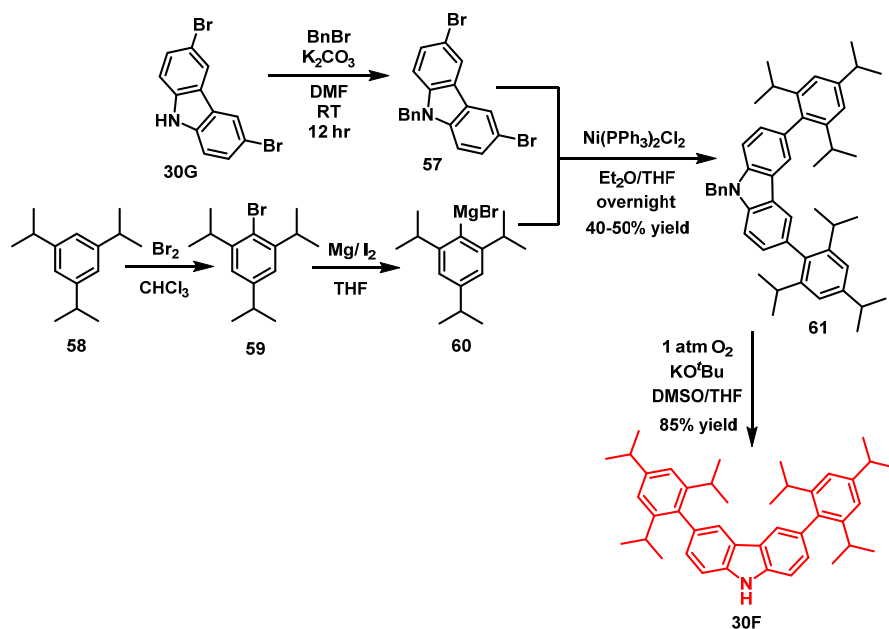


Figure 37. Preparation of carbazole **30F**.

**Preparation of compound 59:** A solution of commercially available 1,3,5-triisopropylbenzene **58** (50 g, 244.7 mmol) in DMF (150 mL) were placed in a 500 mL, 3 neck round bottom and stirred at 0 °C. Bromine (13.2 mL, 259 mmol) was added dropwise for 10 min. After the addition was complete, the reaction was stirred at room temperature for 2 hours. After this time, 100 mL of DCM was added and the reaction was washed with 100 mL of 10% solution of Na<sub>2</sub>SO<sub>3</sub>, 100 mL of 10% NaOH and finally with brine. The combined organic phases were dried over MgSO<sub>4</sub>, and concentrated. The crude residue was distilled under reduced pressure. **Bp** 110 °C (380 mbar). Colorless liquid, isolated yield 58% (40.4 g, 142.6 mmol). The spectral data matched the authentic commercial sample.

#### Preparation of compound 61:

Preparation of the Grignard solution: activated Mg (2.4 g, 98.7 mmol) was suspended in anhydrous THF (50 mL) under an argon atmosphere. A solution of 1-bromo-2,4,6-triisopropylbenzene (25.34 mL, 100 mmol) in anhydrous THF (25 mL) was slowly added at room temperature. The reaction mixture was stirred until only trace amounts of magnesium metal remained unreacted.

9-benzyl-3,6-dibromo-9H-carbazole **57** (8.3 g, 20 mmol) and (Ni(PPh<sub>3</sub>)<sub>2</sub>Cl<sub>2</sub>) (1.62 g, 2 mmol) (Bis(triphenylphosphine)nickel(II) dichloride) were suspended in 60 mL of diethyl ether in a flame dried argon flushed 1 L three-necked flask equipped with a reflux condenser. To the suspension was added the Grignard solution of (2,4,6-triisopropylphenyl)magnesium bromide 2M in THF (98



mmol) prepared above over a period of 30 min. The reaction mixture was heated at 50 °C overnight, cooled to room temperature, and quenched with 1 M HCl solution and extracted with EtOAc (3x 100 mL). The organic phase was treated two times with 100 mL of brine, combined, dried over MgSO<sub>4</sub>, and concentrated. The crude material was purified over silica gel (gradient hexane:Et<sub>2</sub>O from 100:1 to 1:1) and recrystallized in boiling hexane:Et<sub>2</sub>O to yield 8.13 g (61% yield) of a white solid.

**Preparation of compound 30F:** 9-benzyl-3,6-bis(2,4,6-triisopropylphenyl)-9H-carbazole **61**, (8.1 g, 12.3 mmol) was dissolved in DMSO/THF (120 mL:60 mL) and subsequently potassium *tert*-butoxide (8.3 g, 73.8 mmol) was added. Dried oxygen was insufflated into the reaction mixture until the starting compound was completely consumed. The reaction was quenched with water and then the mixture was extracted with EtOAc (3 x 100 mL). The organic phase was treated two times with 100 mL of brine. The organic phases were combined, dried over MgSO<sub>4</sub>, and concentrated. The crude material was recrystallized from boiling hexanes:Et<sub>2</sub>O to yield 8.74 g (71% yield) of a white solid.

#### 4.9.2. Preparation of Different Carbazole Derivatives type Catalysts XXIX.

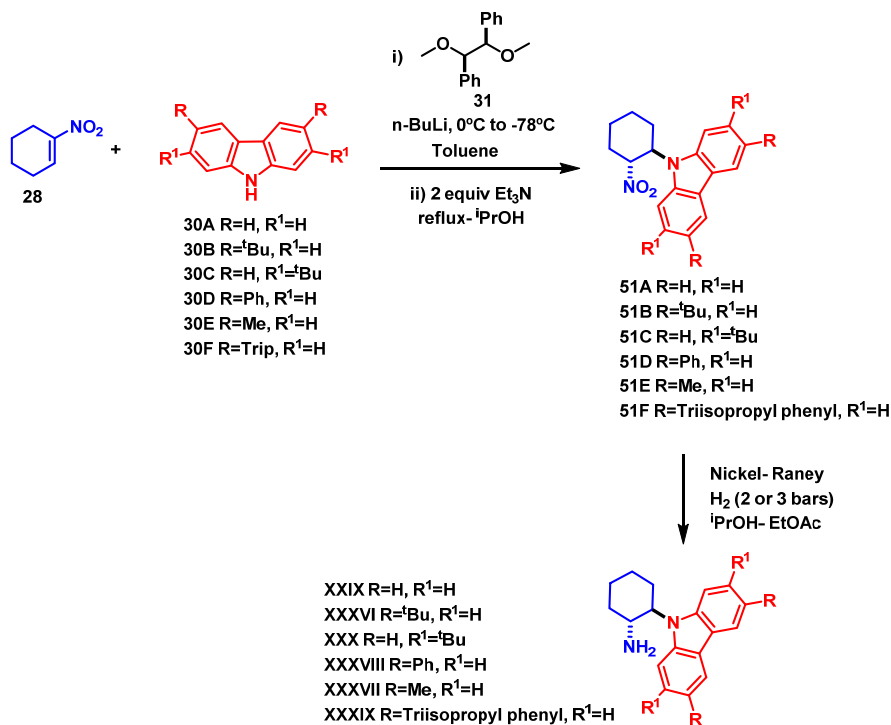


**Figure 38.** Synthetic route to synthesize catalysts XXIX and analogs thereof. The structure of compound **51F** and catalyst **XXXVI** were unambiguously determined by anomalous dispersion X-ray crystallographic analysis.

**General procedure for preparing enantioenriched primary amine catalysts:** *n*-BuLi (2.72 mL, 2.18 M in hexane solution, 5.93 mmol) was added to a solution of the 3,6-di-*tert*-butyl-9H-carbazole (1.58 g, 5.65 mmol) in toluene (100 mL) at 0 °C over 10 min under an argon atmosphere. After stirring for 30 minutes, the chiral ligand (1*R*,2*R*)-1,2-dimethoxy-1,2-diphenylethane **31** (436 mg, 1.8 mmol) was added and the mixture was stirred for 1 hour at 0 °C. The mixture was cooled down at -78 °C and 1-nitrocyclohex-1-ene **28** (1.77 mL, 6.22 mmol) was added. Stirring was continued overnight at -78 °C. The reaction was quenched with 50 mL of saturated aqueous NH<sub>4</sub>Cl solution and extracted with EtOAc (3 x 100 mL). The organic phase was treated two times with 100 mL of brine, dried over MgSO<sub>4</sub>, and concentrated. The crude material was then filtered through a pad of silica gel and eluted with hexane:Et<sub>2</sub>O (20:1).

The crude residue was placed in a 250 mL round bottom flask equipped with a reflux condenser and diluted with isopropanol (or *n*-BuOH when XXXIX catalyst is used). Triethylamine (1.5 mL, 11.3 mmol) was added and the mixture was heated to reflux overnight. The crude material was then filtered through a pad of silica gel rinsed with DCM: Et<sub>2</sub>O (20: 1). The crude residue was placed in a 100 mL Parr vessel diluted with isopropanol (20 mL) (or *n*-BuOH when XXXIX catalyst is used) and EtOAc (5 mL). 2 spoons of commercial Raney-Nickel were added and the vessel was placed in a Parr low pressure hydrogenation apparatus equipped with a shaker with a pressure of 3 bars of H<sub>2</sub>. Hydrogenation was conducted overnight (three days were required for catalyst XXXIX due to insolubility issues) and then the reaction mixture was filtered through a pad of Celite rinsing with EtOAc. The solvents were removed *in vacuo* to afford the crude catalyst. Purification was performed using flash chromatography on silica gel (DCM/MeOH, gradient from 99:1 to 95:5). All the carbazole-based primary amine catalysts were obtained with an overall yield, over three steps, ranging from 40 to 50%.

**Measurement of enantiomeric excess:** The following procedure was used due to the nature of the catalysts and to facilitate the enantiomeric excess determination. Preparation of HPLC sample: 5 mg of the catalyst was placed in a sample vial and dissolved in DCM (3 mL) followed by the addition of a drop of triethylamine and one drop of 1-fluoro-2,4-dinitrobenzene (Sanger's reagent).<sup>51</sup> The vial was shook for ten seconds before evaporation of the volatiles. The crude material was then filtered through a pipette filled of silica gel using a solution of hexane:EtOAc (9:1). Only the brightly coloured portion of the filtrate was collected. The enantiomeric excess of the functionalized product was determined to be 80% by HPLC analysis on a Daicel Chiralpak IC-3.

<sup>51</sup> Toshimasa Toyo'oka, *Modern Derivatization Methods for Separation Science*, 1999, John Wiley and sons, New York

**General procedure for preparing racemic primary amine catalysts:** Under an argon atmosphere, *n*-BuLi (2.72 mL, 2.18 M in hexane solution, 5.93 mmol) was added to a solution of the 3,6-di-*tert*-butyl-9H-carbazole (1.58 g, 5.65 mmol) in toluene (100 mL) at 0 °C over 10 min. After stirring for 30 min, the mixture was cooled down at -78 °C and 1-nitrocyclohex-1-ene (1.77 mL, 6.22 mmol) was added. The solution was allowed to reach -20 °C before being quenched with 50 mL of saturated aqueous NH<sub>4</sub>Cl solution and extracted with EtOAc (3 x 100 mL). The organic phase was treated two times with 100 mL of brine. The organic phases were combined and dried over MgSO<sub>4</sub>, and concentrated. The crude material was then filtered through a pad of silica gel and eluted with hexane: Et<sub>2</sub>O (20:1). The crude residue was placed in a 250 mL round bottom flask equipped with a reflux condenser and diluted with isopropanol (or *n*-BuOH when XXXIX catalyst is used). Triethylamine (1.5 mL, 11.3 mmol) was added and the mixture was heated to reflux overnight. The crude material was then filtered through a pad of silica gel rinsed with DCM:Et<sub>2</sub>O (20:1). The crude residue was placed in a 100 mL Parr vessel diluted with isopropanol (20 mL) (or *n*-BuOH when catalyst XXXIX was used) and EtOAc (5 mL). 2 spoons of commercial Raney-Nickel were added and the vessel was placed in a Parr low pressure hydrogenation apparatus equipped with a shaker with a pressure of 3 bars of H<sub>2</sub>. Hydrogenation was conducted overnight (three days were required for catalyst XXXIX due to insolubility issues) before the reaction mixture was filtered through a pad of Celite rinsing with EtOAc. The solvents were removed *in vacuo* to afford the crude catalyst. Purification was performed using flash chromatography on silica gel (DCM/MeOH 99:1 to 95:5). All the products were obtained with an overall yield, over three steps, ranging from 40 to 50%.

#### 4.9.3. Resolution of the Enantiopure Primary Amine Catalysts.

Resolution of catalysts XXIX and XXXVI:

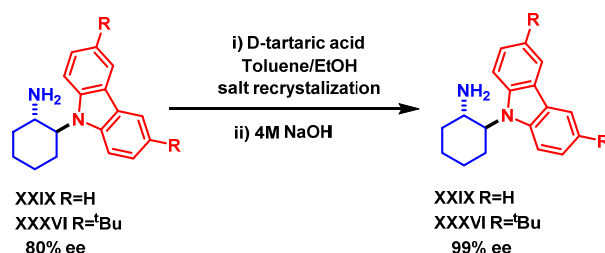
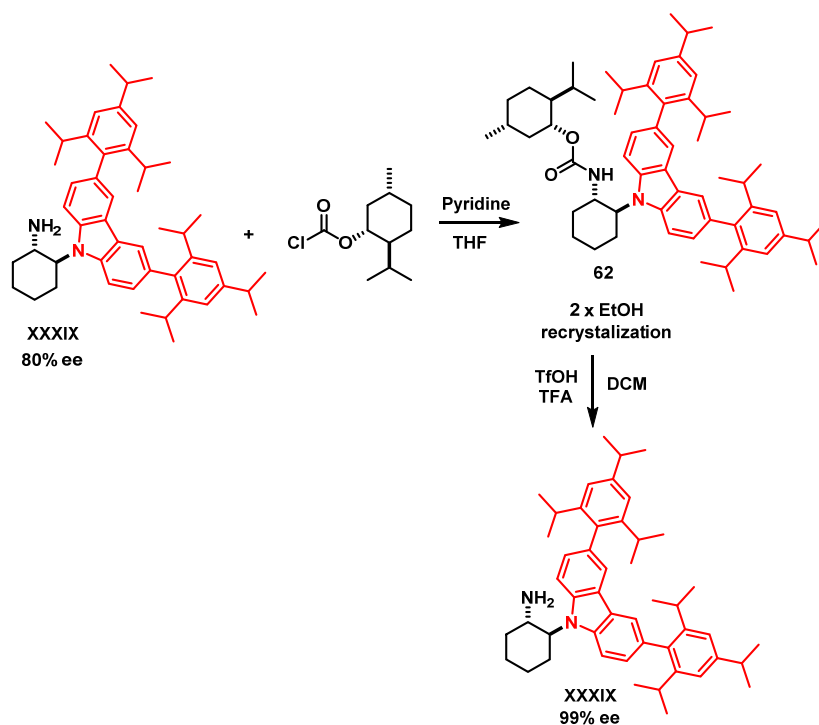


Figure 39. Resolution of catalysts XXIX and XXXVI.

**General procedure for the resolution of catalysts XXIX and XXXVI:** In a 100 mL round bottom flask, 1 g of the enantioenriched carbazole-derived catalyst (about 80% ee) and 1 equivalent of *D*-tartaric acid were dissolved in 0.5 mL of EtOH was added. The mixture was heated at 80 °C. If the sample was not dissolved, EtOH was added dropwise until it was completely dissolved. When the mixture was homogenous, 10 volumes of toluene (vs. ethanol) were added. The mixture was then heated to 100 °C under vigorous stirring (open flask) until

most of the EtOH was evaporated and a precipitate was visible. As soon as the precipitate appeared, it was filtered out and washed with hot toluene and, when the toluene had cooled sufficiently, with ether. The collected salt was placed in 100 mL of a 1:1 mixture of DCM and 4M NaOH and, after stirring over 5 minutes, the organic phase was separated and washed with 20 mL of brine, dried over  $\text{MgSO}_4$ , and concentrated to afford the enantiopure free amine catalyst.

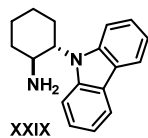
Resolution of catalyst **XXXIX**:



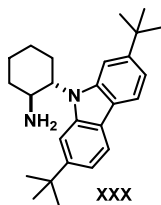
**Figure 40.** Resolution of catalyst **XXXIX**.

**General procedure for the resolution of catalyst **XXXIX**:** (1*R*)-(-)-menthyl chloroformate (0.916 mL, 4.27 mmol) was added to a solution of enantio-enriched (1*S*,2*S*)-2-(3,6-bis(2,4,6-triisopropylphenyl)-9*H*-carbazol-9-yl)cyclohexan-1-amine **XXXIX** (2.4 g, 3.56 mmol, 80% ee) and pyridine (401  $\mu\text{L}$ , 4.98 mmol) in tetrahydrofuran (40 mL) at 0  $^{\circ}\text{C}$  under an argon atmosphere. The reaction was stirred overnight at room temperature. The mixture was diluted with DCM and washed with 2M HCl and then with brine. The organic phases were combined, dried over  $\text{MgSO}_4$ , and concentrated. The crude material was then filtered through a pad of silica gel rinsed with hexane:EtOAc (2:1) and purified by flash chromatography on silica gel (DCM:pentane 1:1). The residue was recrystallized from boiling ethanol until an enantiopure compound was obtained, as inferred by HPLC analysis on a chiral IC Daicel Chiralpak column.

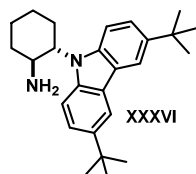
The enantiopure carbamate **62** (1.6 g, 1.88 mmol) was placed in a 100 mL round bottom flask equipped with a reflux condenser and diluted with DCM (10 mL). Trifluoroacetic acid (1.4 mL, 18.8 mmol) and trifluoromethanesulfonic acid (498  $\mu$ L, 5.64 mmol) were sequentially added, and the reaction was stirred at reflux for 2 hours. Then, the reaction was cautiously quenched with a saturated solution of NaHCO<sub>3</sub>, diluted with DCM and extracted with DCM (2 x 20 mL). The organic phases were combined, dried over MgSO<sub>4</sub>, and concentrated. The enantiopure catalyst **XXXIX** was obtained with an overall yield of 60-70% over two steps.



The pure enantiomer was isolated following the general procedure for the resolution of catalysts (see 4.9.3). The enantiomeric excess was determined to be 99% by HPLC analysis on a Daicel Chiralpak IC-3 column: 70/30 hexane/isopropanol, flow rate 0.8 mL/min,  $\lambda = 350$  nm:  $\tau_{Major} = 13.78$  min,  $\tau_{Minor} = 8.8$  min after preparation of HPLC sample following the procedure described in 4.9.2 as a white solid.  $[\alpha]_D^{26} = -61.4$  ( $c = 0.58$ , CHCl<sub>3</sub>). HRMS *calcd* for (C<sub>18</sub>H<sub>21</sub>N<sub>2</sub>): 265.1699, found 265.1695. <sup>1</sup>H NMR (500 MHz, CDCl<sub>3</sub>)  $\delta$  8.14 (dd,  $J = 12.6, 7.7$  Hz, 2H), 7.68 (d,  $J = 8.3$  Hz, 1H), 7.58 – 7.38 (m, 3H), 7.26 (t,  $J = 7.2$  Hz, 2H), 4.23 (ddd,  $J = 12.4, 10.3, 3.9$  Hz, 1H), 3.78 (td,  $J = 10.6, 4.2$  Hz, 1H), 2.60 – 2.34 (m, 1H), 2.28 – 2.09 (m, 1H), 1.97 (dddd,  $J = 16.9, 9.1, 3.9, 1.9$  Hz, 3H), 1.65 – 1.51 (m, 2H), 1.52 – 1.35 (m, 1H). <sup>13</sup>C NMR (126 MHz, CDCl<sub>3</sub> ppm).  $\delta$  141.7, 138.5, 125.8, 125.3, 124.1, 122.70, 120.5, 120.1, 118.9, 118.9, 111.6, 109.0, 63.3, 51.9, 35.4, 29.4, 26.2, 25.2.

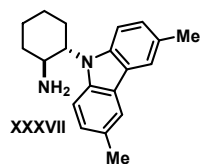


The pure enantiomer was isolated by HPLC analysis on a semi-preparative Daicel Chiralpak IA column: 90/9.9/0.1 hexane/DCM/DEA (diethylamine), flow rate 1 mL/min,  $\lambda = 254$  nm:  $\tau_{1st\ enantiomer} = 7.01$  min,  $\tau_{2nd\ enantiomer} = 12.93$  min as a white solid.  $[\alpha]_D^{26} = -34.4$  ( $c = 0.32$ , CHCl<sub>3</sub>). HRMS *calcd* for (C<sub>26</sub>H<sub>37</sub>N<sub>2</sub>): 377.2951, found 377.2939. <sup>1</sup>H NMR (500 MHz, CDCl<sub>3</sub>)  $\delta$  7.99 (dd,  $J = 13.1, 8.1$  Hz, 2H), 7.63 (s, 1H), 7.42 (s, 1H), 7.30 (dd,  $J = 8.3, 1.6$  Hz, 2H), 4.19 (ddd,  $J = 12.4, 10.2, 4.0$  Hz, 1H), 3.79 (td,  $J = 10.6, 4.1$  Hz, 1H), 2.42 (qd,  $J = 12.3, 3.7$  Hz, 1H), 2.24 (dt,  $J = 13.4, 3.0$  Hz, 1H), 2.05 – 1.92 (m, 3H), 1.66 – 1.54 (m, 2H), 1.47 (s, 18H), 1.45 – 1.41 (m, 1H). <sup>13</sup>C NMR (126 MHz, CDCl<sub>3</sub> ppm).  $\delta$  148.9, 148.2, 142.0, 139.1, 121.6, 120.4, 119.6, 119.3, 117.0, 116.8, 107.9, 105.1, 62.9, 52.2, 35.4, 35.3, 35.1, 31.9, 31.9, 29.5, 26.2, 25.4.

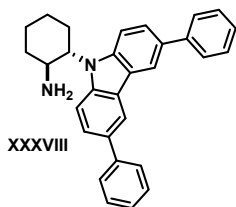


The pure enantiomer was isolated following the general procedure for the resolution of catalysts 4.9.3. The enantiomeric excess was determined to be 99% by HPLC analysis on a Daicel Chiralpak IC-3 column: 70/30 hexane/isopropanol, flow rate 0.8 mL/min,  $\lambda = 350$  nm:  $\tau_{Major} = 12.34$  min,  $\tau_{Minor} = 8.33$  min after preparation of HPLC sample following the procedure described in 4.9.2 as a white solid.  $[\alpha]_D^{26} = -65.4$  ( $c = 0.06$ ,  $\text{CHCl}_3$ ). HRMS *calcd* for ( $\text{C}_{26}\text{H}_{37}\text{N}_2$ ): 377.2942, found 377.2951.  $^1\text{H}$  NMR (500 MHz,  $\text{CDCl}_3$ )  $\delta$  8.12 (d,  $J = 8.9$  Hz, 2H), 7.60 – 7.37 (m, 4H), 4.14 (ddd,  $J = 12.4, 10.2, 3.9$  Hz, 1H), 3.72 (td,  $J = 10.6, 4.1$  Hz, 1H), 2.39 (qd,  $J = 12.6, 3.7$  Hz, 1H), 2.25 – 2.12 (m, 1H), 1.94 (t,  $J = 13.3$  Hz, 3H), 1.67 – 1.52 (m, 2H), 1.48 (s, 18H), 1.45 – 1.34 (m, 1H).  $^{13}\text{C}$  NMR (101 MHz,  $\text{CDCl}_3$  ppm).  $\delta$  141.6, 137.0, 124.0, 123.5, 122.9, 122.5, 116.4, 116.0, 111.0, 108.4, 63.2, 52.1, 35.4, 34.6, 32.01, 29.5, 26.2, 25.2.

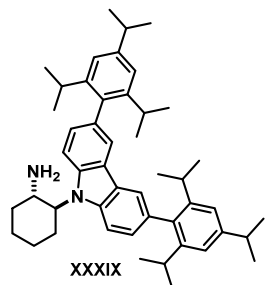
The structure of compound **XXXVI** was unambiguously determined by anomalous dispersion X-ray crystallographic analysis.



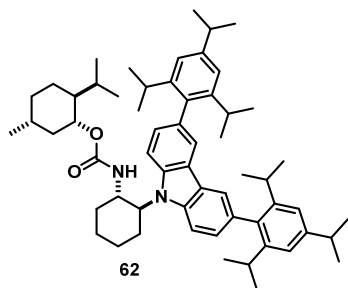
The pure enantiomer was isolated by HPLC analysis on a semi-preparative Daicel Chiralpak IB-3 column: 90/9.9/0.1 hexane/EtOH/DEA (diethylamine), flow rate 1 mL/min,  $\lambda = 254$  nm:  $\tau_{1st\ enantiomer} = 6.02$  min,  $\tau_{2nd\ enantiomer} = 7.29$  min as a white solid. HRMS *calcd* for ( $\text{C}_{20}\text{H}_{25}\text{N}_2$ ): 293.2005, found 293.2012.  $^1\text{H}$  NMR (500 MHz,  $\text{CDCl}_3$ )  $\delta$  7.89 (d,  $J = 17.0$  Hz, 2H), 7.44 (dd,  $J = 29.6, 8.4$  Hz, 2H), 7.31 – 7.18 (m, 2H), 4.28 – 4.01 (m, 1H), 3.85 – 3.58 (m, 1H), 2.54 (s, 6H), 2.41 – 2.29 (m, 1H), 2.22 – 2.13 (m, 1H), 1.96 (d,  $J = 13.9$  Hz, 3H), 1.54 (t,  $J = 10.3$  Hz, 2H), 1.48 – 1.38 (m, 1H).  $^{13}\text{C}$  NMR (101 MHz,  $\text{CDCl}_3$  ppm)  $\delta$  140.2, 136.9, 128.0, 127.0, 126.4, 124.1, 122.6, 120.4, 120.0, 111.2, 108.7, 29.4, 26.1, 25.2, 25.1, 21.3.



The pure enantiomer was isolated by HPLC analysis on a semi-preparative Daicel Chiralpak IA column: 75/24.9/0.1 hexane/DCM/DEA (diethylamine), flow rate 1 mL/min,  $\lambda = 254$  nm:  $\tau_{1st\ enantiomer} = 9.69$  min,  $\tau_{2nd\ enantiomer} = 15.18$  min as a white solid.  $^1\text{H}$  NMR (500 MHz,  $\text{CDCl}_3$ )  $\delta$  8.38 (d,  $J = 15.9$  Hz, 2H), 7.80 – 7.66 (m, 7H), 7.59 (d,  $J = 8.5$  Hz, 1H), 7.49 (t,  $J = 7.6$  Hz, 4H), 7.35 (t,  $J = 7.4$  Hz, 2H), 4.31 – 4.20 (m, 1H), 3.80 (td,  $J = 10.6, 4.1$  Hz, 1H), 2.44 (qd,  $J = 12.9, 12.0, 4.1$  Hz, 1H), 2.25 – 2.11 (m, 1H), 2.06 – 1.91 (m, 3H), 1.69 – 1.39 (m, 3H).  $^{13}\text{C}$  NMR (101 MHz,  $\text{CDCl}_3$  ppm).  $\delta$  141.9, 132.7, 129.5, 129.4, 128.8, 128.2, 128.1, 127.9, 127.3, 126.6, 125.6, 125.0, 124.8, 123.4, 119.0, 118.7, 109.4, 63.4, 52.1, 35.3, 29.7, 29.6, 26.1, 25.2.



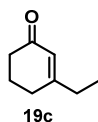
The pure enantiomer was isolated following the general procedure for the resolution of catalysts (see 4.9.3) as a pale yellow solid. The enantiomeric excess was determined to be 99% by HPLC analysis on a Daicel Chiralpak IC-3 column: 86/10/4 hexane/IPA/DCM, flow rate 0.5 mL/min,  $\lambda = 350$  nm:  $\tau_{Major} = 9.05$  min,  $\tau_{Minor} = 9.46$  min after preparation of HPLC sample following the procedure described in 4.9.2.  $[\alpha]_D^{26} = -16.6$  ( $c = 0.52$ , CHCl<sub>3</sub>). HRMS *calcd* for (C<sub>48</sub>H<sub>65</sub>N<sub>2</sub>): 669.5154, found 669.5142. <sup>1</sup>H NMR (500 MHz, CDCl<sub>3</sub> ppm)  $\delta$  7.85 (d,  $J = 15.2$  Hz, 2H), 7.68 (d,  $J = 8.5$  Hz, 1H), 7.55 (d,  $J = 8.5$  Hz, 1H), 7.29 (d,  $J = 8.6$  Hz, 1H), 7.23 (d,  $J = 8.3$  Hz, 1H), 7.09 (s, 4H), 4.29 (ddd,  $J = 12.5, 10.2, 4.1$  Hz, 1H), 3.88 (td,  $J = 10.6, 4.1$  Hz, 1H), 2.97 (p,  $J = 6.9$  Hz, 2H), 2.84 – 2.68 (m, 4H), 2.50 (td,  $J = 12.7, 8.8$  Hz, 1H), 2.27 – 2.18 (m, 1H), 2.13 – 1.88 (m, 3H), 1.66 – 1.52 (m, 2H), 1.52 – 1.41 (m, 1H), 1.33 (d,  $J = 6.9$  Hz, 12H), 1.09 (t,  $J = 6.4$  Hz, 24H). <sup>13</sup>C NMR (126 MHz, CDCl<sub>3</sub> ppm)  $\delta$  147.8, 147.4, 140.9, 137.7, 137.6, 131.4, 128.26, 127.7, 123.7, 122.4, 121.4, 120.9, 120.7, 111.2, 108.6, 63.5, 52.2, 35.7, 34.4, 30.4, 29.7, 26.4, 25.3, 24.6, 24.5, 24.3.



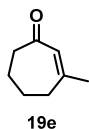
The pure diastereoisomer of compound **62** was isolated following the general procedure for the resolution of catalysts XXXIX (see 4.9.3) as a white solid. The purity was determined to be 99% by HPLC analysis on a Daicel Chiralpak IA column: 90/10 hexane/DCM, flow rate 0.8 mL/min,  $\lambda = 254$  nm:  $\tau_{Major} = 7.99$  min,  $\tau_{Minor} = 7.00$  min. HRMS *calcd* for (C<sub>59</sub>H<sub>83</sub>N<sub>2</sub>O<sub>2</sub>): 851.6475, found 851.6449. <sup>1</sup>H NMR (500 MHz, CDCl<sub>3</sub>)  $\delta$  7.85 (d,  $J = 1.7$  Hz, 2H), 7.65 (br, 2H), 7.28 (t,  $J = 4.2$  Hz, 3H), 4.61 (d,  $J = 29.0$  Hz, 2H), 4.36 (td,  $J = 10.7, 4.1$  Hz, 1H), 3.00 (p,  $J = 6.9$  Hz, 2H), 2.78 (s, 4H), 2.52 (m, 2H), 2.20 – 1.82 (m, 4H), 1.77 – 1.48 (m, 6H), 1.37 (d,  $J = 6.9$  Hz, 12H), 1.31 – 1.20 (m, 2H), 1.12 (d,  $J = 6.6$  Hz, 24H), 1.32 – 0.91 (m, 4H), 0.92 – 0.78 (m, 3H), 0.83 – 0.27 (m, 6H). <sup>13</sup>C NMR (75 MHz, CDCl<sub>3</sub> ppm)  $\delta$  155.6, 147.6, 147.3, 147.2, 137.5, 131.3, 127.7, 121.0, 120.6, 120.6, 74.5, 58.7, 52.5, 47.6, 41.3, 34.3, 31.4, 30.2, 30.0, 26.7, 25.9, 25.1, 24.6, 24.5, 24.8, 24.4, 24.1, 22.1, 20.0, 16.6.

The structure and the stereochemistry of compound **62** was unambiguously determined by anomalous dispersion X-ray crystallographic analysis.

#### 4.9.4. Preparation of Starting Enones and Benzodioxole.



**3-Ethylcyclohex-2-en-1-one:** Was prepared according to literature.<sup>52</sup> An oven-dried, argon purged two neck round bottomed flask fitted with a vacuum adaptor and septum was charged with 3-ethoxycyclohex-2-en-1-one<sup>53</sup> (1.4 g, 10 mmol, 1 eq.) dissolved in anhydrous THF (20 mL). The solution was cooled to 0 °C and ethylmagnesium bromide (6.67 mL, 3 M in Et<sub>2</sub>O, 20 mmol, 2 eq.) was added dropwise over 30 minutes. The mixture was allowed to RT and stirred for 12 hours. The reaction was quenched by the addition of aqueous HCl (10 mL, 1 M, 10 mmol, 1 eq.) and stirred was continued for 30 minutes at room temperature. The reaction was then transferred to a separatory funnel and extracted with diethyl ether (2 x 50 mL). The organic phase was then washed with water, brine and then dried over magnesium sulfate before concentration *in vacuo*. The orange residue was purified by flash chromatography (Hexane:Et<sub>2</sub>O 4:1), to give the title compound as a pale yellow oil, 1.06 g (83%). <sup>1</sup>H NMR (400 MHz, CDCl<sub>3</sub>)  $\delta$  5.86 (s, 1H), 2.38 – 2.31 (m, 2H), 2.30 – 2.18 (m, 4H), 2.01 – 1.92 (m, 2H), 1.08 (t, *J* = 7.4 Hz, 3H). <sup>13</sup>C NMR (101 MHz, CDCl<sub>3</sub>)  $\delta$  200.0, 167.9, 124.6, 37.4, 30.9, 29.7, 22.7, 11.2



**3-Methylcyclohept-2-en-1-one:** Was prepared according to literature.<sup>54</sup> An oven-dried, argon purged two neck round bottomed flask fitted with a vacuum adaptor and septum was charged with cyclohept-2-en-1-one (2.23 mL, 20 mmol, 1 eq.) dissolved in anhydrous THF (25 mL). The mixture was cooled to -78 °C and methyllithium (25 mL, 1.6 M in Et<sub>2</sub>O, 40 mmol, 2 eq.) was added dropwise over 1 hour. After a further 20 minutes at -78 °C the reaction was allowed to RT until a vibrant blue colour was observed. At this point the reaction was poured into water and extracted with diethyl ether (2 x 50 mL). The organic phase was then washed with water, brine and then dried over magnesium sulfate before concentration *in vacuo*. The crude 1-methylcyclohept-2-en-1-ol obtained was used directly in the next step. To a solution of the crude tertiary alcohol (approx. 20 mmol, 1 eq.) in methylene chloride (75 mL) was added NaIO<sub>4</sub> impregnated silica gel<sup>55</sup> (40 mmol, 1 eq.) and TEMPO (156 mg, 1 mmol, 2 mol%). The reaction was vigorously stirred at room temperature for 12 hours to achieve full conversion of the tertiary alcohol. The reaction mixture was then filtered and the silica gel washed with an abundance of methylene chloride. The filtrate was concentrated and the orange residue was purified by flash chromatography (Hexane:Et<sub>2</sub>O 4:1), to give the title compound as a pale yellow oil, 1.39 g (56%). <sup>1</sup>H NMR (300

<sup>52</sup> S. Kehrl, D. Martin D. Rix, M. Mauduit, A. Alexakis, Formation of Quaternary Chiral Centers by N-Heterocyclic Carbene-CuCatalyzed Asymmetric Conjugate Addition Reactions with Grignard Reagents on Trisubstituted Cyclic Enones. *Chem. Eur. J.* **2010**, *16*, 9890.

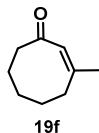
<sup>53</sup> M. Zhou, T-L. Liu, M. Cao, Z. Xue, H. Lv, X. Zhang, Highly enantioselective synthesis of chiral cyclic allylic amines via Rh-catalyzed asymmetric hydrogenation. *Org. Lett.*, **2014**, *16*, 3484.

<sup>54</sup> D. Müller, A. Alexakis, Formation of Quaternary Stereogenic Centers by Copper Catalyzed Asymmetric Conjugate Addition Reactions of Alkenyl Aluminums to Trisubstituted Enones, *Chem. Eur. J.* **2013**, *19*, 15226.

<sup>55</sup> Y-L. Zhong, T. K. M. Shing, Efficient and Facile Glycol Cleavage Oxidation Using Improved Silica Gel-Supported Sodium Metaperiodate, *J. Org. Chem.*, **1997**, *62*, 2622.



MHz, CDCl<sub>3</sub>) δ 5.87 (s, 1H), 2.57 – 2.48 (m, 2H), 2.36 (dd, *J* = 6.9, 4.6 Hz, 2H), 1.90 (s, 3H), 1.80 – 1.68 (m, 4H). <sup>13</sup>C NMR (75 MHz, CDCl<sub>3</sub>): δ 203.6, 158.5, 129.8, 42.5, 34.5, 27.6, 25.1, 21.5.

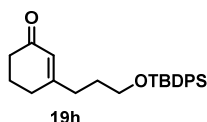


**3-Methylcyclooct-2-en-1-one:** An oven-dried, argon purged two neck round bottomed flask fitted with a vacuum adaptor and septum was charged with cyclooct-2-en-1-one<sup>56</sup> (2.48 g, 20 mmol, 1 eq.) dissolved in anhydrous THF (25 mL). The mixture was cooled to -78 °C and methyllithium (25 mL, 1.6 M in Et<sub>2</sub>O, 40 mmol, 2 eq.) was added dropwise over 1 hour. After a further 20 minutes at -

78 °C the reaction was allowed to RT and stirred for 30 minutes. At this point the reaction was poured into water and extracted with diethyl ether (2 x 50 mL). The organic phase was then washed with water, brine and then dried over magnesium sulfate before concentration *in vacuo*. The crude 1-methylcyclooct-2-en-1-ol obtained was used directly in the next step. To a solution of the crude tertiary alcohol (approx. 20 mmol, 1 eq.) in methylene chloride (75 mL) was added NaIO<sub>4</sub> impregnated silica gel<sup>5</sup> (40 mmol, 1 eq.) and TEMPO (156 mg, 1 mmol, 2 mol%). The reaction was vigorously stirred at room temperature for 12 hours to achieve full conversion of the tertiary alcohol. The reaction mixture was then filtered and the silica gel washed with an abundance of methylene chloride. The filtrate was concentrated and the orange residue was purified by flash chromatography (Hexane:Et<sub>2</sub>O 4:1), to give the title compound as a pale yellow oil, 1.41 g (51%). Spectral characteristics correspond with literature precedent.<sup>57</sup> <sup>1</sup>H NMR (300 MHz, CDCl<sub>3</sub>) δ 6.01 (s, 1H), 2.76 – 2.62 (m, 2H), 2.60 – 2.50 (m, 2H), 1.92 (s, 3H), 1.81 – 1.48 (m, 8H). <sup>13</sup>C NMR (75 MHz, CDCl<sub>3</sub>) δ 204.1, 153.5, 130.6, 42.3, 33.5, 27.9, 24.2, 23.6, 22.9.

<sup>56</sup> R. C. Larock, T. R. Hightower, G. A. Kraus, P. Hahn, D. A. Zheng, Simple, Effective, New, Palladium-Catalyzed Conversion of Enol Silanes to Enones and Enals. *Tetrahedron Lett.* **1995**, 36, 2423.

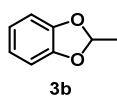
<sup>57</sup> P. Eskola, J. A. Hirsch, Medium-Ring Systems. 6.1 Synthesis and Isomerizations of Medium-Ring 3-Methylenecycloalkanones and 3-Methylcycloalkanones, *J. Org. Chem.* **1997**, 62, 5732.

**3-(3-((Tert-butyldiphenylsilyloxy)propyl)cyclohex-2-en-1-one:**

prepared according to a literature procedure.<sup>58</sup> An oven-dried, argon purged two neck round bottomed flask fitted with a vacuum adaptor and septum was charged with 3-(3-hydroxypropyl)cyclohex-2-en-1-one (327 mg, 2.12 mmol, 1 eq.) dissolved in

anhydrous methylene chloride (5 mL) and TBDPSCI (606  $\mu$ L, 2.33 mmol, 1.1 eq.). The mixture was cooled to 0 °C and freshly crystallized imidazole (289 mg, 4.24 mmol, 2 eq.) was added. The reaction was stirred at RT for 24 hours before being diluted with diethyl ether and washed with a saturated solution of NaHCO<sub>3</sub>, water, brine and dried over magnesium sulfate. A thick yellow residue was obtained upon concentration *in vacuo* which was purified by flash chromatography (Hexane:EtOAc 8:1), to give a pale yellow gum, 791 mg (95%). <sup>1</sup>H NMR (300 MHz, CDCl<sub>3</sub>)  $\delta$  7.74 – 7.67 (m, 4H), 7.49 – 7.36 (m, 6H), 5.92 (t, *J* = 1.4 Hz, 1H), 3.72 (t, *J* = 6.2 Hz, 2H), 2.35 (dt, *J* = 8.0, 6.0 Hz, 4H), 2.30 – 2.23 (m, 2H), 2.01 – 1.93 (m, 2H), 1.78 (ddt, *J* = 9.0, 7.6, 6.2 Hz, 2H), 1.10 (s, 9H). <sup>13</sup>C NMR (101 MHz, CDCl<sub>3</sub>)  $\delta$  199.7, 166.1, 135.6, 133.7, 129.7, 127.7, 125.8, 63.1, 37.4, 34.4, 29.9, 29.7, 26.9, 22.7, 19.2.

**2-methylbenzo[d][1,3]dioxole:** prepared according to a literature procedure.<sup>59</sup> An oven-

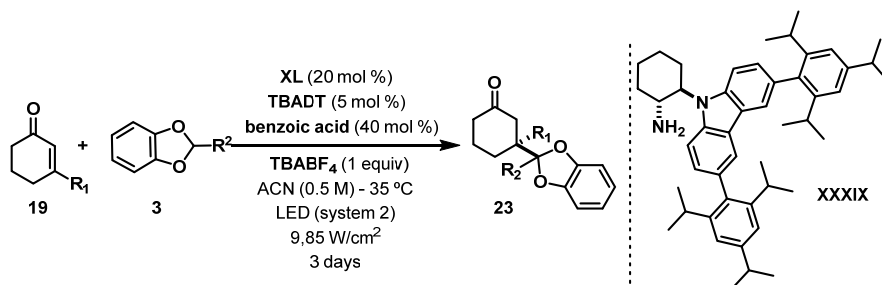


dried, argon purged two neck round bottomed flask fitted with a vacuum adaptor and septum was charged with 5.51 g (50 mmol) of catechol, 12.9 mL (140 mmol) of vinyl acetate, 50 mg of HgO, and 200  $\mu$ L of BF<sub>3</sub>·Et<sub>2</sub>O in 50 mL of dry toluene. Stirring was continued under argon over 12 h. The reaction mixture was extracted with 3 x 30 mL of 0.5 M NaOH and dried (K<sub>2</sub>CO<sub>3</sub>). A brown oil residue was obtained upon concentration *in vacuo* which was purified by flash chromatography (Heptane then pentane), to give colourless oil, 4.48 g (66%). Spectral characteristics correspond with literature precedent.<sup>59</sup> <sup>1</sup>H NMR (300 MHz, CDCl<sub>3</sub>)  $\delta$  6.80 (m, 4H), 6.26 (q, *J* = 4.9 Hz, 1H), 1.70 (d, *J* = 4.9 Hz, 3H).

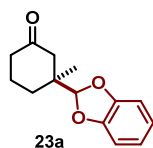
<sup>58</sup> D. Gaugele, M. E. Maier, Approach to the Core Structure of the Polycyclic Alkaloid Palthinine A, *Synlett*, **2013**, 24, 955.

<sup>59</sup> D. E. Nichols, L. J. Kostuba, Steric Effects of Substituents on Phenethylamine Hallucinogens. 3,4- (Methylenedioxy)amphetamine Analogues Alkylated on the Dioxole Ring, *J. Med. Chem.*, **1979**, 22, 1264.

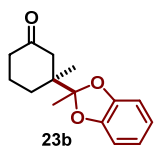
#### 4.9.5. General Procedure of the Photochemical Enantioselective $\beta$ -Alkylation of Enones.



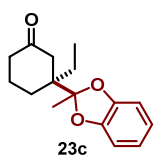
All the reactions were carried out in acetonitrile (synthesis grade, >99%). An ordinary vial equipped with a Teflon-coated stir bar was charged with amine **XXXIX** (0.04 mmol, 26.8 mg, 20 mol %), TBADT (0.01 mmol, 32mg), tetrabutylammonium tetrafluoroborate (0.2 mmol, 64 mg), and benzoic acid (0.08 mmol, 9.8 mg). The reaction vial was sealed with a teflon septum and purged with argon three times prior to adding liquid reagents. Then acetonitrile (0.4 mL, 0.5 M), 3-methyl-2-cyclohexenone (0.2 mmol, 22,6  $\mu$ L) and 1,3-benzodioxole (0.6 mmol, 69  $\mu$ L), were sequentially added. The reaction mixture was stirred in the system 3 described above maintaining the temperature at 35°C inside the vial and irradiance of 9,85 W/cm<sup>2</sup> of 365nm single LED . Stirring was continued over 72 hr. Solvent was removed under reduced pressure and the alkylated product **23** isolated by flash column chromatography.



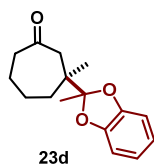
The reaction was carried out following the general procedure to furnish the crude product. The title compound **23a** was isolated by flash column chromatography (eluent hexane/ethyl acetate = 5/1) in 73% yield (33.8 mg) of a colourless oil. The enantiomeric excess was determined to be 93% by HPLC analysis on a Daicel Chiralpak ID-3 column: 95/5 hexane/IPA, flow rate 0.8 mL/min,  $\lambda = 280$  nm:  $\tau_{Major} = 10.21$  min,  $\tau_{Minor} = 9.79$  min.  $[\alpha]_D^{26} = +4.7$  ( $c = 0.18$ , CHCl<sub>3</sub>). <sup>1</sup>H NMR (400 MHz, CDCl<sub>3</sub>)  $\delta$  6.83 – 6.75 (m, 4H), 5.79 (s, 1H), 2.51 (d,  $J = 13.9$  Hz, 1H), 2.41 – 2.27 (m, 2H), 2.20 (dt,  $J = 13.8, 1.8$  Hz, 1H), 2.09 – 2.00 (m, 1H), 1.98 – 1.83 (m, 2H), 1.73 – 1.65 (m, 1H), 1.07 (s, 3H). <sup>13</sup>C NMR (101 MHz, CDCl<sub>3</sub>)  $\delta$  210.2, 147.7, 121.5, 121.5, 115.2, 108.2, 108.2, 46.8, 43.5, 41.0, 29.9, 21.3, 19.0.



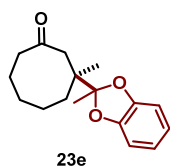
The reaction was carried out following the general procedure to furnish the crude product. The title compound **23b** was isolated by flash column chromatography (eluent hexane/ethyl acetate = 5/1) in 69% yield (34.0 mg) of a colourless oil. The enantiomeric excess was determined to be 98% by UPC<sup>2</sup> analysis on a Daicel Chiralpak IC-3 column with a gradient (100% CO<sub>2</sub> to 60/40 CO<sub>2</sub>/EtOH) over 4 minuts, flow rate 3 mL/min,  $\lambda = 283$  nm:  $\tau_{Major} = 2.21$  min,  $\tau_{Minor} = 2.27$  min.  $[\alpha]_D^{26} = -1.7$  ( $c = 0.69$ , CHCl<sub>3</sub>). <sup>1</sup>H NMR (500 MHz, CDCl<sub>3</sub>)  $\delta$  6.91 – 6.66 (m, 4H), 2.58 (dt,  $J = 13.8$ , 0.9 Hz, 1H), 2.39 – 2.28 (m, 2H), 2.24 (dt,  $J = 13.8$ , 1.9 Hz, 1H), 2.10 – 1.97 (m, 2H), 1.92 – 1.78 (m, 1H), 1.76 – 1.69 (m, 1H), 1.58 (s, 3H), 1.13 (s, 3H). NMR (126 MHz, CDCl<sub>3</sub>)  $\delta$  210.9, 147.4, 147.3, 121.5, 121.3, 121.2, 108.3, 108.3, 47.1, 46.9, 40.6, 29.9, 21.4, 19.8, 19.7.



The reaction was carried out following the general procedure to furnish the crude product. The title compound **23c** was isolated by flash column chromatography (eluent hexane/ethyl acetate = 5/1) in 57% yield (29.6 mg) of a colourless oil. The enantiomeric excess was determined to be 85% by by UPC<sup>2</sup> analysis on a Daicel Chiralpak IC-3 column with a gradient (100% CO<sub>2</sub> to 60/40 CO<sub>2</sub>/ACN) over 4 minuts, flow rate 3 mL/min,  $\lambda = 283$  nm:  $\tau_{Major} = 2.37$  min,  $\tau_{Minor} = 2.49$  min  $[\alpha]_D^{26} = -1.1$  ( $c = 0.60$ , CHCl<sub>3</sub>). <sup>1</sup>H NMR (500 MHz, CDCl<sub>3</sub>)  $\delta$  6.91 – 6.69 (m, 4H), 2.55 (d,  $J = 14.4$  Hz, 1H), 2.36 – 2.30 (m, 2H), 2.26 (dt,  $J = 14.3$ , 1.5 Hz, 1H), 2.09 – 1.99 (m, 1H), 1.93 (ddd,  $J = 14.7$ , 10.7, 4.0 Hz, 1H), 1.89 – 1.75 (m, 2H), 1.69 – 1.57 (m, 2H), 1.56 (s, 3H), 1.02 (t,  $J = 7.5$  Hz, 3H). <sup>13</sup>C NMR (126 MHz, CDCl<sub>3</sub>)  $\delta$  211.0, 147.2, 146.9, 122.2, 121.2, 121.2, 108.4, 108.3, 49.2, 45.8, 40.3, 27.1, 27.0, 21.2, 20.2, 8.8.

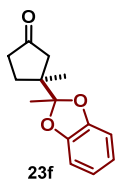


The reaction was carried out following the general procedure to furnish the crude product. The title compound **23d** was isolated by flash column chromatography (eluent hexane/ethyl acetate = 5/1) in 70% yield (36.4 mg) of a colourless oil. The enantiomeric excess was determined to be 94% by by UPC<sup>2</sup> analysis on a Acquity AMY-1 column with a gradient (100% CO<sub>2</sub> to 60/40 CO<sub>2</sub>/MeOH) over 4 minuts, flow rate 2 mL/min,  $\lambda = 283$  nm:  $\tau_{Major} = 3.13$  min,  $\tau_{Minor} = 3.03$  min  $[\alpha]_D^{26} = +25.3$  ( $c = 0.80$ , CHCl<sub>3</sub>). <sup>1</sup>H NMR (500 MHz, CDCl<sub>3</sub>)  $\delta$  6.90 – 6.68 (m, 4H), 2.94 (d,  $J = 11.8$  Hz, 1H), 2.61 – 2.48 (m, 2H), 2.37 (ddd,  $J = 18.3$ , 11.2, 4.7 Hz, 1H), 2.03 – 1.72 (m, 5H), 1.58 (s, 3H), 1.56 – 1.44 (m, 1H), 1.07 (s, 3H). <sup>13</sup>C NMR (126 MHz, CDCl<sub>3</sub>)  $\delta$  213.1, 147.4, 147.4, 122.3, 121.1, 108.4, 108.2, 48.3, 44.1, 43.8, 36.4, 29.7, 24.28, 23.8, 19.9, 19.1.

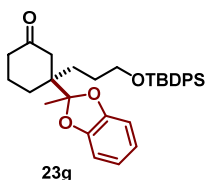


The reaction was carried out following the general procedure to furnish the crude product. The title compound **23e** was isolated by flash column chromatography (eluent hexane/ethyl acetate = 5/1) in 63% yield (34.5 mg) of a colourless oil. The enantiomeric excess was determined to be 99% by UPC<sup>2</sup> analysis on a Acquity CEL-1 column with a gradient (100% CO<sub>2</sub> to 60/40 CO<sub>2</sub>/MeOH) over 4 minuts, flow rate 2 mL/min,  $\lambda = 283$  nm:  $\tau_{Major} = 2.54$  min,  $\tau_{Minor}$

= 2.48 min  $[\alpha]_D^{26} = +28.9$  ( $c = 1.3$ ,  $\text{CHCl}_3$ ).  $^1\text{H}$  NMR (500 MHz,  $\text{CDCl}_3$ )  $\delta$  6.92 – 6.67 (m, 4H), 3.05 (d,  $J = 10.8$  Hz, 1H), 2.43 (ddd,  $J = 15.7, 6.3, 2.4$  Hz, 1H), 2.30 – 2.22 (m, 1H), 2.22 – 2.10 (m, 2H), 1.83 – 1.65 (m, 4H), 1.50 – 1.64 (m, 2H), 1.58 (s, 3H), 1.20 (s, 3H), 1.16 – 1.05 (m, 1H).  $^{13}\text{C}$  NMR (126 MHz,  $\text{CDCl}_3$ )  $\delta$  214.6, 147.5, 147.4, 122.54, 121.1, 121.1, 108.3, 108.2, 47.5, 45.5, 42.5, 30.6, 28.7, 21.2, 20.0, 19.2, 18.9.



The reaction was carried out following the general procedure to furnish the crude product. The title compound **23f** was isolated by flash column chromatography (eluent hexane/ethyl acetate = 5/1) in 99% yield (45.9 mg) of a colourless oil. The enantiomeric excess was determined to be 88% by UPC<sup>2</sup> analysis on a Daicel Chiralpak IC-3 column with a gradient (100%  $\text{CO}_2$  to 60/40  $\text{CO}_2$ /IPA) over 4 minutes, flow rate 3 mL/min,  $\lambda = 283$  nm:  $\tau_{\text{Major}} = 2.22$  min,  $\tau_{\text{Minor}} = 2.37$  min  $[\alpha]_D^{26} = +30.1$  ( $c = 0.45$ ,  $\text{CHCl}_3$ ).  $^1\text{H}$  NMR (500 MHz,  $\text{CDCl}_3$ )  $\delta$  6.81 – 6.71 (m, 4H), 2.57 (d,  $J = 18.1$  Hz, 1H), 2.39 – 2.33 (m, 2H), 2.31 – 2.23 (m, 1H), 2.02 (dt,  $J = 18.0, 1.2$  Hz, 1H), 1.78 (dddd,  $J = 12.9, 8.7, 4.6, 1.8$  Hz, 1H), 1.60 (s, 3H), 1.29 (s, 3H).  $^{13}\text{C}$  NMR (126 MHz,  $\text{CDCl}_3$ )  $\delta$  218.1, 147.9, 147.7, 121.7, 121.7, 121.6, 108.8, 108.7, 48.2, 47.4, 37.0, 30.1, 22.6, 21.0.



The reaction was carried out following the general procedure to furnish the crude product. The title compound **23g** was isolated by flash column chromatography (eluent hexane/ethyl acetate = 5/1) in 57% yield (60.3 mg) of a colourless oil. The enantiomeric excess was determined to be 85% by UPC<sup>2</sup> analysis on a Acquity AMY-1 column with a gradient (100%  $\text{CO}_2$  to 65/35  $\text{CO}_2$ /IPA) over 8 minutes, flow rate 3 mL/min,  $\lambda = 283$  nm:  $\tau_{\text{Major}} = 4.81$  min,  $\tau_{\text{Minor}} = 4.73$  min  $[\alpha]_D^{26} = +0.33$  ( $c = 1.23$ ,  $\text{CHCl}_3$ ).  $^1\text{H}$  NMR (500 MHz,  $\text{CDCl}_3$ )  $\delta$  7.70 (dq,  $J = 6.5, 1.7$  Hz, 4H), 7.56 – 7.37 (m, 6H), 6.92 – 6.73 (m, 4H), 3.74 – 3.62 (m, 2H), 2.59 (d,  $J = 14.3$  Hz, 1H), 2.36 – 2.30 (m, 2H), 2.26 (dd,  $J = 14.3, 1.6$  Hz, 1H), 2.05 – 1.96 (m, 1H), 1.96 – 1.90 (m, 1H), 1.88 – 1.74 (m, 3H), 1.71 – 1.57 (m, 3H), 1.55 (s, 3H), 1.10 (s, 9H).  $^{13}\text{C}$  NMR (126 MHz,  $\text{CDCl}_3$ )  $\delta$  210.7, 147.3, 146.9, 135.6, 135.6, 133.9, 133.8, 129.62, 127.7, 122.0, 121.2, 121.2, 108.4, 108.3, 64.1, 48.8, 46.5, 40.3, 30.7, 30.4, 27.3, 27.1, 26.9, 21.03, 20.2, 19.2.

#### 4.9.6. Single Crystal X-Ray Diffraction Data

X-ray structure determinations: Crystals of **catalyst XXXVI** were obtained by slow evaporation of a Hexane/ $\text{Et}_2\text{O}$  mixture (3:1) at room temperature, the crystals of **62** were obtained by evaporation  $\text{EtOH}$  and the crystals of compound **51F** were obtained by slow evaporation of a Hexane/ $\text{Et}_2\text{O}$  mixture (3:1) at room temperature. The measured crystals were stable under atmosphere conditions; nevertheless they were prepared under inert conditions immersed in perfluoropolyether as protecting oil for manipulation.

Data Collection. Measurements were made on a Bruker-Nonius diffractometer equipped with an APPEX 2 4K CCD area detector, a FR591 rotating anode with MoK $\alpha$  radiation, Montel

mirrors and a Cryostream Plus low temperature device ( $T = -173\text{ }^{\circ}\text{C}$ ). Full-sphere data collection was used  $\omega$  and  $\varphi$  scans.

Programs used: Data collection Apex2 V2010 7.0 (Bruker-Nonius 2008), data reduction Saint + Version 7.60A (Bruker AXS 2008) and absorption correction SADABS. Structure Solution. SIR2007 program was used.<sup>60</sup> Structure Refinement. SHELXTL-97.<sup>61</sup>

Crystal data for **XXXVI** at 100(2) K:

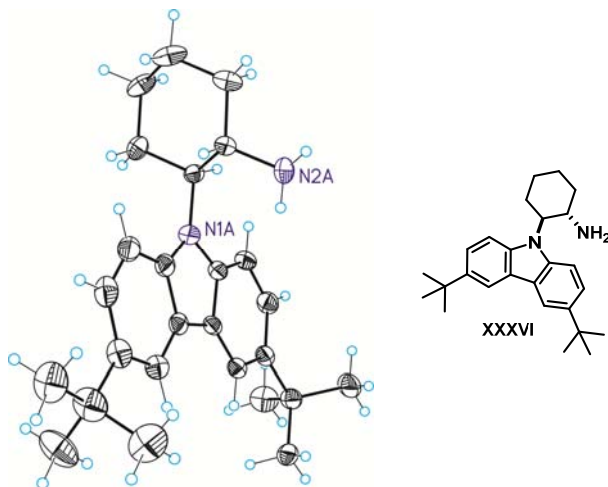


**Figure 41.** Crystal data of catalyst **XXXVI**.

**Table 11.** Crystal data and structure refinement for mo\_DBB07crys03\_0m.

Empirical formula	C <sub>26</sub> H <sub>36</sub> N <sub>2</sub>
Formula weight	376.57
Temperature	100(2) K
Wavelength	0.71073 Å
Crystal system	Monoclinic
Space group	P2(1)
Unit cell dimensions	
a = 13.8162(6)Å	$\alpha = 90^{\circ}$ .
b = 10.7641(5)Å	$\beta = 93.8753(13)^{\circ}$ .
c = 15.1909(6)Å	$\gamma = 90^{\circ}$ .
Volume	2254.01(17) Å <sup>3</sup>
Z	4
Density (calculated)	1.110 Mg/m <sup>3</sup>
Absorption coefficient	0.064 mm <sup>-1</sup>
F(000)	824
Crystal size	0.20 x 0.20 x 0.10 mm <sup>3</sup>

<sup>60</sup>R. Caliandro, B. Carrozzini, G. L. Cascarano, L. De Caro, C. Giacovazzo, D. Siliqi, Advances in *ab initio* Protein Phasing by Patterson Deconvolution Techniques. *J. Appl. Cryst.* **2007**, *40*, 883.

<sup>61</sup>G. M. Sheldrick, A Short History of SHELX. *Acta Cryst.* **2008**, *A64*, 112.

Theta range for data collection	1.344 to 32.314°.
Index ranges	-20<=h<=20,-15<=k<=11,-22<=l<=14
Reflections collected	22533
Independent reflections	10437[R(int) = 0.0234]
Completeness to theta =32.314°	86.4%
Absorption correction	Empirical
Max. and min. transmission	0.994 and 0.948
Refinement method	Full-matrix least-squares on F2
Data / restraints / parameters	10437/ 402/ 673
Goodness-of-fit on F2	1.040
Final R indices [I>2sigma(I)]	R1 = 0.0562, wR2 = 0.1403
R indices (all data)	R1 = 0.0757, wR2 = 0.1532
Flack parameter	x =-0.3(10)
Largest diff. peak and hole	0.505 and -0.562 e.Å <sup>-3</sup>

Crystal data for **51F** at 100(2) K:

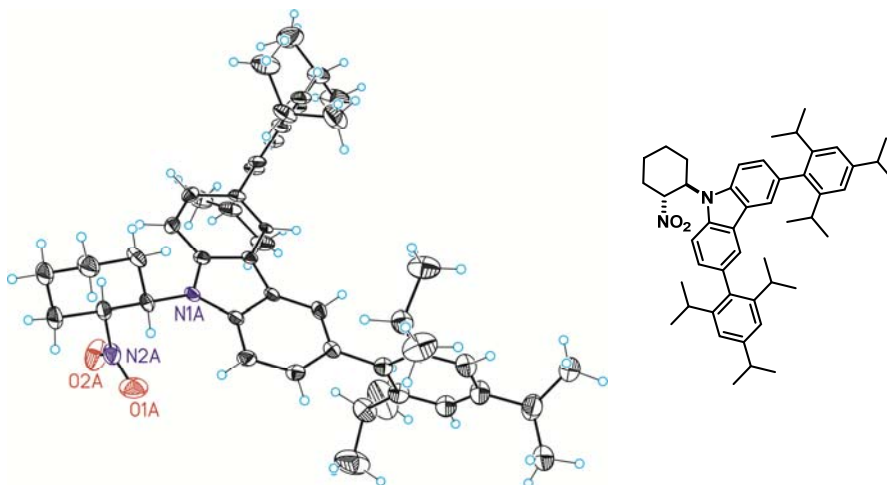


**Figure 42.** Crystal data of compound **51F**.

**Table 12.** Crystal data and structure refinement for DBB07crys02\_b.

Empirical formula	C <sub>49.75</sub> H <sub>64</sub> N <sub>2</sub> O <sub>2</sub>
Formula weight	722.03
Temperature	100(2) K
Wavelength	0.71073 Å
Crystal system	Triclinic
Space group	P-1
Unit cell dimensions	
a = 12.868(4) Å	α = 89.205(10)°.
b = 17.479(5) Å	β = 80.097(9)°.
c = 21.009(6) Å	γ = 69.683(7)°.

Volume 4360(2) Å<sup>3</sup>  
Z 4  
Density (calculated) 1.100 Mg/m<sup>3</sup>  
Absorption coefficient 0.066 mm<sup>-1</sup>  
F(000) 1570  
Crystal size 0.20 x 0.20 x 0.20 mm<sup>3</sup>  
Theta range for data collection 2.278 to 27.638°.  
Index ranges -16<=h<=16,-22<=k<=22,-27<=l<=27  
Reflections collected 58463  
Independent reflections 19727[R(int) = 0.0656]  
Completeness to theta =27.638° 97.1%  
Absorption correction Empirical  
Max. and min. transmission 0.987 and 0.759  
Refinement method Full-matrix least-squares on F<sup>2</sup>  
Data / restraints / parameters 19727/ 2371/ 1886  
Goodness-of-fit on F<sup>2</sup> 1.136  
Final R indices [I>2sigma(I)] R1 = 0.1460, wR2 = 0.3720  
R indices (all data) R1 = 0.1646, wR2 = 0.3800  
Largest diff. peak and hole 0.631 and -0.451 e.Å<sup>-3</sup>

X-ray crystallographic analysis of the single crystal **62** was good enough to unambiguously determine the absolute configuration of the major enantiomer of the catalyst obtained.

Crystal data for **62** at 100(2) K:

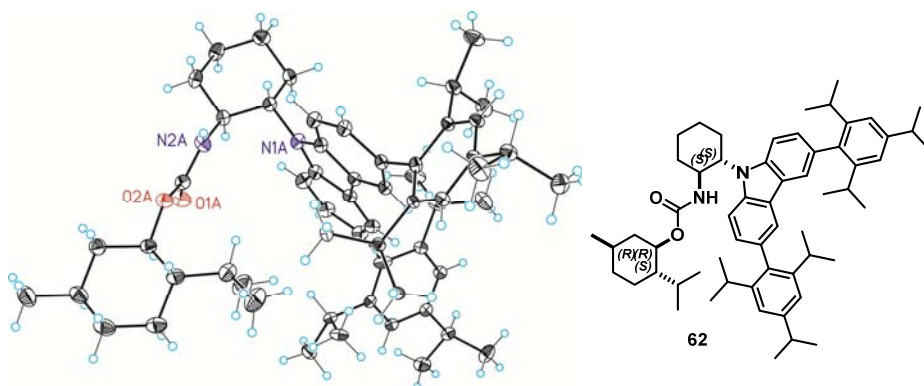


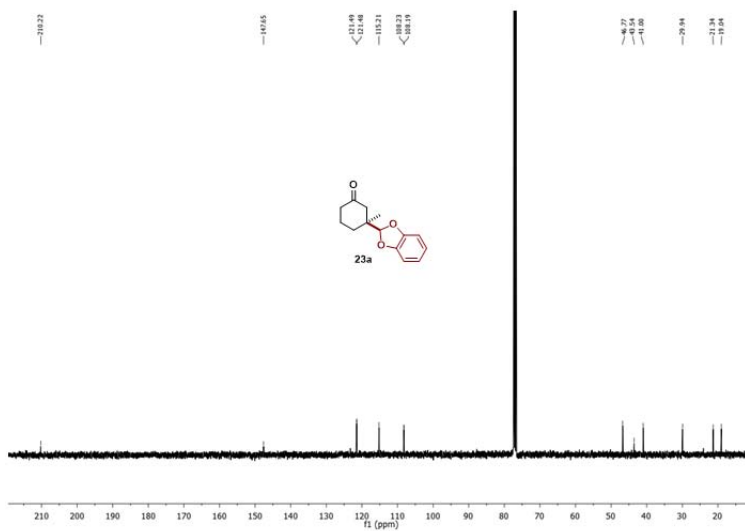
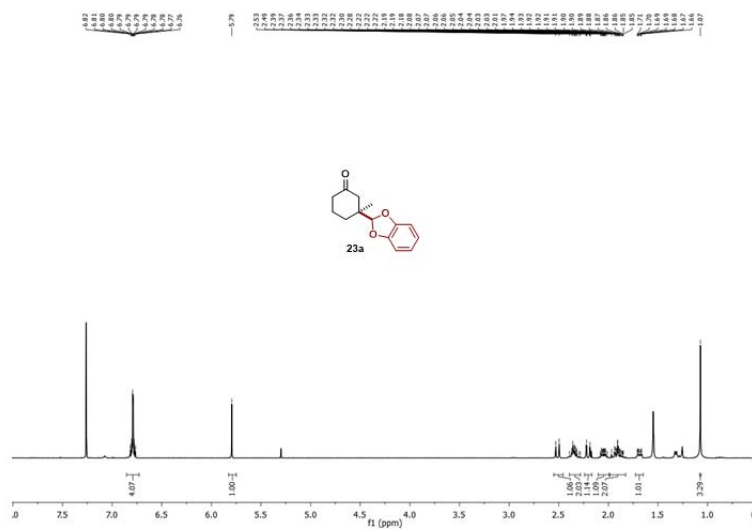
Figure 43. Crystal data of compound 62.

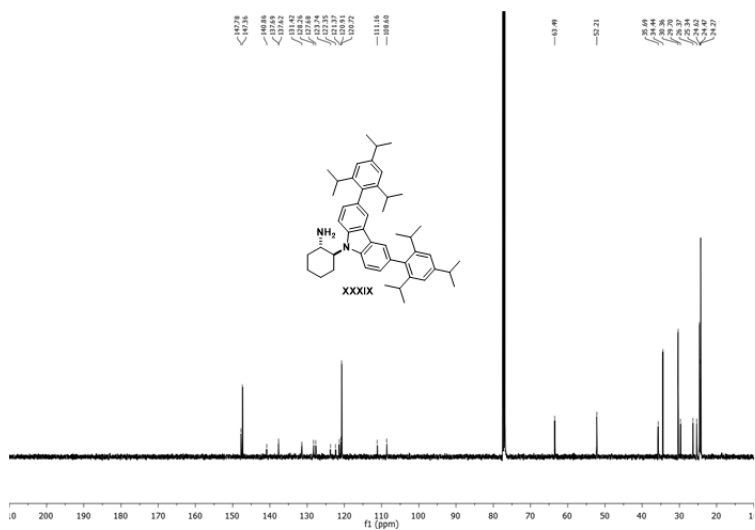
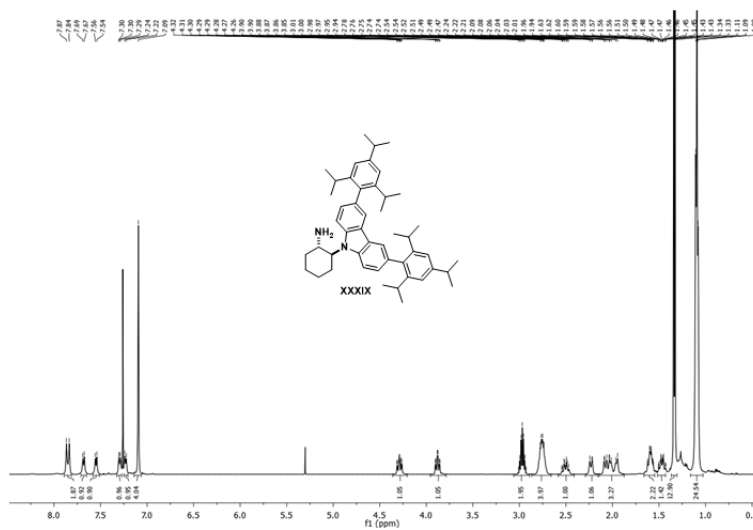


**Table 13.** Crystal data and structure refinement for JM-TRIPCARE.

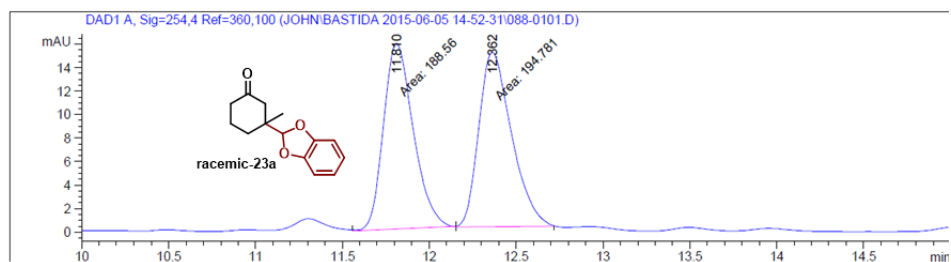
Empirical formula	C66 H103 N2 O5.50
Formula weight	1012.50
Temperature	100(2) K
Wavelength	0.71073 Å
Crystal system	Triclinic
Space group	P1
Unit cell dimensions	
a = 12.6555(14)Å	$\alpha$ = 101.834(3)°.
b = 14.3909(15)Å	$\beta$ = 91.8154(5)°.
c = 17.7283(19)Å	$\gamma$ = 98.931(3)°.
Volume	3115.1(6) Å <sup>3</sup>
Z	2
Density (calculated)	1.079 Mg/m <sup>3</sup>
Absorption coefficient	0.067 mm <sup>-1</sup>
F(000)	1114
Crystal size	0.30 x 0.30 x 0.20 mm <sup>3</sup>
Theta range for data collection	2.066 to 45.339°.
Index ranges	-25<=h<=25,-25<=k<=28,-35<=l<=34
Reflections collected	122569
Independent reflections	65782[R(int) = 0.0236]
Completeness to theta =45.339°	84.6%
Absorption correction	Multi-scan
Max. and min. transmission	0.983 and 0.756
Refinement method	Full-matrix least-squares on F <sup>2</sup>
Data / restraints / parameters	65782/ 892/ 1811
Goodness-of-fit on F <sup>2</sup>	1.023
Final R indices [ $I > 2\sigma(I)$ ]	R1 = 0.0513, wR2 = 0.1423
R indices (all data)	R1 = 0.0641, wR2 = 0.1568
Flack parameter	x = 0.17(13)
Largest diff. peak and hole	0.710 and -0.715 e.Å <sup>-3</sup>

#### 4.9.7. NMR traces of compound 23a and catalyst XXXIX.



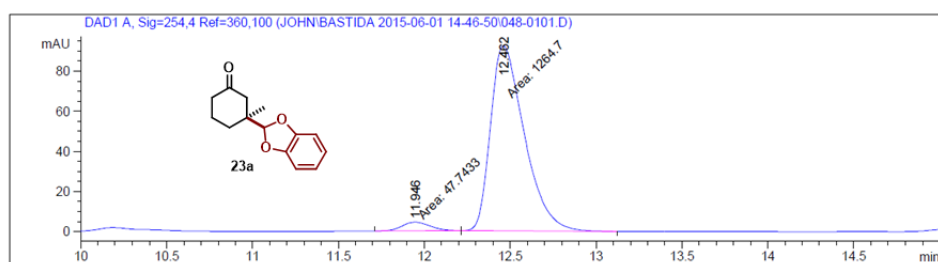


## 4.9.8. HPLC traces of compound 23a.



Signal 1: DAD1 A, Sig=254,4 Ref=360,100

Peak #	RetTime [min]	Type	Width [min]	Area [mAU*s]	Height [mAU]	Area %
1	11.810	MM	0.1986	188.55975	15.82049	49.1886
2	12.362	MM	0.2185	194.78065	14.85641	50.8114



Signal 1: DAD1 A, Sig=254,4 Ref=360,100

Peak #	RetTime [min]	Type	Width [min]	Area [mAU*s]	Height [mAU]	Area %
1	11.946	MM	0.1850	47.74335	4.30145	3.6377
2	12.462	MM	0.2284	1264.69873	92.27348	96.3623

## 4.10. ANNEX 2 Features, Descriptions and Technical Issues of the Irradiation Systems.

System 1 and system 2 consist of 6 LEDs distributed in 2 series of 3 LEDs in parallel with a resistor to give a longer lifetime to the LEDs. This array was incorporated into an aluminum block featuring six vial wells with an aperture to allow a single LED to enter each well. The aluminum block itself houses a system which allows liquid, connected to a thermo/cryostat, to circulate through the block to control the temperature of the vial wells.

The energy applied to the electrical circuit is controlled by a variable power supply which allows regulation of the current and the voltage applied to the order of 0.01 A and 1 mV respectively. The light intensity (in  $\mu\text{A}$ ) was measured using a photodiode.

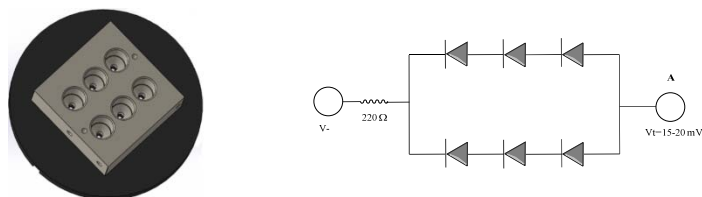


Figure 44. Solid works representation of the single LED set up, and schematic electric circuit.

Table 14. LED circuit voltage Irradiance equivalences

LEDS	Factor	V (V) applied	(I mA) mesured	(W/cm <sup>2</sup> ) irradiance
<i>Wavelength</i> 365 nm	<b>130,78</b>	<b>20</b>	<b>0,09</b>	<b>11,25</b>
		<b>19</b>	<b>0,08</b>	<b>10,72</b>
		<b>18</b>	<b>0,08</b>	<b>9,85</b>
		<b>17</b>	<b>0,06</b>	<b>8,44</b>
		<b>16</b>	<b>0,06</b>	<b>7,30</b>
		<b>15</b>	<b>0,05</b>	<b>6,21</b>
<i>Wavelength</i> 355 nm	<b>185,46</b>	<b>20</b>	<b>0,02</b>	<b>4,40</b>

UNIVERSITAT ROVIRA I VIRGILI  
NOVEL ENANTIOSELECTIVE AMINOCATALYTIC PROCESSES BY MEANS OF VINYLLOGOUS  
REACTIVITY AND PHOTOREDOX CATALYSIS  
David Bastida Borrell